Towards the synthesis of imines and iminiums and their reactions *in situ*

Philip Geoffrey Arthur Winkworth

Submitted in accordance with the requirements for the degree of

Doctor of Philosophy

University of Leeds

School of Chemistry

September 2014

Intellectual Property and Publication Statements

The candidate confirms that the work submitted is his own and that appropriate credit has been given where reference has been made to the work of others.

This copy has been supplied on the understanding that it is copyright material and that no quotation from the thesis may be published without proper acknowledgement.

Acknowledgments

Abstract

Functionalised amines are important targets for organic chemists. Various methods are used to functionalise amines, however often these reactions will involve the use of toxic or expensive reagents and therefore must be controlled, especially when used as active pharmaceutical ingredients (API). These reagents could potentially increase the cost associated with API and fine chemical synthesis. There has been an impetus to directly activate the C-H bonds adjacent to amine groups, thus increasing the reactivity of the group.

Metal complexes have been used to stoichiometrically activate amines, however catalytic methods would be more favourable due to potential cost reduction. Metal complexes are used widely for hydrogen transfer reaction, which have provided a new methodology to activate non-electrophilic substrates by forming their electrophilic analogues. This methodology has been used extensively with alcohols, however there remains the opportunity to form imines by amine activation.

The research disclosed in this thesis discusses efforts toward the formation of imines or iminium ions from their amine precursors. Analysis of the *N*-alkylation of several amines has been carried out, with discussion of methods to inhibit *N*-alkylation to form more of the desired imine. Mechanistic analysis of the various species in the reactions has given information including a potential pathway for *N*-alkylation, amine iridium binding and a potential inhibition product.

The optimisation of an indole cyclisation reaction has been probed, with different a range of conditions investigated. A discussion of an attempted telescoped reaction has been given as well, together with a study on the expansion of the methodology to include diverse structural motifs. The attempted incorporation of different nucleophiles has also been disclosed with a discussion of the results and potential improvements to these reactions. Finally, an overview of the future for this research has been presented with potential new avenues for exploitation.

Table of Contents

List of Tables

List of Figures

List of Schemes

List of Abbreviations

APIs	Active Pharmaceutical Ingredients
Ac	Acetyl
AcOH	Acetic acid
Ar	Aryl
BArF	(*Tetrakis*-[3,5-*Bis*-(trifluoromethyl)phenyl]borate)
BINAP	2,2′-*Bis*(diphenylphosphino)-1,1′-binaphthyl
bp	Boiling point
bppm	2,3-*Bis*-(diphenylphosphino)-*N*-phenylmaleimide,
Bn	Benzyl
Bu	Butyl
$CDCl_3$	Chloroform-d
COSY	Correlation order spectroscopy
COD	1,5-Cyclooctadiene
Cp*	Pentamethylcyclopentadienyl
CSA	Camphor Sulfonic Acid
de	Diastereoisomeric excess
DIAD	Diisopropyl azodicarboxylate
DIBAL	Diisobutylaluminium hydride
DIOP	1,4-*bis*-diphenylphosphinobutane
DKR	Dynamic kinetic resolution
DMBQ	2,4-dimethoxybenzoquinone

DME	1,2-Dimethoxyethane
DMF	N,N'-Dimethylformamide
DMSO	Dimethyl sulfoxide
DNA	Deoxyribonucleic acid
DOSY	Diffusion ordered spectroscopy
dr	Diastereoisomeric ratio
EDTA	Ethylenediaminetetraacetic acid
ee	Enantiomeric excess
EI	Electron impact
equiv.	equivalents
er	Enantiomeric ratio
ES	Electrospray
ESI-MS	Electrospray ionisation mass spectrometry
Et	Ethyl
GC	Gas chromatography
GC-MS	Gas chromatography mass spectrometry
HPLC	High performance liquid chromatography
HRMS	High resolution mass spectrometry
Hz	Hertz
i-PrOH	*iso*-Propylalcohol
IR	Infrared
LHMDS	Lithium hexamethyldisilazide
LRMS	Low resolution mass spectrometry

MAO	Monoamine oxidases
MAO-N	*Aspergillus niger* derived MAO
Me	Methyl
MeCN	Acetonitrile
m.p.	Melting point
MS	Molecular sieves
m/z	Mass–charge ratio
NMP	*N*-Methyl pyrrolidine
NMR	Nuclear magnetic resonance spectroscopy
Nu	Nucleophile
Pet	Petroleum 40-60 °C fraction
PGSE	Pulsed field gradient spin-echo
PGIs	Potential Genotoxic Impurities
Ph	Phenyl
PhH	Benzene
PhMe	Toluene
PHOX	Phosphinooxazolines
PMA	Phosphomolybdic acid
ppm	Parts per million
Pr	Propyl
Py	Pyridine
Re	Rectus
rt	Room temperature

SCRAM	Diiodo(pentamethylcyclopentadienyl)iridium(III) dimer
Si	Sinister
Sol	Solvent
TBAF	Tetrabutylammonium fluoride
TEAF	Tetraethylammonium formate
Tf	Trifluoromethanesulfonyl (triflyl)
TFA	Trifluoroacetic acid
TFAA	Trifluoroacetic anhydride
THF	Tetrahydrofuran
TLC	Thin layer chromatography
TMS	Trimethylsilyl (tetramethylsilane)
TMSCN	Trimethylsilyl cyanide
TON	Turnover number
TOF	Turnover frequency
Ts	*p*-Toluenesulfonyl
TsOH	*p*-Toluenesulfonic acid
TsDPEN	*N-para*-Toluenesulfonyl-1,2-diphenylethylenediamine
TTC	Thresholds of Toxicological Concern
UPLC-TOF-MS	Ultra high performance liquid chromatography time of flight mass spectrometry
UV	Ultraviolet
Yr	Year

Chapter 1 Introduction

1.1 Functionalised amines and the pharmaceutical and fine chemical industries

1.1.1 The financial and medicinal importance of functionalised amines

Functionalised amines are of great economic importance to drug companies; active pharmaceutical ingredients (APIs) **1.1**-**1.4** had combined revenues of greater than $21 billion in 2011 (Figure 1.1).[1]
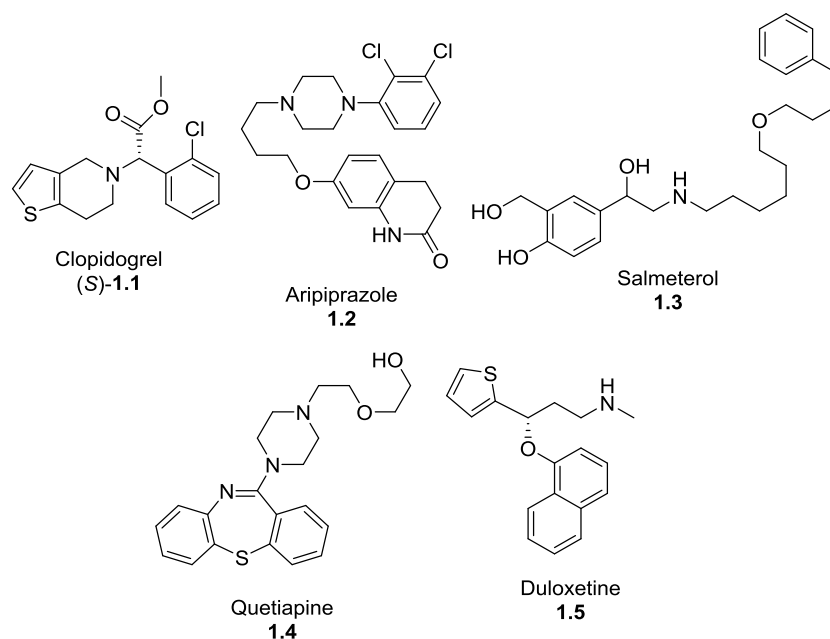
Figure 1.1 Important amine containing APIs: (*S*)-1.1, Clopidogrel by Bristol Myers-Squibb; 1.2 Aripiprazole by Otsuka; 1.3, Salmeterol by GlaxoSmithKline; 1.4 Quetiapine by AstraZeneca and 1.5 Duloxetine by Eli Lilly.

These drugs not only represent lucrative financial targets, but are also used in the treatment of debilitating diseases. Clopidogrel, **1.1**, is a platelet-aggregate inhibitor, also used in the treatment of ischemic events in symptomatic atherosclerosis sufferers as well as in the treatment of acute coronary syndrome without ST-segment elevation; these diseases affect

80-90% of the population and cause the death of 1 in 5 men and 1 in 7 women, respectively. Aripiprazole, **1.2** and Quetiapine, **1.4**, are antipsychotics which are used in the treatment of bipolar disorder, a disease that affects 1 in 100 people. Salmeterol, **1.3**, is a corticoid used in the treatment of asthma a disease affecting 235 million people globally (2011).[2] The importance of these and similar drugs medicinally and economically has required the design of cheap and efficient formation of functionalised amines on an industrial scale.

1.1.2 Functionalization of amines and the pharmaceutical industry

The functionalization of amines is a broadly researched subject, the scope and characterisation of which has been thoroughly examined. The synthesis of optically active functionalised amines in the pharmaceutical industry has been reviewed by Hauer and co-workers.[3] Whilst there are numerous methodologies for the formation of functionalised amines many of the well characterised techniques may not be suitable for use in pharmaceutical synthesis, due to regulatory restraints on the concentration of certain chemicals within these methods and these will now be described.

1.1.2.1 *N*-Alkylations with alkyl halides

APIs **1.1-1.5** contain *N*-alkylated amines. This type of functionalisation can happen in numerous ways. One conventional method for the *N*-alkylation of amines involves the use of toxic alkylating agents, such as haloalkanes to alkylate ammonia and other amines (Scheme 1.1).[4]
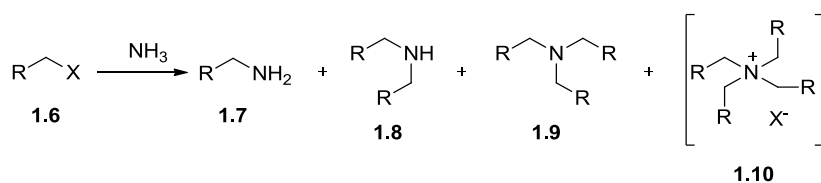
Scheme 1.1 The *N*-alkylation of haloalkanes by ammonia, leading to a mixture of primary, secondary, tertiary or quaternary amines.

One of the drawbacks of this reaction is the lack of selectivity, with the formation of side-products **1.7-1.10** that can lead to difficult separations and add to the waste stream and give poor yields, reducing the economic efficacy of the reaction. It should be noted, however, that *N*-alkylation using halo-alkanes is still used to form APIs, the synthesis of prasugrel hydrochloride being one such example (Scheme 1.2).[5]
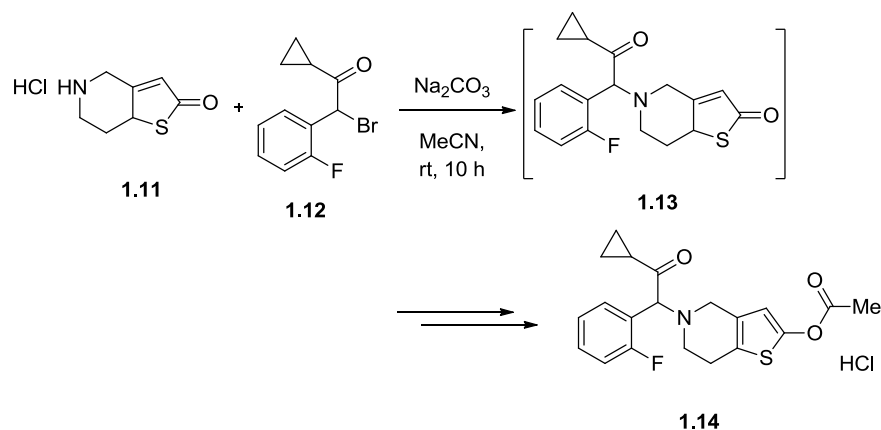
Scheme 1.2 Key step in Vummenthala's synthesis of prasugrel hydrochloride, 1.14 involving use of a halo alkane to make intermediate 1.12.

Furthermore, haloalkanes like compound **1.6**, must themselves be controlled in the final pharmaceutical product because, as alkylating agents, since they are potential genotoxic impurities (PGIs).[6, 7] From a regulatory standpoint, there are specific levels of PGIs that are permissible within a drug, *e.g.* methyl iodide has a time weighted average exposure limit of 12 mg m^{-3}. Lipczynski and co-workers have evaluated the methyl iodide levels that are required in a range of pharmaceuticals.[6, 7] They described how the testing method for the antiemtic azasetron hydrochloride, **1.15** (Figure 1.2), showed that methyl iodide levels were less than 41.3 ng. There is a major impetus within the pharmaceutical industry to move away from using these genotoxic reagents, as there is an increased cost associated with the testing required to prove that these impurities are not present at high concentrations. The drug industry has tried to avoid the use of PGIs, where possible, and has tried to develop numerous methodologies for the functionalization of amines that build-on developed *N*-alkylation, reductive amination and amide reduction reactions (Scheme 1.4 and Scheme 1.6, *vide infra*).
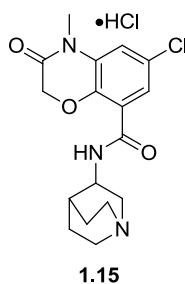
Figure 1.2 Azasetron hydrochloride, 1.15.

When considering the synthesis of APIs **1.1-1.4**, atom inefficient methodologies have often been employed.[8] In the case of Clopidogrel **1.1**, the literature suggests numerous routes towards its synthesis including the one reported in Scheme 1.3 as a representative example.
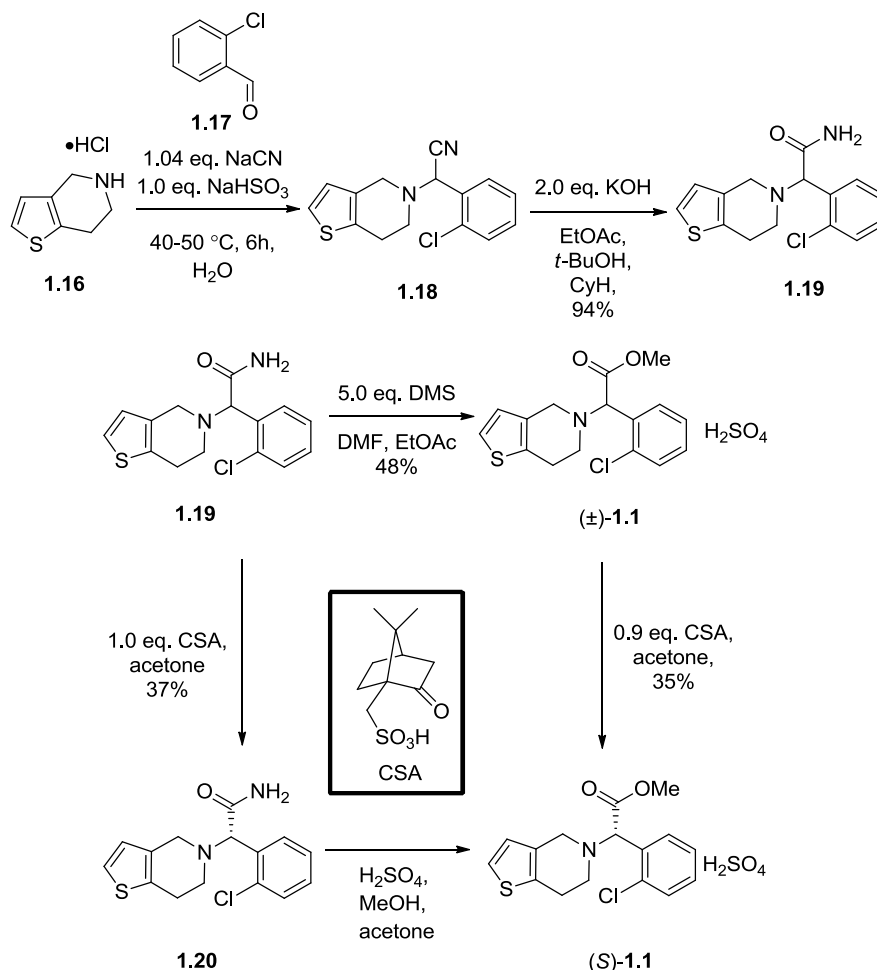
Scheme 1.3 Literature methods for the synthesis of Clopidogrel, 1.1.

This route to (+)-Clopidogrel, is wasteful as diastereomeric crystallisation, a chiral resolution, with camphor sulfonic acid, CSA, is used to remove the undesired enantiomer. The maximum theoretical yield during diastereomeric crystallisation is 50%, leading to the low yields observed; the waste associated with this process is expensive in terms of disposal and procurement of materials. Furthermore the use of DMF as a solvent is undesirable, as it is also a PGI.

1.1.2.2 *N*-Alkylation using reductive aminations

Further to using alkyl halides to carry out *N*-alkylations, reductive aminations can also be used, reacting an amine with a carbonyl compound and reducing the subsequent imine (Scheme 1.4).
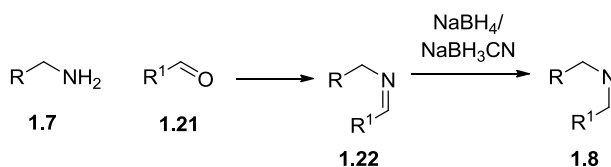
Scheme 1.4 Other methods for the functionalisation of amines: a) reductive amination.

These reactions can be used successfully, as has been shown recently by Li and co-workers at Janssen Pharmaceuticals in the multi-hundred gram synthesis of a potential type 2 diabetes therapeutic currently in phase 2 clinical trials.[9] As part of their synthesis they used a reductive amination to form the functionalised *N*-methyl piperidine in a good yield (88%) on a 1.56 mol scale (Scheme 1.5). One drawback associated with reductive aminations is the atom inefficiency of the process. Li's reduction has greater than stoichiometric quantities of waste containing sodium, boron as well as unreacted reductant, all of which must be disposed of safely post reaction (Scheme 1.5).
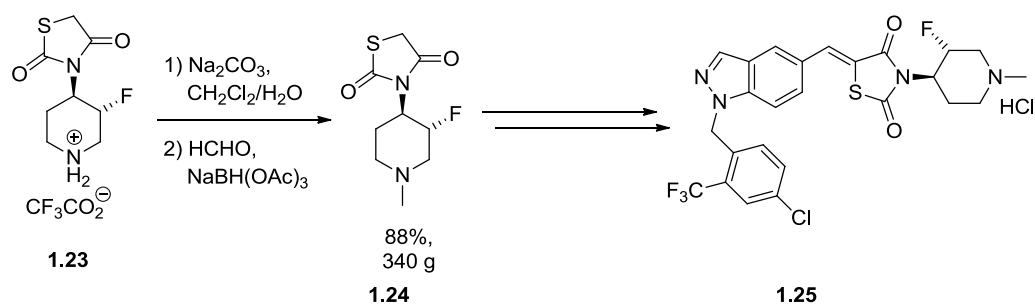
Scheme 1.5 Li and worker's synthesis of type 2 diabetes therapeutic 1.25 *via* reductive amination of functionalised piperidine 1.23 and formaldehyde.

1.1.2.3 *N*-Alklyations by the reduction of amides

As well as using haloalkanes and reductive aminations, *N*-alkylated amines can be produced *via* the reduction of amides (Scheme 1.6). The reaction involves the formation of waste streams of the reductants required and also of the carbonyls required, which are an added

cost during synthesis. The reaction also requires anhydrous conditions (due to the reductants generally employed, typically lithium aluminium hydrides) and these conditions can be costly to achieve.
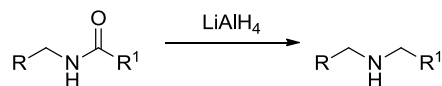
Scheme 1.6 Amide reduction for the formation of a secondary amine.

A review by Magano and Dunetz has discussed several examples of process scale reductions and the need for safety and economy during these processes.[10] The review discussed the use of DIBAL in Shieh and Prasad's formation of a bicyclic fused piperidine functionalised pyrrole ring system, **1.27** during the synthesis of bicyclic amine, **1.28**, an important structural motif implicated in cancer therapy (Scheme 1.7).[11] The reaction being carried out at cryogenic temperatures, will have an associated risk, as will the added fire hazard due to using a pyrophoric reagent, however the reaction was carried out on a 3 L scale.
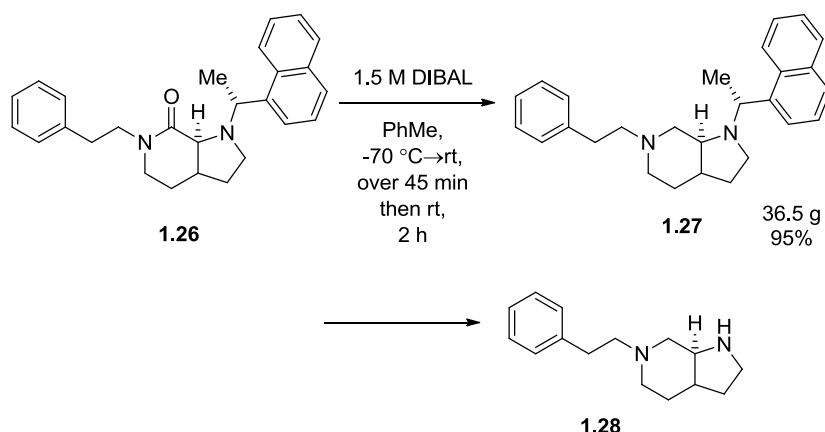
Scheme 1.7 Shieh and Prasad's use of DIBAL in the formation of intermediate 1.27 in the synthesis of the potential cancer therapeutic 1.28.

Magano and Dunetz's review also highlighted work carried out at Glaxo-Smith Kline on a multi-hundred gram synthesis of compound **1.29**. In this instance the use of borane as a reductant led to milder reaction conditions at room temperature (Scheme 1.8).[12]
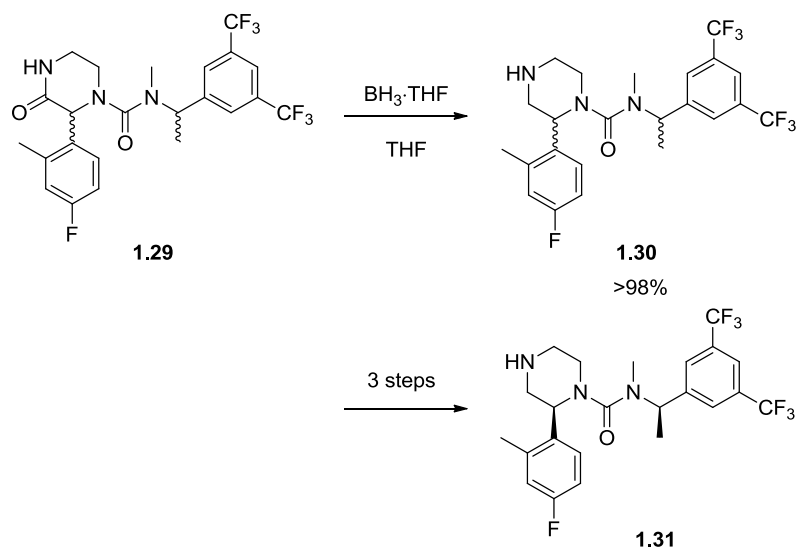
Scheme 1.8 Glaxo-Smith Kline's synthesis of GW597599 (1.31) *via* reduction of intermediate compound 1.29 by borane.

1.1.2.4 The regulation of PGIs and toxic by-products in pharmaceuticals

The control of certain chemicals that are used in API synthesis is important due to the risk of averse affects if they remain after final purification. Certain chemicals, for example halo-alkanes, will readily alkylate DNA causing its mutation, leading to possible disease manifestation. Regulatory authorities seek to control the concentration of these species within the API from the clinical trial stage and maintain them below certain thresholds of toxicological concern, TTCs, depending on their exposure limits. Table 1.1 outlines the general TTCs for genotoxic impurities in medicines.[13]

Table 1.1 ICH guidelines for acceptable genotoxic and carcinogenic concentration in APIs.

Duration of Treatment	≤ 1 month	>1 month- 12 months	>1 year-10 years	>10 years
Genotoxic and carcinogenic impurity threshold (μg/day)	120	20	10	1.5

The levels of PGI impurities must be certified before a product is allowed onto the market by national/international regulatory bodies, which adds further cost to pharmaceutical development. There is currently an industrially driven impetus in academic research for the development of methodologies that are alternatives to the use of alkylhalides, reductive aminations and amide reductions that can functionalize amines in a more efficient way, reducing the amount of testing required; these methods will be discussed in the following sections.

1.1.3 Stoichiometric methods for C−H bond activation of amines for amino functionalization

Attempts have been made in the literature to overcome the problems associated with multi-step functionalization of amines. Many of the methods suffer from the need for stoichiometric quantities of toxic oxidants. For example, Barton and co-workers developed a modification of the Strecker reaction, which is an effective method for synthesising protected imines and amino acids directly from amines.[14] The group were able to demonstrate that phenylselenic anhydride or the acid derivative in mild conditions could be used to oxidise **1.30**, to an imine *via* transfer dehydrogenation. Subsequent reaction of the imine *in situ* with sodium cyanide or its safer derivative trimethylsilyl cyanide, TMSCN, (forming cyanide *in situ*) would produce *α*-cyanopyrrolidine, **1.31**, (Scheme 1.9) in excellent yield. The reaction proved to be applicable to various cyclic secondary amines; where the use of TMSCN was also shown to be more efficient with yields ranging from 49-95%.
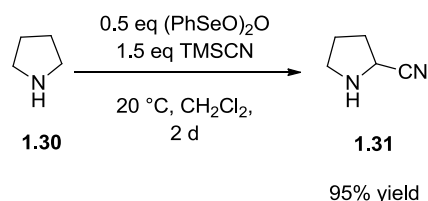
Scheme 1.9 Phenylselenic anhydride activation of pyrrolidine 1.30 to a Strecker reaction with TMSCN to form α-cyanopyrrolidine 1.31.

Barton and co-workers were unable to completely determine the mechanism and the role of the oxidant during the dehydrogenation of pyrroles using phenylselenic anhydride, which may not have been the only oxidant. The reaction required expanding to incorporate primary or tertiary amines as well as shorter reaction times to increase its value as a synthetic tool.[14]

Similarly, Uskokovic and co-workers' synthesis of the heteroyohimbine alkaloids[15] used stoichiometric quantities of 1:1 mercuric acetate−EDTA to synthesise racemic ajmalicine, **1.33**, from functionalised tryptamine amine **1.32**, *via* iminium ion formation (Scheme 1.10).

1) 1:1 Hg(OAc)₂:EDTA
2.5 % AcOH,
40 °C

2) NaBH₄,
MeOH

1.32

1.33

28% yield
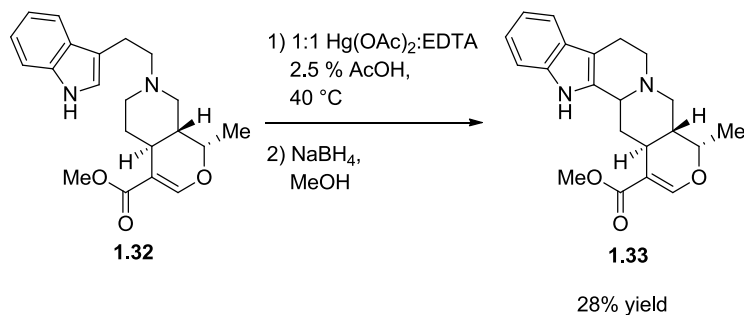
Scheme 1.10 Uskokovic and co-workers C−H activation of amine 1.32 during the synthesis of racemic heteroyohimbine alkaloid, ajmalicine, 1.33.[15]

A low yield was observed in this reaction, presumably due to the reaction having to proceed through the strained 5-membered spiro-cyclic intermediate, **1.34** and facile over-oxidation of the product to iminium by-product **1.35** requiring a reductive work-up (Figure 1.3). The expense and toxicity associated with this oxidant, coupled with the poor yield and formation of the over-oxidation product, preclude this method's use on an industrial scale.

1.34

1.35
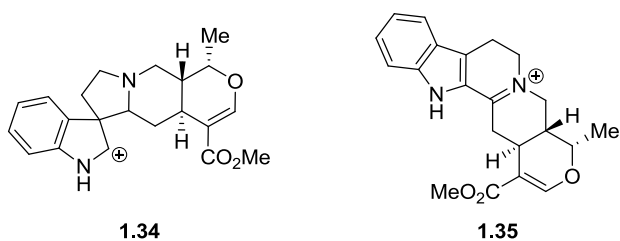
Figure 1.3 Spiro-cyclic intermediate 1.34 and over-oxidation product 1.35 formed during heteroyohmibine alkaloid synthesis.

Murahashi and co-workers have developed a method for the cyclisation of tertiary amine **1.36** and amides that proceeds *via* a ruthenium catalysed dehydrogenation to the corresponding iminium ion intermediate.[16] Whilst the method has a moderate to high yield, it employs *tert*-butylhydroperoxide as a stoichiometric oxidant, which has undesirable toxic and suspected genotoxic properties (Scheme 1.11).
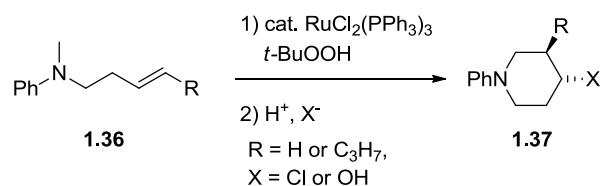
Scheme 1.11 Murahashi and co-worker's oxidation of tertiary amines with alkyl hydroperoxides.[16]

Li[17] has also developed a dehydrogenation reaction with amine **1.38** using *tert*-butyl peroxide as a stoichiometric oxidant and copper as a catalyst, where the imines formed were trapped *in situ* with malonate to afford functionalised amine **1.39** (Scheme 1.12). Whilst this group had developed one pot reactions which proceeded from the amine to the α-substituted or cyclisation product directly, the stoichiometric quantities of toxic and sometimes hazardous oxidant required was not desirable.
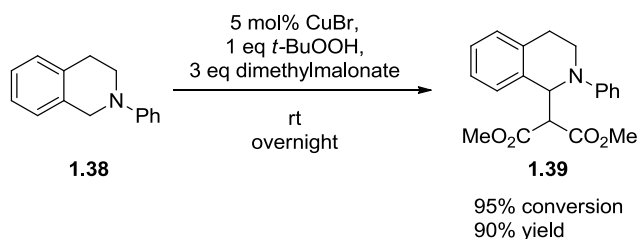
Scheme 1.12 Li's copper catalysed oxidation of *N*-phenyl-tetrahydroisoquinoline, 1.38, with *in situ* trapping by dimethylmalonate.

The majority of the stoichiometric methods that have been developed for the dehydrogenation of amines are not suitable for industrial scale-up. The oxidants employed *tert*-butyl hydrogen peroxide, phenylselenic anhydride and mercuric acetate: EDTA, are all potentially hazardous to use. Furthermore, when these oxidants are used in stoichiometric quantities they are expensive and, with the drive toward sustainable processes, are wasteful. The development of catalytic dehydrogenation methodologies that do not require expensive or highly hazardous oxidants has become a point of increasing interest within both academia and industry.

1.2 Hydrogenations, Transfer-Hydrogenations and Hydrogen-Borrowing

Transfer-hydrogenation and hydrogen-borrowing methodologies are a logical development from metal-catalysed hydrogenations in organic chemistry (Scheme 1.13 a, b and c, respectively). Hydrogenation reactions have a wide scope within the realm of organic chemistry. There are three main branches of hydrogenation reactions: biological, heterogeneous and homogeneous reactions.[18] There are a number of recent reviews that highlight current work in the field of heterogeneous catalytic hydrogenation, with a current focus being on the immobilisation of homogeneous catalysts.[19-21] Within these three branches, homogeneous catalytic hydrogenation is the most relevant to this work. The field of homogeneous hydrogenation is continually growing and expanding and new methods are constantly being developed by chemists. This section will give a brief outline of homogeneous hydrogenations providing examples of historical and more recent work in the field.
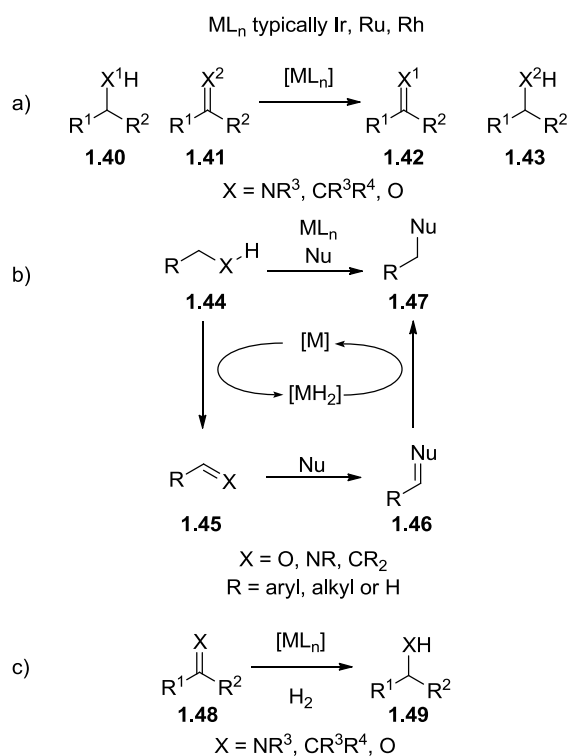
Scheme 1.13 Generic schemes for a) transfer hydrogenation; b) hydrogen-borrowing and c) hydrogenation reactions.

1.2.1 The reduction of imines by homogeneous hydrogenation catalysts

One of the first homogeneous hydrogenation catalysts developed was the *tris*-triphenylphosphinylrhodium(I) chloride complex, known as Wilkinson's catalyst, **1.50** (Figure 1.4), developed by the Nobel Laureate Sir Geoffrey Wilkinson and co-workers.[22]

1.50   **1.51**
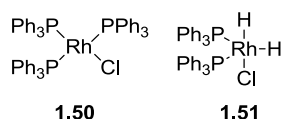
Figure 1.4 Wilkinson's catalyst 1.50 and with coordinated dihydrogen 1.51.

In the catalytic process, the catalyst loses a triphenylphosphine ligand and reacts with hydrogen gas to form the active catalyst, rhodium(III) complex **1.51** (Figure 1.4), which then goes onto hydrogenate unsaturated olefinic bonds.[5] Noyori and co-workers demonstrated that modification of complex **1.51** with the chiral, bidentate, C_2 symmetric 2,2'-Bis(diphenylphosphino)-1,1'-binaphthyl (BINAP) ligand, **1.52**, could lead to enantioselective hydrogenations. High enantiomeric excesses, *ee*, for the hydrogenation of α-(acylamino) acrylic acids were possible (79->99% *ee*) in high yields (93-99%).[23] BINAP is atropisomeric due to the steric interactions of hydrogens and biphenylphosphines on the napthyl rings (Figure 1.5),[4] this fact ensures that there is restricted rotation about the aryl−aryl axis, leading to the ligand being chiral.[24] The axial chirality of the BINAP ligand influences the spatial environment around the metal centre and its coordination sites, which lead to the stereoselectivity of the reaction.[25] A recent review of the use of chiral phosphorus ligands in enantioselective synthesis by Tang and Zhang provides a comprehensive review of chiral phosphorus ligands in synthesis, as well as their use in asymmetric imine hydrogenations.[26]

1.52   (*R*)-**1.52**   (*S*)-**1.52**
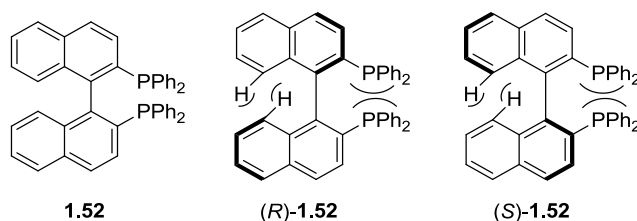
Figure 1.5 Steric interaction in BINAP, 1.52, that induce atropisomerism in the compound.[4]

A different system for the homogeneous asymmetric hydrogenation of enamides was developed by Kagan and Dang. Using the (*R, R*)- 1,4-*bis*-diphenylphosphinobutane [(*R, R*)-DIOP] ligand, (*R, R*)-**1.54**, they were able to form chiral (*R*)-*N*-acetylphenylalanine, 1.**55**, from the corresponding α-acetamidocinnamic acid, **1.53**, in 95% yield with an *ee* of 72% (Scheme 1.14). This early example paved the way for the incorporation of further imines into homogeneous asymmetric hydrogenation.[27]

(R,R)-**1.54**

1.53 → **1.55**

0.2 mol% (Rh(*R,R*)-**1.54**)ClSol)

20 °C

95% yield,
72% *ee*
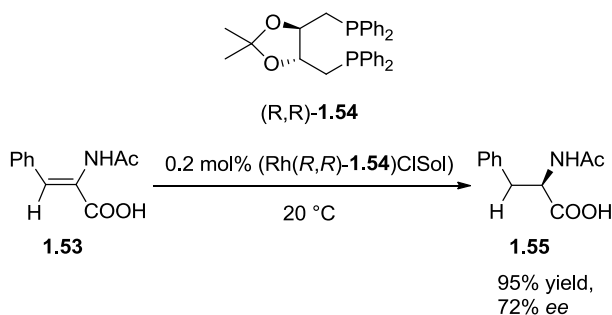
Scheme 1.14 Kagan and Dang's rhodium catalysed asymmetric hydrogenation of α-acetamidocinnamic acid 1.53, using chiral (*R*,*R*)-DIOP, (*R*,*R*)-1.54.

The incorporation of enamides into hydrogenation reactions paved the way for imines to be used. In the field of homogeneous imine hydrogenation Spindler and Blaser have noted the preferred use of only a few noble metals, namely iridium, rhodium and ruthenium as well as group IV titanium species as catalysts.[28] Further work by these authors has noted that diphosphinoiridium complexes used as catalysts give low activities, even at hydrogen pressures greater than 70 bar.[29] These processes are therefore inefficient and uneconomic with low catalyst activity requiring high loadings of expensive precious metal catalysts. High pressures of hydrogen are required that necessitate the use of specialised robust equipment and extra safety measures that are costly to implement and maintain. These low activities must be improved upon to reduce the economic expenditure of process scale synthesis.

One of the first industrially important uses of imine hydrogenation was discovered by Blaser and co-workers for the synthesis of the active stereoisomers, (α*R*,1'*S*)-**1.56** and (α*S*,1'*S*)-**1.56**, of the herbicide (*S*)-Metolachlor (Figure 1.6).[30, 31]
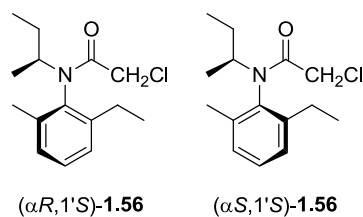
Figure 1.6 Active stereoisomers, (α*R*,1'*S*)-1.56 and (α*S*,1'*S*)-1.56, of (*S*)-Metolachlor.

(*S*)-Metolachlor was released into the market in the USA as the 90% (1'*S*)-diastereomer in 1997, but was sold previously as the racemate (from 1976). The key step in the synthesis of (*S*)-Metolachlor was the hydrogenation of imine intermediate **1.57** to amine **1.59** (Scheme 1.15), here the use of the xyliphos ligand, **1.58**, led to a good *ee* of 80%. The turnover number, TON, and initial turnover frequency, TOF, however, were high at 10^6 and $>1.8 \times 10^6$ per hour, respectively.[32] The synthesis also requires high hydrogen pressures of 80 bar, which are potentially hazardous, however the large TON and TOF coupled with the good *ee* has led to the synthesis being carried out on a $>10^5$ tonnes per year scale, thus exemplifying the industrial relevance of the process.
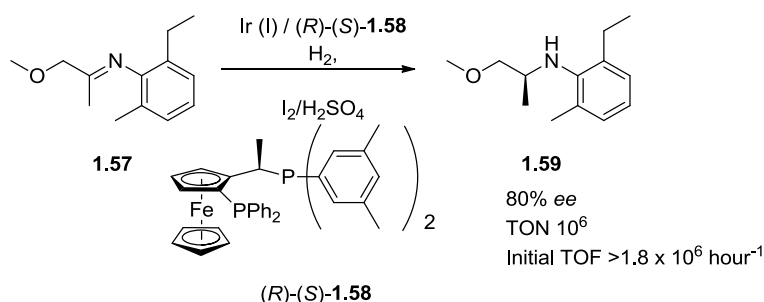
Scheme 1.15 The key step in the asymmetric synthesis of (*S*)-Metalochlor, 1.56, the hydrogenation of imine 1.57 to amine 1.59 by iridium catalyst 1.58.

Han and co-workers reported a bi-dentate chelate, spiro compound with phosphine and pyridine coordinating sites that can be used in the reduction of *N*-phenyl-acetophenone imine, **1.60**. The method used a chiral iridium catalyst (*S*)-**1.61** to reduce imine **1.60** with hydrogen, 50 atm, in dimethyether for 24 hours at rt to its amine analogue, (*S*)-**1.62** (Scheme 1.16).[33] The method was encouraging as the iridium catalyst gave the product in almost quantitative yield; however the *ee* of 58% was modest. The synthesis of the spiro ligand involved 6 steps with overall yield being 42%. The low yield made the catalyst expensive to produce and was compounded by a high catalyst loading of 1 mol%.[33]
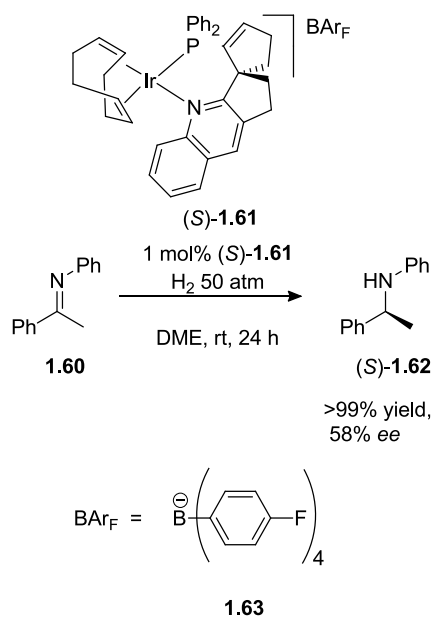
Scheme 1.16 Han and co-workers' hydrogenation of *N*-phenyl acetophenone imine, 1.60.[33]

Baeza and Pfaltz attempted to modify the iridium centre in a similar fashion to Han and co-workers using phosphorus or nitrogen bidentate ligands. Their research aimed to improve selectivity of imine hydrogenation using Ir-PHOX complexes, **1.64-1.66** (Scheme 1.17), with the BAr$_F$, **1.63**, counterion that proved critical in giving high activity.
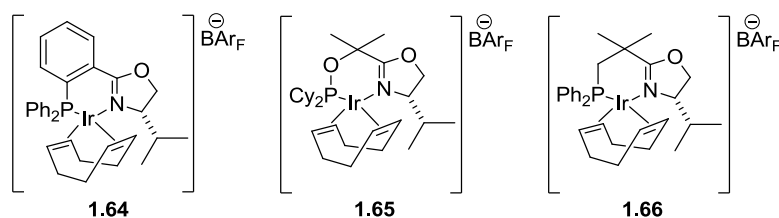
Scheme 1.17 Ir-PHOX complexes 1.64-1.66, used by Baeza and Pfaltz to induce asymmetry during imine dehydrogenation.

The authors altered the alkyl to aryl substituents of the phosphine ligand, as they believed this would increase the selectivity by changing the electronic properties of the iridium when changing from a more σ-donating ligand to a more π-accepting ligand.[34] The researchers found that catalysts **1.64-1.66** (Scheme 1.17) successfully converted a number of different aryl substituted imines to amines with generally high conversions (85-99%) and modest to good *ee* of (74-96%) at moderate hydrogen pressures (Scheme 1.18). The system accepted a

variety of *N*-alkyl-aryl substituted secondary imines, **1.66**, with little effect from the substituents on the conversion or *ee*. A poor conversion of 20% was observed for benzyl-substituted imine, **1.69**, with catalyst **1.64**; and 56% for *N*-(4-methoxyphenyl) substituted imine, **1.70**, with catalyst **1.65** (Figure 1.7).
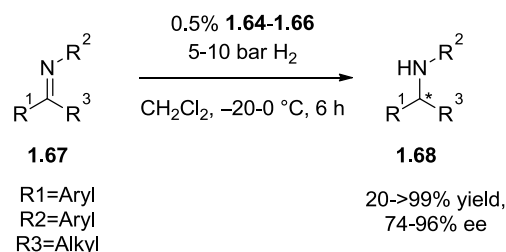
Scheme 1.18 Baeza and Pfaltz's Ir-PHOX complex catalysed imine hydrogenation.
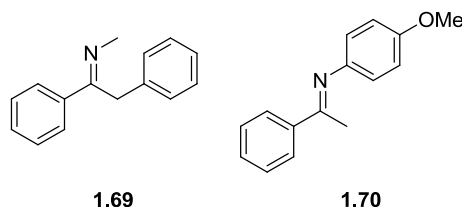
Figure 1.7 Imines 1.69 and 1.70 which had poor conversions of 20% and 56%, respectively, during hydrogenation.

1.2.2 Transfer hydrogenation of imines

The development of transfer hydrogenation or hydrogen transfer reactions was a logical development from the methodologies described previously (Scheme 1.19). In this reaction, instead of hydrogen gas being used as the reductant an organic molecule is oxidised, which then reduces the desired substrate.[35] The use of organic molecules as the reductant negates the need to deal with hazardous hydrogen atmospheres, *i.e.* flammable *etc.*, as in the previous examples.[11-26] A number of reviews have been published which highlight the work in this area. A review of the early work in this field by Brieger and Nestrick gives an insight into the early heterogeneous and homogeneous catalyst systems,[35] whilst Zassinovich and co-workers provide a thorough analysis of work with asymmetric rare-earth metal homogeneous catalysts until 1992. Their review gave examples of the most commonly used organic molecules as reductants.[36] Williams and co-workers have provided two excellent reviews giving an insight into C–N, C–O and C–C bond forming reactions possible *via* hydrogen transfer reactions of alcohols.[37, 38] Crabtree[39] and Guillena, Ramón and Yus[40] and

others[40-45] have reviewed recent work on hydrogen transfer reactions and Crabtree's review placed particular emphasis on its role industrially *via* dehydrogenation for substrate activation. In the following section early examples of hydrogen transfer reactions, as well as reactions that utilise the methodology shall be discussed.
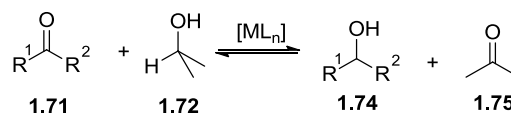
Scheme 1.19 A generic transfer hydrogenation reaction.[46]

1.2.2.1 The Meerwein–Ponndorf–Verley reaction, metal centred hydrogen transfer

The Meerwein–Ponndorf–Verley reaction was an important early use of transfer hydrogenation. Huskens and co-workers have written a comprehensive review on the Meerwein–Ponndorf–Verley reaction.[47] The reaction involves the reduction of carbonyl **1.76** to alcohol **1.77** by the alkoxy-aluminium intermediate, **1.78**, generated *in situ via* coordination of isopropanol, **1.77**, to aluminium(III), with concomitant oxidation of alcohol **1.77** to acetone, **1.81** (Scheme 1.20).[48-50] The reaction is often stoichiometric in aluminium, as the aluminium forms a tight complex with the aldehyde or ketone formed, **1.81**, which deactivates the catalyst and also due to slow ligand exchange. Since this early reaction, catalytic metal mediated transfer hydrogenations have been developed; these methodologies will be discussed during the rest of this section.
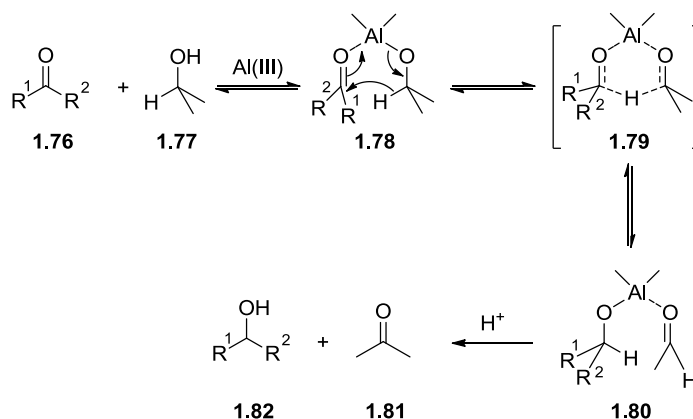
Scheme 1.20 Meerwein–Ponndorf–Verley transfer hydrogenation of carbonyls using
***in situ* generated aluminium alkoxy species, 1.79.**

Noyori and co-workers discovered a novel asymmetric transfer hydrogenation of secondary imines using ruthenium-η-aryl complexes, **1.84,** and TEAF as the reductant (Scheme 1.21).[51] The use of various chiral *N*-tosylated-1,2-diamine ligands led to asymmetric reduction of the imine in moderate to high *ee* with moderate to quantitative yields, 77-96% and 72-99%, respectively. As well as the model dihydroisoquinoline substrate **1.83** the system was tolerant of other cyclic imines as well as acyclic imines. Carbon dioxide formation led to higher yields as the reverse reaction, for the formation of formic acid and **1.83** from **1.85**, was not possible.
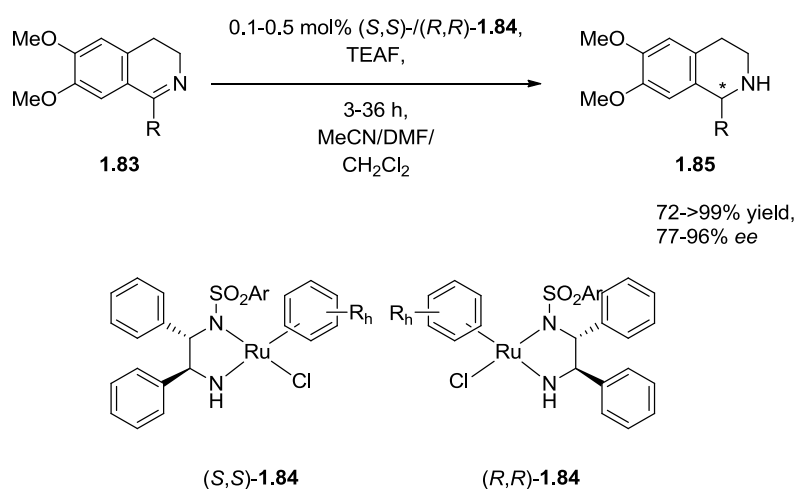
Scheme 1.21 Noyori and co-workers' ruthenium catalysed asymmetric transfer hydrogenation of secondary imines.

Bäckvall and Chowdhury demonstrated that other reductants are tolerated in transfer hydrogention, using cheap and water soluble sodium hydroxide as a co-catalyst to reduce ketone **1.86** with isopropanol, **1.77**, as the reductant (Scheme 1.22).[52] The reaction used low catalyst loadings (0.1 mol%) and achieved a maximum reported TON of 890 turnovers and TOF of up to 900 turnovers per hour, at significantly lower temperatures than previously reported. Using *tris*-(triphenylphosphinyl)-*bis*-chloro-ruthenium(II), they were able to convert cyclic or aromatic ketones to the corresponding alcohols, **1.87**, in 39-89% yield. The ability to boil off the acetone, **1.81**, that was formed, made the reaction desirable compared to using a hydrogen atmosphere; however the protocol required expansion to incorporate further ketones.
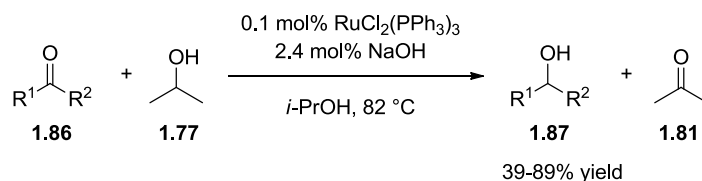
Scheme 1.22 Bäckvall and Chowdhury's protocol for the ruthenium catalysed hydrogenation of ketones.

The same authors have also disclosed mechanistic aspects of the hydrogenation of imines, showing experimentally that the hydrogen transfer occurs after the imine binds to ruthenium.[53] The authors examined the hydrogenation of a model imine compound (**1.89**) with Shvo's catalyst (**1.91**) and either H_2 or D_2 as a reductant. NMR analysis of the hydrogen transfers at both room and low temperatures established that the nitrogen of the imine must bind directly to the ruthenium centre, with the hydroxyl group being involved in hydrogen transfer to form the amine. An inner sphere mechanism for the reduction was established and the authors were able to discern the effect of deuterium on the rate of reaction and showed that the rate determining step was the cleavage of the C-H bond, alpha to the nitrogen. The authors also showed that the transfer of hydrogen from the amine to the complex was not a concerted process and that, unlike aldehydes, hydrogen transfer is not rate limiting.
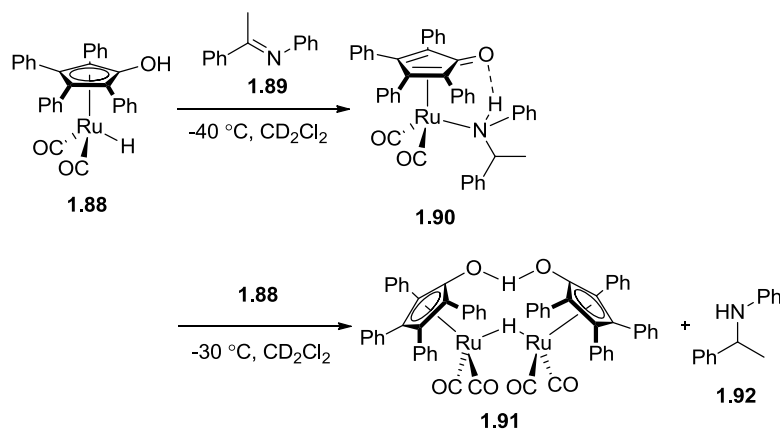
Scheme 1.23 Mechanistic study of hydrogen transfer carried out by Backvall and Chowdury, showing that the reaction occurs *via* an inner-sphere mechanism.

Blacker and Mellor have also developed an asymmetric route for the hydrogenation of imines to their amine analogues using potassium hydroxide-isopropanol as the reductant (Scheme 1.24).[54] In this instance rhodium, rather than ruthenium was used, the authors

found that by using (*1S,2R*)-2-amino-1,2-diphenylethanol as an asymmetric ligand they could induce the rhodium complex to carry out asymmetric reduction of imine **1.93,** *via* formation of complex **1.94**.
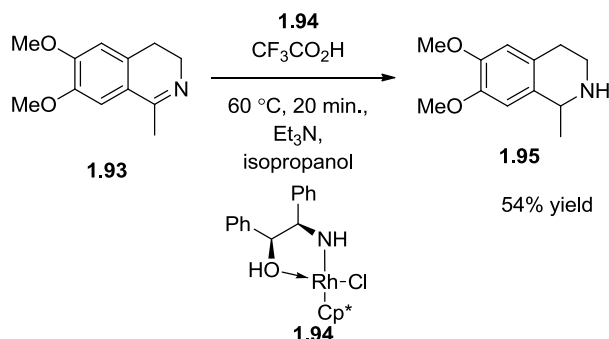
Scheme 1.24 Blacker and Mellor's asymmetric transfer hydrogenation of imines.

Baker and Mao have developed an asymmetric protocol for the rhodium-catalysed transfer hydrogenation of imine **1.96** using TEAF as a reductant at room temperature (Scheme 1.25).[55] Similarly to Noyori and co-workers, they employed the 1, 2-diamine ligand, (*S,S*)-*N-para*-toluenesulfonyl-1,2-diphenylethylenediamine [(*S,S*)-TsDPEN, (*S,S*)-**1.97**), and its enantiomer, (*R,R*)-TsDPEN, to convert imine **1.96** in high yields (85-96%) to the corresponding amine, **1.98**, with generally moderate to excellent *ee* (67-99%). The reaction did not achieve good selectivity for the phenyl- and 3,4-dimethoxyphenyl- substituted dihydroisoquinolines, **1.99** and **1.100** (4.4% and 3.2%, respectively) or for the *N*-benzyl-substituted imines, **1.101** and **1.102** (both 8.4%). This poor selectivity can be rationalised due to acidic, benzylic proton of the desired product allowing for rapid reformation of the imine (and possible non-selective dehydrogenation). The reaction used low catalyst loadings of 0.5-0.1 mol% and would be completed in 10-180 min. Whilst the lower loading reduced reactivity and enantioselectivity, the conversions were still high, 94% at 0.1 mol% and 96% at 0.5 mol%, as were *ee*, 93% compared to 99% for imine **1.103** (Figure 1.8).
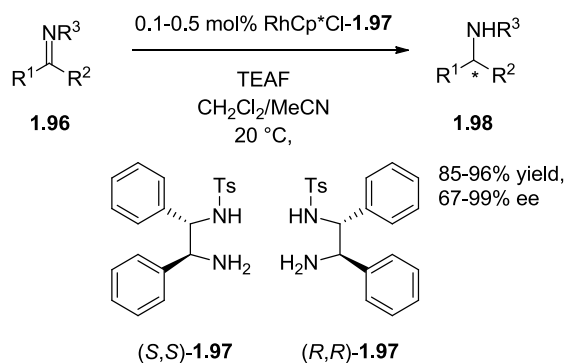
Scheme 1.25 Baker and Mao's rhodium catalysed asymmetric reduction of imine 1.96 using chiral TsDPEN ligand, 1.97.
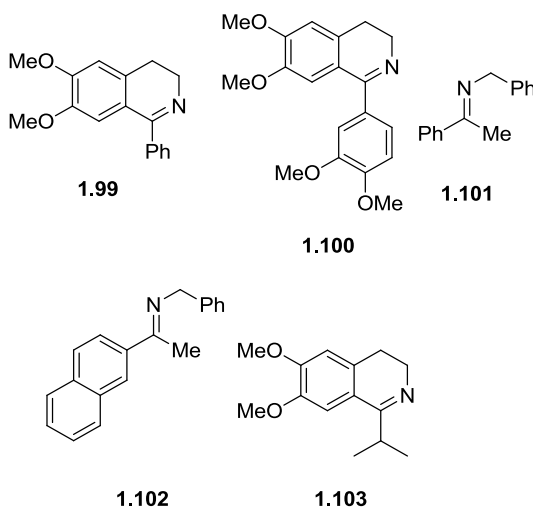
Figure 1.8 Imines 1.99-1.102 that achieved poor selectivity during asymmetric hydrogenation and imine 1.103 which achieved excellent yield and *ee* at 0.1 or 0.5 mol% catalyst loading.

1.2.3 Enzymatic hydrogen transfer reactions

Before examining the utility of chemo-catalytic hydrogen transfer reactions, a brief aside will describe the academic community's development of a variety of enzymatic tools to carry out hydrogen transfer reactions. Numerous biologically based, enzymatic systems, have been detailed and reviewed comprehensively by Turner[56] and further by Fleury[57] for the activation of amines and alcohols. Of particular note was work carried out using monoamine oxidases (MAO) that have been used for amine activation, which included work by Singer and co-workers that described the *Aspergillus niger* derived MAO (MAO-N) oxidation of amines (Scheme 1.26).[58] The work was important from both a chemical and

21

biological standpoint as the precursors to mammalian MAO used to oxidise specific amines gave an insight into the chemical origins of life.
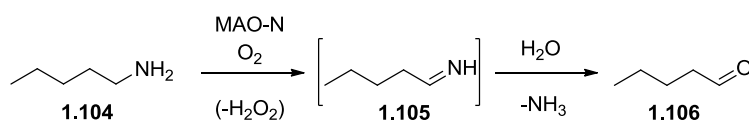
Scheme 1.26 Oxidation of amine 1.104 to imine 1.105 via enzymatic catalysis with monoamine oxidase derived *Aspergillus niger* (MAO-N) with molecular oxygen as an oxidant.
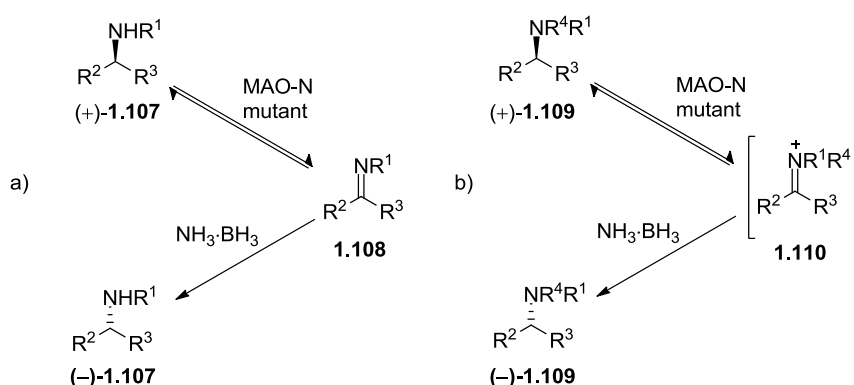
Scheme 1.27 Deracemisation of a) primary and secondary amines, 1.107, and b) tertiary amines, 1.109, via chemo-enzymatic methods using MAO-N mutants, *via* imine 1.108 and iminium ion 1.110 formation, respectively.

Work by Turner has shown that *via* a combination of chemical and enzymatic methods primary and secondary, **1.107**, and tertiary amines, **1.109**, can all be deracemised using different mutants of wild-type MAO-N, and a chemical reductive method (Scheme 1.27a and b, respectively).[59-62] Whilst only a small sample of amines has been shown to work with this methodology, there is scope for expansion to a wider range of amines using this methodology. A similar system which further exploits the dehydrogenation to carry out other transformations, would be an ideal method to selectively functionalize amines.
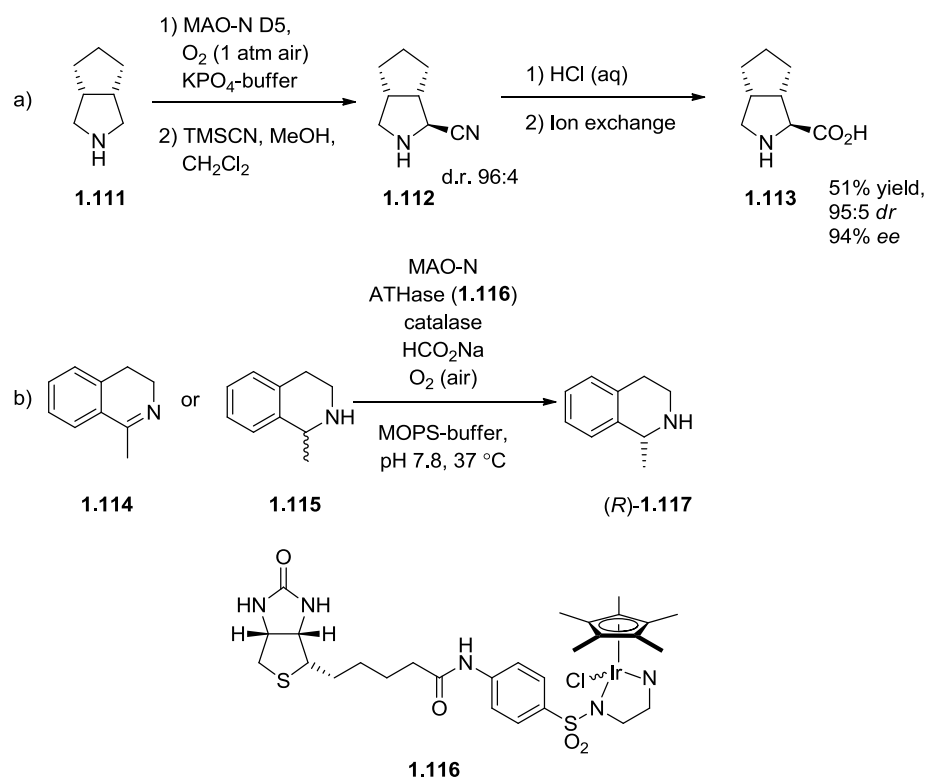
Scheme 1.28 a) Enzymatic Strecker reaction via amine dehydrogenation; b) Enzymatic Dynamic Kinetic Resolution (DKR) or 2-methyl-tetrahydroisoquinoline.

Further developments in the Turner group have shown that the MAO-N pathway can be used for the addition of other nucleophilic substrates to imines formed *in situ* (Scheme 1.28.a).[63] The Strecker reaction used to produce fused cyclopentane-α-cyanopyrrolidine, **1.112**, is less hazardous than Barton's[14] protocol (Scheme 1.9 *vide supra*) as phenylselenic anhydride is not required and the reaction is catalytic. Recently, the group has reported the use of biological-chemical cascade reactions utilising an iridium biotin catalyst, **1.116**, anchored within a streptavidin isoform to produce an ATHase and biological co-factors to carry out amine dehydrogenations (Scheme 1.28b).[64] The incorporation of iridium catalysts, used widely in hydrogen transfer reactions, within an enzyme environment, was an interesting development.

1.2.3.1 Reactions utilising chemical hydrogen transfer reactions

Grigg and co-workers demonstrated that *tetrakis*-triphenylphosphine rhodium(I) hydride complex, RhH(PPh$_3$)$_4$, was the most active catalyst in the *N*-alkylation of primary and secondary amines using methanol. The catalyst system was favourable compared to a palladium on carbon catalyst, with a higher yield (97% compared to 6%) and shorter

reaction time (4 hours compared to 46 hours) for the conversion of pyrrolidine, **1.22**, to
N-methylpyrrolidine, **1.118** (Scheme 1.29). Both systems had a catalyst loading of 5 mol%,
which would need to be reduced to be made industrially viable; however the promising
yield and quicker reaction time meant that the protocol could be of interest to industry.[65]
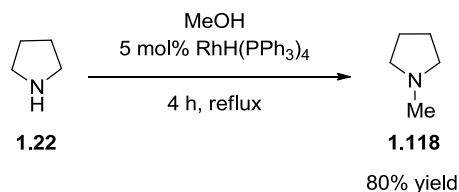
**Scheme 1.29 Grigg and co-workers' protocol for the *N*-alkylation of pyrrolidine, 1.22,
to *N*-methylpyrrolidine, 1.118.**

Homogeneous platinum group metal catalysts also improve the efficiency of the
Leuckart−Wallach reaction. The Leuckart−Wallach reaction, a reductive amination of
carbonyls using formic acid as the reductant, is not very attractive as a route for the
synthesis of primary and secondary amines from aldehydes and ketones, respectively.[66] The
uncatalysed reaction requires high temperatures (>180 °C) for the reaction to proceed and a
high number of equivalents (3 equiv. of TEAF for the reaction with benzophenone) of
reagents to achieve acceptable yields (80%, at 200 °C after 30 min.).[66] The high
temperatures and large equivalents of reagents required have led to the reaction being
avoided. Kitamura and co-workers have demonstrated that rhodium could be used as an
effective catalyst in the reaction. Cp*-*bis*-µ-chloro-rhodium(II) dimer ([RhCp*Cl$_2$]$_2$) proved
to be a good catalyst providing a selective route from acetophenone, **1.119**, to
bis-α-methylbenzylamine, **1.120**, (Scheme 1.30). The reaction can now be carried out at a
much milder temperature of 70 °C in a relatively short reaction time of two hours. The
reaction also benefits from a high yield of 98%.[67]
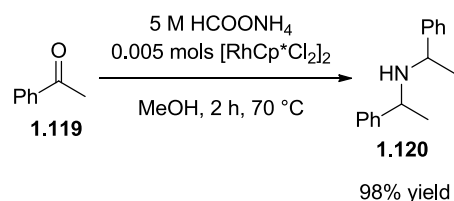
Scheme 1.30 Kitamura and co-workers catalytic Leuckart−Wallach reaction.

Further utility of transfer hydrogenation reactions has been demonstrated by Berke and co-workers, using the methodology as a form of hydrogen storage.[68] They demonstrated that at mild temperatures (20-60 °C) using ammonia−borane, **1.122** they could transfer hydrogenate imine **1.121** to amine **1.123**, *via* oxidation of ammonia−borane to the unsaturated compound **1.124** (Scheme 1.31).
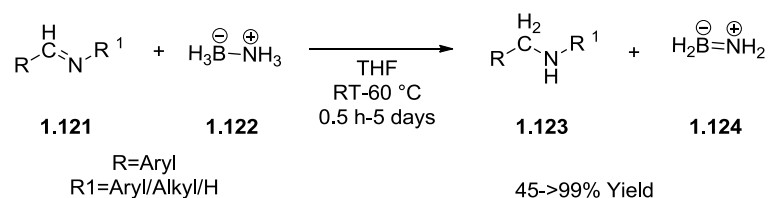
Scheme 1.31 Yang and co-workers transfer hydrogenation of imines using ammonia−borane.

The rate of the transfer hydrogenation was slower at room temperature (5 days *c.f.* 7 hours at 60 °C). Ammonia−borane decomposes at temperatures greater than 60 °C, therefore further heating to increase the rate of reaction was not possible. The reaction did have a moderately broad scope, as a large number of alkyl amines could be formed in addition to aromatic amines, however rates were slower and in the case of the extremely hindered *N*-tertiary butyl benzylamine the reaction was extremely slow. The reaction was subject to side reactions of the ammonia−borane with the production of cyclic and polymeric adducts. They surmised that ammonia−borane could thus be used during this process as a form of hydrogen storage as small amounts of hydrogen gas were released during the process.

Fujita and co-workers have asserted that oxidant-free reactions to oxidise alcohols would be an ideal protocol for the highly atom efficient synthesis of carbonyl compounds. The critical step in alcohol oxidation is the catalytic dehydrogenative oxidation of alcohol **1.126** where the dehydrogenation forms the metal−hydride intermediate **1.129** *via* β-elimination of ketone **1.128** (Scheme 1.32).[69]
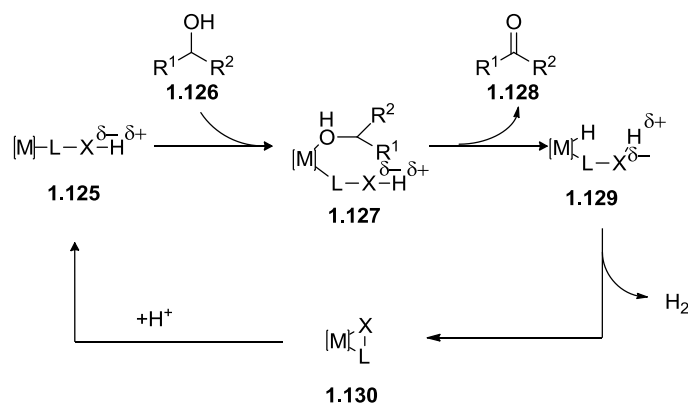
Scheme 1.32 Fujita and co-workers proposed mechanism for the dehydrogenation of alcohols by metal catalysts.

In the same paper Fujita and co-workers established a protocol for oxidant free oxidation of secondary alcohols. The authors developed a class of Cp*Ir(III) catalysts; 2-hydroxypyridine containing **1.131** and 2-pyridonate containing **1.132** were used in the dehydrogenation of secondary alcohol **1.133** to carbonyl **1.134** (Scheme 1.33). Their method allowed dehydrogenation of secondary alcohols containing various aromatic and alkyl substituents even with low catalyst loadings of 0.2 mol% in refluxing toluene (PhMe). Deactivated aromatic systems required longer reaction times and higher loadings; cyclohexanol required 1.0 mol% catalyst loading as did 1-tetralol, with an increased reaction time of 50 hours. This new reaction showed promise, with its ability to oxidise benzylic alcohols using low catalyst loadings, however an optimisation of the reaction to reduce the temperature and increasing the substrate scope, to include more alkyl substituted alcohols, was required.[69]
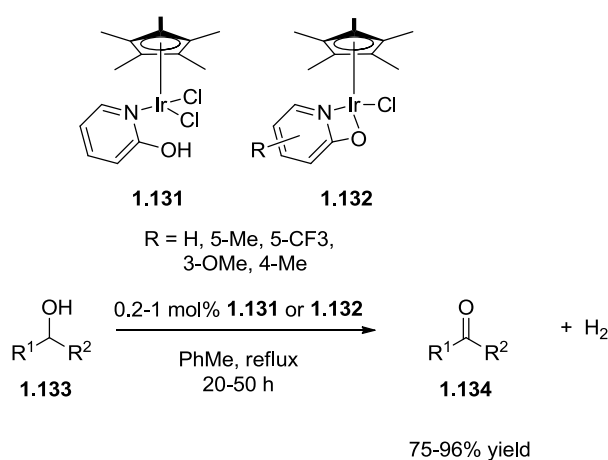
Scheme 1.33 Fujita and co-workers iridium catalysed alcohol dehydrogenation.

The hydrogen-transfer technology is not only applicable to alcohols, but also for amines. Bäckvall and co-workers have demonstrated that using a ruthenium catalyst, **1.136**, a cobalt-salen co-catalyst, **1.137**, and 2,4-dimethoxybenzoquinone (DMBQ) that they could dehydrogenate a range of secondary amines to their imine derivatives (Scheme 1.34). [70]
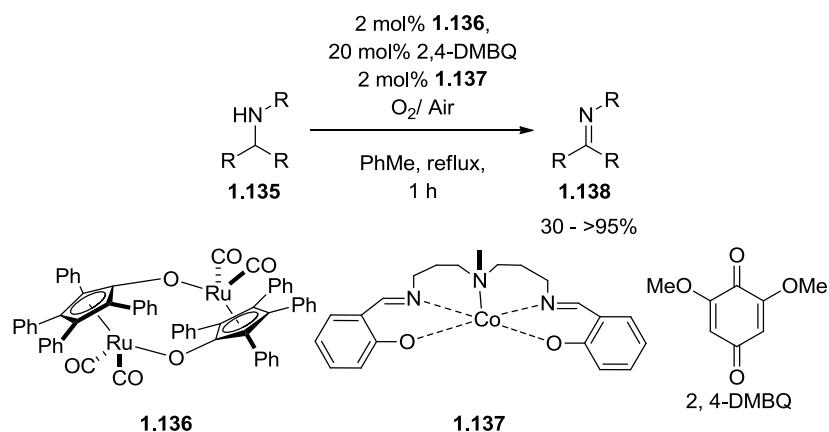
Scheme 1.34 Bäckvall's biomimetic ruthenium catalysed dehydrogenation of amines.

The biomimetic system was able to use oxygen from air, as the oxidant, to reform the catalytic species, with no observed catalyst deactivation. The reaction tolerated various *N*-aryl amines, with yields varying from 30-95%, which, coupled with a short reaction time of 1 hour, makes this an attractive protocol. The authors noted one serious drawback however, when air and toluene are mixed at 100 °C in the gas phase, explosive mixtures form and such a situation is not desirable on scale. Further investigation was required to prevent this potentially dangerous situation from occurring. The authors also carried out a Mannich reaction with the isolated product, using L-proline, propionaldehyde (**1.141**) and *N*-methyl pyrrolidine (NMP) as solvent, to form amine (**1.142**), proving the efficacy of the protocol (Scheme 1.35).[71]
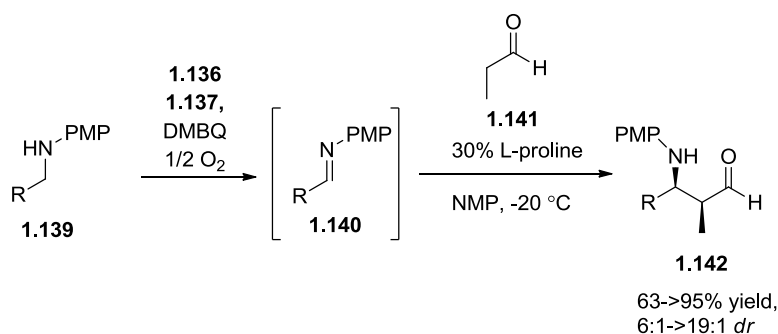
Scheme 1.35 Incorporation of hydrogen transfer to activate an amine to its imine analogue to carry out a Mannich reaction.

Fujita and co-workers established the first iridium catalysed homogenous reversible dehydrogenation–hydrogenation of nitrogen heterocycles, **1.158,** to their unsaturated analogues **1.159**, *via* hydrogen transfer from the system (Scheme 1.36a).[72]
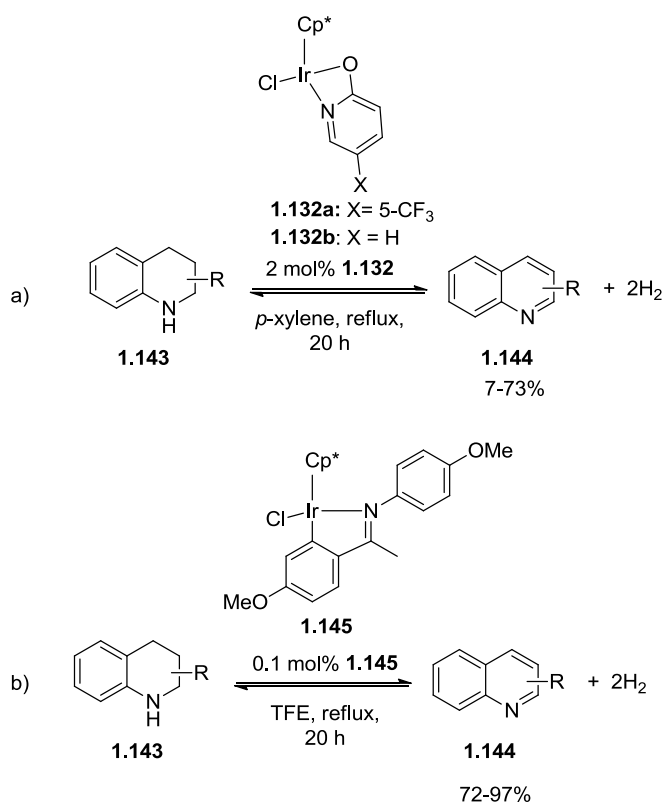
Scheme 1.36 a) Fujita and co-workers b) Xiao and co-workers iridium catalysed dehydrogenation of substituted tetrahydroquinolines.

The group found that incorporation of catalyst **1.132b**, proved incompatible with tetrahydroquinoline giving only a 7% yield. However catalyst **1.132a** was effective in the

28

reaction when the 2-pyridonate ring was substituted (73% yield). Furthermore, Fujita was able to hydrogenate 1-decene with catalyst **1.50** and the hydrogen gas evolved from the dehydrogenation in a separate reaction vessel. The reaction was tolerant of different methyl substitution patterns on the tetrahydroquinoline substrate; however the reaction required the use of refluxing *p*-xylene (138 °C), high catalyst loadings (2.0 mol%) and was applicable to a narrow substrate range. The costs associated with the catalysts in these reactions precludes their use at a process scale. Recently, work by Xiao and co-workers has further improved upon Fujita's work by use of iridium-imine complex, **1.145**, for the dehydrogenation reaction (Scheme 1.36b). Complex **1.145** could be used at far lower catalyst loadings (0.1 mol%) and at much lower temperatures to give moderate to excellent yields of the dehydrogenated product (72-97%).[73]
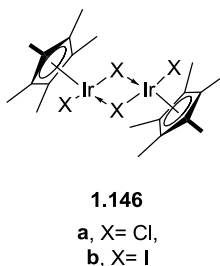
1.146
a, X= Cl,
b, X= I

Figure 1.9 Iridium chloride dimer catalyst, 1.146a, and SCRAM catalyst 1.146b, employed by Blacker and co-workers for the racemisation of chiral secondary and tertiary amines.

Blacker and co-workers have further shown the applicability of transfer hydrogenation *via* the use of pentamethylcyclopentadienyliridium(III) halide dimer ([IrCp*X$_2$]$_2$) catalysts, **1.146** (Figure 1.9).[74] Their system used the equilibrium that can be formed between two stereoisomers, due to reversible hydrogenation−dehydrogenation reactions (known as 'hydrogen−borrowing'; Scheme 1.37), to racemise a stereocentre. This racemisation, or scrambling, of the stereocentre has led to [IrCp*I$_2$]$_2$ being known as SCRAM catalyst. The original work demonstrated that a model 2-methyltetrahydroisoquinoline structure, (*S*)-**1.147**, containing a conformationally rigid secondary amine, could be racemised from the single enantiomer under mild conditions and at low catalyst loadings [40 °C, 0.2 mol% ([IrCp*I$_2$]$_2$)] (Scheme 1.37).
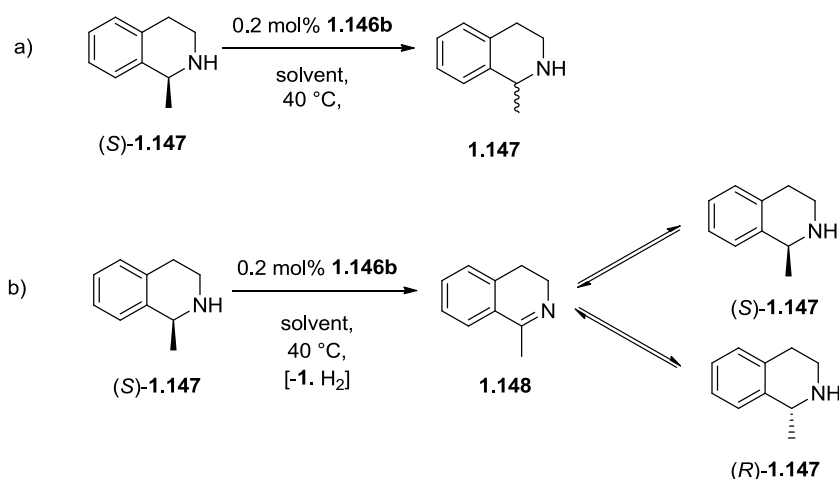
Scheme 1.37 Iridium catalysed racemisation of amine (*S*)-1.147, by reversible dehydrogenation-hydrogenation that leads to racemisation of the stereocentre.

Further work by the group proved the system was tolerant of numerous secondary and even tertiary amines; however primary amine racemisation proved elusive due to the formation of *N*-alkylation products (work has shown that this can be overcome by slow addition of substrate).[75] The group found that the use of the iodide dimer **1.146b**, originally formed *in situ*, *via* salt exchange between the chloride dimer **1.146a** and potassium iodide, was more active than the chloride analogue. The ability of the catalyst to racemise tertiary amines was impressive as it involved the formation of the kinetically high energy, cationic nitrogen of an iminium species, **1.149**, during dehydrogenation (Figure 1.10). The iminium ion species formed at a slower rate than secondary imines, however the iminium species was also reduced at a faster rate. Rates were faster for the cyclic tetrahydroisoquinoline structure **1.147**, where reduced temperatures and low catalyst loadings were tolerated (40-80 °C, 0.2-0.5 mol%), than for acyclic structures (80-90 °C, 0.1-1.0 mol%). The reaction could then be used in a dynamic kinetic resolution with a chiral enzyme to discriminate the required stereoisomer and selectively form one stereoisomeric product.[76]
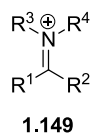
1.149

Figure 1.10 The reversible formation of iminium ion species, 1.149, formed during the dehydrogenation of tertiary amines by Blacker and co-workers.

Blacker and co-workers' method was shown to be efficacious during the synthesis of sertraline, (1*S*,4*S*)-**1.150**, the API in the Pfizer drug Zoloft. Using a dynamic kinetic resolution protocol (DKR), coupled with diastereomeric crystallisation with mandelic acid, that had already been established to selectively form a single stereoisomer, a reduction in waste was possible to 1 kg/kg of product (not including solvent) during the isolation of the desired enantiomer. The synthesis of the substrate is complicated due to the presence of two asymmetric centres. These centres can lead to the formation of four different diasteromers, (1*S*,4*S*)-**1.150**; (1*S*,4*R*)-**1.150**; (1*R*,4*S*)- **1.150** and (1*R*,4*R*)- **1.150** (Figure 1.11).[77]

(1*S*,4*S*)-**1.150**   (1*S*,4*R*)-**1.150**   (1*R*,4*S*)-**1.150**   (1*S*,4*S*)-**1.150**
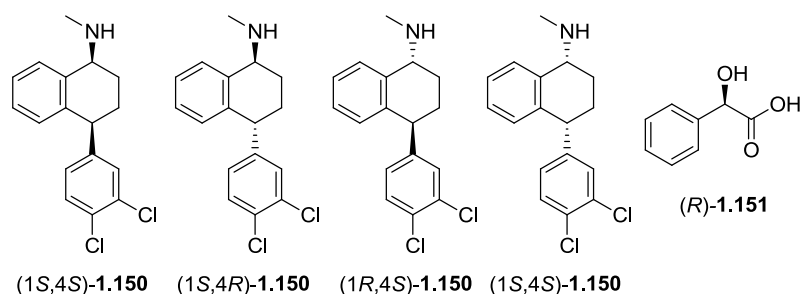
Figure 1.11 The 4 diastereomers of sertraline, 1.150, the active stereoisomer is (1S,4S)-1.150 and (R)-mandelic acid, (R)-1.151, used during crystallisation induced diastereomeric transformation (CIDT).

Williams and co-workers[78] have demonstrated several uses for the SCRAM (**1.146b**) catalyst including alkylation of amines, **1.152**, with alcohols, in water in the absence of base to the *N*-alkylation product, **1.153**, in 60-98% (Scheme 1.38).[79] They were able to form a range of secondary amines and tertiary amines. They found no real trend between the isolated yield achieved and the electronic or steric nature of the parent amine. The formation of electron-deficient *N*-propyl 4-(trifluoromethyl)- and *N*-propyl-4-cyano-anilines was achieved with poor yields of 18 and 23%, respectively. The direct alkylation of amines in an environmentally benign solvent without the use of hazardous alkylating agents was desirable.

1 mol% **1.146b**

R^3-OH

H_2O,
115 °C, 10 h

1.152   **1.153**

18-98% yield

R^1 = Alkyl, Aryl
R^2 = Alkyl, H
R^3 = Aryl, Alkyl
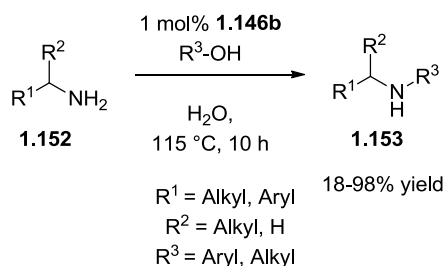
Scheme 1.38 Williams and co-worker's alkylation of amines with alcohols.

A range of complex 2,3,5-substituted pyrroles, **1.157**, have recently been synthesised by Kempe[80] using the hydrogen borrowing methodology (Scheme 1.39). The work was of particular interest as sustainable feedstocks were used and the reaction was tolerant of a diverse range of functional groups on the different R-groups. The ability to produce highly functionalised pyrroles, which are used in a variety of industrial and medicinal applications, across a range of yields 37-88% (for the fused cyclododecyl-benzyl and fused cycloheptyl-ethyl analogues) at low loadings of as little as 0.03 mol% (84% yield fused cycloheptyl-*iso*-propyl analogue) has demonstrated how important this methodology can be.

Ir cat. **1.156**

KO^tBu

(-2H_2)
(-2H_2O)

1.154   **1.155**   **1.157**

37-88%

1.156
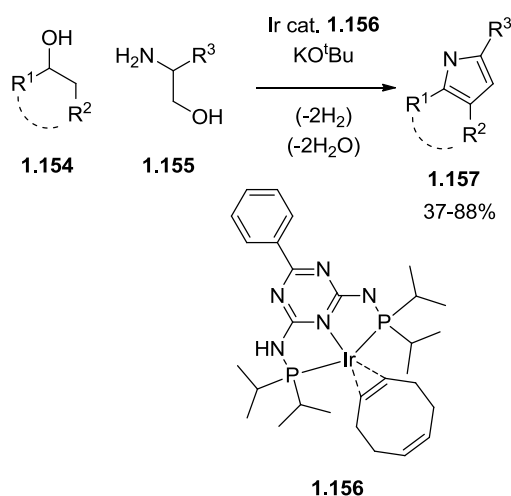
Scheme 1.39 Kempe's synthesis of 2,3,5-substituted pyrrole.

The industrial efficacy of the hydrogen-transfer methodology has been demonstrated during the multi-kilogram synthesis of an API. Chemists at Pfizer developed a synthesis of the GlyT1 inhibitor **1.161**, a potential schizophrenia therapeutic, of which the key step involved an iridium catalysed *N*-alkylation of alcohol **1.158** by amine **1.159** (Scheme 1.40). Of note was the ability to form 4.8 kg of product **1.160** with a substrate-catalyst ratio (S/C) of 2000. This ratio was a vast improvement on similar reactions of the time, where many would have

S/Cs of 50-100. The low loadings of catalyst make the procedure more financially viable and the work demonstrated that hydrogen-borrowing could be a valuable technology to the pharmaceutical industry. Similar processes that work as efficiently and on a similar scale to the Pfizer method are highly sort after by industry. In addition to these reactions, understanding what reactions are currently possible with imines is important.
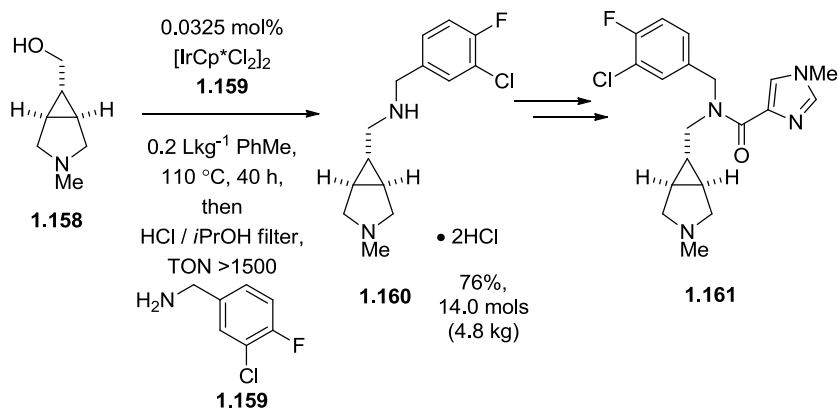
Scheme 1.40 Pfizer's synthesis of GlyT1 inhibitor, 1.161, with iridium catalysed
***N*-alkylation the key step in the synthesis.**

1.3   Nucleophilic reactions of imines

The *in situ* formation of imines *via* the hydrogen-transfer methodology outlined previously is important, as the imine formed can react subsequently with nucleophiles *in situ* at the imine carbon, which is electrophilic unlike the parent amine, allowing for a change in reactivity. The coupling of the dehydrogenation protocol with concomitant nucleophilic reactions would lead to the expeditious formation of functionalised amines, reducing waste and increasing efficiency during synthesis. Currently the main nucleophiles used in hydrogen transfer reactions are amines, with either homo or hetero dimerization popular reactions (*vide supra*), however an expansion to include more nucleophiles is required to increase the applicability of this protocol. As such, an overview of possible reactions of imines with nucleophiles is advantageous to establish which reactions could be studied with the hydrogen-transfer protocol. This subject has been extensively reviewed by Kobayashi and Ishitani, detailing enantioselective catalytic additions to imines.[81] Amongst the reactions mentioned of interest were the enantioselective Strecker reaction, enantioselective aza-Mannich reactions, enantioselective reductive aminations, enantioselective alkylation and enantioselective Diels–Alder reactions have already been carried out and some key examples will be highlighted in this section.

1.162   **1.163**
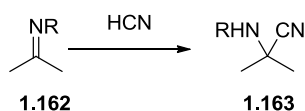
Scheme 1.41 A generic Strecker reaction involving the formation of the α-amino nitrile 1.163 *via* nucleophilic attack of cyanide on the imine 1.162.

The Strecker reaction, *vide supra*, has high potential due to the ability to functionalize the α-amino nitrile **1.163**, formed through the addition of cyanide to an imine **1.162** (Scheme 1.41).[14]

1.164

69-99% yield,
37-95% *ee*
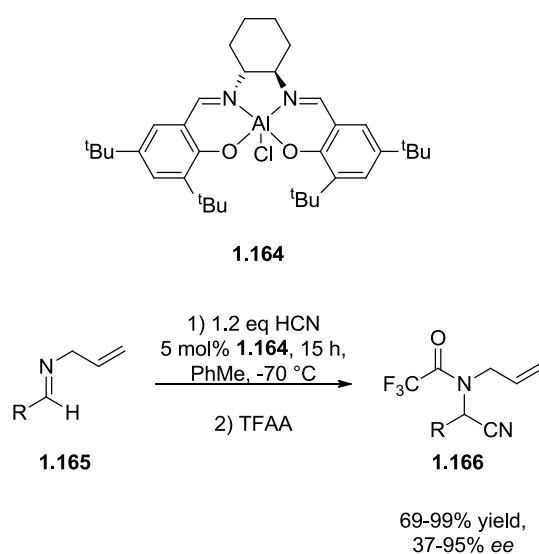
Scheme 1.42 Jacobsen and Sigman's aluminium salen catalysed asymmetric Strecker reaction.

Jacobsen and Sigman have shown that aluminium(III) salen complex, **1.164**, could be used in asymmetric Strecker reactions (Scheme 1.42).[82] This work demonstrated that α-aminonitriles, **1.166**, can be formed from a number of *N*-ally-aryl substituted imines, **1.165**, in good to excellent yields (91-99%) and moderate to excellent *ee* (79-95%). Cyclohexyl-substituted imine, **1.167**, and *tert*-butyl substituted imine, **1.168** (Figure 1.12), were converted in lower yields, 77% and 69%, respectively and with moderate and poor *ee*, 57% and 37%. The reaction required cryogenic conditions, -70 °C, high catalyst loadings, 5 mol%, and long reaction times, 15 hours, which on process scale would be costly. The high yields possible with the aryl substituents were promising, but the reaction requires optimisation to become applicable industrially.

1.167   **1.168**
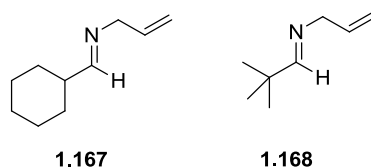
Figure 1.12 The imines 1.167 and 1.168 that were converted in lower yields (77% and 69%, respectively) to the corresponding α-amino nitrile by Jacobsen and Sigman's aluminium salen complex, 1.164.

North and co-workers expanded on Jacobsen and Sigman's system employing vanadium(V) salen complex, **1.169**, in an asymmetric Strecker reaction with *N*-benzyl imine **1.170** to *N*-benzyl substituted α-amino nitrile **1.171** (Scheme 1.43).[83] North and co-workers' system was tolerant of numerous *N*-benzylated imines. The reaction had generally modest to good yields, 46-85%, and *ee*, 31-74%. Phenyl substituted imine, **1.172**, achieved the highest conversion and *ee* of 88% and 75% respectively, however *N*-benzylpivaldehyde, **1.173**, was converted with a good overall yield, 85%, but the *ee* was poor at 16% (Figure 1.13). Similarly to Jacobsen and Sigman, the reaction required expensive cryogenic conditions; however the temperature was slightly warmer at -40 °C. The reactions reached completion within 3 hours; however the reaction did require high catalyst loadings of 10 mol%. The reaction also required optimisation to achieve better enantioselectivities at higher temperatures and lower catalyst loadings, as well as increasing reaction scope, in spite of these drawbacks the reaction has subsequently been carried out on a >100 L scale.[84]

1.169
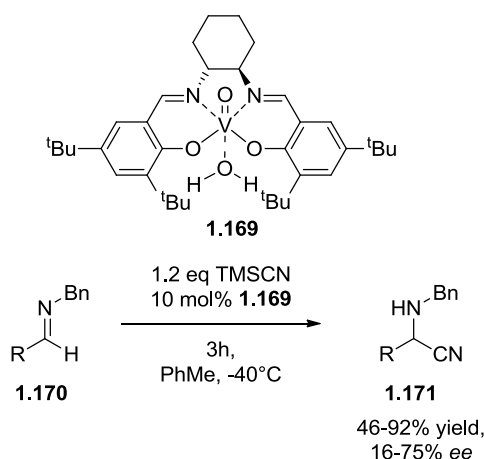
Scheme 1.43 North and co-workers' vanadium(V) salen catalysed asymmetric Strecker reaction.[83]

35

1.172   **1.173**
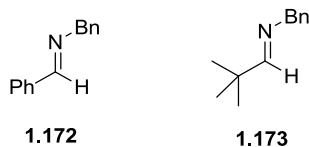
Figure 1.13 Imine 1.172 which achieved good conversion and *ee* (88 and 75%, respectively) and imine 1.173 which achieved good conversion but poor *ee* (85 and 16%, respectively), during North and co-workers asymmetric Strecker reaction.

Nitromethane can be used in nucleophilic reactions with imines during the aza-Henry (nitro-Mannich) reaction to form β-nitroamine **1.175** (Scheme 1.44). The nitroamine product formed by the aza-Henry reaction can be subsequently functionalised *via* further reactions, to give different functionality. The aza-Henry reaction involves the attack of nitromethane on imine **1.174**, however the reaction is reversible and there is the possibility for the formation of the nitro-alkene elimination product, (**1.176**).[85]

1.174   **1.175**   **1.176**
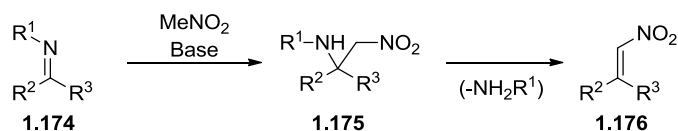
Scheme 1.44 A generic aza-Henry reaction for the formation of β-nitroamine 1.175 from imine 1.174 and nitromethane, with potential formation of 1.176.

Asymmetric variations of the aza-Henry reaction have been disclosed by Ruano and co-workers[53] with *N-p*-tolylsulfinylimines, **1.177**. The group was able to react nitromethane under two different reaction conditions to give either of the optical isomers from either *Re* or *Si* facial attack. Using sodium hydroxide and 4 Å molecular sieves they were able to achieve up to 90% conversion to β-nitroamine **1.178** with a diastereoselectivity of up to 94% diastereomeric excess, *de*, for one of the diastereomers (Scheme1.45a). Furthermore, using *tert*-butylammonium fluoride, TBAF, they were able to produce the other diastereomer of **1.178** with up to 100% conversion and a *de* of up to 48% (Scheme1.45b). The reaction was tolerant of numerous unsymmetric secondary sulfinylimines containing both alkyl and aryl substituents at the imine carbon, as well as converting the challenging isopropyl-substituted analogue in 32% and 79% yield for each protocol.[85]

36
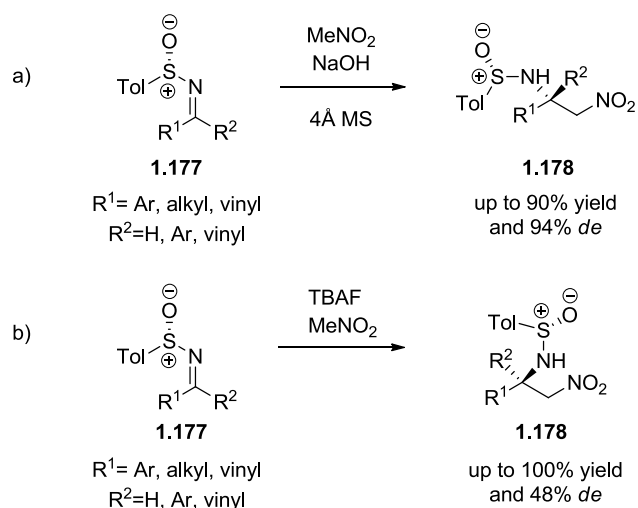
Scheme1.45 Ruano and co-workers protocol for asymmetric aza-Henry reactions, to form either diastereomer of β-nitro amine 1.78 from tolylsulfinylimine 1.177.

Work by Okino and co-workers disclosed a bifunctional organocatalyst, **1.179** (Figure 1.14), to also achieve an enantioselective addition to a phosphinoyl protected imine, during aza-Henry reactions with nitromethane.
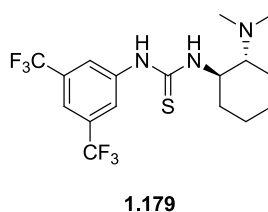
Figure 1.14 Okino and co-workers bifunctional organocatalyst, 1.179.

The reaction was optimised to give a maximum yield of 99% for the tosyl protected imine (dichloromethane, 4.5 hours, rt), however this reaction proceeded with only 4% *ee* for the (−)-isomer. The isolated yield and *ee* were 85% and 76%, respectively, for the *N*-diphenylphosphinoyl protected 2-furyl imine (rt, dichloromethane, 24 hours). The reaction was chemoselective, which was proven when the reaction was tolerant of olefin-containing substrates. The reaction with imine **1.181** exhibited chemoselectivity for the 1,2- (and not 1,4-) addition product (Scheme 1.46), with a yield of 68% of the kinetic product, **1.182**. Furthermore, the work highlighted that although non-polar solvents would give higher enantioselectivities, they led to slower reactions than polar solvents. Although the reaction demonstrated the ability of organocatalyst **1.179** to carry out the reaction, the long reaction time for a comparatively low yield and *ee* would need to be significantly improved upon,

otherwise DKR reactions, such as those described previously, would be required if the process where to be used on an industrial scale.[86]
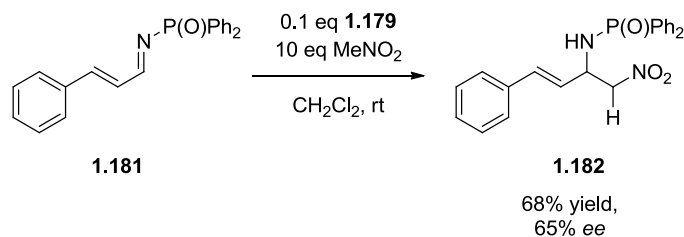
Scheme 1.46 Okino and co-workers organocatalysed enantioselective *aza*-Henry reaction.

Aziridines, **1.183** (Figure 1.15), the nitrogen analogues of epoxides, can be synthesised in a number of ways. Sweeney comprehensively reviewed the structure, reactivity, biological and synthetic importance and synthesis of aziridines.[87] The review highlighted many methods for the synthesis of this moiety many of which include nucleophilic attack of carbon nucleophiles on imines.
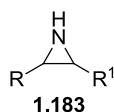
Figure 1.15 General structure of an aziridine, 1.183.

Sweeney's review of aziridine chemistry highlighted Davis and co-workers asymmetric aziridine synthesis *via* an aza-Darzens reaction. Davis and co-workers established new synthetic procedure used α-haloenolates and optically active sulfinylimines to form aziridines (Scheme 1.47).[88] They formed aziridine (2*R*,3*S)*-**1.186** from *α*-haloester **1.185** and sulfinylimine **1.184** using lithium hexamethyl disilylazide (LHMDS) at -78 °C in 30 min. with a good yield and *de* (85 and 90%, respectively). Aryl ring systems with electron withdrawing groups proved to be difficult to convert, the *p*-trifluoromethyl substituted phenyl ring analogue converting in 22% isolated yield, however the diastereomeric excess for the reaction was 98%. Furthermore, although it is generally assumed that activated imines should have a higher conversion rate, the *p*-methoxyphenyl analogue was formed in 74% yield and with 98% *de*. Thus a new method for the asymmetric production of these biologically important compounds was discovered.
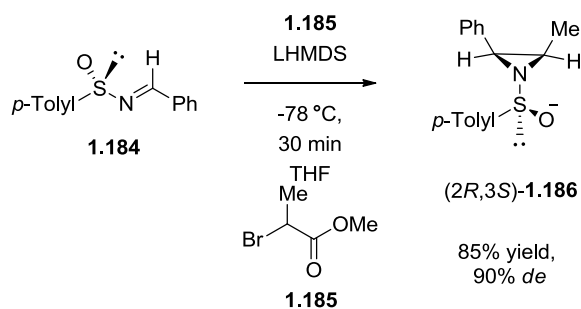
Scheme 1.47 Davis and co-worker's diastereoselective aza-Darzens reaction for the formation of (2*R*, 3*S*)-1.186.

Imines can be further utilised in aza-Diels–Alder reactions, Clive and co-workers used this methodology in the synthesis of aza-bicyclic compound **1.190** a constituent of castoreum, a mixture used in the perfume industry.[89] The aza-Diels–Alder reaction occurs at the second stage of the synthesis using a zinc chloride mediated cycloaddition (Scheme 1.48).
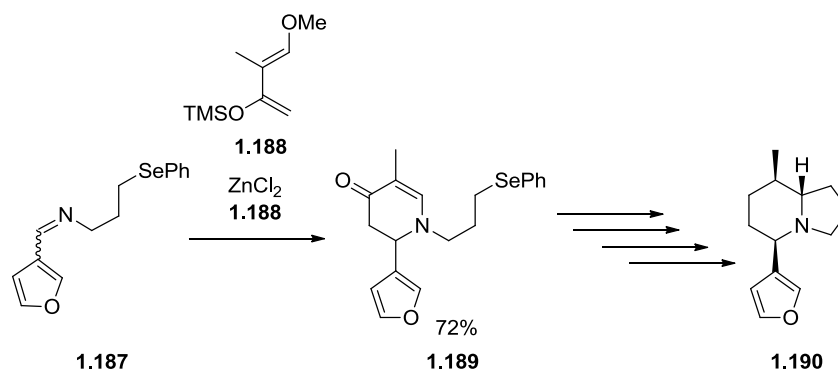
Scheme 1.48 aza-Diels–Alder reaction in the synthesis of castoreum constituent 1.190.

1.4   Summary, challenges and opportunities

Functionalised amines are a ubiquitous chemical moiety and are important from a financial and therapeutic standpoint to the pharmaceutical industry. Classic methods for the functionalization of amines have suffered from numerous problems, from cost through to their hazardous nature in scalable synthesis. Historic methods for stoichiometric C−H bond activation adjacent to nitrogen have been developed, however the use of toxic oxidants in stoichiometric quantities during C−H bond activation is not desirable, and their use is undesirable on scale.

The field of transfer hydrogenation has gained major impetus as an alternative method to classic hydrogenation and has provided new routes for the formation of chemical bonds. Efficient asymmetric transfer hydrogenation reactions have been developed that can be used as part of the method of formation of carbon−carbon bonds in API synthesis. These methods have increased the overall efficiency of the procedures, reducing waste during drug synthesis. The introduction of 'hydrogen borrowing' methodologies have provided an alternative method to activate numerous chemical bonds. 'Hydrogen borrowing' is a viable alternative for chiral resolution methods and the use of chiral auxiliaries that were only previously available, through DKR protocols. Using this methodology the maximum theoretical yields of a single enantiomer can be increased to 100%, where previously the maximum theoretical yield was 50% when chiral resolution was used. The successful implementation of hydrogen-borrowing in industry can be seen as Pfizer has successfully developed a multi-kilogram scale synthesis of an API using the methodology.

Imines, which are formed *in situ* during hydrogen-borrowing reactions, can undergo a number of reactions when preformed separately and the literature has disclosed numerous protocols that utilise the electrophilic nature of imines. The Strecker, aza-Henry, aza-Darzens and aza-Diels−Alder reactions to synthesise α-aminonitriles, β-nitroamines, aziridines and (hetero)-cyclic compounds which are all important intermediates in organic chemistry. There are potential problems when reacting nucleophiles with imines, these include that the imine is susceptible to hydrolysis, primary imines are incredibly reactive and so the secondary and tertiary analogues are preferred as they are more stable.

The ability to carry out efficient, clean, safe and cheap reactions is a key goal of organic chemistry and its proponents. In this regard the hydrogen transfer and hydrogen-borrowing methodologies provide the opportunity for the development of a synthetic tool that does not require the use of toxic reagents that are currently required for C−H bond activation of amines. There is the opportunity to combine the hydrogen-borrowing methodology with nucleophilic reactions of imines to establish novel, synergistic protocols that can synthesise functionalised amines rapidly, *via* metal catalysis (Scheme 1.49).
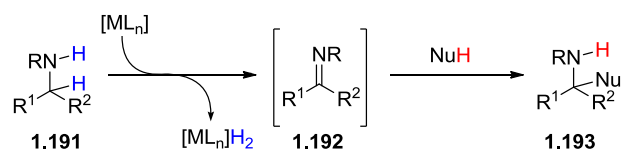
Scheme 1.49 Ideal synthetic strategy for the functionalization of amines *via* metal catalysis.

The following chapters will discuss the work carried out to achieve the metal catalysed functionalization of amines, *via* formation of an imine intermediate. Discussion of amine dehydrogenation, the cyclisation of substituted indoles, the mechanistic knowledge gained and the evaluation of a range of nucleophiles will be discussed and the conclusions of this work given.

Chapter 2 The dehydrogenation of primary amines an optimisation study

2.1 Background

The literature review in Chapter 1 established precedent for the activation of C-H bonds adjacent to amines using amine dehydrogenation to form an imine intermediate. Its subsequent reaction with a suitable nucleophile could be performed *in situ* and has the potential to become a useful tool in synthetic chemistry. The availability of cheap, simple amines, and the ubiquity of functionalised amines in synthetic pharmaceuticals/agrochemicals and bioactive natural products, encourage this methodology to become an important tool for the green atom efficient synthesis of high value chemicals. Before this endeavour can be achieved, a greater knowledge of the reaction and understanding how to form imines using this methodology is required.[39]

2.1.1 Aims and objectives

The dehydrogenation approach has a number of advantages over the existing direct oxidative methods for imine/iminium ion formation including: i) the ability to carry out multiple transformations in a one-pot process; ii) the absence of hazardous reagents (e.g. peroxides, oxygen) and iii) that molecular hydrogen is the only by-product formed in the process (although it is worth noting that this must be handled in a safe manner). The activation of C-H bonds adjacent to a variety of amines *via* transfer dehydrogenation to form imines using a variety of catalysts known to participate in this type of reaction was investigated (Scheme 2.1, a and b).
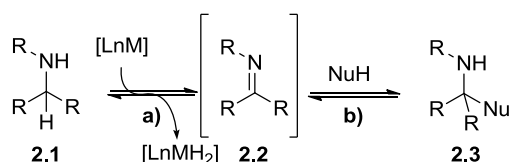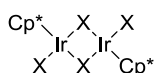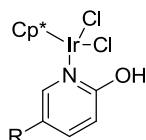
Scheme 2.1 a) The proposed iridium catalysed dehydrogenation of an amine to an imine, b) nucleophilic attack on the in situ generated imine.

To establish an efficient dehydrogenation protocol a range of primary amines were tested (Scheme 2.1a). The catalysts that were screened had been previously shown to be active in hydrogen transfer reactions,[1] including the dehydrogenation of secondary and tertiary amines[72, 76] and in the dehydrogenation of alcohols.[69, 79]

2.2   Results and Discussion

2.2.1 Investigation into the dehydrogenation of a model amine substrate

Benzhydrylamine (**2.6**) was selected as a model compound being a cheap and commercially, available primary amine (Scheme 2.2). Furthermore, dehydrogenation of this amine produces benzophenone imine (**2.7**) which is stable and isolable. Imine **2.7** is commercially available, as such its formation during the dehydrogenation reaction can be observed *via* comparison to the commercially available standard in gas chromatography (GC) analysis. Investigation into the effect of different catalysts, concentrations and additives across a range of temperatures was undertaken. Moreover, *in situ N*-alkylation of the imines to either the saturated or unsaturated homo-dimer, **2.8** or **2.9** respectively, was investigated.
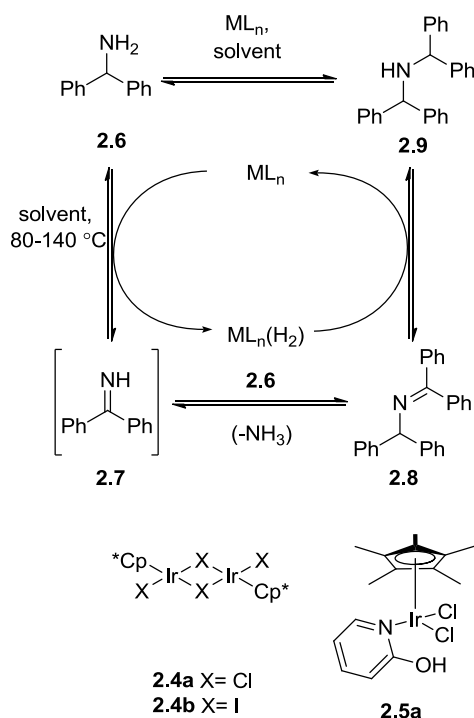
Scheme 2.2 *N*-alkylation products formed *via* iridium catalysed hydrogen transfer.

2.2.2 The *N*-alkylation of imine 2.7

Williams and co-workers have demonstrated that SCRAM catalyst **2.4b** can be used to catalyse the cross-coupling of amines.[79] In addition, Blacker and co-workers have also reported that homo-coupling *N*-alkylation products are formed when using primary amines during the iridium catalysed deracemisation of chiral amines.[76] It was reasoned that the SCRAM catalyst **2.4b** was catalysing the *in situ N*-alkylation of the intermediate imines formed during the reaction leading to their transient appearance in GC analysis.
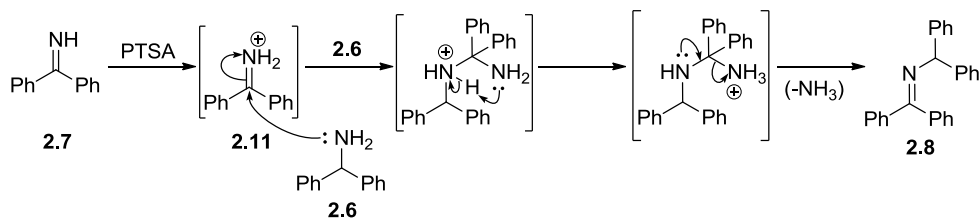
Scheme 2.3 Proposed mechanism for formation of 2.8.

Table 2.1 The effect of metal and Bronstead acid catalysts on the reaction rate of imine 2.7 *N*-alkylation, Scheme 2.2.[a]

Entry	Catalyst	Catalyst loading / mol%	Rate of Amine Consumption / µmoles/min[b]
1	**2.4b**	1	29
2	**PTSA**	50	20
3	-	-	No Reaction[c]

[a] Amine (2 mmols), imine (2 mmols) and catalyst (if required) were stirred in solvent (4 mL) at 80 °C and monitored *via* GC analysis.

[b] Calculated *via* GC analysis and comparison to pre-prepared standards.

[c] No reaction after 24 hours at temperature.

To test this hypothesis *N*-alkylation reactions were carried out with and without SCRAM catalyst and as a further control with *para*-toluene sulfonic acid, PTSA, (*i.e.* to generate the iminium ion from the preformed imine, Table 2.1). No reaction was observed when only equimolar quantities of imine and amine where mixed in toluene at 80 °C for 8 hours (Entry 3). However, when either metal **2.4b** or Bronsted acid catalyst (PTSA) were present in the reaction mixture the unsaturated *N*-alkylation homo-dimer product, **2.8** was formed rapidly (Scheme 2.2 and Scheme 2.3, respectively). The control reaction using PTSA showed that formation of the iminium ion 2.11 (Scheme 2.3), was sufficient to activate it towards the amine nucleophile **2.6**. Loss of ammonia may also be acid catalysed.

Blacker and co-workers have proposed a catalytic cycle for the dehydrogenation of amines.[77] The iridium catalysed *N*-alkylation reaction is thought to occur *via* dehydrogenation of amine **2.6** to imine **2.7** (Scheme 2.4). Imine **2.7** was presumed to react *in situ* with substrate **2.6** to form *N*-alkylation product **2.8**. *N*-Alkylation of amine **2.6** was proposed to occur *via* coordination of the imine nitrogen onto the iridium centre, to afford hydrogen iodide. Coordination of the benzophenone imine nitrogen to the Lewis acidic iridium catalyst activated it to nucleophilic addition. In the presence of a large excess of amine **2.6**, nucleophilic addition occurs to give the *gem*-aminal **2.16** with concomitant loss of iridium-coordinated ammonia. A proton transfer then occurs between the iminium ion and the catalyst bound ammonia affording neutral **2.8** and the iridium complex **2.17**. Finally, a second equivalent of substrate **2.6** coordinates onto the iridium centre, leading to loss of ammonia and a continuation of the catalytic cycle (Scheme 2.4).Evidence for this pathway is limited and forms the basis for Chapter 3. With the knowledge that SCRAM catalyses the *N*-alkylation of primary amines and a hypothetical mechanism for *N*-alkylation, it was

possible to alter reaction conditions to optimise the formation of imine **2.7**, or for the *N*-alkylation product.
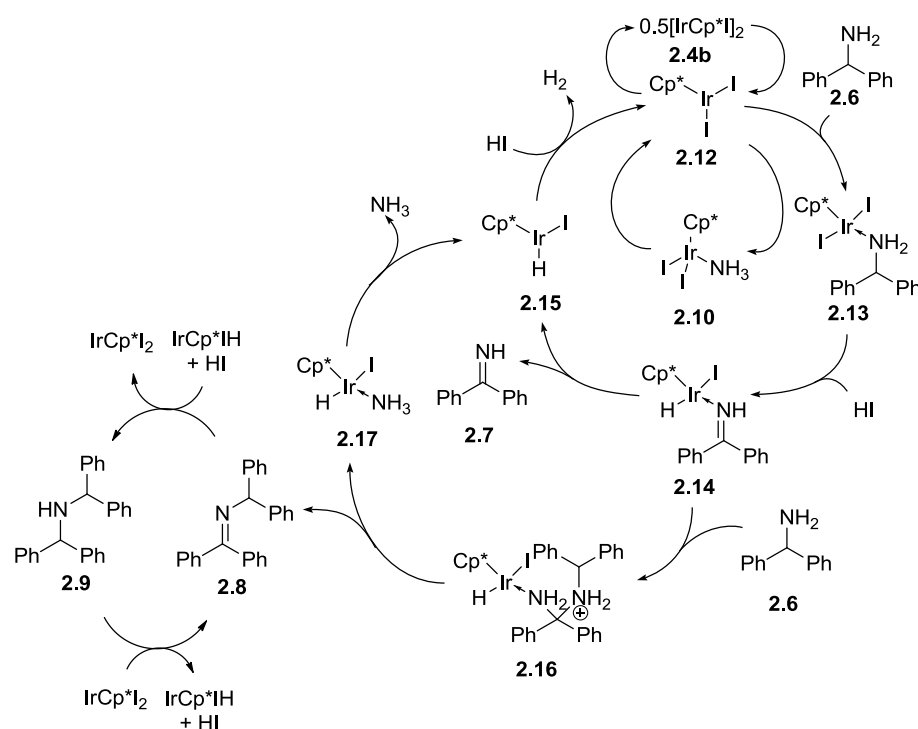
Scheme 2.4 Proposed catalytic cycle for SCRAM (2.4b) catalysed *N*-alkylation of benzhydrylamine 2.4.[77]

2.2.3 Ammonium additives as *N*-alkylation inhibitors

The proposed catalytic cycle is believed to have a number of steps that are in equilibrium (Scheme 2.4). If the *N*-alkylation occurred as proposed, with evolution of ammonia to form the *N*-alkylation product, the addition of ammonia would reverse the formation of dimer **2.8** and increase the amount of imine **2.7** (Scheme 2.5). The Blacker group has shown previously that ammonia will complex to the iridium centre to form a toluene insoluble complex [IrCp*I$_2$(NH$_3$)], **2.10**,[77] therefore addition of ammonia might slow the rate. If the addition of ammonia did not lead to formation of species **2.10**, micro-reversibility would lead, however to the concentration of imine **2.7** increasing. An initial reaction was performed heating a solution of amine **2.6**, with the SCRAM catalyst **2.4b** and an aqueous ammonia solution in toluene at reflux to test this hypothesis (Scheme 2.5, Table 2.2, Entry 2). 2 equiv. of ammonia gave a marked improvement over the reactions conducted in its absence, with an observed 17% conversion of to imine **2.7a** after 6 hours. Increasing the number of moles of ammonia to 10 equiv. gave 26% conversion after 6 hours (Table 2.2,

Entry 3). Although complete conversion to imine **2.7** was still not achieved, the observation of increased imine formation merited further investigation.
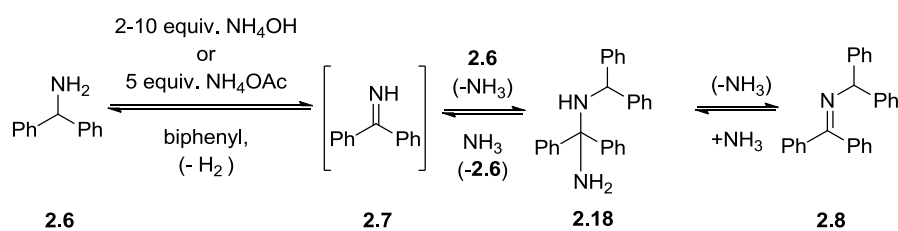
Scheme 2.5 Use of ammonium additives to reduce *N*-alkylation of amine 2.6.

Table 2.2 Effect of aqueous ammonia on the initial rate of reaction during the iridium catalysed dehydrogenation of 2.6.[a]

Entry	Ammonium additive	Quantity (mmole)	GC yield[b, c, d] (%) 2.7	GC yield [b,e] (%) 2.8	Initial rate (µmoles/min)
1	ammonia (aq)	0	<1	37	9
2	ammonia (aq)	2	17	38	5
3	ammonia (aq)	10	26	14	7
4	ammonia (aq)	10[f]	0	0	0
5	ammonium acetate	5	11	6	9

[a] Amine **2.6** (2.00 mmols), complex **2.4b** (1 mol%) and toluene (2 mL) were heated to reflux under nitrogen for 6 hours.

[b] GC yields to the nearest percent ± 0.5%.

[c] Calculated *via* GC and comparison to a biphenyl internal standard and commercially available standard of **2.7**.

[d] Yield after 5 hours.

[e] Calculated *via* GC and comparison to a biphenyl internal standard and pre-prepared standard of **2.8**.

[f] Initially 8 mmols of aqueous ammonia, with a further 12 mmols added dropwise over 1.75 hours.

Since ammonia is a volatile reagent it will be readily lost when carrying out reactions at the temperature required for successful dehydrogenation (110 °C). To overcome this issue and increase the amount of imine **2.7** formed, dropwise addition of aqueous ammonia to the reaction was carried out (Table 2.2, Entry 4). Initially, aqueous ammonia (8mmols) was heated to reflux under the standard conditions and aqueous ammonia (12 mmols) was added after 2 mins. *via* drop-wise addition over 1.75 hours. Surprisingly this procedure resulted in no products being formed, which may be due to catalyst deactivation.

As a further probe of the reaction ammonium acetate was used to help overcome the problem of using ammonia. Ammonium acetate was unfortunately less successful than aqueous ammonia and only 11% yield of the desired imine was observed (Table 2.2, Entry 5), however it also reduced the formation of the *N*-alkylation product **2.8** to 6%. With these promising results, further optimisation of the *N*-alkylation conditions was carried out to try and increase the amount of imine formed.

2.2.4 The effect of reaction temperature

Previous work by Williams and others has identified the need for high temperatures during amine *N*-alkylation. The reaction of amine **2.6** with iridium catalyst **2.4b** in non-polar aprotic solvents at different temperatures was undertaken to assess the formation of *N*-alkylation products and to determine if any imine 2.7 was formed (Scheme 2.2**,** Table 2.3, Entry 1).

Table 2.3 The effect of temperature upon dimer 2.8 formation using catalyst 2.4b in non-polar a-protic solvents.[a]

Entry	Solvent	Temp / ^{o}C	Percentage of 2.6 in reaction / %[b]	Yield of 2.8 / %[b,c]	Initial Rate of Consumption of 2.6 / µmols min^{-1}
1	Toluene	80	>99	<1	-
2	Toluene	110	64	34	<1
3	Xylenes	137-140	5	37	11

[a] Amine **2.6** (2 mmols.), complex **2.4b** (2 mol%) were heated in solvent (4 mL) for 5 hours.

[b] Product yield, determined by GC analysis and comparison to internal biphenyl standard.

[c] GC yields to the nearest percent, ±0.5%.

Little to no reaction was observed when **2.6** was heated in the presence of 1 mol% of complex **2.4b** in toluene to 80 °C for 24 hours with only trace quantities of the products observed (Table 2.3, Entry 1). When the temperature was increased to 110 °C, reflux, in toluene (Table 2.3, Entry 2), dimers **2.8** and **2.9** were formed, , 34% and <1% and respectively, however conversion of the starting material was incomplete, 24%. The reaction was repeated in refluxing xylenes and 37% of dimer **2.8** was formed (Table 2.3, Entry 3). Analysis of the initial rate of consumption of **2.6** by GC showed a marked improvement from <1 to 11 µmols min^{-1}. Nevertheless, the reaction still did not reach full conversion of amine **2.6** after 21.5 hours at reflux. The GC traces also showed compounds

with retention times at 12.8 and 13.2 in a ratio of 20:2. The two peaks were found to have masses m/z = 209 and 224, respectively and were tentatively assigned the structures **2.20** and **2.22** (Figure 2.1, Scheme 2.6). The formation of **2.20** is proposed to occur *via* a Ritter type reaction (Scheme 2.6a). Whilst the structure **2.22** might be formed by reaction of the amine with iridium activated acetonitrile (Scheme 2.6b).
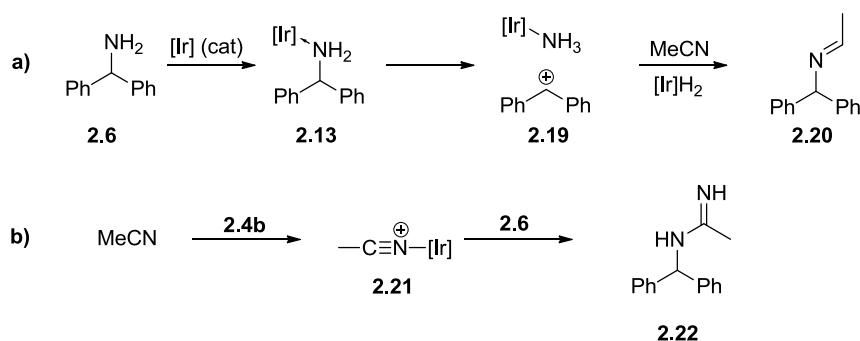
Scheme 2.6 Proposed formation of a) 2.20 and b) 2.22.
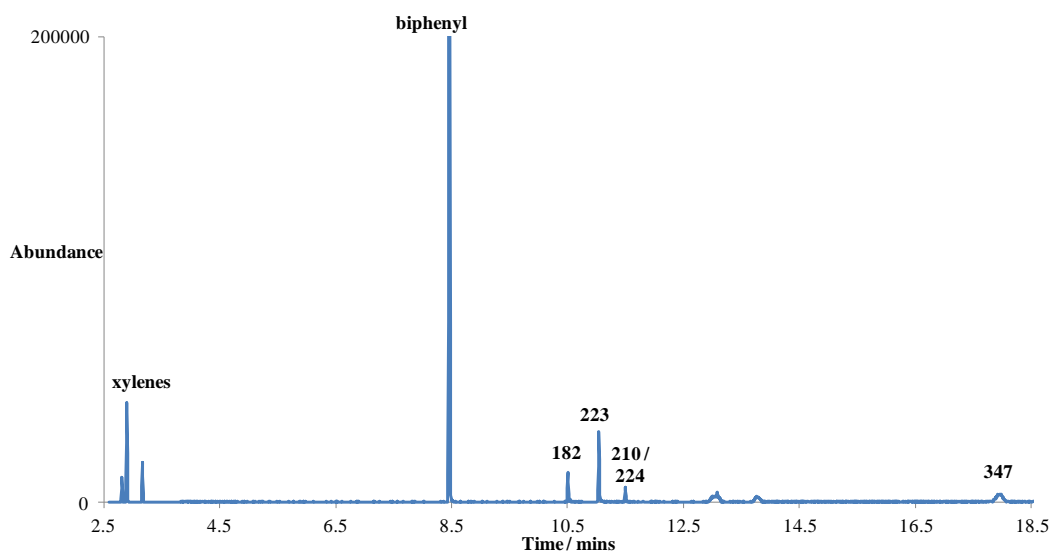
Figure 2.1 Total Ion Chromatogram highlighting relevant peaks, from the GC-MS analysis of the iridium catalysed dehydrogenation of amine 2.6.

The temperature study suggested that the activation energy of the dehydrogenation reaction has a high thermal barrier. Indeed the reaction kinetics appeared non-linear because the rate at 80 °C would be expected to be about 8 times less than at 110 °C, rather than hundreds of times slower (Figure 2.2, *vide infra*). One possible explanation is the endothermic loss of

hydrogen to form imine **2.7**, this endothermic loss of hydrogen has been observed in other dehydrogenation reactions, including work by Jensen on iridium catalysed alkane dehydrogenation.[90]

2.2.5 The effect of reaction atmosphere

The proposed catalytic cycle invokes the formation of iridium-hydride species **2.15** (Scheme 2.2),[77] suggesting that if the cleavage of the iridium-hydride bond during the reaction is rate limiting, then the use of an oxidant would accelerate the rate of reaction (Scheme 2.7).
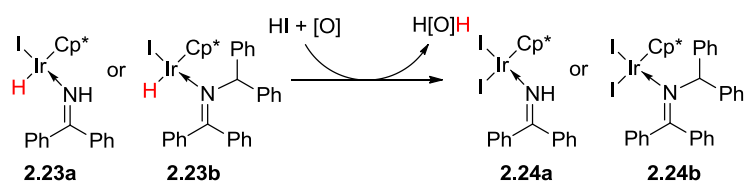
Scheme 2.7 The use of an oxidant to form active catalyst 2.24 from iridium-hydride complex 2.23 that is formed during the dehydrogenation reaction.

Table 2.4 The rates of amine 2.6 conversion and yields of *N*-alkylation product 2.8 with various reaction conditions (Scheme 2.2).[a]

Entry	Temperature	Atmosphere	Rate of consumption of amine / mmols $min^{-1[b]}$	Product 2.8 (%)[d]	Product 2.9 (%)[d]
1	80	Air	0.0063	2	<1
2	80	Air	0.0083	2	<1
3	80	Air	0.0032	2	<1
4	80	Nitrogen	0.0006	2	<1
5	80	Nitrogen[c]	0	<1	<1
6	100	Nitrogen[c]	0.0068	<1[e]	<1
7	100	Nitrogen[c]	0.0004	1[e]	<1
8	110	Nitrogen[c]	0.0154	34	<1
9	137	Air	0.0322	86	<1
10	137	Nitrogen[c]	0.0114	37	<1
11	137	Nitrogen[c]	0.0055	37	<1
12	137	Nitrogen	0.0017	67	<1
13	137	Nitrogen	0.0126	67	<1

[a] Amine **2.6** (2 mmols), complex **2.4b** (2 mol%) and solvent (4 mL) were heated with a sparge or under an atmosphere of nitrogen

[b] Rate determined by GC analysis and comparison to a biphenyl internal standard.

[c] No sparge.

[d] GC yields to the nearest percent, ±0.5%.

[e] Yield calculated after 120 mins.

The use of the oxygen might cleave the metal-hydride bond of intermediate **2.23** and would generate water, as a by-product. The use of an air or nitrogen sparge has been demonstrated previously to accelerate hydrogen transfer reactions.[77] The use of an air sparge should accelerate the *N*-alkylation of primary amine **2.8**.
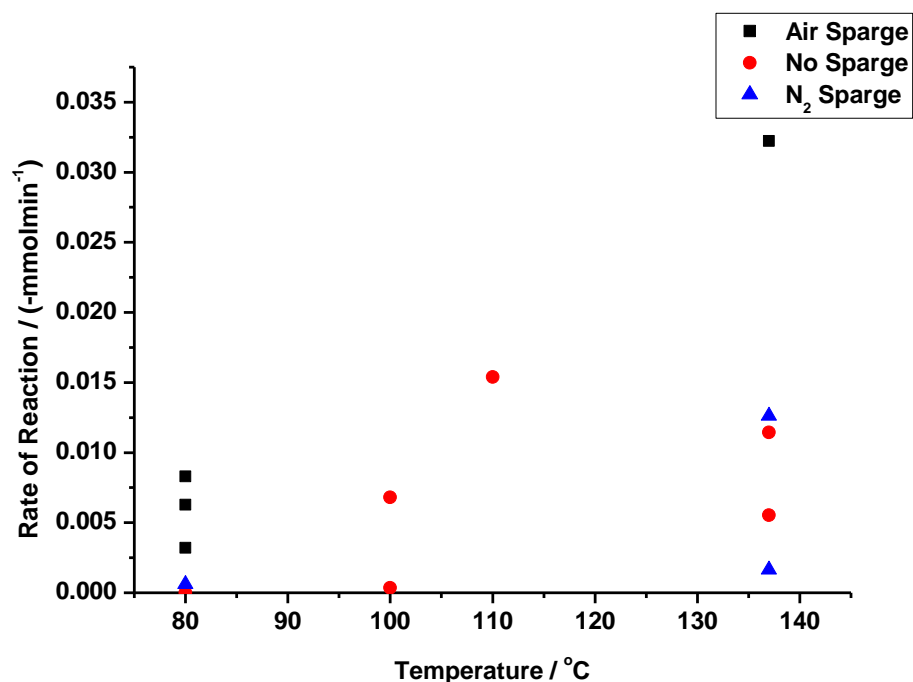
Figure 2.2 Initial rates of reaction for different SCRAM catalysed dehydrogenations of amine 2.6 in various aprotic solvents, at 80–137 °C with a sparge of compressed air, nitrogen or no sparge (Table 2.4).

Air was bubbled through the reaction mixture at a rate of 6-32 µmol min⁻¹ and reaction temperatures ranging from 80 to 138 °C and the rate of conversion of starting amine **2.6** was noted (Table 2.4, entries 1-3 and 9). At all temperatures, the air sparge gave a higher rate and conversion compared to the non-sparged systems (Entries 1–3 and 9 *cf* 5-8, 10 and 11; Figure 2.2).[77] Nitrogen used as a sparge demonstrated lower rates and conversions (Entries 4, 12 and 13). In contrast with the literature, in which a nitrogen sparge enhanced the rates of hydrogen transfer reactions, this system did not.[77] Contrary to the results observed with secondary amines, the *N*-Alkylation product **2.8** was produced in significant amounts using both the air and nitrogen sparged reactions (86 and 67% GC yield, respectively) with no imine **2.7** detected. Despite these promising results, the conditions are not scalable due to the temperatures required; *cf.* 137-140 °C, in the presence of oxygen could be explosive on a large scale. Nevertheless, the result showed potential for further optimisation, which will constitute future research efforts.

2.2.6 Catalyst screening for reaction optimisation

The SCRAM catalyst **2.4b** has proven useful in the dehydrogenation of amines, nevertheless iridium-Cp* catalysts have been developed and reported in the literature for hydrogen transfer reactions.[91-94] A small screen of different moisture and oxygen stable amine dehydrogenation iridium-Cp* complexes was carried out with the aim of identifying more active catalysts (Table 2.5).[72, 76]

Table 2.5 Dehydrogenation of amine 2.6 catalysed by Ir (III) complexes (Scheme 2.2).[a]

Entry	Catalyst	Initial Rate of Amine conversion [b, c, d] / $\mu mol\ min^{-1}$
1	[IrCp*I$_2$]$_2$, **2.4b**	-14
2	IrCp*(2-hydroxypyridine)Cl$_2$, **2.5a**	-11
3	[IrCp*Cl$_2$]$_2$, **2.4a**	-16

[a] Amine **2.6** (2.mmols), catalyst (2 mol%) in toluene (4 mL) were heated to reflux.

[b] Rate determined by comparison with biphenyl internal standard (1.00 mmol).

[c] Rates determined for single experiments.

[d] Rate to the nearest μmol +/-0.5 $\mu mol\ min^{-1}$.

Catalysts **2.4b**, **2.5a** and **2.4a** have all proven to be useful in iridium catalysed amine dehydrogenation and were assessed in the benzhydrylamine system (Table 2.5).[72, 95] The initial rate of 11 $\mu mol\ min^{-1}$ shown by complex **2.5a** (Entry 2) was comparable to the initial rate for complex **2.4b**, 14 $\mu mol\ min^{-1}$ (Entry 1). The difference in activity between complexes **2.4a**, **2.4b** and **2.5a** was not significant. The [IrCp*Cl$_2$]$_2$ catalyst **2.4a** has similar activity to complexes **2.4b** and **2.5a** (16 $\mu mol\ min^{-1}$, Entry 3). Both catalysts **2.4a** and **2.4b** gave similar amounts of the dimer **2.8**, 30 and 28%, respectively. None of the catalysts produce imine **2.7**, further suggesting that it is catalyst bound and susceptible to amine attack, analogous to Scheme 2.3.

2.2.7 Evaluation of low substrate concentration to inhibit *in situ N-alkylation*

Since the formation of dimer **2.8** is bimolecular and dependent upon the concentration of amine **2.6** experiments were carried out at low concentration of amine **2.6** (51.3 μM) by slow portion-wise addition. This method would reduce the concentration of free amine available to react with imine **2.7** thereby minimising the *N*-alkylation reaction.[75] Amine **2.6**

was added slowly to a solution of toluene and SCRAM catalyst **2.4b** (1 mol%) with biphenyl as an internal standard at 80 °C over 3 hours (20 µL every 10 min.). Unexpectedly there was no less *N*-alkylation product, indicating that the rate of *N*-alkylation was faster than the rate of dehydrogenation of amine **2.6**. This observation supports the mechanistic hypothesis that the imine remains coordinated to the catalyst, which is acting as a Lewis acid activating the imine to nucleophilic attack (Scheme 2.4).

2.2.8 Mechanistic investigation into SCRAM catalysed *N*-alkylation of primary amines

Having examined the dehydrogenation of model amine substrate **2.6**, an investigation of how other primary amines would interact with SCRAM catalyst **2.4b** was undertaken. The electronic and steric properties of the substituents on the primary amine substrate will affect the rate of dehydrogenation if the migration of the hydride is rate limiting and will give mechanistic insights (Scheme 2.8).
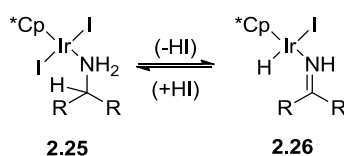
Scheme 2.8 Proposed rate determining step during imine dehydrogenation.

Amines **2.27** and **2.31** were evaluated in the SCRAM catalysed dehydrogenation reaction to investigate the effect of proton acidity (Scheme 2.9).
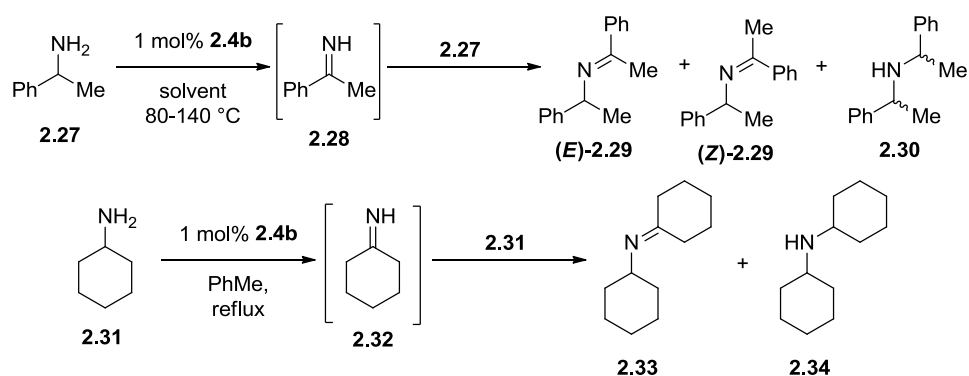
Scheme 2.9 Dehydrogenation reactions of aryl-alkyl and dialkyl amines.

The SCRAM catalysed dehydrogenation and racemisation of α-methylbenzylamine, **2.27**, has been previously reported,[76] showing that (+)-**2.27** will racemise when heated at 80 °C in toluene in the presence of the SCRAM catalyst **2.4b**. Blacker and co-workers found that **2.27** preferentially formed two different imine dimers (**2.35** and **2.36**, Figure 2.3) in 70% yield, with the remainder as racemised amine **2.27**. Unpublished work from the same group also showed that dimer formation could be averted by slow addition of the amine into a DKR with enzymatic acylation of the desired amine enantiomer.[75]

2.35   **2.36**
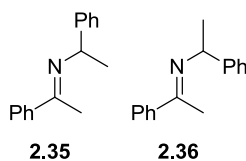
Figure 2.3 The two diastereomeric secondary imines formed due to *N*-alkylation of *a*-methylbenzylamine.

In this study (+/-)-α-methyl benzyl amine **2.27**, SCRAM catalyst **2.4b**, biphenyl standard and toluene were heated to 80 °C (Table 2.6). The rate of conversion of amine **2.27** was 1 μmol min^{-1} (Entry 1), the reaction was repeated in refluxing xylenes with a rate of conversion of 26 μmol min^{-1} (Entry 2). The rate was three times higher than that of amine **2.6** (Entry 5), which can be rationalised through a reduced steric encumbrance about the iridium catalyst.

Table 2.6 Investigation into the effect of amine constituent on the rate of iridium catalysed dehydrogenation of primary amines.[a]

Entry	Starting amine	*N*-alklyation product	Solvent	Temp / °C	Initial rate of consumption of substrate / μmol min^{-1b}	GC Yield / % [c]
1	**2.27**	**2.30**	Toluene	80	1	6
2	**2.27**	**2.30**	Xylenes	137-140	26	82
3	**2.31**	**2.34**	Toluene	110	14	52
4	**2.6**	**2.8**	Toluene	110	15	34[c]
5	**2.6**	**2.8**	Xylenes	137-140	8	37[c]

[a] Amine (2 mmols), complex **2.4b** (2 mol%) and solvent (4 mL) were heated under a nitrogen atmosphere.

[b] Rate of consumption calculated to the nearest μmol min^{-1}, ±0.5 μmol min^{-1}.

[b] GC yield calculated *via* comparison to a biphenyl internal standard, to the nearest percent, ±0.5%.

[c] GC yield after 5 hours.

In the first instance amine **2.27** formed four by-products in GC analysis, eluting at retention times of 12.6, 12.9 and 13.7 min. Those of 12.6 min and 12.9 min were identified by GC-MS, *m/z* = 225 and comparison to a standard as *N*-alkylation product (*R,R*)-**2.30** and (*R,S*)-**2.30**.
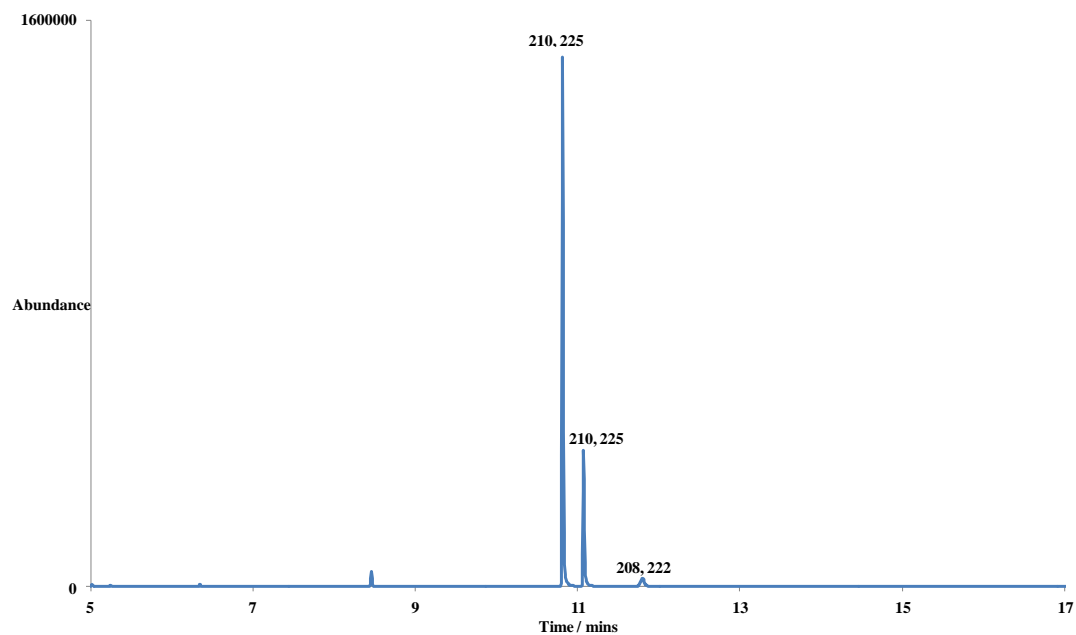
Figure 2.4 GC-MS chromatogram of the SCRAM catalysed dehydrogenation of amine 2.27.

The peak at 13.7 min. was identified as the dehydrogenated *N*-alkylation product **2.29** with *m/z* of 223. One interpretation for the two diastereomers, **2.30**, is shown in Scheme 2.10. A further possibility is the non-specific condensation of either enantiomer of **2.27**. To test this hypothesis, the commercially available diastereomer (*R,R*)-**2.30**, SCRAM catalyst **2.4b** and toluene were stirred at reflux (Scheme 2.10).
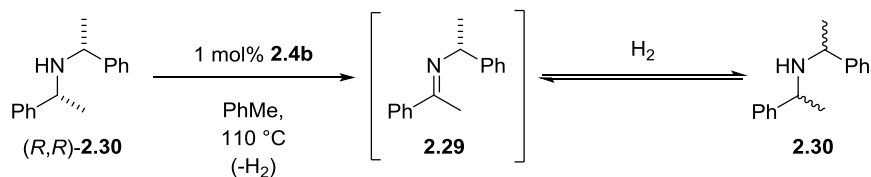
Scheme 2.10 Iridium catalysed racemisation of (*R,R*)-2.30 *via* formation of imine 2.29.
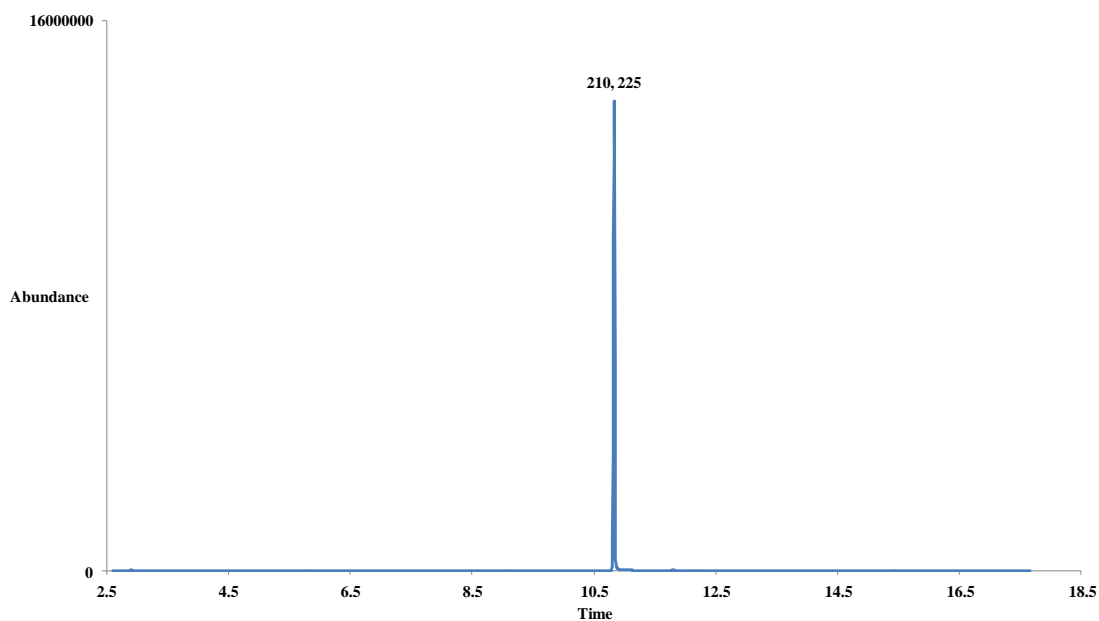
Figure 2.5 GC-MS analysis of the dehydrogenation of (*R,R*)-*bis*-α-methyl benzylamine (2.30) showing the starting material.
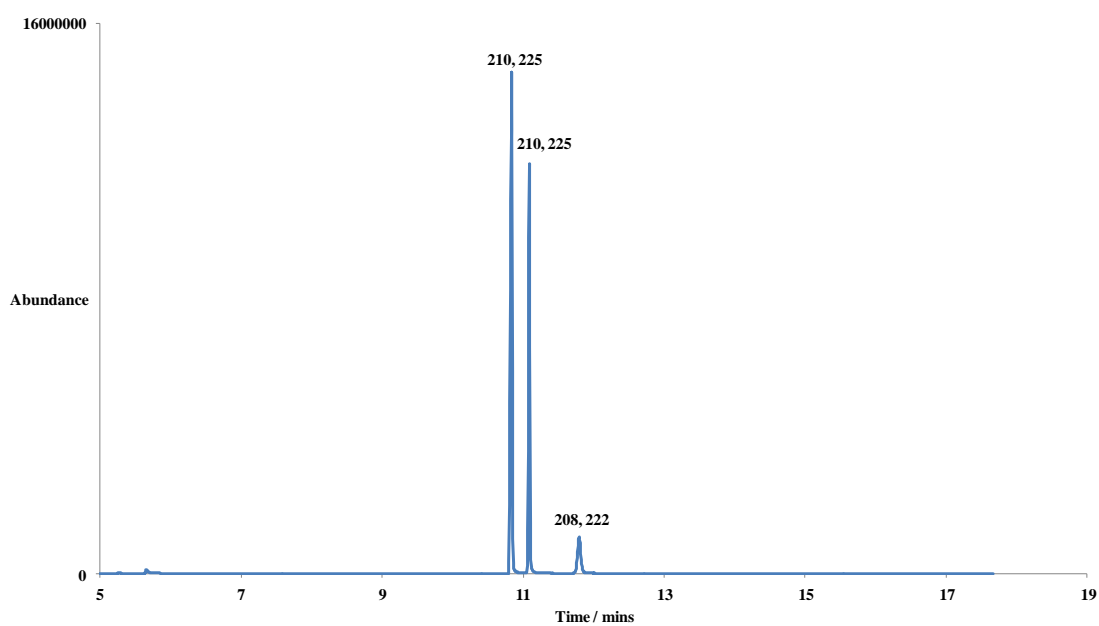
Figure 2.6 GC-MS analysis of the dehydrogenation of (*R,R*)-*bis*-α-methyl benzylamine (2.30), 1.5 hour sample.

Analysis *via* GC-MS showed the peak for the single diastereomer (Figure 2.5) became two peaks (with ratios 12:7,Figure 2.6) both having the same fragment ion *m/z* of 210 and molecular ion of 225. A smaller peak with mass corresponding to imine **2.29** 222 and its molecular ion 208 was also generate. This result confirmed that the product of the *N*-alkylation of amine **2.30** was itself able to undergo racemisation.

Of further interest was the GC conversions observed for the unsaturated dimers **2.29** and the saturated dimer **2.30**. The saturated dimer **2.30** was observed as one peak corresponding to 82% conversion and then 9% conversion to what has been assigned as the imine dimer **2.29**. These observed conversions are in contrast to that observed with the *N*-alkylation of amine **2.6**, the increased stability of the unsaturated dimer was rationalised as being due to the conjugation into the both aryl ring systems and the increased steric bulk around the iridium centre. Imine **2.28** was not observed.

The dialkylamine cyclohexylamine (**2.31**) was heated with SCRAM catalyst **2.4b** and biphenyl in refluxing toluene at reflux (Entry 3) and formed amine **2.34** in 6% isolated yield. Amine **2.31** was consumed at an initial rate of 14 μmol min^{-1}, *via* GC analysis with biphenyl as an internal standard and amine **2.34** was formed in 6% isolated yield. It was not possible to carry out the reaction in refluxing xylene due to the amines lower boiling point, without carrying out under pressure. Formation of **2.34** indicates a hydrogen-borrowing mechanism, with neither the unsatured dimer **2.33** or the monomer imine **2.32** observed. The data showed that dehydrogenation and dimerisation of the benzylic amines was more rapid than that of the aliphatic amines (Scheme 2.11).
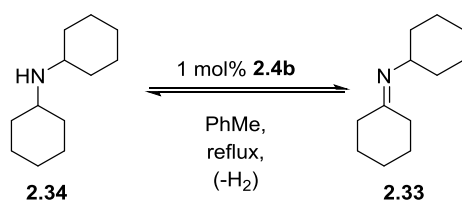
Scheme 2.11 Analysis of dicyclohexylamine (2.34) dehydrogenation.

To check this hypothesis, amine **2.34**, toluene and SCRAM catalyst **2.4b** (1 mol%) were stirred at reflux (Scheme 2.11). Trace quantities of imine **2.33** were observed in GC-MS analysis indicating the equilibrium lies far to the left, toward saturated product. As the starting material was not chiral it was not possible to observe if rapid dehydrogenation-hydrogenation was occurring, which would be observable with chiral GC analysis. Future

work will involve using deuterium exchange reactions to prove that imine formation is occurring during this reaction.

2.3 Conclusions

Primary amines are active towards dehydrogenation with iridium catalysts, however, as has been shown previously in the literature,[37, 79, 96] they readily undergo *N*-alkylation reactions with trace observation of primary imine *via* GC analysis. The *N*-alkylation reaction of benzhydrylamine revealed that the main *N*-alkylation product is the unsaturated imine homo dimer. The rate of the *N*-alkylation reaction was enhanced by using elevated temperatures or by employing different Cp*-iridium catalysts. An indication of the probable rate limiting step during the dehydrogenation pathway has been found, as the presence of an oxidant (an air sparge) dramatically increased the rate of *N*-alkylation. This enhancement is thought to be due to facilitated cleavage of the iridium-hydride bond to generate water. Efforts to inhibit the *N*-alkylation and form solely primary imine were unsuccessful; however the use of ammonia and ammonium salts to change the equilibrium toward imine monomer formation were successful, thus warranting further investigation (Chapter 5). Stereo-electronic effects have been evaluated using aryl and alkyl substituted primary amines, showing that aryl or diaryl primary amines reacted faster than dialkyl amines. These results have given insight into the mechanism of the reaction and with knowledge of primary amine dehydrogenation study of the *in situ* generated imines was carried out and discussed in Chapter 5. Further analysis of the mechanism using a range of analytical techniques is reported in Chapter 3.

Chapter 3 Mechanistic studies of amine dehydrogenation *via* NMR, mass-spectrometry and X-ray diffraction studies

3.1   Introduction

N-Alkylation of the amine starting material was the predominate observation in metal-catalysed primary amine activation reactions discussed in Chapter 2. The reaction of amines with alcohols *via* iridium-catalysed hydrogen borrowing has been characterised mechanistically *in silico* and experimentally by Madsen, providing insight into the intermediates of the reaction, showing that the more electro-withdrawing substituents will increase the rate of *N*-alkylation (Scheme 3.1, Figure 3.1).[97]
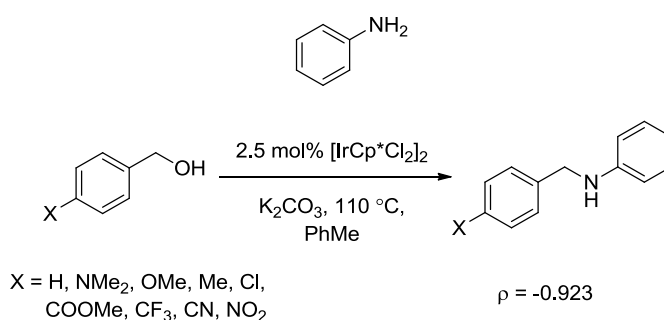
Scheme 3.1 Previous mechanistic work into *N*-alkylation of alcohols by amines.
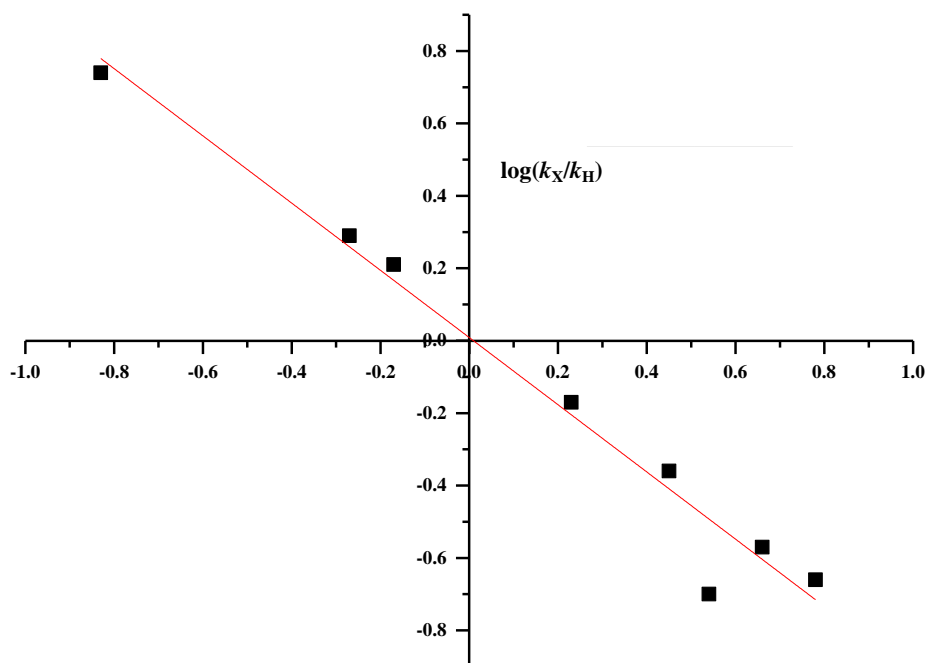
Figure 3.1 Madsen's Hammett analysis graph of the *N*-alkylation of 4-substituted benzylalcohols by aniline via iridium catalysis.

There remains, however, a broad scope for the direct elucidation of the mechanism of iridium(III) half-sandwich complex amine activation, as this field is not currently well characterised, except *in silco*.[98] Nevertheless, mechanistic understanding has been gained through studies of Shvo catalyst catalysed proton/deuterium exchange with tertiary amines *via* NMR analysis (Scheme 3.2).[99]
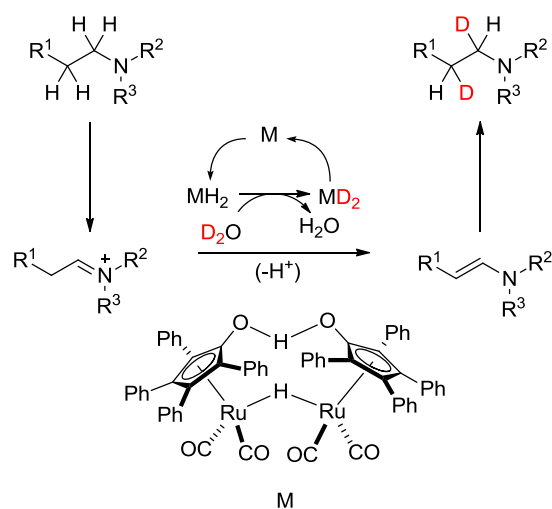
Scheme 3.2 Proton deutrium exchange during tertiary amine dehydrogenation.

Whilst analysis of electronic effects have been carried out on several systems (Scheme 3.3),[91, 100] except for Madsen's work, the main investigations have focused on alcohol dehydrogenation reactions and considered only the yield of the reactions without an in depth analysis of the rate of formation of the final product. Analysis of these rates of reaction will probe the mechanism, establishing whether or not a build of charge occurs in the transition state of the reaction.

R^1 = 4-H, 88%
R^1 = 4-MeO, 95%,
R^1 = 4-Me, 92%,
R^1 = 4-NO$_2$, 86%,
R^1 = 4-Cl, 83%
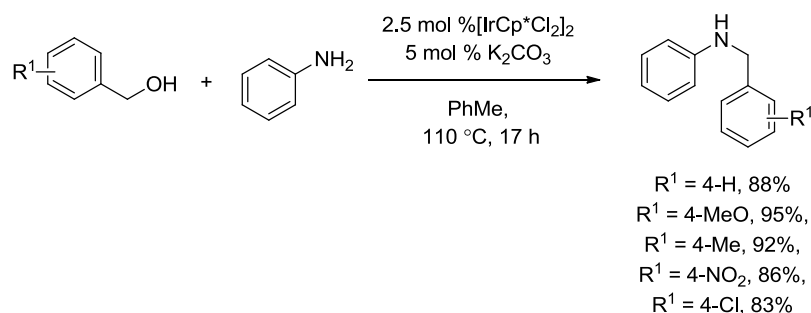
Scheme 3.3 Analysis of different substitution pattern on alcohol dehydrogenation and *N*-alkylation product yield.

Blacker and co-workers have observed reaction intermediates, forming iridium-amine complex **4.4**, an insoluble catalyst inhibition product formed during amine dehydrogenation (Scheme 1.37, *vide infra*).[77] Observation of potential intermediates, through X-ray diffraction, NMR studies and mass spectrometry analysis will enable a greater understanding of the conditions required to achieve preferential amine dehydrogenation, without the immediate undesired *N*-alkylation reaction. Further analysis in this way will help gain understanding of how and why Williams' observed preferential cross-coupling, rather than homo-coupling of amines when isopropanol and benzylamine were used in the dehydrogenation process (Scheme 3.4).

R^1 = 4-H-, 4-Me-, 4-MeO-,
4-Cl-, 4-F-, 3,4-(MeO)$_2$,
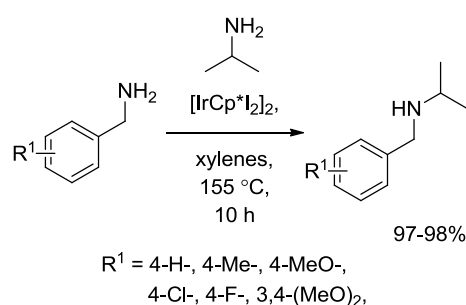
Scheme 3.4 Williams and co-workers' iridium catalysed amine cross-coupling.

2D-NMR spectroscopic techniques including ^{1}H DOSY experiments can be used to provide structural information on the size and structure of components of complex mixtures.[101] ^{1}H DOSY NMR uses pulsed field gradient spin-echo (PGSE) or stimulated echo nuclear magnetic resonance, to separate components of a mixture by their diffusion gradients. A smaller molecule will therefore move faster along an NMR tube than a larger component, giving indication of size and structure, through elucidation of diffusion coefficient (Figure 3.2).[102, 103] DOSY NMR has been employed extensively to analyse mixtures, including hydrocarbon mixtures in fuels, the size distribution of different polymers in a solution, protein-ligand binding and for to detect the formation of π-π complexes.[104-112] The technique benefits from being non-destructive, but providing important insight into the structure of components of complex mixtures. The use of this technique coupled with similar 2D-NMR analysis can be used to elucidate the structure of intermediates formed during the reaction of amines with iridium catalysts.
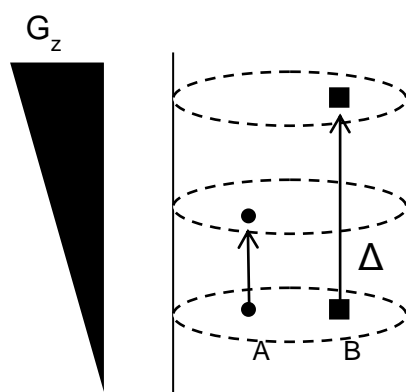
Figure 3.2 The application of a pulsed field gradient used for DOSY NMR to give different attenuations for particle B compared to particle A due to different diffusion coefficients.[113]

3.1.1 Aims and Objectives

The interaction and reaction of different primary, secondary and tertiary amines with SCRAM catalyst, **3.1** were monitored by 1D- and 2D-NMR, and the intermediates analysed by LC-MS and HRMS to elucidate the structure of species within the reaction mixture. The rates of amine dehydrogenation of a range of substituted benzylamines were investigated by ^{1}H NMR analysis allowing investigation of the mechanism and transition state *via* a Hammett plot. Crystallisation and X-ray diffraction were used to elucidate the structure of

any stable intermediates formed during the reaction, which may affect the course of the reaction.

3.2 Results and Discussion

3.2.1 Analysis of reactive intermediates

The recrystallisation of solids formed when commercially available amines or imines were mixed with catalyst complexes allowed for the expedient elucidation of the structure of intermediates that form during the reaction through X-ray analysis. Preliminary investigations involved looking for the existence of iridium-imine complexes (**3.3**). A pre-formed iridium complex (**3.1**) was mixed with benzophenone imine (**3.2**) and the recrystallized solid was analysed by X-ray diffraction (Scheme 3.5).
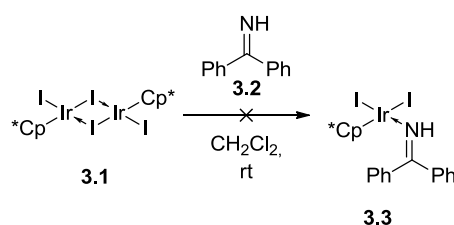
Scheme 3.5 Attempted formation of iridium-imine complex, 3.3.

Two different sets of crystals were formed during the recrystallisation procedure. X-ray studies (X-ray analysis carried out by Dr H. Sheppard, University of Leeds) revealed that two distinct species were formed. The iridium-amine complex **3.4** was identified as the structure for one set of crystals (Figure 3.3) and the second set, the unreacted iridium dimer, **3.1**. There was no evidence for the formation of the desired iridium-imine complex formation.
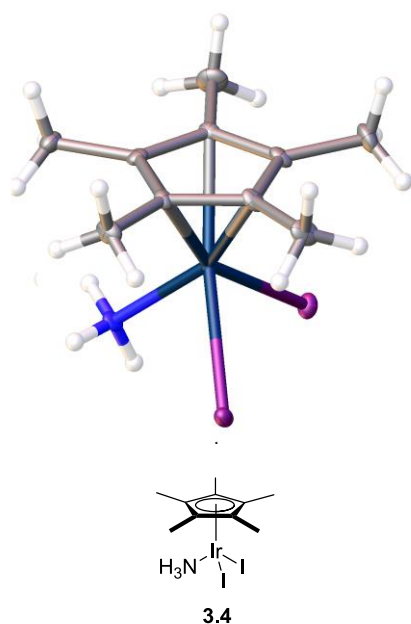
Figure 3.3 X-ray crystal structure of the iridium-amine complex 3.4 formed when SCRAM complex (3.1) and benzophenone imine (3.2) were mixed in dicholoromethane and then recrystallised.

Comparison of the crystal structure of iridium-amine complex **3.4** at room temperature revealed that the Ir-N bond length was 2.159 Å, the Ir-C_g distance was 1.799 Å and the average Ir-I bond length was 2.746 Å, which were all in accordance with the literature (similar to 2.133 (Ir-N), 1.783 (Ir-C_g) and 2.715 Å (Ir-I), respectively).[77] The presence of these two compounds within the reaction mixture indicated that instead of the desired coordination complex being formed the N=C bond of the imine was cleaved, presumably facilitated by the imine nitrogen being iridium bound, leading to the formation of the iridium-amine complex, reported by Blacker and co-workers (Scheme 3.6).
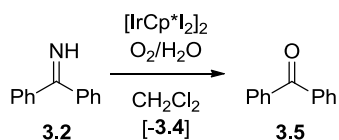
Scheme 3.6 Formation of iridium-amine complex 3.4, *via in situ* oxidation of benzophenone imine (3.2) to benzophenone (3.5) by SCRAM catalyst (3.1) and an oxidant.

Absence of the characteristic imine-proton peak at 9.34 ppm,[114] further showed that benzophenone imine was not present in the ^{1}H NMR of the mother liquor (Figure 3.4).

Benzophenone **3.5** however was observed, indicating that the imine had in fact undergone an *in situ* oxidation or hydrolysis, presumably due to oxygen and/or water in the atmosphere of the crystallisation vessel.
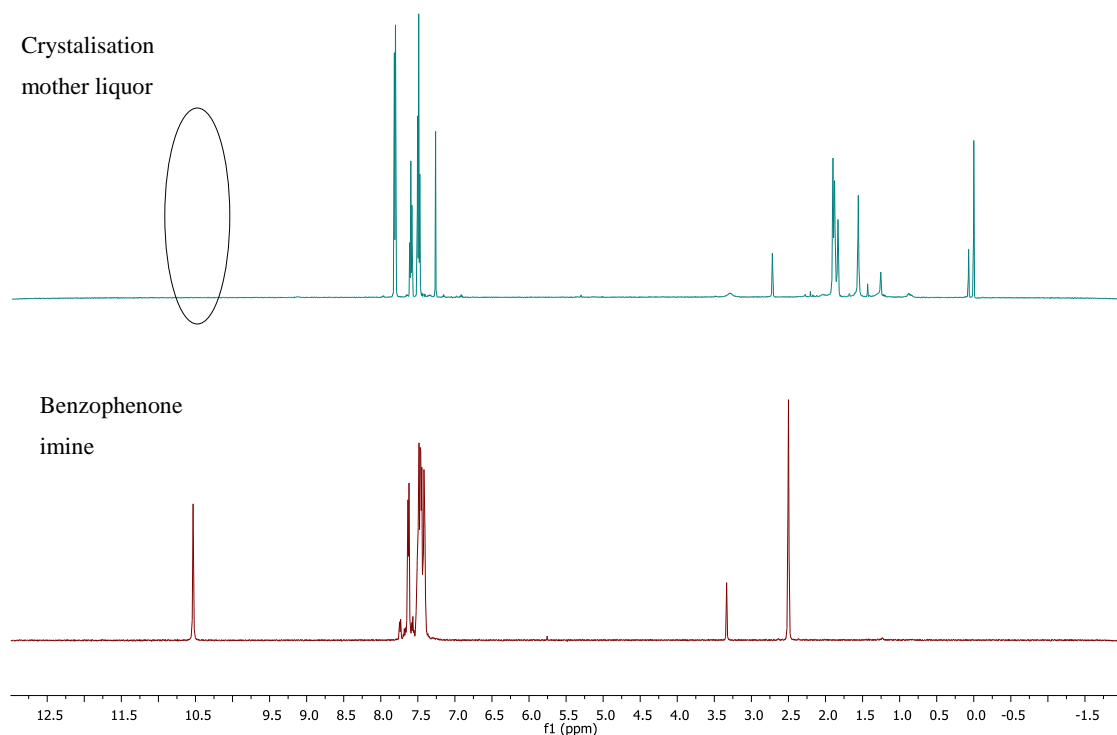
Figure 3.4 ^{1}H NMR of benzophenone imine 3.2 and SCRAM complex (3.1) mother liquor not containing highlighted peak (top) and benzophenone imine 3.2 standard containing the characteristic imine proton.

As solid state analysis of the key catalyst bound imine intermediate was not possible, further solution phase reaction structural characterisation was instead used to give greater insight into the mechanism in solution.

3.2.2 1D and 2D NMR studies of amine *N*-alkylation and substrate catalyst binding

3.2.2.1 1D NMR

The binding of the amine to the catalyst can be monitored during catalyst-substrate binding studies *via* ^{1}H NMR analysis, as the amine and the α-proton to the amino-group undergo

chemical shift changes between the non-bound and bound states. Stoichiometric studies using NMR titration were carried out with a range of primary, secondary and tertiary amines and the iridium catalyst complex **3.1** (Scheme 3.7), allowing direct comparison of benzylic and alkyl-amines, **3.6** and **3.10**, and therefore, studies on electronic effects, **3.7-3.8**. Amine (**3.6-3.15**) was added to an NMR tube containing the iridium complex in DMSO-d$_6$ or CDCl$_3$ and ^{1}H NMRs were taken after each addition (Scheme 3.7, Table 3.1).
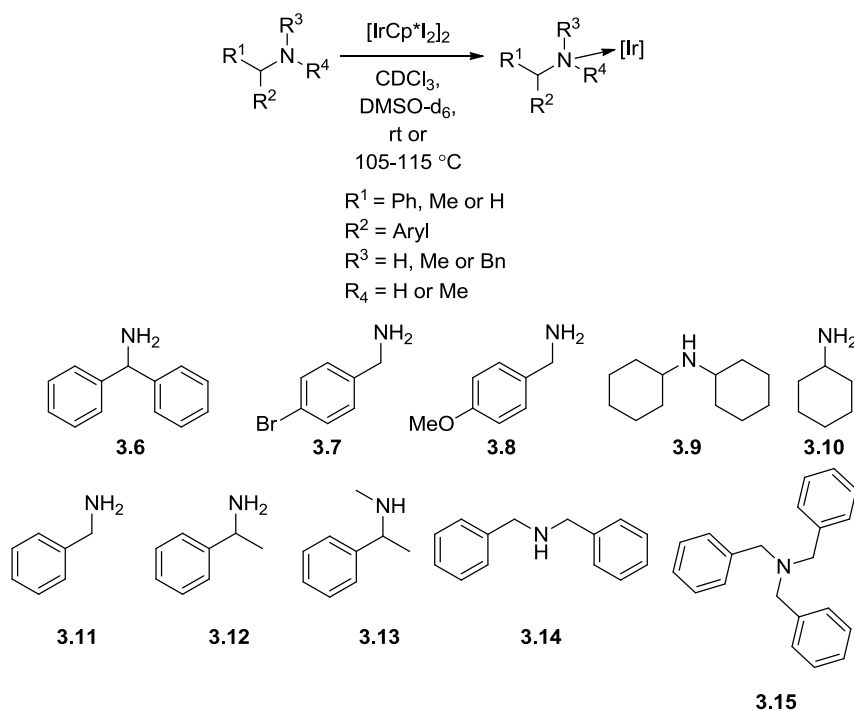
Scheme 3.7 Analysis of amine iridium catalyst binding.

Benzhydrylamine (**3.6**), used during the *N*-alkylation studies (Chapter 2), and catalyst complex **3.1** were initially investigated in the amine-binding study. It was envisioned that after the lone-pair of the nitrogen bound to the catalyst centre, the amino protons would assume a down-field chemical shift, due to lower electron density at the nitrogen *via* formation of the coordinate bond, in the catalyst bound amine complex. Furthermore, during the course of the experiment the amino protons would move from down- to up-field chemical shifts (ppm) as the equivalence of the iridium was decreased and there would be a lower probability of the amine binding to the catalyst centre.
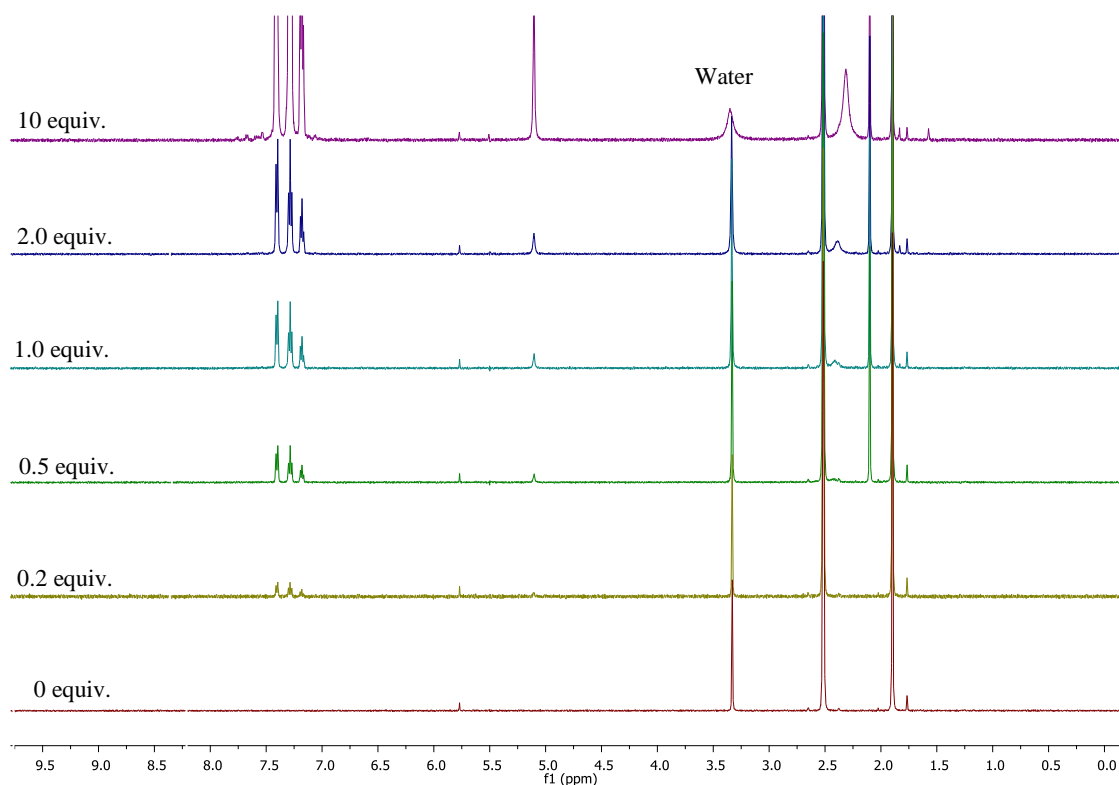
Figure 3.5 ^{1}H NMR spectra of iridium catalyst (3.1) in DMSO-d$_6$ with 0, 0.2, 0.5, 1.0, 2.0 or 10.0 equiv. of benzhydrylamine 3.6.

Amine **3.6** was added to iridium catalyst (**3.1**, 4.2 μmols, 9.4 μmols of iridium) in DMSO-d$_6$ and analysis of the resulting ^{1}H NMR spectra showed that there was a change in the chemical shift of the amine protons. As the equivalences of amine **3.6** increased in the reaction (Figure 3.5), a change in the chemical shift of the amino-proton of amine **3.6** was observed (Table 3.1). The observed, up-field chemical shift with increasing amine equivalence suggested there was no longer the presence of the amine-catalyst bond. The lack of down-field shifted signal (from the catalyst bound amine) indicated that amine coordination/decoordination is in rapid equilibrium, and at low iridium concentration a time averaged observation of free amine signal was predominant.

71

Table 3.1 Change in amino-proton chemical shift after benzhydrylamine, 3.6, addition to iridium complex, 3.1, and comparison with the free amine.[a]

Entry	Molar equivalence of amine added to the solution[b]	Δppm of amino-proton (*c.f.* free amine)	Observed Chemical shift of amino-proton / ppm
0	0	n/a	n/a
1	0.5	0.2	2.43
2	1	0.17	2.4
3	2	0.14	2.37
4	10	0.07	2.3
5	Free amine	0	2.23

[a] Iridium complex **3.1** (0.5 equiv.) was suspended in DMSO-d_6 (0.7 mL) and shaken for 60 seconds. The resulting suspension was analysed by ^{1}H NMR. Amine **3.6** (0.5-10 equiv.) was added to the resulting pale orange suspension and shaken for 60 seconds. The resulting suspension was then analysed by ^{1}H NMR, this process was then repeated for each entry.

[b] Equivalence related to the amount of iridium in solution (*i.e.* two moles of amine = two moles of iridium monomer).

The environment of the Cp*-protons, will give an insight into the environment at the iridium centre. Focusing on this region, there was a dramatic change noticeable in the Cp*-proton chemical shifts (Figure 3.6). At 0.5 equiv. of amine **3.6** the chemical shift of the Cp*-protons changed from being solely at 1.88 ppm (the pure complex) to have an additional peak at 2.10 ppm. The ratio of the two different Cp*-proton peaks was 11:4-10:5 (1.88 ppm: 2.10 ppm, Figure 3.6, Table 3.2).

Table 3.2 Changes to the chemical shifts of Cp*-protons at different equivalences of various benzylic amines.[a]

Entry	Amine	Equivalence of amine[b]	Cp* proton ppm / number of protons		
			1.88	**2.1**	
1	**Benzhydrylamine, 3.6**	0	30	0	
		0.2	29	0	
		0.5	29	0	
		1	9	21	
		2	20	10	
		10	20	10	
			1.88	**1.85**	**1.82**
2	**Benzylamine, 3.11**	0	0	0	0
		0.2	3	27	0
		0.5	0	23	7
		1	0	22	8
		2	0	15	15
		10	0	15	15
			1.88	**2.09**	
3	**Dibenzylamine, 3.14**	0	30	0	
		0.2	27	3	
		0.5	27	3	
		1	26	4	
		2	26	4	
		10	26	4	

[a] Iridium complex **3.1** (0.5 equiv.) was suspended in DMSO-d_6 (0.7 mL) and shaken for 60 seconds. The resulting suspension was analysed by ^{1}H NMR. Amine (0.2-10 equiv.) was added to the resulting pale orange suspension and shaken for 60 seconds. The resulting suspension was then analysed by ^{1}H NMR, this process was then repeated for each entry in the table.

[b] Molar equivalence related to the amount of iridium in solution (*i.e.* one mole of catalyst **3.1** was equivalent to 2 moles of iridium).

Entry	Amine	Equivalence of amine[b]	Cp* proton ppm / number of protons	
			1.88	1.75
	Tribenzylamine,	0	30	0
	3.15	0.2	29.5	0.5
		0.5	29.5	0.5
4		1	29	1
		2	29	1
		10	26	4

[a] Iridium complex **3.1** (0.5 equiv.) was suspended in DMSO-d_6 (0.7 mL) and shaken for 60 seconds. The resulting suspension was analysed by ^{1}H NMR. Amine (0.2-10 equiv.) was added to the resulting pale orange suspension and shaken for 60 seconds. The resulting suspension was then analysed by ^{1}H NMR, this process was then repeated for each entry in the table.

[b] Molar equivalence related to the amount of iridium in solution (*i.e.* one mole of catalyst **3.1** was equivalent to 2 moles of iridium).

Figure 3.6 ^{1}H NMR spectra of iridium catalyst (4.1) in DMSO-d_6 with 0, 0.2, 0.5, 1.0, 2.0 or 10.0 equiv. of benzhydrylamine 3.6; focused on the Cp*-protons region.

This observation indicated that two different iridium species were present within the reaction mixture, the new peak was either the catalyst bound amine complex **3.16** or the active catalyst monomer complex (**3.16**), similar to that which has been suggested in the

74

literature from *in silico* studies.[97] Further analysis of the NMR values of the different Cp*-environments could potentially indicate the direction of any equilibrium.

Analysis of the concentrations of different species at different concentrations was used to give a potential value for the equilibrium constant, K_c. The equilibrium between the free amine and dimeric catalyst with the monomeric amine bound catalyst was believed to be the equilibrium that was observed (Scheme 3.8).
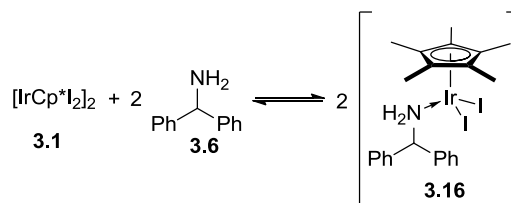
Scheme 3.8 Potential equilibrium between non-bound and catalyst bound amine.

The Cp* protons of the dimeric catalyst in solution have a chemical shift of 1.88 ppm, the new species, which was assigned as a monomeric iridium species, has Cp* protons with a chemical shift of 2.10 ppm, which has been shown in previous literature.[97] These two species were compared to that for the benzylic protons of the free amine at a chemical shift of 5.09 ppm at different concentrations (Table 3.3), in order to give an indication of the equilibrium constant of the amine bound catalyst.

Table 3.3 Concentration of different species within the ^{1}H NMR analysis of benzhydrylamine and catalyst 3.1 coordination.[a, b]

Amine in solution / equiv.	Volume of DMSO-d$_6$/ μL	Concentration in solution / species mL^{-1}		
		Dimeric catalyst complex (1.88 ppm)	Monomer catalyst complex (2.10 ppm)[c]	Free benzhydrylamine
0	700	4.69	0	0
0.2	717	5.31	0.08	2.93
0.5	742	4.76	4.02	6.46
1	784	4.21	3.80	10.71
2	869	3.43	3.10	16.57
10	869	3.15	3.18	81.14

[a] Iridium complex **3.1** (0.5 equiv.) was suspended in DMSO-d$_6$ (0.7 mL) and shaken for 60 seconds. The resulting suspension was analysed by ^{1}H NMR. Amine (0.2-10 equiv.) was added to the resulting pale orange suspension and shaken for 60 seconds. The resulting suspension was then analysed by ^{1}H NMR, this process was then repeated for each entry in the table

[b] Calculated by normalising the spectrum to DMSO-d$_6$ (if applicable over the range including the amine integral and ensuring that this does not affect the integral, 6 protons), then dividing the new integrals by the volume of DMSO-d$_6$ added.

[c] Monomer value was multiplied by 2 as the ratio of dimeric to monomeric protons was 2:1

From these results it became apparent that there was an optimum concentration for the formation of the complex with chemical shift 2.10 ppm (Figure 3.7), after which both dimeric catalyst **3.1** and the monomeric derivative **3.16** had higher concentrations. The graph suggested that the highest concentration of the monomeric species was between 0.5-0.6 equiv. of amine.
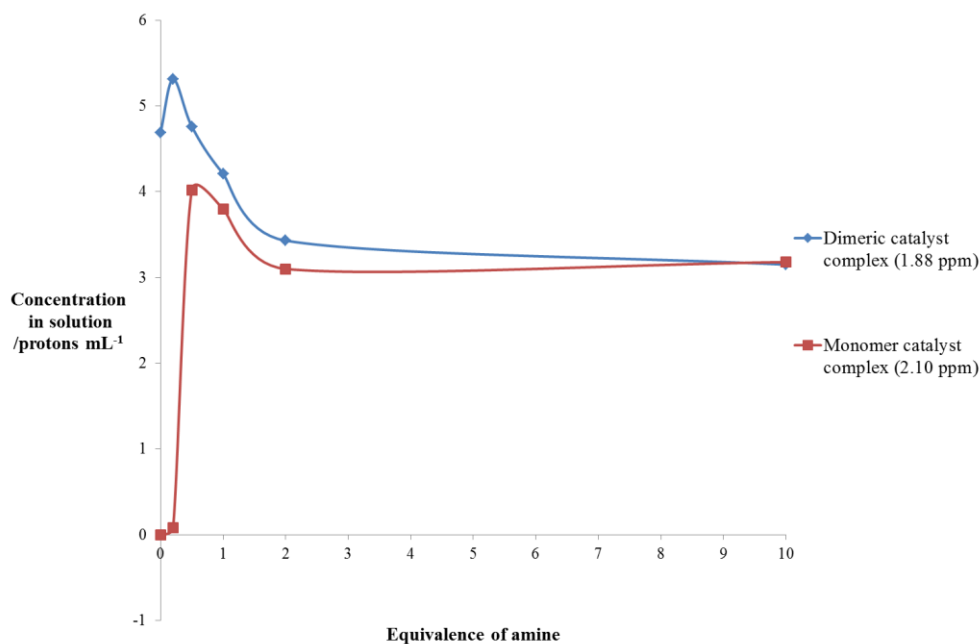
Figure 3.7 Concentration of species in solution vs amine equivalence for benzhydrylamine iridium catalyst coordination experiment.

To calculate a potential equilibrium constant, K_c, Equation 3.1 was used. The concentrations for both dimeric and monomeric complex when monomeric complex was at its maximum were 4.65 and 4.1 species mL^{-1}, respectively. When these values were used for the calculation, along with a benzhydrylamine concentration of 6.3 species mL^{-1}, K_c was 0.574. This value represents a potential figure for K_c, as the reaction may behave differently in the non-polar solvents generally used for dehydrogenation reactions. These solvents also have differences in solubility, such that each species considered may not have been completely in solution. However, this value indicated that the equilibrium lied toward free amine and dimer, thus supporting literature evidence that breaking of the dimer to the monomer is important for successful dehydrogenation reactions.
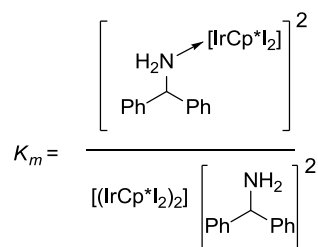
Equation 3.1 Equilibrium equation for benzhydrylamine catalyst binding.

To further assess the affects observed on both the amino- and the Cp*-protons and gain further mechanistic and structural understanding a range of amines were evaluated using the same methodology.

Benzylamine, **3.11**, a benzylic primary amine is not as sterically encumbered as amine **3.6** after binding to the iridium centre, which would be more facile. Amine **3.11** was added to a solution of iridium complex (**3.1**) in DMSO-d_6 and ^{1}H NMR analysis was again carried out to probe for any changes in environment caused by the amine binding to the iridium centre (Table 3.1, Figure 3.8).
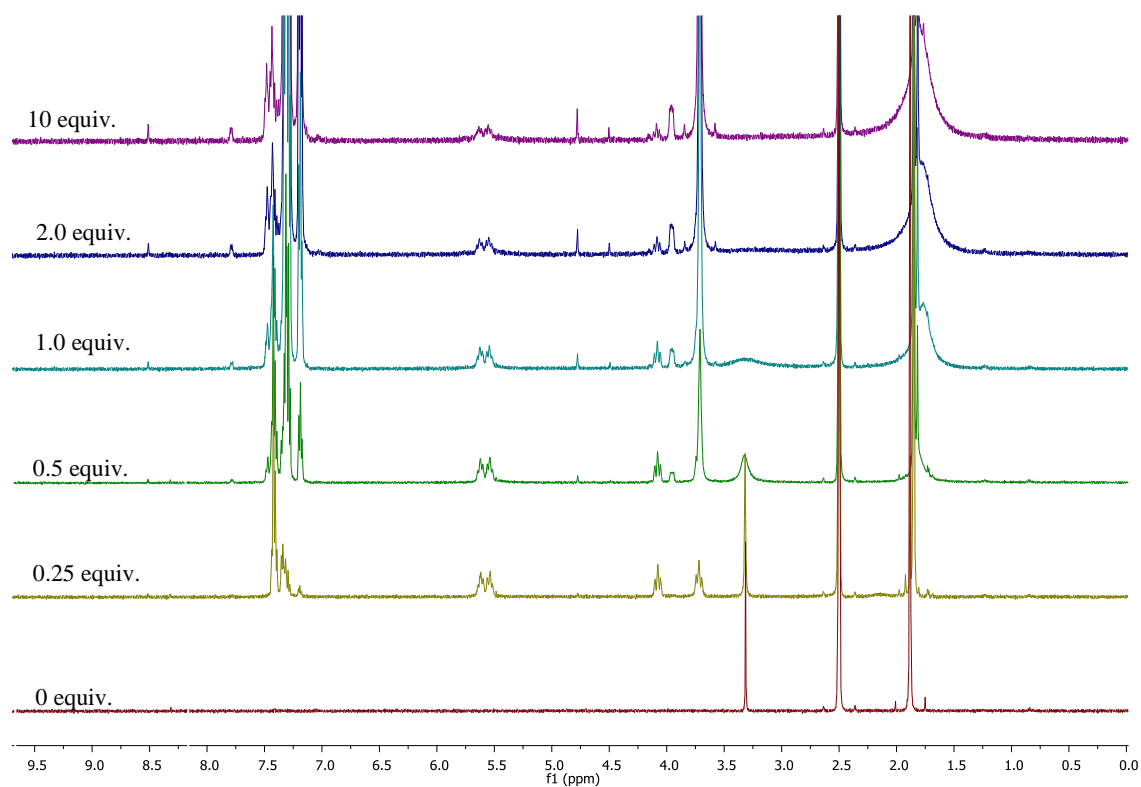
Figure 3.8 ^{1}H NMR spectra [IrCp*I$_2$]$_2$ in DMSO-d_6 with 0, 0.2, 0.5, 1.0, 2.0 or 10 equiv. of benzylamine, 3.11.
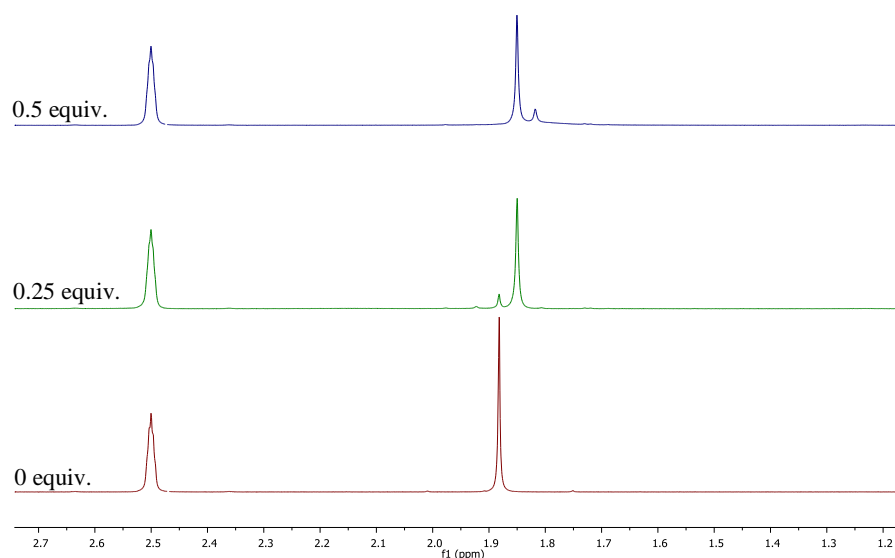
Figure 3.9 ^{1}H NMR spectra focused on the Cp*-protons, containing [IrCp*I$_2$]$_2$ (0.5 equiv. of dimer, 1 equiv. of iridium monomer) and 0, 0.2 or 0.5 equiv. of amine 3.11 in DMSO-d$_6$ (0.7 mL).

The ^{1}H NMR analysis showed the presence of three different Cp*-proton environments (Figure 3.9, Table 3.2), similar to benzhydrylamine, however the chemical shift for these peaks was 1.88 (free Cp*-dimer), 1.85 (after 0.2 equiv. of amine addition) and 1.82 ppm (0.5-10 equiv.) respectively.

With the 0, 0.2 and 0.5 equiv. of amine NMRs there is an observable progression in the Cp* region from 1.88 to 1.82 ppm (Table 3.2). The ratio of the Cp*-proton environments between 1.88, 1.85 and 1.82 ppm was 1:0:0, 2:13:0 and 0:12:3; for the 0, 0.2 and 0.5 equiv. respectively. Quantitative analysis of the ratios for the three environments was not possible for the spectra with 1, 2 and 10 equiv. of amine as the amino-protons for the free benzylamine (1.73 ppm) altered the intergration of the Cp*-protons. Qualitatively however, there is no evidence for the 1.88 ppm species in the spectra, but the peak heights for the 1.85 and 1.82 ppm species have become equivalent. The removal of the 1.88 ppm species indicated that the dimer complex must break before reaction can take place, providing empirical evidence for Madsen's *in silico* postulate of a monomeric species being the active catalyst.[97] Comparison of mono-benzylamine through to tribenzylamine has shown that as substitution increases there is a reduction in the amount that the Cp*-protons are affected and the formation of a third species not being observed nor a reduction in the amount of a second species at 2.10 or 1.75 ppm being observed for both di-and tri-benzylamine, respectively, also.

The region of the spectra between 3.5 and 6.0 ppm showed a change as the equivalences of amine increased through the course of the reaction (Figure 3.10). Firstly the protons at 3.72 and 4.08 ppm were two separate sets of triplets, assigned as the benzylic protons. The first proton at 3.72 ppm was at the same chemical shift as the benzylic protons of the free amine, as indicated most noticeably in the top stacked spectra (Figure 3.10). A triplet however, was more downfield at 4.08 ppm and integration of the spectrum confirmed that each peak was a separate proton. In the free amine the benzylic protons appeared as a singlet, whereas in the recorded spectrum the inequivalency observed indicated a change to a more constrained structure of amine **3.6** and catalyst complex **3.1** where proton exchange cannot take place.
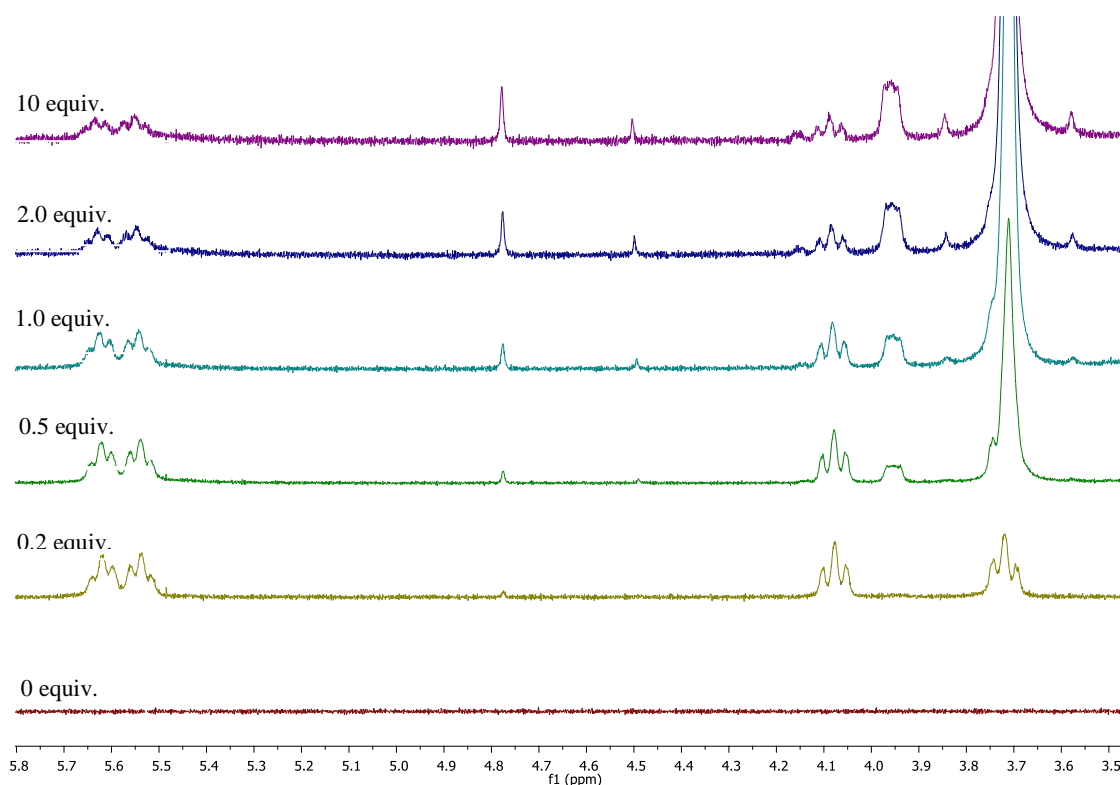
Figure 3.10 ^{1}H NMR spectra of [IrCp*I$_2$]$_2$ in DMSO-d$_6$ and 0, 0.2, 0.5, 1.0, 2.0 or 10.0 equiv. of benzylamine, 3.11; focusing on the region 3.5-6.0 ppm.

The protons observed at 5.58 ppm as a doublet of triplets, were assigned as the amino-protons of an iridium-bound benzylamine (Figure 3.11). The change in the chemical shift of the amino-protons of 3.85 ppm (to 5.58 ppm) places their environment in a region between that of the free amine (1.73 ppm) and those of the ammonium hydrochloride (8.46 ppm).[115] The intermediate environment displayed by the amino-protons showed that the lone-pair of the amino-nitrogen was now coordinating to the iridium centre, reducing electron density to a level between that of free amine and ammonium ion.
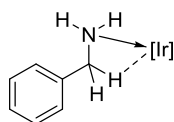
Figure 3.11 Rationale for the different chemical environments observed during ^{1}H NMR substrate-catalyst binding studies.

Table 3.4 Concentration of the three amine species at different concentration of amine in solution.[a,b]

Equivalence of benzylamine	Ratio of species		
	Free Amine (3.7 ppm)	Catalyst bound amine 1 (4.08 ppm)	Catalyst bound amine 2 (3.95 ppm)
0.2	0	1	0
0.5	9	2	1
1	16	1	1
2	42	1	2
10	70	1	3

[a] Iridium complex **3.1** (0.5 equiv.) was suspended in DMSO-d_6 (0.7 mL) and shaken for 60 seconds. The resulting suspension was analysed by ^{1}H NMR. Amine (0.2-10 equiv.) was added to the resulting pale orange suspension and shaken for 60 seconds. The resulting suspension was then analysed by ^{1}H NMR, this process was then repeated for each entry in the table

[b] Ratios calculated by integrating the species and normalising the values to the lowest value.

Further analysis revealed that a third environment for the benzylic protons was being formed at a chemical shift of 3.95 ppm after 0.5 equiv, of amine was added. The three different environments were present at different concentrations depending on the amine loading (Table 3.4, Figure 3.12). At low equiv. of amine, a catalyst bound amine species with benzylic protons at a chemical shift of 4.08 ppm predominated, being the sole species present at 0.2 equiv. of benzylamine. As the equiv. of amine increased the second species with benzylic protons at a chemical shift of 3.95 ppm began to predominated, at a ratio of 3:1 at 10 equiv.
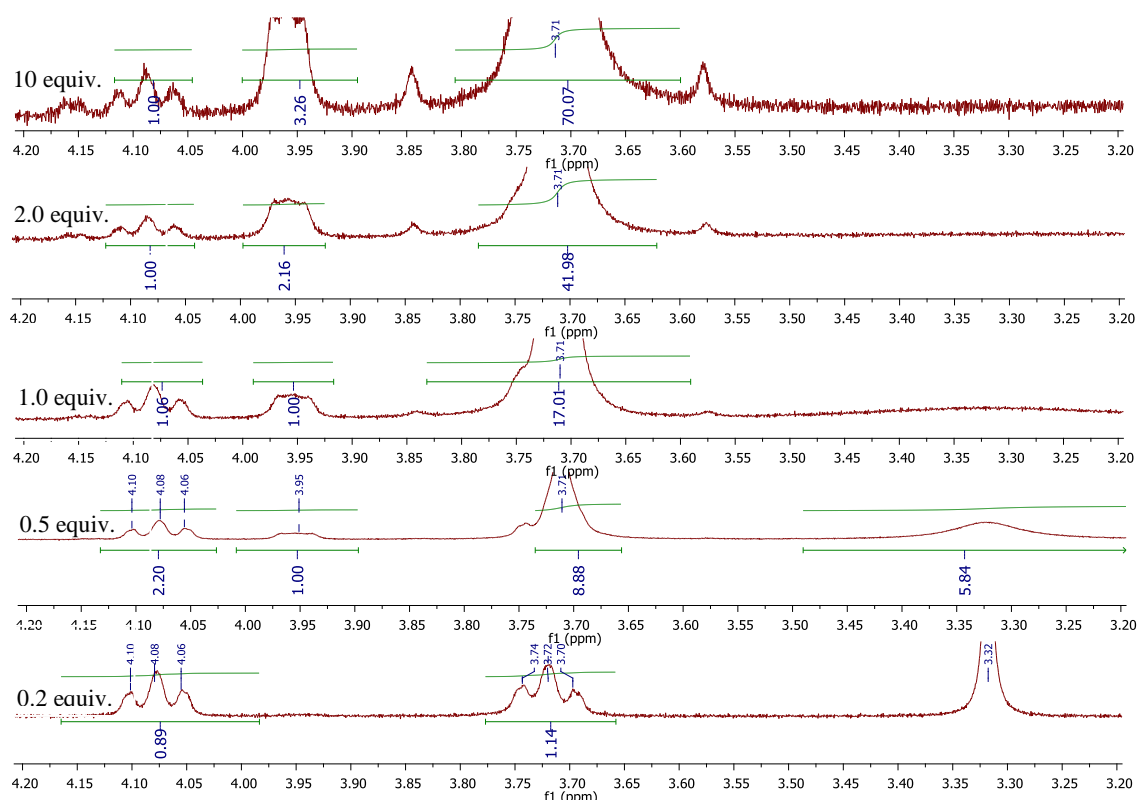
Figure 3.12 Stacked integrated spectra for the benzylic protons of free benzylamine, and two different catalyst bound amine species when 0.2, 0.5, 1, 2 or 10 equiv. of benzylamine 3.11 was added to [IrCp*I$_2$]$_2$ in DMSO-d$_6$.

Overall free amine was the predominant species, due to the large equivalences present, however the change between two different catalyst bound amine species, gave an indication of the potential mechanism for binding of amine to the catalyst during amine dehydrogenation. At low amine concentration it suggests that there would be only one amine bound to the iridium centre or that multiple iridiums may be bound to an amine centre (Scheme 3.9). At high equivalences of iridium multiple amines would be expected to bind to the iridium centre, however further analysis was required to ensure whether this hypothesis was correct. Analysis of different substitution patterns on the arene ring was carried out to see how these substrates were affected by iridium binding.
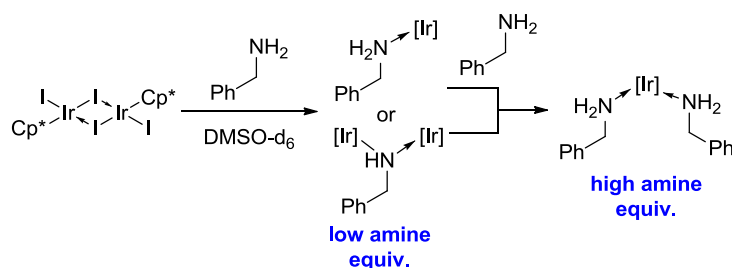
Scheme 3.9 Potential change in amine catalyst binding at first low then high equivalence of benzylamine.

Table 3.5 Change in amine proton chemical shift for different amines when mixed with [IrCp*I$_2$]$_2$.[a]

Amine	Free NH proton δ-chemical shift	NH proton δ-chemical shift with [IrCp*I$_2$]$_2$	Change in chemical shift
Cyclohexylamine, 3.10	2.48[b, 116]	2.93	0.45
Benzhydrylamine, 3.6	2.23	2.43	0.20
Dibenzylamine, 3.14	2.67	2.63	0.04
Benzylamine, 3.11	1.73	5.58	3.85
Dicyclohexylamine, 3.9	0.77	2.47	0.38
α-Methyl benzylamine, 3.12	1.25	1.47	0.22
N-Methyl-α-methyl benzylamine, 3.13	1.25	1.44	0.19
4-Bromo benzylamine, 3.7	1.4	5.57	4.17
4-Methoxy benzylamine, 3.8	1.42[117]	5.52 and 5.45	4.1 and 4.03

[a] Amine (1 equiv.) and [IrCp*I$_2$]$_2$ (0.5 equiv.; 1.0 equiv. of iridium) in DMSO-d$_6$ (0.7 mL) were shaken together for 60 seconds and then analysed by ^{1}H NMR.

[b] Value quoted as the mid-point from the literature value of 2.40-2.55 ppm.

Comparison of the different amine environments showed that the substituted benzylamines changed significantly when in the presence of $[IrCp*I_2]_2$ complex, compared to the free amine, this was more pronounced with the electron deficient 4-bromo, than the unsubstituted analogue and was in comparison to the electron-rich 4-methoxy analogue. The increased proximity of the nitrogen to the iridium centre due to the reduced sterics of the benzyl amines compared to benzhydrylamine, the cyclohexylamines and the α-methylbenzylamines was believed to cause the larger change in amino-proton environment.

When the α-protons to the amine were considered, these showed little variance. The only noted difference was with the benzylic protons of the benzylamines, and it was rationalised as a steric affect with the benzylamines, with the close proximity of the benzylic C-H to the iridium centre causing the proton to become more acidic, increasing its ppm chemical shift, above that of the free amine. Of further note was that the substituted benzylamines were not affected by the substituent at the 4-position, as the 4-methoxy and 4-bromo both underwent larger changes in chemical shift of their amine protons compared to that of the unsubstituted benzylamine, inspite of their activating and deactivating properties, respectively. This result suggested that there was no effect of ring system on amine-iridium bonding.

Finally, a difference between the Cp*-protons within the initial NMR containing only the iridium complex (1.88 ppm for DMSO-d_6 and 1.83 for CDCl$_3$) and that containing the various amines was observed (Table 3.6). The changes to the cyclohexylamine and dicyclohexylamine reactions, were not easy to interpret due to the reactants substrate proton environments masking the Cp*-protons. Nevertheless, at 10 equiv. of cyclohexylamine there was no evidence of the 1.88 ppm Cp* species, conversely this species was observed with dicyclohexylamine, an indication that more sterically hindered amines were not binding to the iridium centre. Of further note was that tribenzylamine, dibenzylamine and *N*-methyl-α-methylbenzylamine were also able to influence the iridium centre, indicating that although they are substituted, the reduced sterics of their substituents allowed for interaction with the iridium centre.

Table 3.6 Cp*-proton environments for different alkyl and aryl substituted amines.[a]

Entry	Amine	Equivalence of amine[b]	Cp* proton ppm / number of protons	
			1.88	
1	Dicyclohexylamine, **3.9**	0	30	
		0.2	30	
		0.5	30	
		1	30	
		2	30	
		10	30	
			1.84	1.81
2	α-Methyl benzylamine, **3.12**	0	30	0
		0.2	30	0
		0.5	15	15
		1	3	27
		2	0	30
		10	0	30
			1.83	2.04
3	*N*-Methyl-α-methyl benzylamine, **3.13**	0	30	0
		0.2	30	0
		0.5	30	0
		1	30	1
		2	30	1
		10	30	5

[a] Iridium complex **3.1** (0.5 equiv.) was suspended in DMSO-d_6 (0.7 mL) and shaken for 60 seconds. The resulting suspension was analysed by ^{1}H NMR. Amine (0.2-10 equiv.) was added to the resulting pale orange suspension and shaken for 60 seconds. The resulting suspension was then analysed by ^{1}H NMR, this process was then repeated for each entry in the table.

[b] Molar equivalence related to the amount of iridium in solution (*i.e.* one mole of catalyst **3.1** was equivalent to 2 moles of iridium).

Entry	Amine	Equivalence of amine[b]	Cp* proton ppm / number of protons 1.88			
4	**4-Bromo benzylamine, 3.7**		**1.88**	**1.84**	**1.92**	
		0	30	0	0	
		0.5	23	6	1	
		1	20	9	1	
5	**4-Methoxy benzylamine, 3.8**		**1.88**	**1.92**	**1.84**	**2.09**
		0	30	0	0	0
		0.5	19	2	6	3
		1	13	2	12	3

[a] Iridium complex **3.1** (0.5 equiv.) was suspended in DMSO-d_6 (0.7 mL) and shaken for 60 seconds. The resulting suspension was analysed by ^{1}H NMR. Amine (0.2-10 equiv.) was added to the resulting pale orange suspension and shaken for 60 seconds. The resulting suspension was then analysed by ^{1}H NMR, this process was then repeated for each entry in the table.

[b] Molar equivalence related to the amount of iridium in solution (*i.e.* one mole of catalyst **3.1** was equivalent to 2 moles of iridium).

These changes in Cp*-proton environment provided further evidence for catalyst bound amines or monomeric iridium species being formed in solution. Whilst these results had shown evidence of amine-catalyst binding, further 2D-NMR analysis was required to establish which Cp*-protons and hence iridium complex was related to these protons. Elevated temperature analysis of the dehydrogenation reactions, to look for evidence of imine in solution was also required.

3.2.2.2 Elevated Temperature Studies

10 molar equiv. of amine in suspension with 0.5 equiv. of iridium catalyst (1 molar equiv. of iridium) in DMSO-d_6 (0.7 mL) were shaken together and then heated in an oil bath (120 °C) and analysed by ^{1}H NMR (Table 3.7). Amines **3.6, 3.9-3.11** and **3.14-3.15** were heated and transient monomeric imine (<1%) formation was observed for benzhydrylamine only (Figure 3.13 and Figure 3.14).
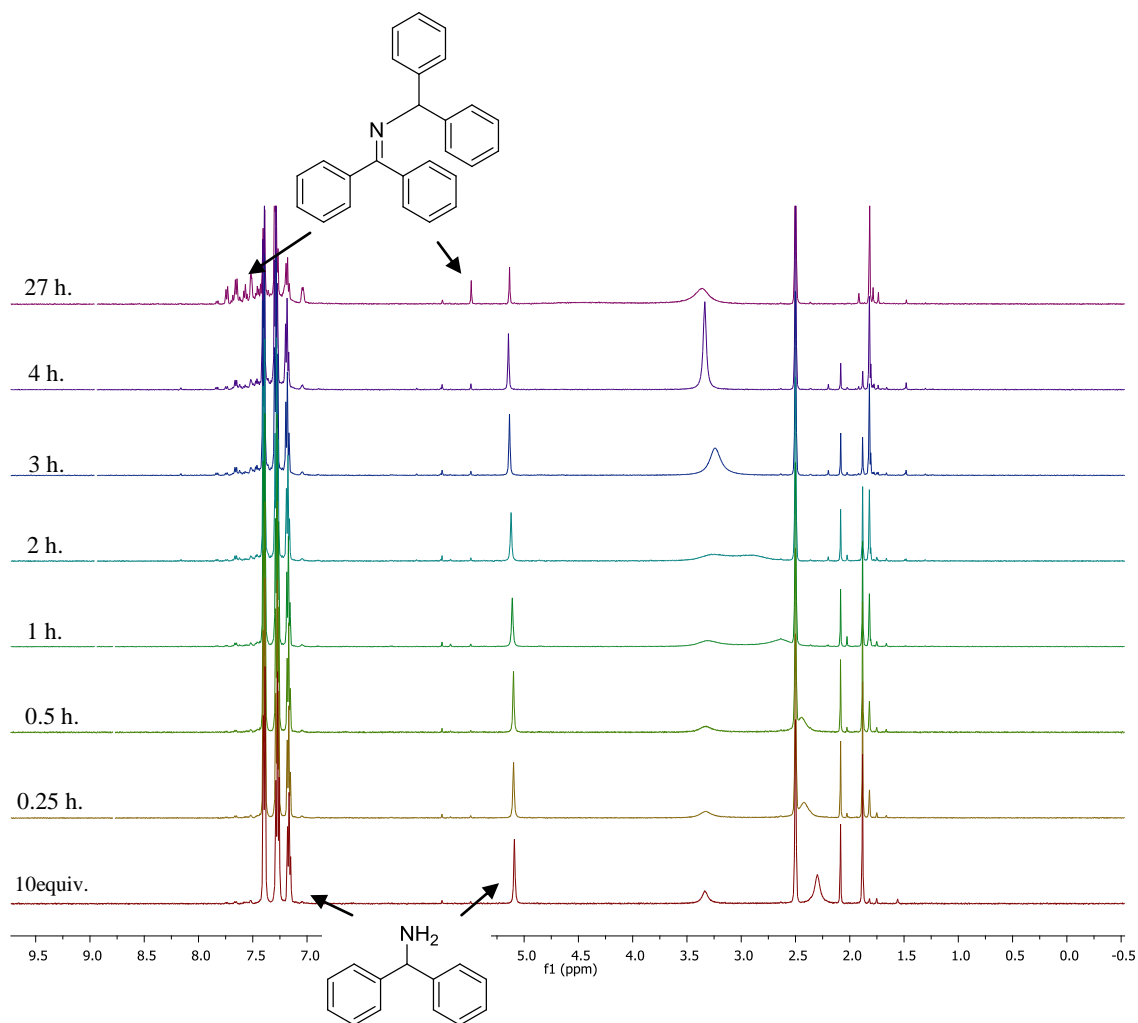
Figure 3.13 Stacked temperature time course experiment of the heating of benzhydrylamine, showing formation of benzophenone imine, *N*-benzhydryldiphenylmethanimine and dibenzhydrylamine.
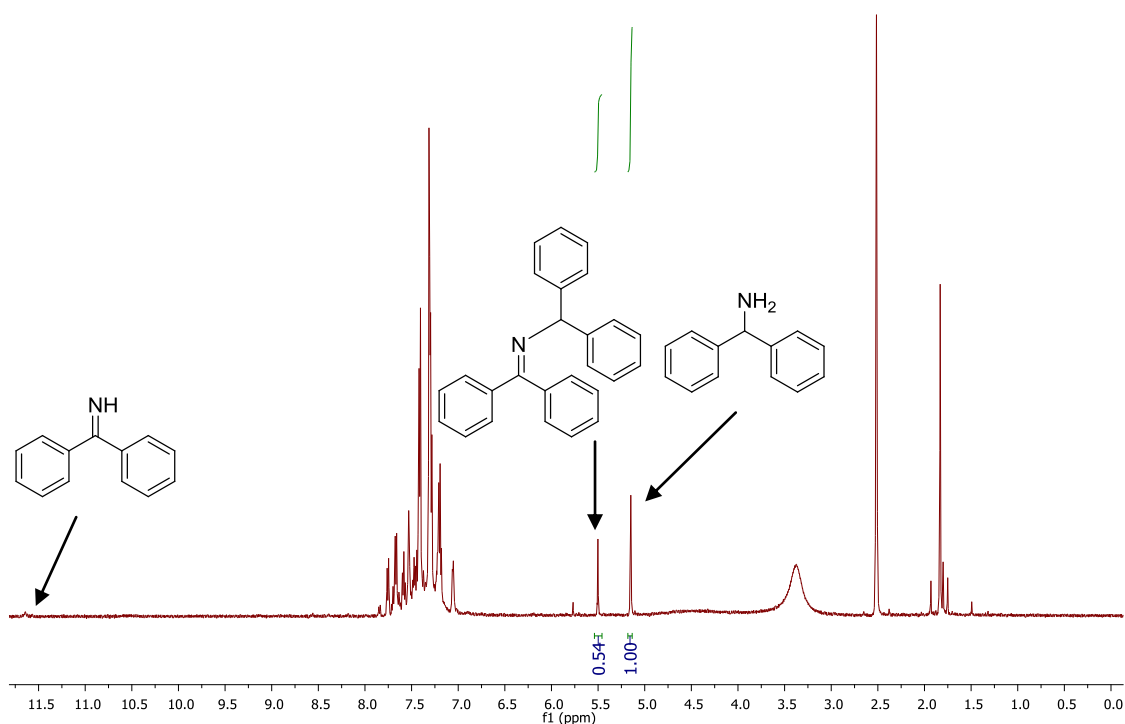
Figure 3.14 Integrated ^{1}H NMR spectrum of benzhydrylamine heated in DMSO-d$_6$, at 110 °C for 27 hours.

Benzylic primary amines and benzhydrylamine however, produced their unsaturated *N*-alkylation products. *N*-benzhydryldiphenylmethanimine was produced in a 2:1 ratio of starting material to product, which was calculated by comparison of the integrals of the benzylic protons of benzhydrylamine and *N*-benzhydryldiphenylmethanimine, after 27 hours of heating. The formation of the unsaturated *N*-alkylation product further evidenced that catalyst bound imine is highly reactive, and will readily undergo the *N*-alkylation reaction. Benzylamine reacted faster than the other primary amines as noticeable quantities of *N*-benzylidene-benzylamine (a ratio of 10:1, of starting material to product) were observed even after 0.25 hours, rising to complete imine product after 27 hours (Figure 3.15 and Figure 3.16).
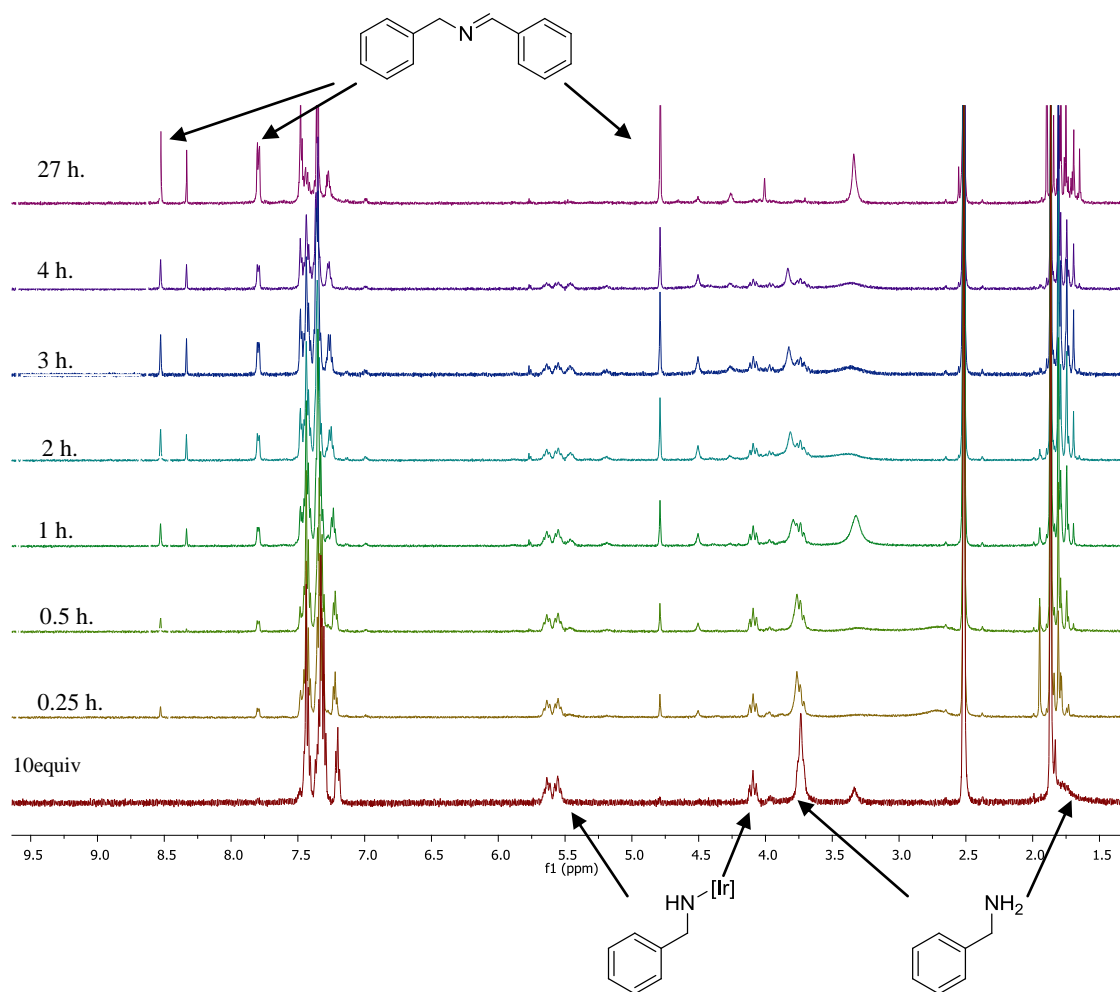
Figure 3.15 Stacked temperature time course experiment of the heating of benzylamine, showing formation of *N*-benzylidene benzylamine, dibenzylamine from potential catalyst bound benzylamine.
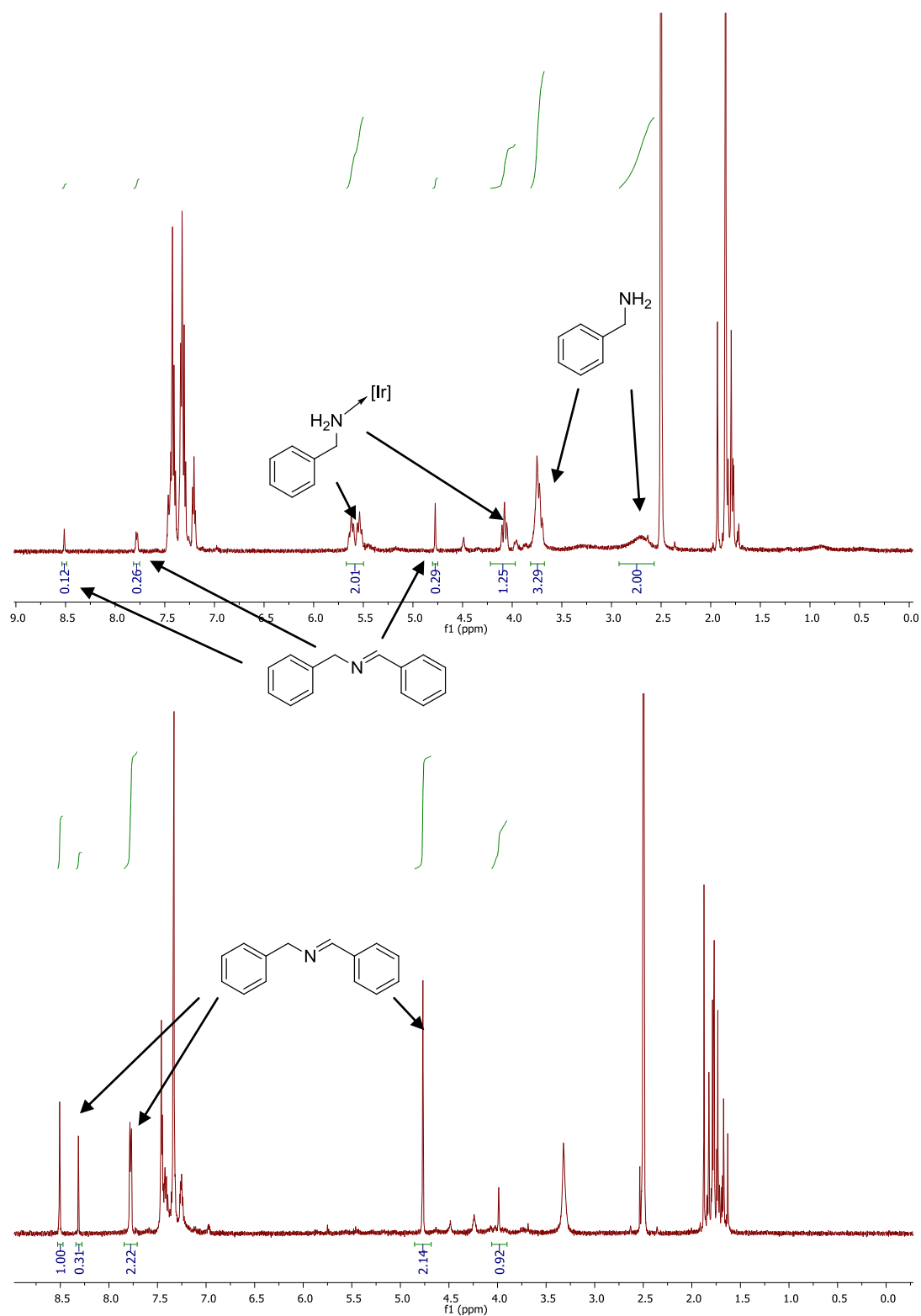
Figure 3.16 Integrated ^{1}H NMR spectrum of benzhylamine heated in DMSO-d$_6$, at 110 °C for 0.25 hours (top) and 27 hours (bottom).

Of further note, no evidence for the dehydrogenation products of either di-or tribenzylamine or dicyclohexylamine, also heated using the same procedure was observed after 4 hours (Figure 3.17 and Figure 3.18).
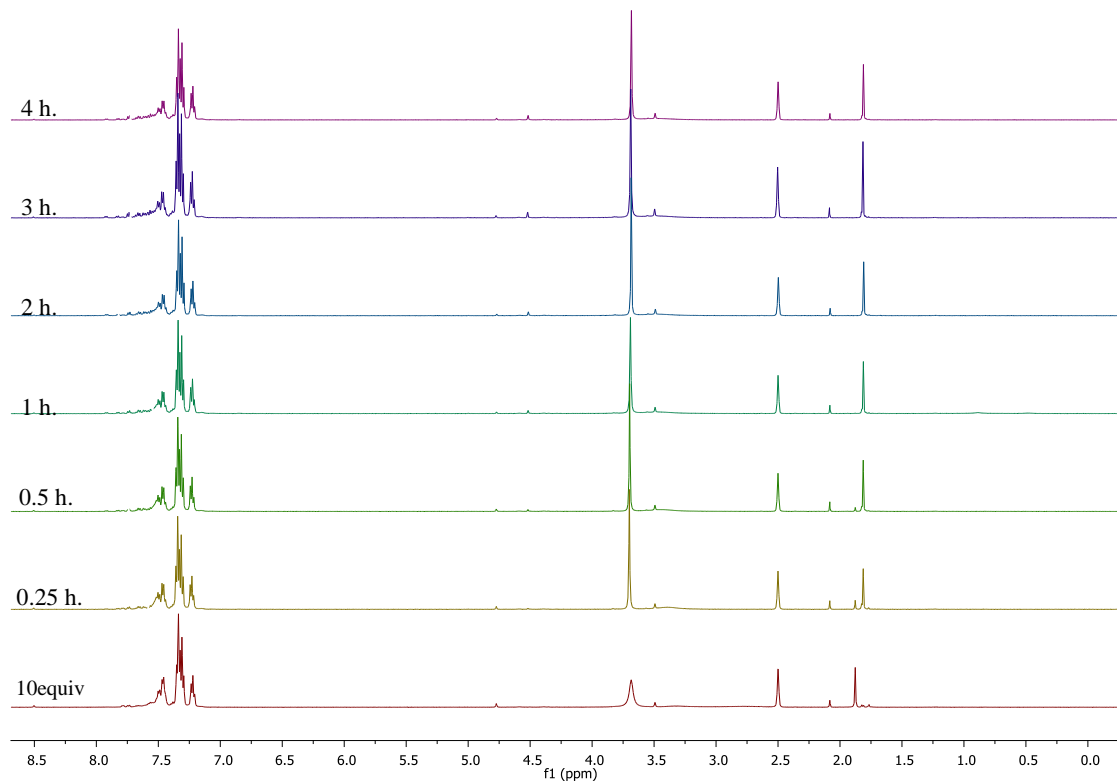
Figure 3.17 Stacked ^{1}H NMR spectra for the heating of dibenzylamine at 115 °C (oil bath temperature) in DMSO-d$_6$.
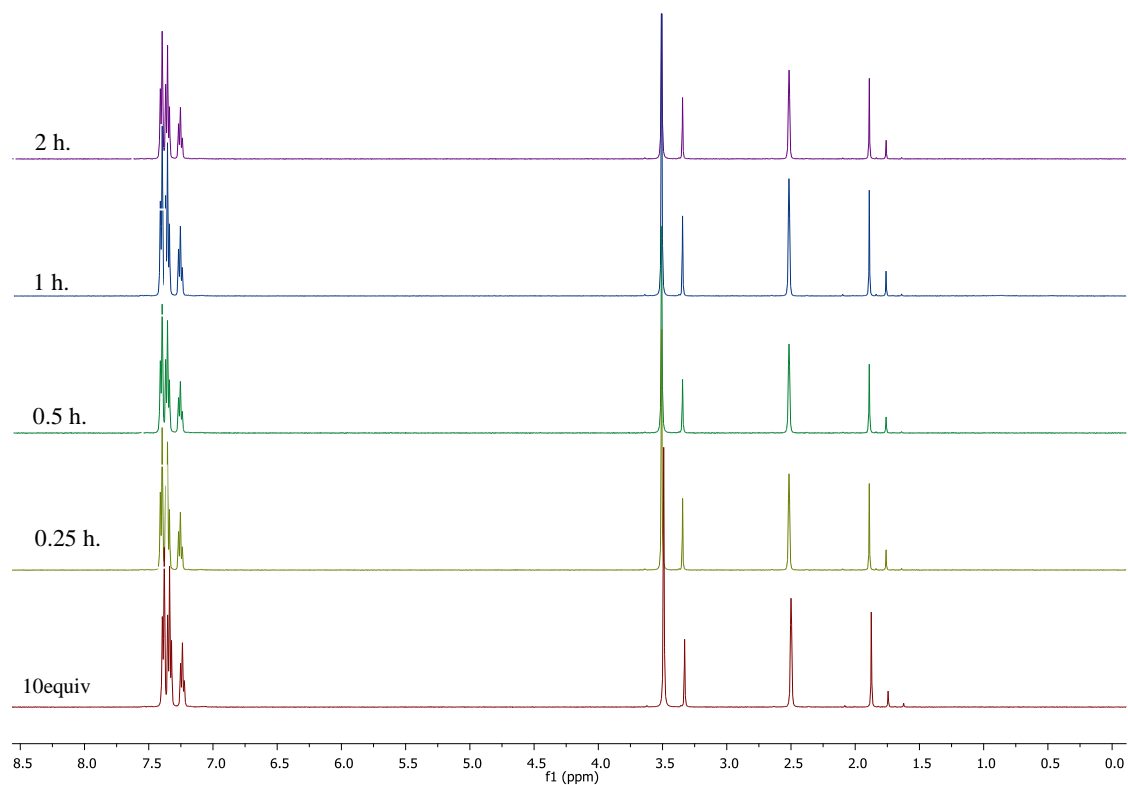
Figure 3.18 Stacked ^{1}H NMR spectra for the heating of tribenzylamine at 115 °C (oil bath temperature) in DMSO-d$_6$.
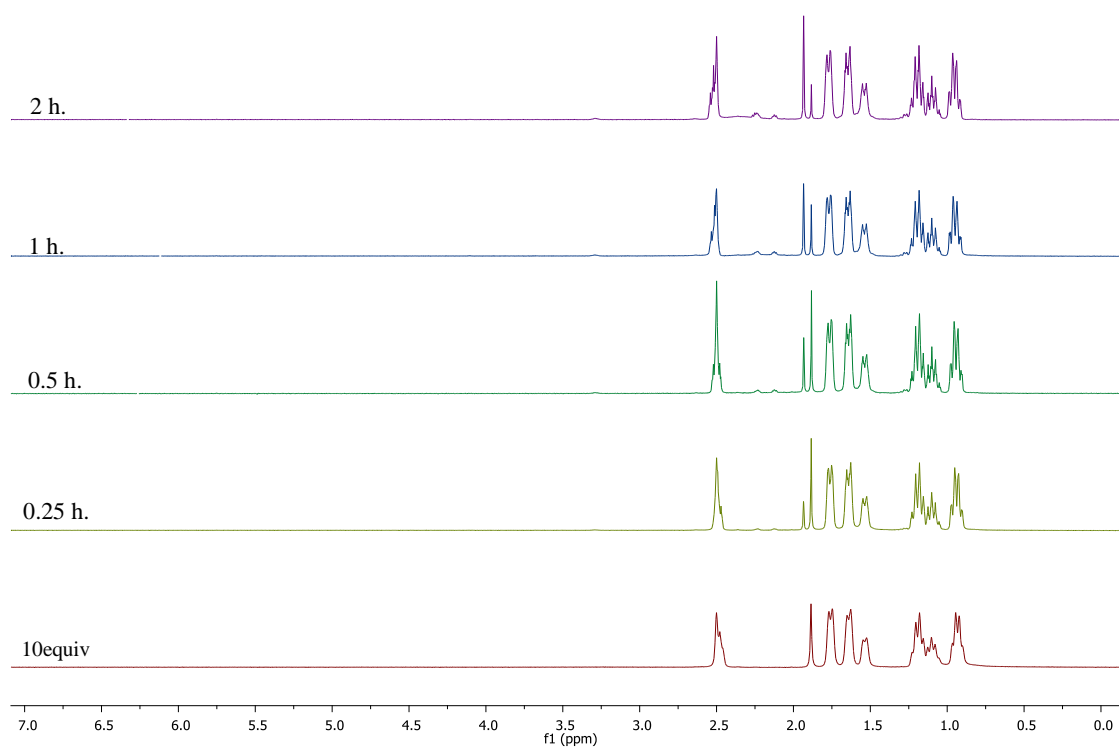
Figure 3.19 Stacked ^{1}H NMR spectra for the heating of dicyclohexylamine at 115 °C (oil bath temperature) in DMSO-d$_{6}$.

Finally cyclohexylamine was assessed, however due to similarities between the solvent and substrate or product-protons full analysis was not possible (Figure 3.20). What was clear however was that the no reaction was observed after heating for two hours. These results indicated that the less sterically crowded and benzylic amines are more active in the dehydrogenation and their ease of coordination may facilitate a quicker reaction.
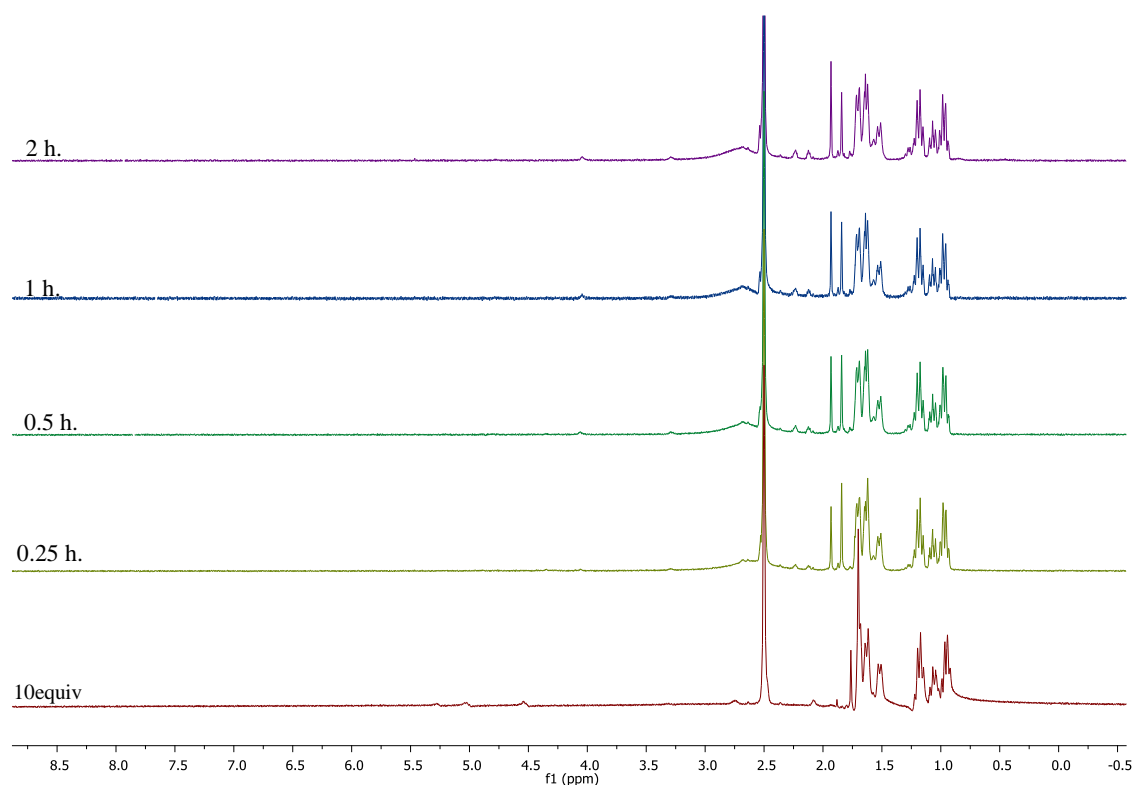
Figure 3.20 Stacked ¹H NMR spectra for the heating of cyclohexylamine at 115 °C (oil bath temperature) in DMSO-d₆.

The observation of rapid dehydrogenation with benzylamine and the slower rate with the secondary amines and alkyl amines provided further evidence to explain Williams' observations during the cross-coupling of benzylamines and isopropyl amines (Scheme 3.4). During the reaction, the benzylamine can self-condense preferentially to form *N*-benzylidene-benzylamine (**3.17**), observed in the ¹H NMR of the high temperature reaction (Scheme 3.10, Figure 3.13). The formation of dimeric imine **3.17**, allowed for the *N*-alkylation of the alkylamine to hemi-aminal **3.20** and then secondary amine **3.22**. Amine **3.22** formed from this process, will preferentially undergo dehydrogenation at the benzylic, over the alkyl centre, as shown by the high temperature experiments, therefore the cross and not-homo-coupled product will predominate.
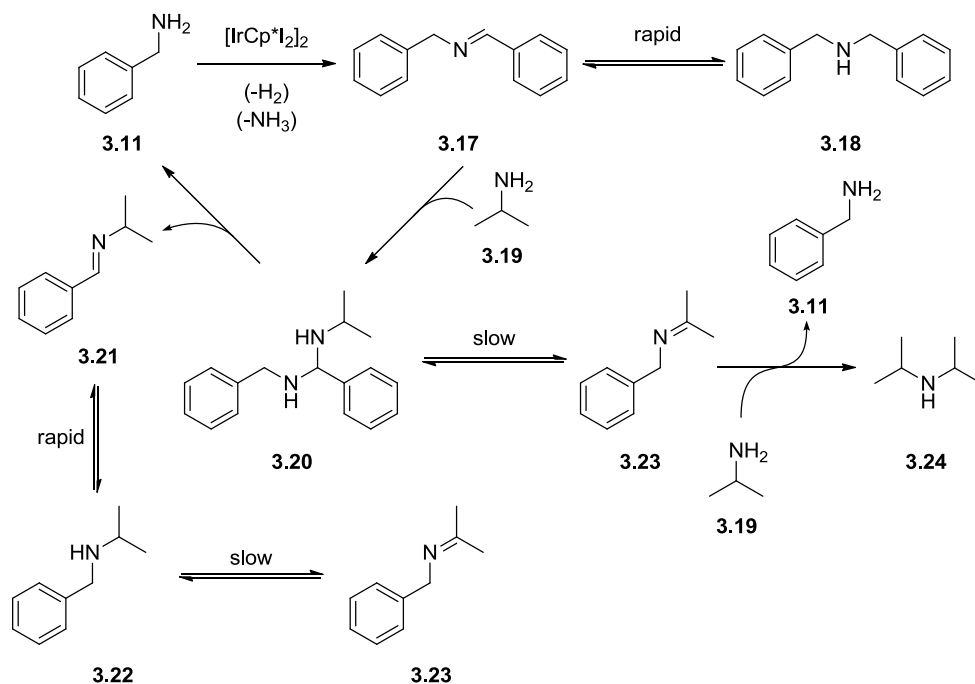
Scheme 3.10 Potential mechanistic rationale for Williams' observed amine cross-coupling over homo-coupling.

The Cp*-protons changed chemical shift during the course of the high temperature reactions. During the benzhydrylamine experiment the Cp*-protons changed from one species at 1.88 ppm to form a new species at 1.82 ppm (after 180 min.) then, after 1620 min., to produce fours species, at 1.88, 1.92, 1.78 and 1.74 ppm. A similar situation was observed with the benzylamine, where the initial species was at 1.85 ppm, and numerous other species were observed after 240 min., by 1680 min. the peak at 1.88 ppm was predominant, but there were still numerous species present in the mixture. When moving to dibenzylamine, the Cp* was less complicated, the protons moved from 1.88 ppm to more upfield 1.83 ppm with heating until after 246 min. a species at 1.81 ppm was predominant. Finally, tribenzylamine showed no change in the Cp*-proton environment. This led to a similar observation as for the stoichiometry investigation, as the greater number of species that are formed with the less substituted amine indicated that the smaller the amine the more it can interact with the metal catalyst, furthermore it showed that heating was required to induce a change in the dibenzylamine, presumably due to the energetic cost of binding to the metal centre.

Table 3.7 ^{1}H NMR monitoring of the dehydrogenation of amines heated in an oil bath at 120 °C.[a]

Amine	Ratio of starting amine protons to solvent protons[b]	Ratio of amine protons to solvent protons [b]	Ratio of dimer imine protons to protons of solvent[b]
Benzhydrylamine, 3.6	4.85	4.0 (0)[c]	0.4 (11.5)[c]
Benzylamine, 3.11	1.94	0.9 (0.3)[c]	0.7 (1.2)[c]
Dibenzylamine, 3.14	8.85	11.1	0.2
Tribenzylamine, 3.15	9.66	9.6[d]	0

[a] Amine (10 equiv.) and [IrCp*I$_2$]$_2$ (0.5 equiv.; 1.0 equiv. of iridium) in DMSO-d$_6$ (0.7 mL) were shaken together for 60 seconds and then analysed by ^{1}H NMR. The mixture was then heated in an oil bath (T = 120 °C), the reaction was monitored by ^{1}H NMR after 0.25, 0.5, 1, 1.5, 2, 3 and 4 hours.

[b] Concentration after 4 hours calculated by comparison of characteristic benzylic proton peaks to the solvent protons to give the number of protons of the molecule per molecule of solvent protons.

[c] Concentration after heating overnight.

[d] After 2 hours at 120 °C.

A similar situation can be seen with dicyclohexylamine, where Cp*-protons changed from 1.88 ppm initially to form a species at 1.93 ppm after 15 min. which dominated after 120 min. Furthermore, with cyclohexylamine there was a change from 1.76 ppm to 1.84 and 1.93 ppm observed after 15 min. of heating, which were in equal quantities. Further NMR analysis was required to gain a greater insight into the mechanism of amine dehydrogenation, as such 2D-NMR techniques, principally [1]H-DOSY was employed to give further insight into the reaction, and to try to elucidate the structure of the different Cp*-protons.

3.2.3 2D NMR analysis

[1]H DOSY spectroscopy was used to establish which Cp*-protons were related to the doublet of triplets and the two distinct triplets observed during the analysis of the ^{1}H DOSY when 0.2 equiv. of benzylamine (**3.11**) was mixed with iridium complex (**3.1**, Figure 3.10). A sample containing 0.5 equiv. of benzylamine, 0.5 equiv. iridium complex and DMSO-d$_6$ was analysed using [1]H-^{1}H DOSY spectroscopy (Figure 3.21, [1]H-DOSY spectroscopic analysis and diffusion coefficient determination carried out by Dr J. Fisher, University of Leeds).
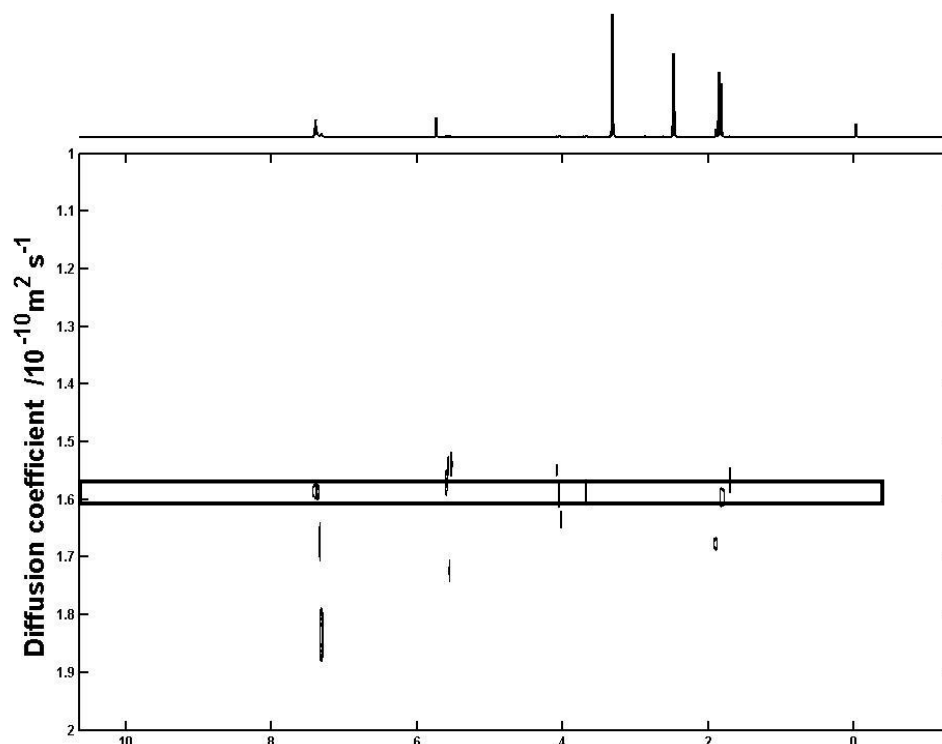
Figure 3.21 DOSY NMR spectra for a sample of benzylamine 0.5 equiv. benzylamine mixed with 0.5 equiv. iridium complex in DMSO-d$_6$, with highlighted catalyst species at diffusion coefficient.1.59 m^{2}s^{-1}.

The analysis of the ^{1}H DOSY spectra established that the doublet of triplets at 5.58 ppm and the two distinct triplets at 3.72 ppm and 4.08 ppm had the same diffusion coefficient, 1.59×10^{-10} m^{2}s^{-1}, as the aryl protons and the Cp*-protons at chemical shift 1.85 ppm. The ratio of integrals of the Cp*-protons, benzylic and amino-protons was: 15:4:4; establishing that the species comprised two benzylamines bound to an iridium centre (Figure 3.22).
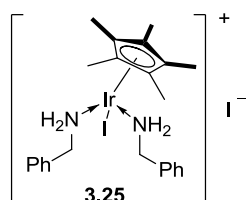
Figure 3.22 Proposed structure (3.25) of the complex formed during addition of benzylamine (3.11) to iridium catalyst (3.1).

The proposed structure implied that the complex was di-cationic (with iodides as the counter ions). Comparison of the stoichiometric analysis confirmed that the initial dimeric iridium complex **3.1**, converts to the monomeric *bis*-amine complex **3.25** or catalyst bound amine complex **3.29**, inferring a potential inner sphere mechanism for the *N*-alkylation process. The ^{1}H DOSY could not, however, confirm whether there were associated amine protons with those observed at 1.82 ppm, which are likely to be associated with the species at 1.85 ppm. HRMS analysis was used to confirm species **3.25** was present and elucidate the potential structure of this species.

3.2.3.1 Hammett analysis of amine dehydrogenation

3.2.3.1.1.   Aryl substitution effects on the rate of dehydrogenation of various 4-substituted benzylamines

The Hammett analysis can prove key to investigate the reaction mechanism and probe the structure of the transition state during the rate determining step, and it was therefore carried out on substituted benzylamines (Scheme 3.11, Table 3.8). It was envisaged that the study would allow understanding of how the activity would change at a benzylic centre depending on the substituents of the aryl ring on the rate of reaction (even at a pKa 9.33).[118, 119]
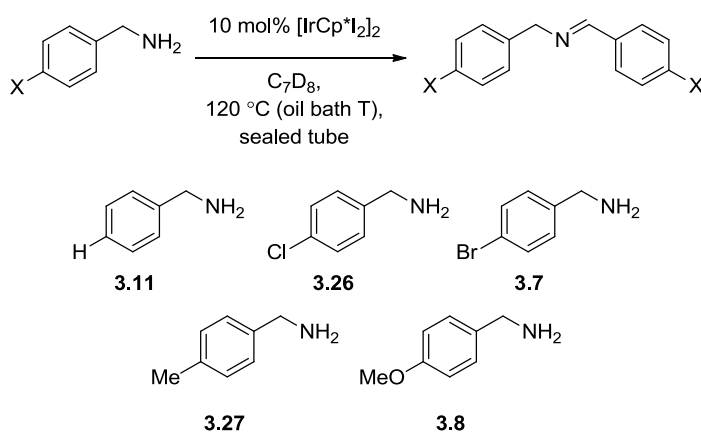
Scheme 3.11 Analysis of the effect of the 4-substituent of aryl rings on benzylamine dehydrogenation.

Table 3.8 Results of the Hammett analysis of the dehydrogenation of 4-substituted benzylamines, 3.7-3.8, 3.11 and 3.17-3.18.

Entry	X	Rate of consumption of substrate (k_X) / μmol min^{-1} [b]	$\log(k_X/k_H)$	σ-value[120]
1	H	-0.000333	0	0
2	MeO	-0.000277	-0.080	−0.268
3	Me	-0.00144	0.636	−0.170
4	Cl	-0.00317	0.979	+0.227
5	Br	-0.0138	1.620	+0.232

[a] Amine (2 mmols), biphenyl and iridium catalyst **4.1** (1 mol%) were heated in toluene-d$_8$ (0.7 mL) to 120 °C (oil bath temperature), in a sealed NMR pressure tube.

[b] Calculated *via* NMR analysis and comparison of proton integral normalised with solvent integration over 180 min.

A variety of 4-substituted benzlyamines were heated, with the iridium catalyst **3.1** in an oil bath and the rate of consumption of starting material was monitored by ^{1}H NMR analysis. The study showed a positive correlation between the rate of amine consumption and the electron donating effect of the substituent (Figure 3.23) due to the *x*-coefficient of 2.1483. The correlation between electronic effects and the rate of dehydrogenation had an R^2 value of 0.6014, which was quite strong, but further experimentation was required to prove the strength of the correlation. From these results it indicated that the rate determining step of the reaction did involve the build up of positive charge. This result supported the mechanistic hypothesis that hydride migration in the dehydrogenation process is rate-limiting, as a more electron rich ring would be expected to make the loss of the hydride more facile at the benzylic position. The rate data showed that the reactions were occurring slower than expected, as it was envisioned that as although the benzyl proton was less acidic, the reduced steric encumbrance of the reactive centre would overcome the problem and lead to comparable rates. This result supported the mechanistic hypothesis that cleavage of the iridium-hydride bond to form the active catalyst was rate limiting, as has been shown with iridium(I) catalysts.

The plot shows $\log(k_{\mathrm{X}}/k_{\mathrm{H}})$ on the y-axis with the following annotations:

$$y = 2.4183x = 0.6208$$

$$R^2 = 0.6014$$
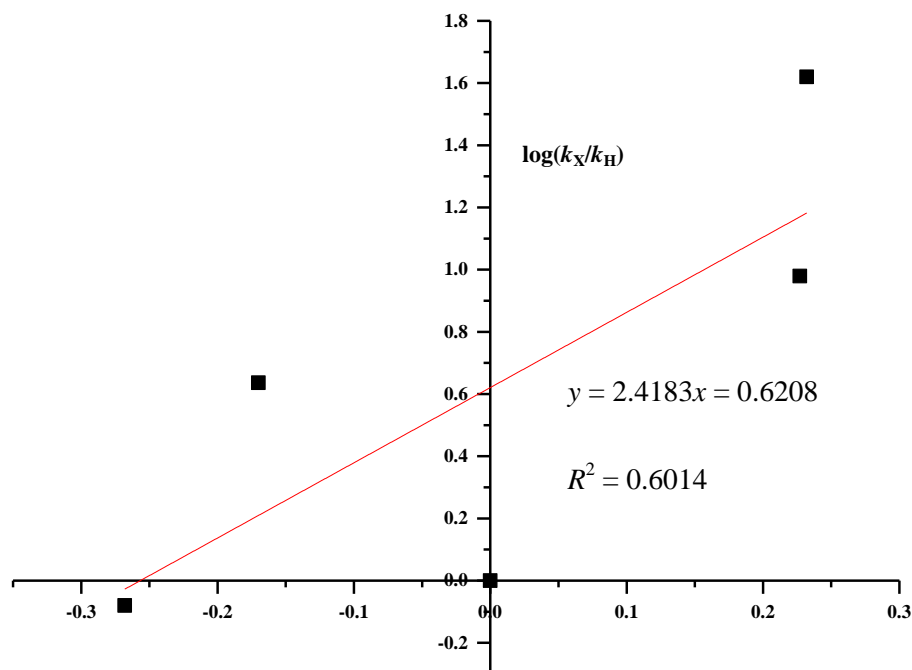
Figure 3.23 Hammett plot for the electronic effects on the rate of consumption of different 4-substituted benzylamines in iridium catalysed amine dehydrogenation in toluene at 105-110 °C.

An alternate explanation for the R^2 value was the possible competing effects of the electron withdrawing groups and electron donating groups on the reaction. If the key intermediate during dehydrogenation is structure **3.28** (Figure 3.24), hydride migration from the benzylic position would be aided by an electron donating group and be hindered by a more electron withdrawing group. Loss of the hydrogen from the amine to form the imine would also be dependent on the pK_a of that proton. Work by Blackwell has shown that more electron withdrawing groups will reduce the pK_a of an ammonium in aqueous solution, as unsubstituted ammoniums had a pK_a of 9.38 whereas 4-bromo and 4-chloro have pK_as of 9.13 and 9.14 resepectively, whereas 4-methyl and 4-methoxy ammoniums have pK_as of 9.54 and 9.51, respectively.[121] These two competing phenomena could act against each other as when the benzylic hydrogen is more hydridic, due to an electron donating group, the amine proton is less acidic and *vice versa*, but in this instance it appeared that the effect of the electron-donating groups was more pronounced.

3.28

X=Me, Br, MeO, Cl
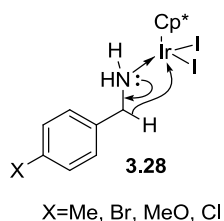
Figure 3.24 Potential intermediate in the iridium catalysed dehydrogenation of amines.

During the Hammett analysis, precipitate formed inside the NMR tubes and it was analysed to ascertain its structure and if it had an effect on the reaction. The solid was therefore isolated and recrystalised from dichloromethane. Examination of the resultant ^{1}H NMR of the crystals showed that a new species had been formed. Comparison of the ^{1}H NMR of the crystals showed that the Cp*-protons were at 1.93 ppm, similar in chemical shift to those observed for benzylamine in CDCl$_3$ (1.92 ppm, Appendix), indicating that this species was produced during the reaction. 4-Methyl benzylamine produced suitable crystals for X-ray diffraction analysis, which confirmed that the structure was a catalyst bound amine species (**3.29**, X-ray analysis carried out by Dr. C. Pask, University of Leeds, Figure 3.25). This observation represents the first example of benzylamine coordinated to an IrCp* centre. Notably, it was in contrast to previous literature observations of iridium–amine formation during amine dehydrogenation.[77]

3.29
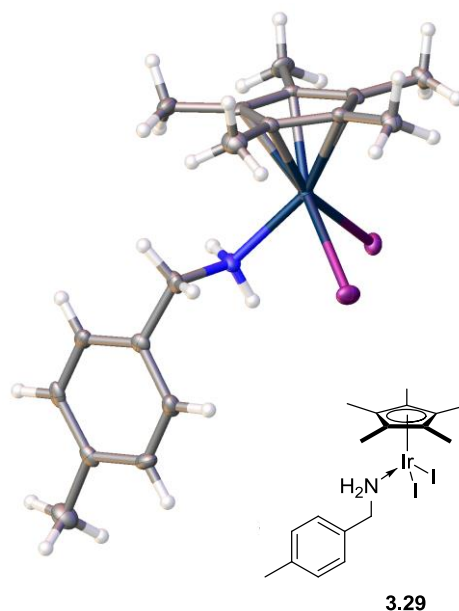
Figure 3.25 X-ray crystal structure of catalyst bound amine species 3.29 formed during the heating of 4-methylbenzylamine and [IrCp*I$_2$]$_2$ in toluene-d$_8$.

Catalyst bound amine **3.29** was not soluble in toluene-d_8, even when heated to reflux, and its insolubility and stability was envisioned to inhibit the dehydrogenation reaction of the amine. This hypothesis was further supported by the results obtained carrying out the reaction in DMSO-d_6, where the now soluble species underwent *N*-alkylation, although at a reduced rate. This result also supported the hypothesis that the catalyst-bound imine complex was highly reactive, as iridium-imine complex has yet to be observed. Even when complex **3.1** was heated to reflux in toluene-d_8 with imine **3.2**, only the hydrogen iodide salt of benzophenone imine was isolated as a stable species, which precipitated from solution.

This observed structure, combined with the DOSY data discussed previously was interesting, as it was contrary to that expected from the original ^{1}H NMR data, as instead of the expected monomeric catalyst bound amine **3.29** becoming the *bis*-amine complex **3.25**, originally hypothesised, the converse was appearing to happen. Complex **3.25** is a 16 electron species, whilst structure **3.29** (Figure 3.25) is an 18 electron mono-dentate species. *bis*-Amine complex **3.25** became the monomeric complex **3.29**. One potential driving force for this phenomenon was solubility, as the monomeric complex was driven out of solution, forming the precipitate. Further analysis of how these complexes form will form the basis of future work, as well as analysis of the crystal structures of similar catalyst bound amines.

3.2.4 Mass spectra analysis of intermediates formed during amine dehydrogenation

Mass-spectrometry (MS) analysis was carried out on the crude mixture containing benzylamine, iridium complex and DMSO (in collaboration with Dr. Stuart Warriner, University of Leeds). Analysis *via* direct injection onto an Ultra-High Performance Liquid Chromatography–Time of Flight mass spectrometer (UPLC–TOF–MS) showed the formation of several different distinct species (Figure 3.26).
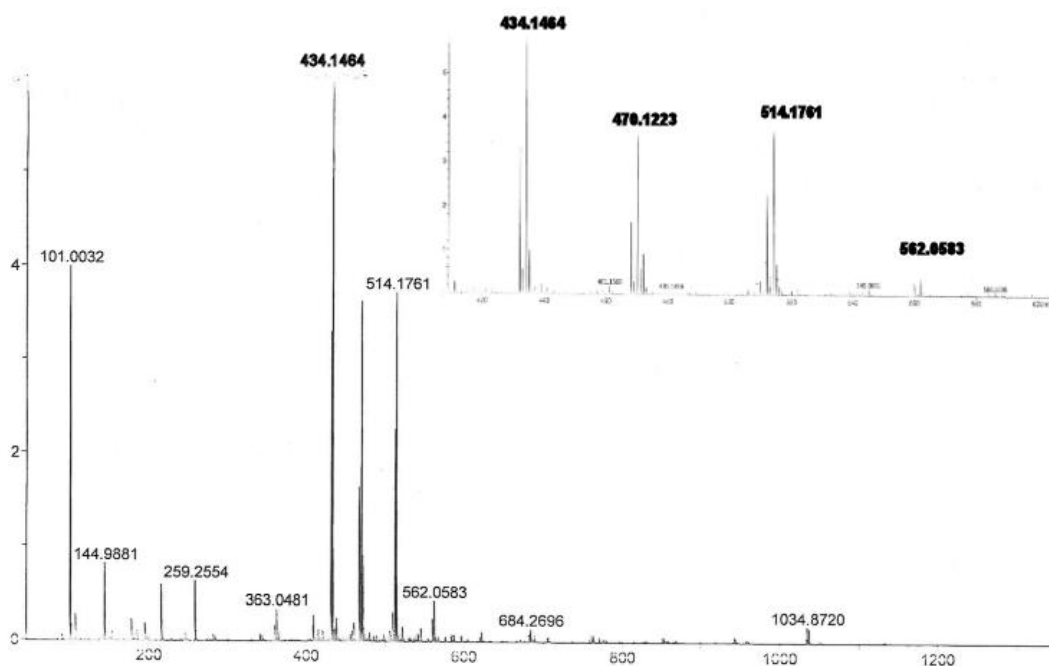
Figure 3.26 UPLC-TOF-MS trace for a mixture of benzylamine, iridium complex and DMSO.

There were four distinct species of interest formed with *m/z*, 434, 470, 562 and 1034. The structure of the species with *m/z*: 1034 was rationalised as being the starting SCRAM complex, **3.1** , which had lost an iodide ion, this can lead to the formation of the triply bridged complex **3.30,** previously observed by Lucas (Figure 3.27).[122] The observation of complex **3.30** was unusual as the complex would have converted between two 18 electron species (with respect to each centre).

3.30
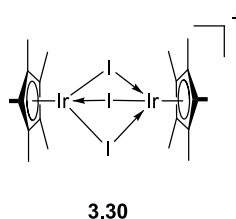
Figure 3.27 Triply bridged iridium dimer complex observed during MS analysis.

The predicted ion for the *bis*-amine complex **3.25**, *m/z* 542, was not observed during analysis, indicating this species was not stable under the ionisation conditions used in this instance. Conversely, iridium-amine complex **3.31**, was observed (*m/z* 562.0583) in the normal and high resolution methods (Scheme 3.12). Of further interest was the observation

103

of a species with *m/z* 434.1464, which was rationalised as being the isobaric, isoelectronic iridium-bound amine **3.32** or imine-iridium species **3.33**.
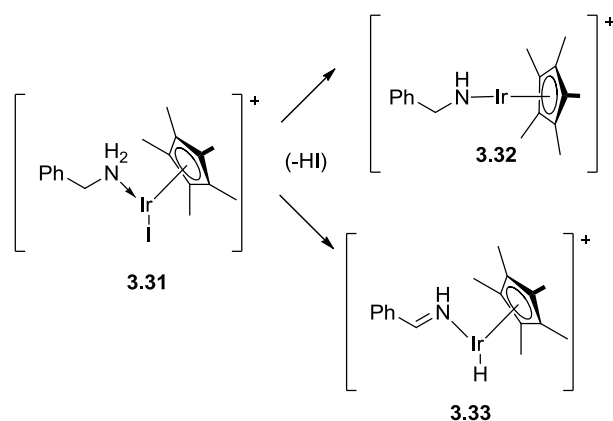
Scheme 3.12 The related iridium-amine complexes formed during SCRAM complex, 3.1, catalysed benzylamine, 3.11, dehydrogenation, conversion occurs via loss of the hydrogen iodide.
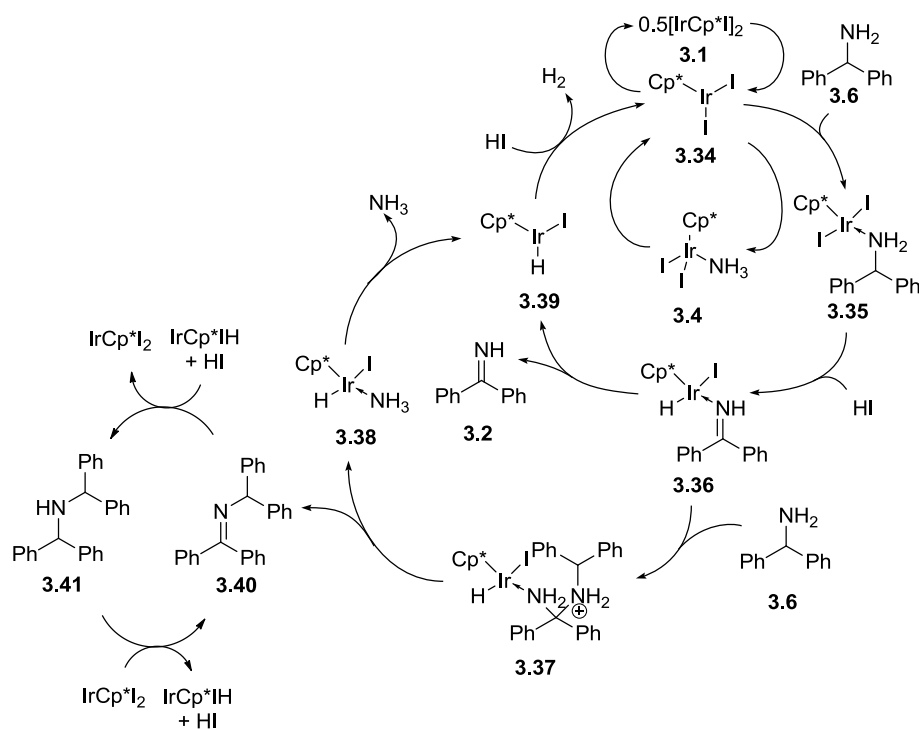
Scheme 3.13 Proposed catalytic cycle for SCRAM (3.1) catalysed *N*-alkylation of benzhydrylamine 3.6.[77]

Chapter 2 discussed Blacker and co-workers proposed catalytic cycle for amine dehydrogenation and *N*-alkylation (Scheme 3.13).[77] The MS evidence showed that two stable species were observed, the difference in mass between the two species was the loss of hydrogen iodide. The two species had two related structures, the first, where the amine was bound *via* a coordinate bond, **3.42** and secondly, after the hydrogen iodide loss, where two isobaric species are possible, either amine bound *via* a formal bond, **3.44** or where the dehydrogenation has already occurred with catalyst-bound imine **3.43** (Scheme 3.12). The observation of these three species would suggest that the dehydrogenation may occur *via* a step-wise process and is supported by the formation of the stable iridium-amine complex **3.29** (Scheme 3.14). NMR analysis of the mixture did not show the presence of any up-field protons in the region expected for iridium-hydride species (-14.5-[-15.5 ppm]).[123] The lack of observed iridium-hydride would indicate that structure **3.44** and not structure **3.43** was observed in the mixture.
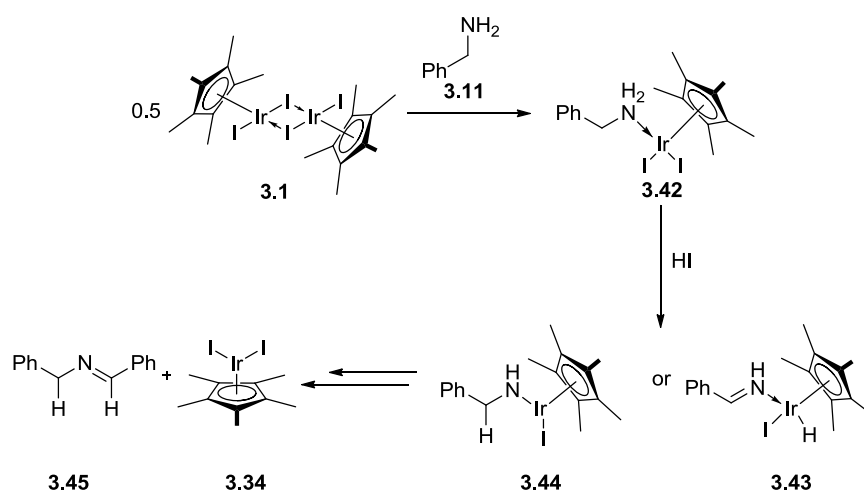
Scheme 3.14 Proposed mechanism for amine coordination and dehydrogenation, observed *via* MS, X-ray and NMR analysis.

The observed formation of the catalyst bound amine complex **3.29** (*vide supra*) has given further support to the mechanistic hypothesis,[77] being the first empirical evidence for catalyst bound amine formation for a non bi-dentate or tethered amine. The observed inhibition when this species is formed indicates that amine-iridium binding is also important in the catalytic cycle, as a strong amine-iridium bond leads to the inert species, whereas more labile amine-iridium coordination allows for faster reactions. This observation could be crucial in future catalyst design.

3.3 Conclusions

The proposed mechanism for the iridium catalysed dehydrogenation of amines and their *N*-alkylation requires elucidation to observe potential intermediates during the reaction and to aid in improving the reaction (Scheme 3.14). Madsen has observed that the formation of active monomer from the dimer must be an initial step in the mechanism.[97] In this work ^{1}H NMR titration experiments have shown how amines interact with the iridium centre when in solution and provided evidence for the second step of the mechanism, amine coordination. This work has confirmed that the more sterically encumbered an amine, the less it will interact with the iridium centre, as evidenced by the formation of several different IrCp* environments in ^{1}H NMR with small amines, such as benzylamines. The first observation of a benzylamine bound to an IrCp* centre, *via* X-ray analysis, has provided further support for the direct formation of catalyst bound amine during the reaction and shown that this is a stable complex. Observations with benzylamines have shown that they have the largest difference between bound and non-bound amine, having protons that are intermediate between amine and ammonium environments, indicating that they are in the process of becoming an imine. Furthermore, preliminary analysis of the equilibrium between bound and non-bound benzhydrylamines have been carried out, a potential K_c value has been determined in DMSO-d_6. A K_c value of 0.57 indicated that the non-bound amine and dimer catalyst species **3.6** and **3.1** were preferred. Future work, will focus on establishing the equilibrium constants of different amines, to prove conclusively which states are preferred.

The direct observation of catalyst bound or free primary imines, or secondary imines from primary or secondary amines, respectively (the proposed third step of the catalytic cycle) have not been observed previously and their observation has not been possible in large amounts during this investigation. The observation of rapid formation of the *N*-alkylation products over imines has supported the hypothesis that the imines formed must remain catalyst bound in the case of primary amines, which are more prone to attack by starting material. Observation of <1% formation in the benzhydrylamine reaction of a potential catalyst bound imine species supported this assertion and evidenced the transient nature of the catalyst bound imine or free imine species. In the case of secondary amines, the results indicate that their reaction was not as facile as the primary amines and that they may be in equilibrium between a non-bound amine and catalyst bound imine state.

This work has given indication of the potential mechanism by which *N*-alkylation occurs. The observation of *bis*-benzylamine iridium complex **3.25** at high iridium concentration by NMR analysis was interesting as the amine bound iridium complex **3.29** was expected to be dominant at high iridium concentration, furthermore as more amine was added to the system the *mono*-benzylamine was the predominant species, whilst it was not clear why this was the case, the insolubility of the mono-amine iridium complex may have been the driving force for its formation. The formation of the *bis*-amine complex however indicated that the *N*-alkylation mechanism maybe *via* an at metal, inner sphere mechanism, at least in the case of benzylamines. Unfortunately, this mechanism could not be proven as there was no evidence for the formation of the *bis*-amine species in MS analysis.

The observation of the *N*-alkylation products during NMR analysis of amine dehydrogenation, confirmed that this was an alternative pathway leading to by-product formation, furthermore the observation of iridium bound ammonia during crystallisation studies with imines supported the literature hypothesis that this is a mechanism for *N*-alkylation, furthermore the insolubility of this species and the catalyst bound amine species were potential inhibition pathways.

Mass spectrometry has shown the formation of ions that have a similar structure to those observed previously in the literature, of an iridium dimer, triply bridged by iodide ions. Ions have also been observed with structures that indicate the formation of iridium-amine species that are part of the proposed catalytic cycle. Iridium-imine or iridium-hydride species were not observed *via* a combination of MS and NMR analysis, which suggested that these species may be transient in nature.

Attempts to probe electronic effects on the dehydrogenation and *N*-alkylation reactions have been carried out. There was no strong correlation between changes in electron donating or withdrawing groups and the rate of reaction for substituted benzylamines, this was believed to be either an effect of insolubility, as precipitates formed, one of which being the characterised as the catalyst bound amine species **3.29**. The other potential reason could be the conflict between benzylic hydrogen nature and amine or ammonium hydrogen nature on the rate of dehydrogenation, where electron withdrawing groups would help the loss of the ammonium or catalyst bound amine hydrogen, but would hinder the loss of the hydride during the hydride migration step. Deuterium labelling experiments could potentially target each interaction and a secondary kinetic isotope effect seen, which would determine which interaction is more important in the reaction, this study will form the basis for future work on this system. Having gained further mechanistic knowledge *via* these methods,

exploitation of this methodology could be used to carry out nucleophilic reactions, investigation of these nucleophilic reactions will be discussed in the remaining chapters.

Chapter 4 Towards an improved synthesis of polycyclic indoles

4.1 Background

During the course of primary amine dehydrogenation described in Chapter 2, *N*-alkylation appeared to be the predominant pathway for the reaction. The further mechanistic work discussed in Chapter 3 demonstrated that secondary amine dehydrogenation was not as facile as primary amine dehydrogenation. To overcome the problems associated with *N*-alkylation, tertiary amines presented an attractive target for their reactions with nucleophiles when converted to their corresponding iminium ions.

4.1.1 The Pictet–Spengler reaction and its variants

The Pictet–Spengler reaction (Scheme 4.1a) has the potential to be incorporated with the hydrogen transfer methodology with iminiums ions. The reaction, known since 1911, was initially used for the formation of isoquinoline **4.6** from phenethylamine, **4.1**, and formaldehyde, **4.2** *via* acid catalysed imine formation, cyclisation and re-aromatisation.[124] Its scope and optimisation has been thoroughly characterised,[125] with variants used for the synthesis of indole **4.12** (Scheme 4.1b).[124, 126-128]
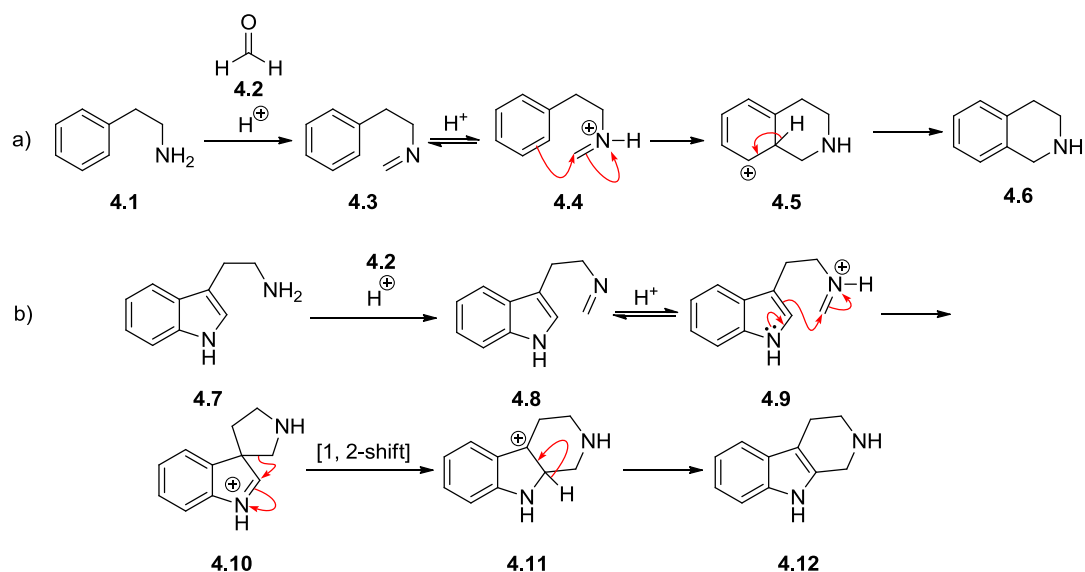
Scheme 4.1 The Pictet–Spengler reaction of a) phenethylamines and b) tryptamines.

Metal mediated variants of the Pictet–Spengler reaction are not extensively characterised, Uskokvic's mercuric acetate mediated amine C-H activation to form penta-cyclic tryptamines from their tetra-cyclic precursors is one example (Scheme 1.10).[15] A change from stoichiometric mercuric acetate to a catalytic method provides an opportunity to further exploit such cyclisations. Recent advances have been seen in the formation of poly-cyclic indoles using iridium complexes, however these reactions proceed *via* allylic dearomatization and require anhydrous conditions, which may be problematic at a large scale.[129] Whilst biosynthetic Pictet–Spengler reactions have been developed recently which utilise MAO-N to form the required iminium, and occur at mild temperatures, there remains the opportunity for the establishment of iridium catalysed protocols.[130]

4.1.2 Hydrogen-transfer methodology in nitrogen heterocycle and Pictet–Spengler type polycyclic indole synthesis

The development of a Pictet-Spengler type cyclisation using a hydrogen-transfer methodology would be desirable to avoid formaldehyde, potentially increase the yield and broader reaction scope, leading to reactions under ambient atmosphere, with formation of hydrogen, water or ammonia as the only by-products, as described in the literature (Chapter 1). Marsden and Blacker have established a method for the activation of tertiary amines to facilitate Pictet–Spengler type intra-molecular cyclisations with 2- and 3-substituted indolyl amines, **4.13**, **4.16** and **4.18**, using the hydrogen-transfer methodology to form a range of polycyclic indoles (Scheme 4.2, Table 4.1).[95]
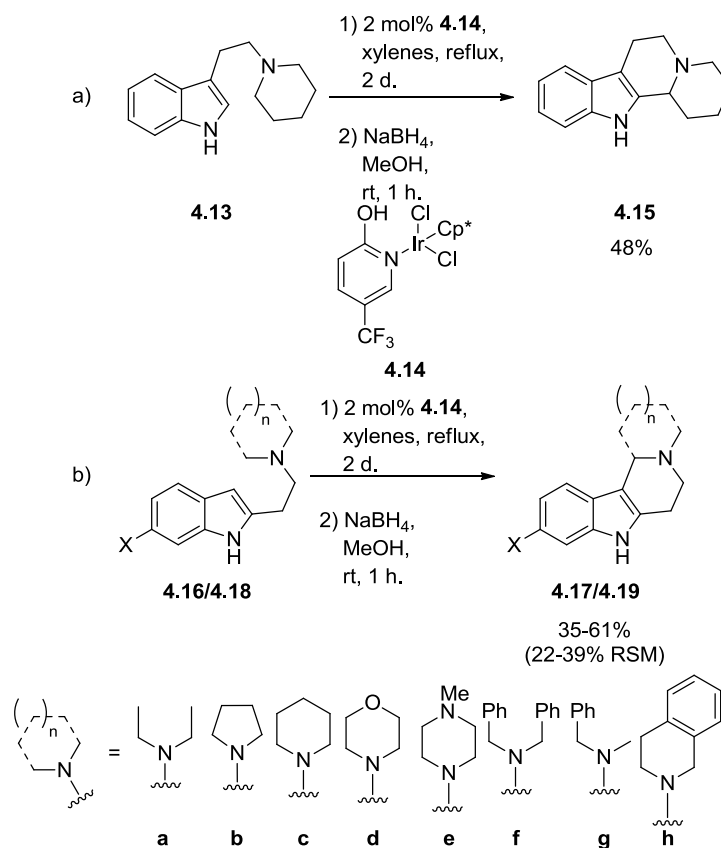
Scheme 4.2 Iridium catalysed cyclisation of: a) 3-substituted indolyl amine, 4.13 and b) 2-substituted indolyl amine, 4.16 and 4.18.

Table 4.1 Pictet–Spengler ring closure of 2-substituted indoles (Scheme 4.2b).[95]

Entry	X	Amine	Yield / % (RSM / %)	Entry	X	Amine	Yield / % (RSM / %)
1	H	**4.16a**	41 (23)	7	H	**4.16g**	0
2	H	**4.16b**	0	8	H	**4.16h**	0
3	H	**4.16c**	61 (35)	9	OMe	**4.18a**	42 (23)
4	H	**4.16d**	35 (39)	10	OMe	**4.18c**	61 (35)
5	H	**4.16e**	54 (24)	11	OMe	**4.18d**	39 (30)
6	H	**4.16f**	0	12	OMe	**4.18e**	49 (22)

The low to moderate yields observed, 35-61%, for the 2-substituted indoles were reasoned to be due to over-oxidation of the product to iminium species **4.21**, as also observed by Uskokovic.[15] This reaction pathway was preferential to further cyclisation, requiring a

reductive work-up before product isolation (Scheme 4.3a). Cyclisation to form (±)-Desbromoarborescidine A from the parent alkylated tryptamine was achieved, but required increased reaction temperature and time scale, presumably due to progressing through a similar 5-membered spiro-cyclic intermediate **4.23** (Scheme 4.3b) as those in the standard Pictet–Spengler and Uskokovic reactions (Scheme 4.a and Scheme 1.10, *vide supra*). Optimisation of the process would make the reaction more attractive to industry.
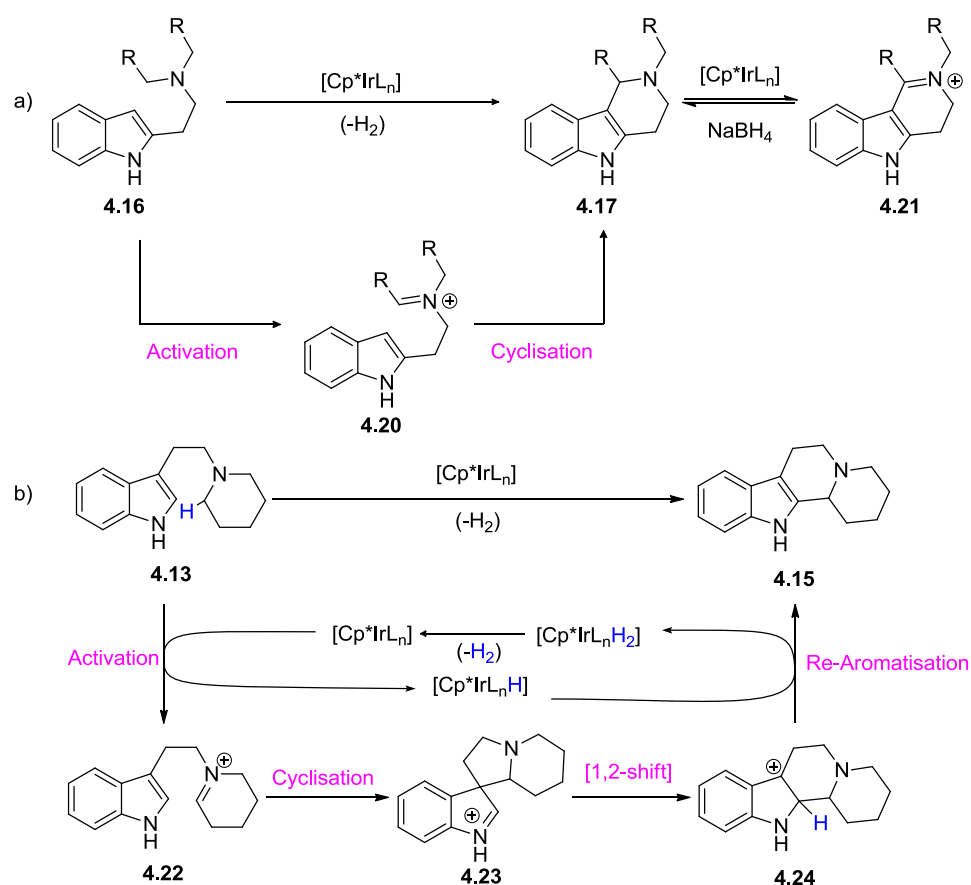
Scheme 4.3 Iridium catalysed cyclisation of: a) 2-substituted indolyl amine 4.16 with formation of over-oxidation product 4.21 and b) 3-substituted indolyl amine 4.13 *via* strained spiro-cyclic indole 4.23.

Incorporation of iridium catalysed hetero-cyclisation reactions developed by Fujita (Scheme 4.4a)[131] and Williams (Scheme 4.4b),[132] provide the opportunity for telescoping the synthesis of polycyclic indoles. This prospect is made more inviting as alkylated tryptamines have been formed from tryptamines and tryptaphols by this technique.
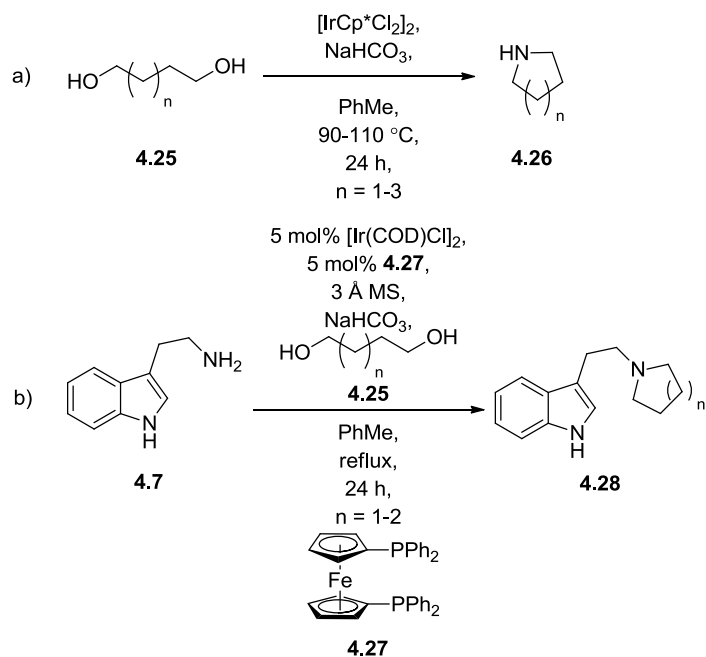
Scheme 4.4 a) Iridium catalysed formation of heterocycles;[131] b) Iridium catalysed synthesis of alkylated tryptamines.[132]

Both reactions require dehydrogenation of both alcohols of diol **4.25** and then *N*-alkylation of the resultant aldehyde. The reaction can be visualised to occur through two possible mechanisms: the first is *via* two sequential dehydrogenation-*N*-alkylation steps (Scheme 4.5, Path A); the second *via* a double dehydrogenation and then double *N*-alkylation reaction (Path B).
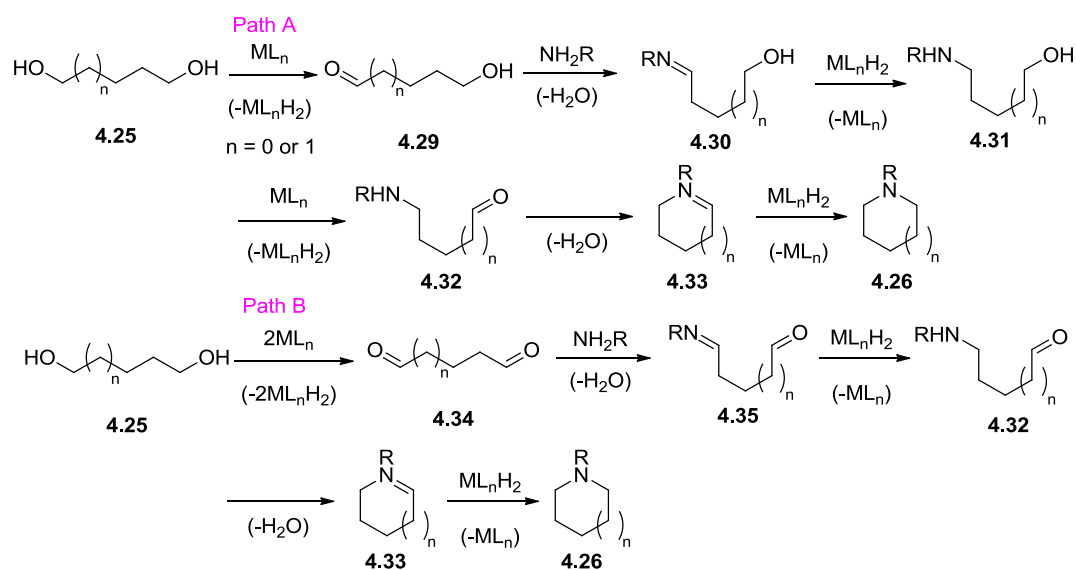
Scheme 4.5 Formation of heterocyclic amine 4.26: Path A) *via* **sequential dehydrogenation and *N*-alkylation or Path B)** *via* **double dehydrogenation and double *N*-alkylation.**

Either mechanism invokes imine or iminium ion formation, which are susceptible to Pictet-Spengler type cyclisations from either indolyl alcohol **4.36** or amine **4.39** (Scheme 4.6a and b), which increase the attractiveness of this approach.
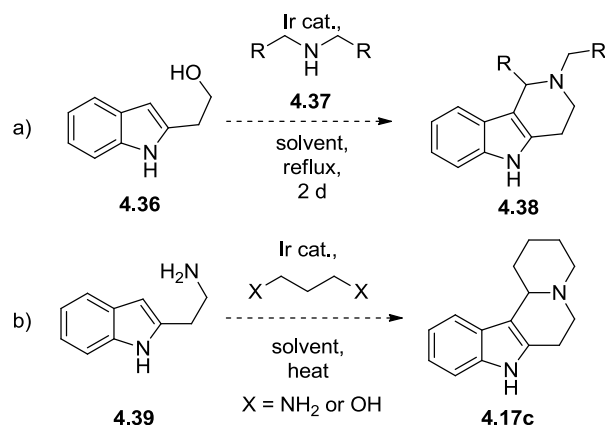
Scheme 4.6 Telescoped synthesis of polycyclic indoles using iridium catalysed heterocyclisation from: a) 2-substituted indolyl alcohol 4.36; b) 2-substituted indolyl amine 4.39.

4.1.3 Indoles in the pharmaceutical industry

Polycyclic indoles were chosen because the moiety is present in the structure of numerous multi-million dollar selling drugs such as Tadalafil, **4.40**, (1.88 billion $/yr)[133] and Octreotide acetate, **4.41**, (649 million $/yr)[134] (Figure 4.1). Compounds **4.40** and **4.41** are used for the treatment of erectile dysfunction and hypothalamic disorder, respectively. As such, drug compounds **4.40** and **4.41** represent both financial and medicinally important drug substances to the pharmaceutical industry.
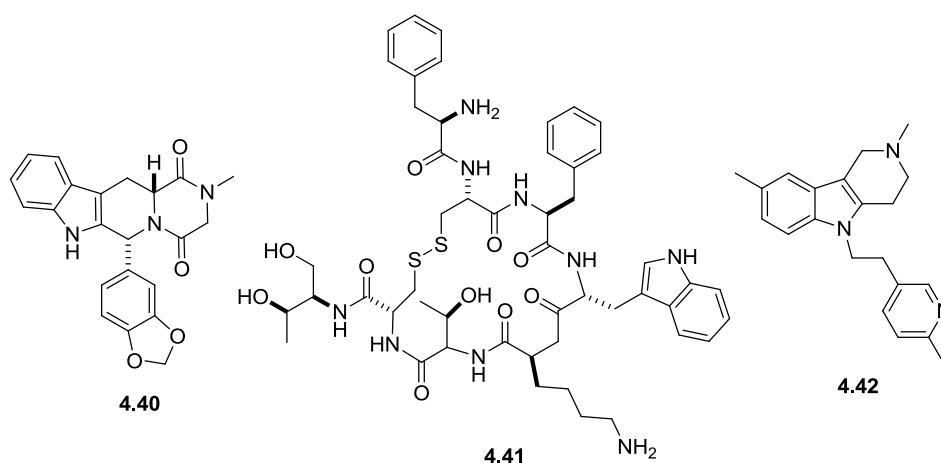
Figure 4.1 Medicinally and economically relevant indole amines.

Indoles and their polycyclic derivatives are prevalent not only as biologically active motifs in lucrative pharmaceuticals, but also as active natural products.[135] Dimebolin, **4.42** is a pharmaceutically active natural product currently used as an antihistamine, however it has also shown potential as an anti-Alzheimer's and anti-Huntingdon's disease therapeutic (Figure 4.1).[136] Compounds **4.40-4.42** provide a snapshot of the significance of indoles and polycyclic indoles to the chemical industries; their cheap and efficient synthesis provide a substantial challenge to process chemists to decrease the cost and ease with which they are synthesised. As polycyclic indoles, drug compounds **4.40** and **4.42** can potentially be synthesised *via* the Pictet–Spengler type cyclisation conditions. Furthermore, telescoping the formation of poly-cyclic indoles could be financially beneficial due to reduced waste streams and conciseness of synthetic strategy compared to a multi-step approach; therefore optimisation of the synthesis of polycyclic indoles *via* hydrogen-transfer was investigated.

4.1.4 Aims and objectives

To increase the efficacy of the cyclisation reaction a range of catalyst systems and reduction methods were probed. Telescoping of the reaction to develop a one-pot multi-component reaction to proceed directly from either a 2-indolyl alcohol and an amine or the 2- or 3-substituted indolyl amine and an alcohol with subsequent cyclisation to the polycyclic indoles **4.17c** or **4.38** (Scheme 4.6a and b, respectively) was investigated, as was its optimisation. Finally an increase in the scope of the reaction was investigated to incorporate substitution of the aryl ring with 4 or 5-substituted indoles and different amines.

4.2 Results and Discussion

4.2.1 Attempted optimisation of the cyclisation of 2-substituted indolyl amines

4.2.1.1 Analysis of different catalyst systems

Other iridium,[73, 137, 138] ruthenium[139] and palladium based systems have been established to catalyse amine dehydrogenation. These methods were incorporated into the cyclisation protocol to improve upon the original conditions and increase cyclised indole formation. Indole amines **4.16c-e** and **g** were synthesised using a literature procedure. *N*-Mesyl-indolyl alcohol, **4.46**, was synthesised from 2-iodo-aniline (**4.43**), subsequent mesylation, *N*-alkylation and deprotection gave the desired free amino indoles (**4.16c-e** and **g**) (Scheme 4.7).[140, 141]
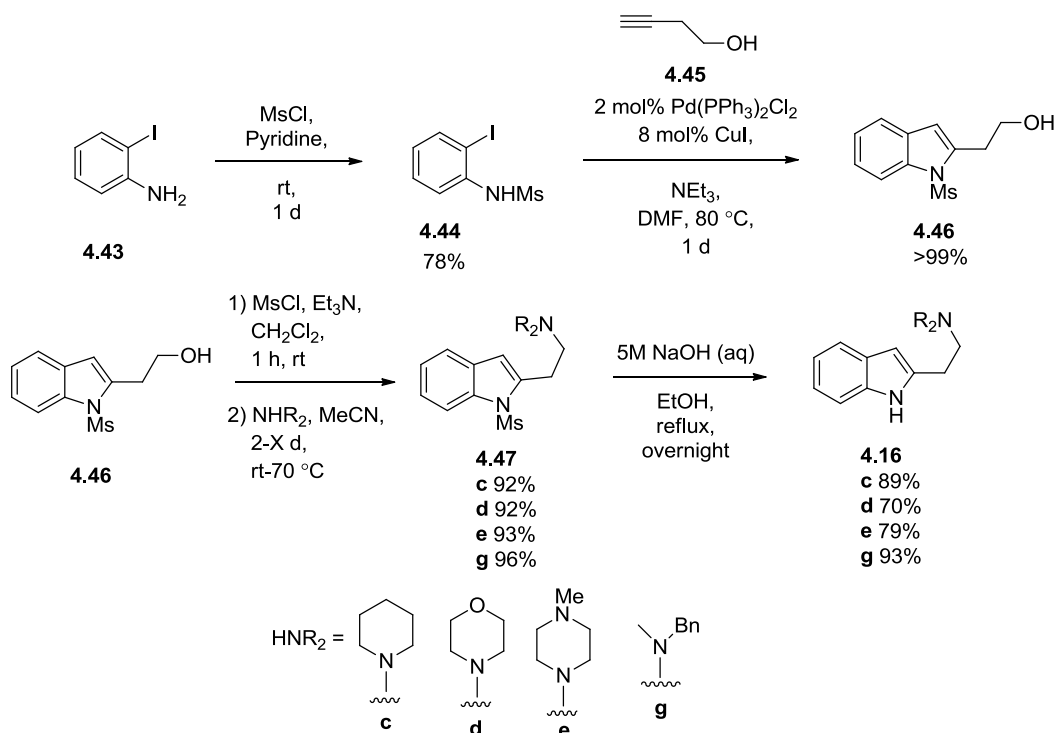
Scheme 4.7 Synthesis of indole starting materials (4.16 c-e and f) from 2-iodo-aniline (4.43).

Ruthenium trichloride monohydrate, has been used to cyanate tertiary amines and similar conditions were used for the cyclisation reaction (Scheme 4.8). Air was sparged through a mixture of indole **4.16g** and ruthenium complex at 60 °C in a MeOH–acetic acid solvent mixture (3:1, *v/v*). Despite the use of a very reactive benzylic amine as shown in Chapter 2 and 3, ^{1}H NMR and LC-MS analysis revealed that overnight heating did not afford the cyclised product. It was therefore hypothesised that the lower temperature used in this modified literature procedure was insufficient to facilitate cyclisation and different catalytic systems were therefore investigated.
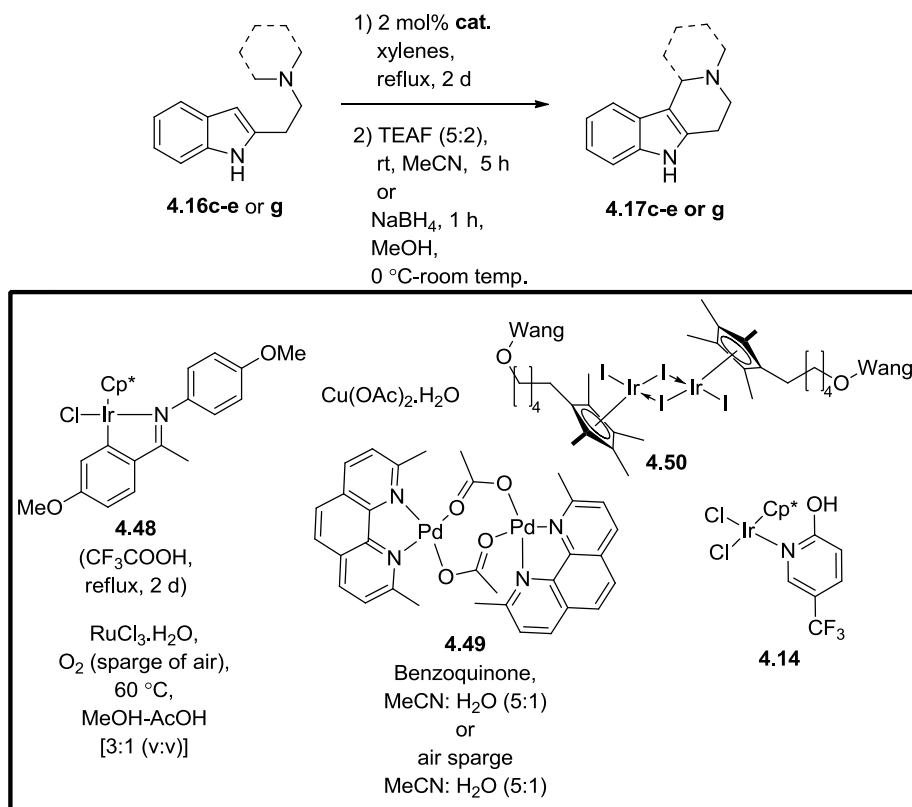
Scheme 4.8 Screening reactions employing various palladium, copper, iridium and ruthenium catalysts.

As palladium based catalysts have been developed for alcohol dehydrogenation, these systems were investigated to achieve the cyclisation reaction (Scheme 4.8). Palladium complex **4.49** was evaluated with indole **4.16e** using two different stoichiometric oxidants, in the first instance an air sparge and in the second benzoquinone was assessed. After stirring for two days at room temperature only starting material was observed by ^{1}H NMR or LC-MS analysis. Several attempts confirmed these results indicating that also this complex was not suitable for amine dehydrogenation.

Copper acetate monohydrate was subsequently employed, as this system has been used to activate oxindoles[142] and dihydro-1,3-oxazines[143] to cyclisations, *via* C-H activation, under similar conditions to those for the cyclisation. It is also worth noting that this catalyst is economically advantageous being £10 g^{-1}, which is cheaper in comparison to [IrCp*Cl$_2$]$_2$ (**4.51**, £590 g^{-1}) the starting material for complex **4.14**.[144] This catalyst afforded promising results, as when the copper complex was incorporated into the standard reaction conditions (after one day) the crude ^{1}H NMR showed a 4% conversion to the desired product (Scheme 4.8). Unfortunately, when the crude reaction mixture was recycled, no further product was

observed after heating for a further day, revealing that the rate of formation of cyclised product was slower compared to Fujita catalyst **4.14** (Table 4.1, Entry 5, 35% after two days). Further catalysts were screened, although it is worth noting that there remain further avenues for exploitation in the field of copper catalysis, which may prove more process friendly from an economic standpoint.

Two iridium catalysts were eventually evaluated in the system (Scheme 4.8, complexes **4.48** and **4.50**). Xiao's catalyst (**4.48**) was evaluated using the literature conditions for secondary amine dehydrogenation,[73] however after two days no product was observed. Furthermore, immobilised complex **4.50**, which has proven successful in benzaldehyde-isopropanol transfer hydrogenations,[138] was evaluated under the standard conditions. After heating for two days, cyclised product was not observed in the reaction. These results proved that the Fujita complex **4.14** was more active under the reaction conditions, however future efforts will focus on further analysis of other Xiao type catalyst systems, which have not been possible due to time constraints.

4.2.1.2 Evaluation of transfer-hydrogenation for over-oxidation product reduction

Use of a different hydrogen source to $NaBH_4$ for the reduction of the over-oxidation product **4.21** formed during the cyclisation reaction was investigated. TEAF solution (triethylamine–formic acid 2:5, azeotropic solution) transfer-hydrogenation allowed for the realisation of a full hydrogen-transfer sequence, forming carbon dioxide as a result of the reduction of the iminium ion by-product formed during the reaction (**4.21**). Using these conditions, the desired product indole **4.17c** was isolated in 78% yield from indole **4.16c** (438 μmol scale, Scheme 4.8). The observed yield enhancement therefore provided a promising starting point for further investigation.

The cyclisation reaction was carried out in a solution of TEAF and MeCN, rather than in previously employed xylenes, using the morpholine adduct **4.16d** to probe the scope of the TEAF modification (Scheme 4.9). After refluxing for the standard two day time period, ^{1}H NMR analysis of the crude reaction mixture showed a 10% yield of the cyclised product. MeCN refluxes at a lower temperature than xylenes (bp_{MeCN} = 81 °C *vs.* $bp_{xylenes}$ = 137-140 °C), the reaction was repeated with the piperidine analogue, heated to 110 °C for one day then 140 °C for one day (bath temperature, sealed tube) to evaluate the effect of increased temperatures, leading to a 41% NMR yield of indole **4.17d**, which was comparable to standard conditions. This result proved promising, as it is believed to be the first reported

example of the oxidation of a tertiary amine in a reductive environment. However, time constraints did not allow further investigation to determine if this reaction will be successful in a TEAF only system. Such investigations will therefore form the bulk of future work to assess the scope of this reaction.
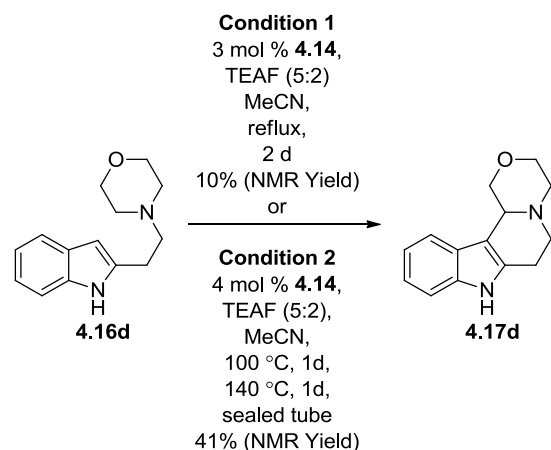
Scheme 4.9 Use of TEAF solution in the cyclisation of 2-substituted indolyl amines.

4.2.2 Telescoping of iridium catalysed polycyclic indole formation

Hydrolysis of the *N*-mesyl group yielded the free indolyl alcohol, **4.36**, in 88% yield (from **4.46**, Scheme 4.10). With indolyl alcohol **4.36** in hand, a test reaction was carried out with piperidine **4.52** and catalyst **4.14** heated to reflux in xylenes for two days for comparison with the standard conditions (Scheme 4.11). A reductive work-up, using NaBH$_4$, was carried out and the crude mixture was analysed by ^{1}H NMR analysis.
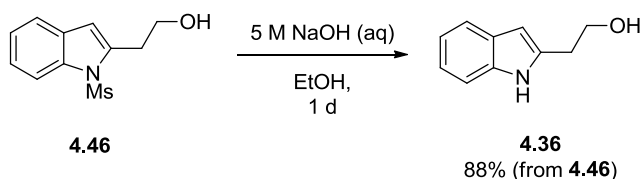
Scheme 4.10 The synthesis of starting material, indolyl alcohol 4.36.
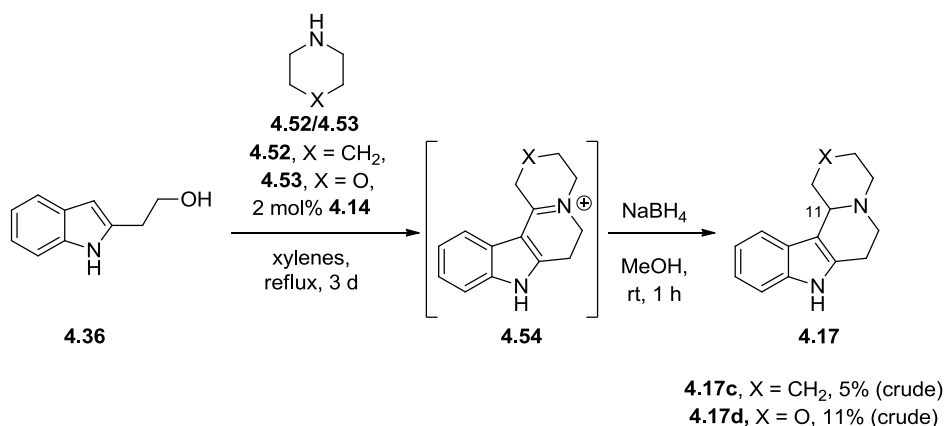
Scheme 4.11 The iridium catalysed multi-component reaction of indolyl alchol 4.36 in the presence of amines 4.52 or 4.53.

Initial analysis was promising, due to the presence of the diagnostic indole protons of compound **4.17c** (C11, 1H, 3.37.ppm, *t* and NH, 1H, 7.90 ppm, *s*, Figure 4.2).
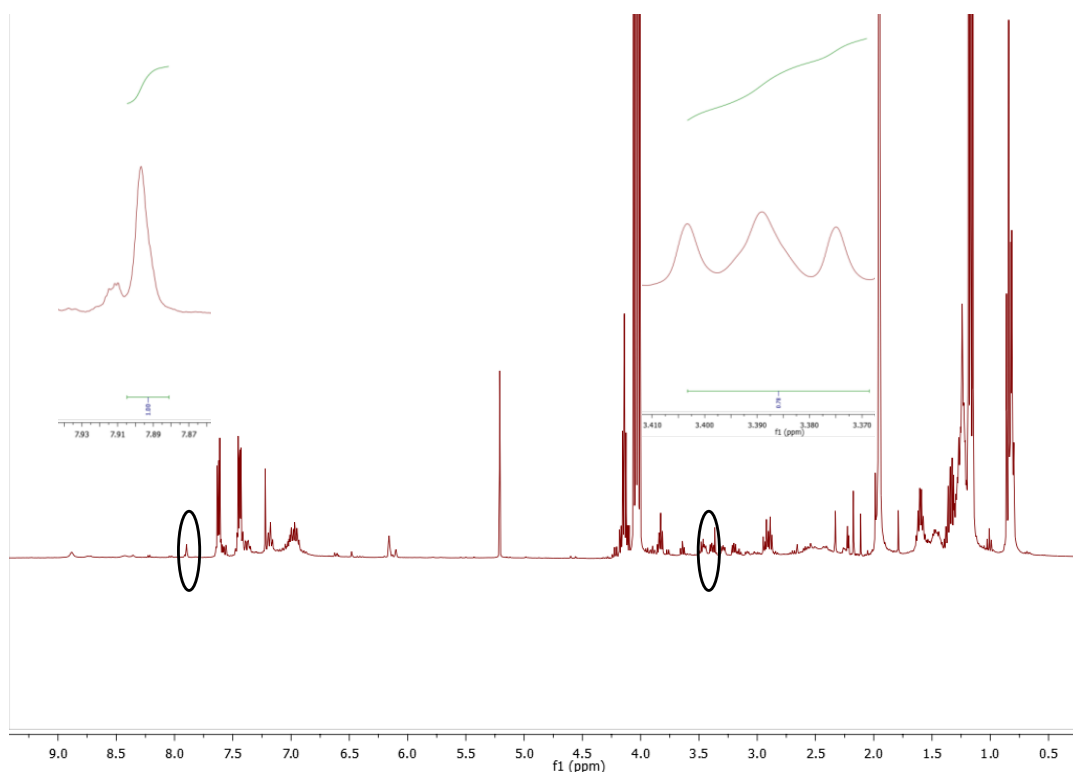
Figure 4.2 Crude ¹H NMR analysis of one-pot multi-component synthesis of indole 4.17c, with highlighted diagnostic protons.

Unfortunately, isolation of the polycyclic indole, **4.17c**, was not possible by column chromatography across a range of solvent polarities. This was due to the range of products

formed during the reaction with similar R_f values, which would not be separated in all solvent mixtures trialled. Optimisation of this initial result was carried out, investigating a range of solvents, temperatures, equivalences of amine and methods of addition of amine **4.52**.

4.2.2.1 Optimisation of the 2-substituted indolyl alcohol multi-component reaction

A range of conditions were screened to optimise the formation of the desired cyclisation product **4.17c** (Scheme 4.11, Table 4.2). HPLC analysis suggested the formation of the cyclisation product **4.17c** (in the UV analysis) for all conditions. LC-MS and ^{1}H NMR analysis did not provide evidence for product formation however, as the mass-spectrum did not correlate with the product [(M–H$^+$), 227] and the characteristic protons were not observed [3.37 ppm, 1H, *d* (*J*=8.4), C11'H].

Formation of the *N*-alkylation product **4.16c** was indeed observed *via* HPLC and LC-MS analysis, which correlated with the literature.[132] A black amorphous precipitate was formed on the sides of the reaction vessel in all instances. The precipitate was insoluble in a range of solvents (including MeOH, petroleum ether, toluene, DMSO and water), which did not allow for its isolation and characterisation. It was however hypothesised that this precipitate could be attributed to indole polymerisation products **4.55a-c** (Figure 4.3)[145, 146] or indole thermal isomerisation (>970 K), which have been observed in the literature.[147-150] As the temperature for the reaction is below that required for thermal isomerisation this reaction appears unlikely, however chemical formation of polyindole occurs at the operating temperature in the prescence of an oxidant, in aqueous buffer and is therefore possible under the reaction conditions. As the desired formation of the tetracyclic cyclisation product **4.17c** would not occur under the conditions screened, a different strategy was required.

Table 4.2 Conditions screened during optimisation of indole *N*-alkylation-cyclisation (Scheme 4.11).[a]

Entry	Solvent	Base	Catalyst	Piperidine / Equiv.	Temperature / °C	Yield of Product / %
1	Xylenes	No	**4.14**	0.8	137-140	0
2	Xylenes	No	**4.14**	1	137-140	0
3	Xylenes	No	**4.14**	1[b]	137-140	0
4	Xylenes	No	**4.14**	1.5	137-140	0
5	Piperidine	No	**4.14**	solvent	106	0
6	PhCl	No	**4.14**	1	100	0
7	PhCl	K$_2$CO$_3$	**4.51**	1	100	0
8	PhCl	No	**4.51**	1	100	0
9	PhCl	K$_2$CO$_3$	**4.51**	1	100	0
10	PhCl	No	**4.51**	1	100	0
11	PhCl	K$_2$CO$_3$	**4.14**	1	100	0
12	PhCl	No	**4.14**	1	100	0
13	AcOH	No	**4.14**	1	100	0
14	PhCl	No	**4.14**	1	110	0
15	Xylenes	No	**4.51**	1	110	0
16	Xylenes	TMG	**4.14**	1	110	0
17	Xylenes	No	**4.14**	1	110	0

[a] Indole alcohol **4.36** (1 equiv.) was added to a suspension of **4.14** or [IrCp*Cl$_2$]$_2$ (**4.51**) (1 mol%) and (if required) base (1 mol%) in solvent (0.5 mL) and was heated to reflux. Piperidine was added to the resultant suspension which was stirred for up to seven days.

[b] Dropwise addition over 1 hour.
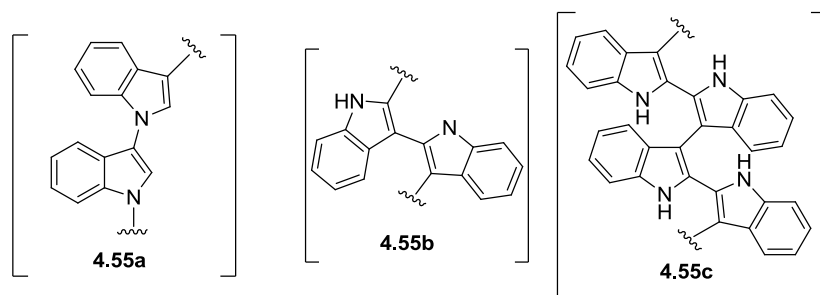
Figure 4.3 Poly-indoles 4.55a-c, potential structures of insoluble precipitate formed in the multi-component reactions.

4.2.3.2. Analysis of potential catalyst inhibition products

To ensure that coordination of indolyl alcohol **4.36** alcohol and nitrogen lone pairs to the iridium centre of complex **4.14** was not reducing or stopping catalytic activity, formation of new iridium complex **4.57** was attempted (Scheme 4.12).
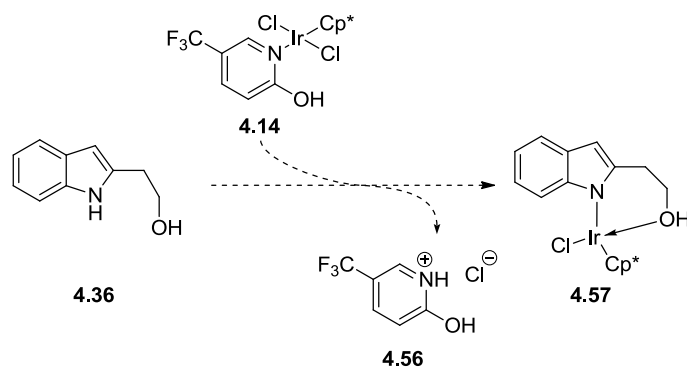
Scheme 4.12 Potential ligand exchange reaction between indolyl alcohol 4.36 and iridium complex 4.14.

X-ray diffraction was used to investigate whether indolyl alcohol **4.36** was binding to the iridium **4.14**, inhibiting the reaction by formation of insoluble coordination complexes. Fujita catalyst **4.14** contains the ligand 2-hydroxy-5-(trifluoromethyl)-pyridine (**4.56**), which has the potential to form a chelation complex with the iridium centre. Analogous complexes have been observed in the literature,[151] therefore iridium dimer complex, $[IrCp*Cl_2]_2$, **4.51** was used to model Fujita catalyst **4.14**. The only limitation of using iridium complex **4.51**, however was that the monomeric iridium chloride complex must be formed before a ligand exchange can occur. Indolyl alcohol **4.36** was mixed with iridium catalyst **4.14** at room temperature in dichloromethane (Scheme 4.13) to probe any chelation effects on the catalyst. A solid was formed which was recrystalised from dichloromethane.
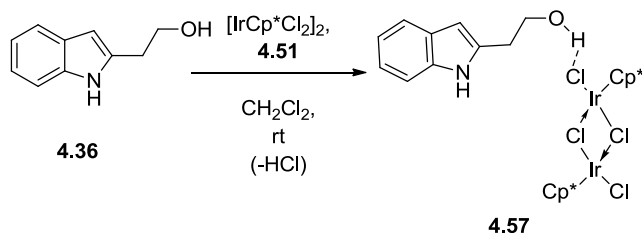
Scheme 4.13 Attempted formation of indolyl alcohol bound iridium.

X-ray diffraction of the resultant crystals did not show that a ligand exchange had occurred. Hydrogen-bonding between a chlorine ligand and alcohol proton of the indole was the only interaction observed (analysis carried out by Dr. H. Sheppard, Figure 4.4). This observation did not support that substrate-catalyst deactivation was inhibiting the reaction at room temperature, the lack of precipitate formation at the reaction temperature before amine formation would have given evidence to support that catalyst inhibition was precluding reaction.
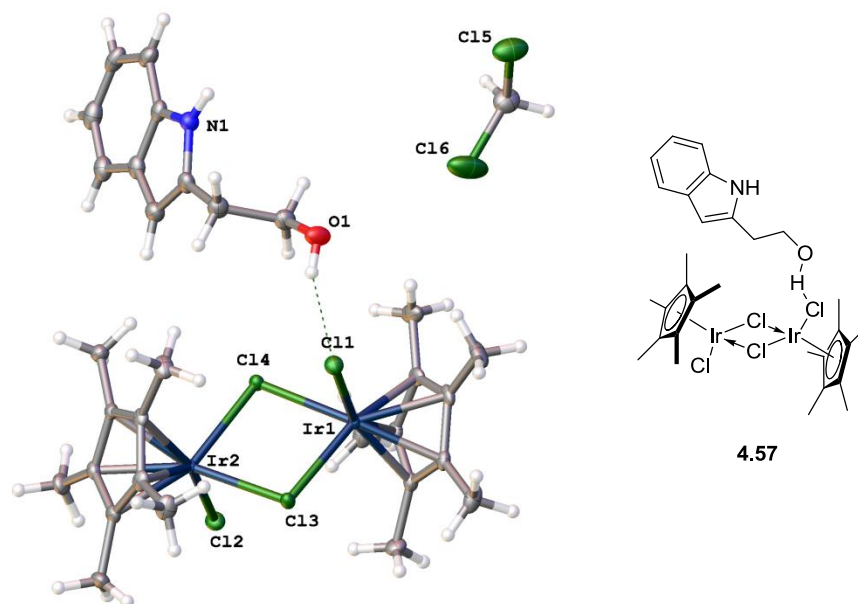
Figure 4.4 X-ray crystal structure 4.57 confirming hydrogen-bonding interaction between substrate and catalyst after mixing at room temperature.

4.2.2.2 Substrate scope of telescoped reaction

Morpholine, **4.53**, was also analysed as the reactive amine to increase the synthetic efficacy and scope of the multi-component reaction. Amine **4.53**, indolylalcohol **4.36**, xylenes and catalyst **4.14** were heated to reflux for 3 days and yielded 11% (15 mg) of impure polycyclic indole, **4.17d** (Scheme 4.11). The poor yield of this reaction suggested that choice of amine was not exerting a major role in the reaction process but that other factors were affecting the reaction. Tryptamine instead of indolyl alcohol was therefore evaluated within the multi-component reaction.

4.2.2.3 Evaluation of indolyl amines in the multi-component reaction

A similar protocol to that employed by Williams was evaluated for the formation of polycyclic indoles.[132] Tryptamine **4.7**, 1, 5-pentandiol **4.25**, xylenes, iridium complex **4.14** and NaHCO$_3$ were heated to 100 °C for 4 h. and then reflux for 2 days. (Scheme 4.14). The reaction was monitored *via* LC-MS and showed the formation of a mixture of products (**4.13**, **4.15** and **4.58**). After an acid work-up and column chromatography, 7% (10.7 mg) of impure cyclised product was obtained.
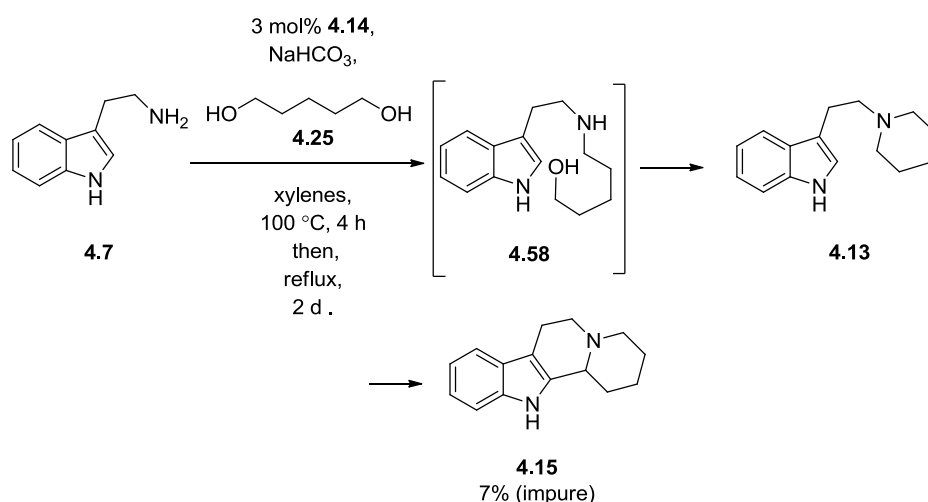
Scheme 4.14 Iridium catalysed multi-component synthesis of polycyclic indole 4.15 in the presence of diol 4.25.

Inspite of the poor yield, the formation of **4.15** was interesting, as it represented an example of hydrogen-transfer methodology being utilised to form two C–N and one C–C bonds within a single reaction, and therefore merits further examination to improve the yield. As with the Williams' chemistry (Scheme 4.4b, *vide supra*),[132] there are different possible pathways for the reaction, and the poor observed yield could be rationalised by the possibility for a number of by-products being formed. Future work therefore necessitates focusing on the determination of the preferred desired pathway and the optimisation of this methodology.

4.2.3 Increase in substrate scope *via* ring functionalisation

Preliminary work to increase the synthetic efficacy of the protocol by incorporating a pre-functionalised indole was carried out. Pre-functionalised indoles would provide more diverse

structural motifs, that could be functionalised post-reaction at not only the indole nitrogen, but also at either the 4'- and, or 5'-positions. Palladium catalysed cross-coupling would be a potential utilisation of the methodology, and the scope has the potential to be expanded to form 5-methyl polycyclic indoles, similar to dimebolin, with potential therapeutic benefits (Scheme 4.15).
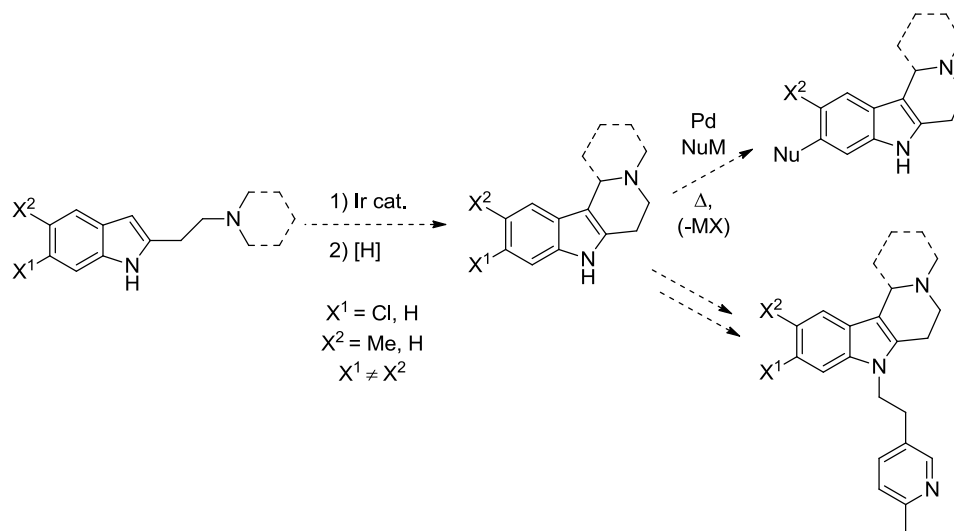
Scheme 4.15 Proposed iridium catalysed cyclisation of 4'-chloro or 5'-methyl-2-substituted indoles.

As an initial test of the functionalised indoles and with a view towards the synthesis of dimebolin type motifs, a test reaction with an *N*-methyl piperazine analogue of 5-methyl-indole **4.64a** was carried out. 4- and 5-substituted indole alcohols **4.62a** and **b** were synthesised from 4-chloro methyl-2-iodo- aniline (**4.60b**) or 4-toluidine (**4.59**) employing a modified literature method, used in the synthesis of indole alcohol **4.36** (Scheme 4.16). 4-Methylindole alcohol **4.62a** was mesylated, *N*-alkylated and hydrolysed to give the *N*-methyl piperazine analogue **4.64a** (416 µmols).
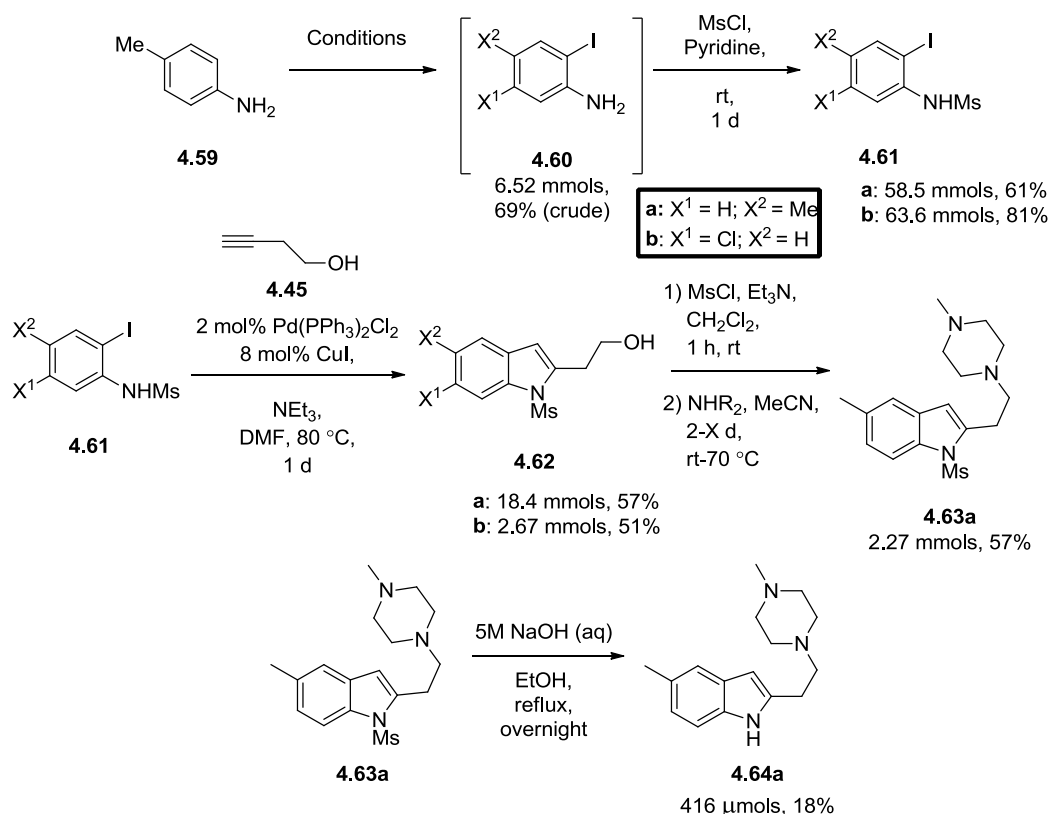
Scheme 4.16 Synthesis of the 4'chloro and 5'-methyl substituted indole starting material.

5-Methylindole amine **4.64a** was evaluated in the cyclisation protocol by refluxing in xylenes in the presence of Fujita catalyst **4.14** for two days on a 156 μmol scale (Scheme 4.17). The reaction was then cooled and a TEAF hydrogenation was carried out in MeCN. No cyclised product was observed however during post work-up analysis *via* ^{1}H NMR and LC-MS analysis. The reaction was repeated on the same scale, but a NaBH$_4$ reduction was carried out; however no product was observed again. It was not clear why the reaction was not successful, as 4'-methoxy substituted indoles (**4.18**) have been successfully cyclised under the similar conditions by Marsden and Blacker,[95] however an initial hypothesis was that the altered steric environment of indole **4.64a** may be precluding the formation of the polycyclic indole. The bulk of future research efforts will focus on investigating this hypothesis and also to expand the scope exploiting 4-chloroindole alcohol **4.62b** and 5-chloro-indoles.
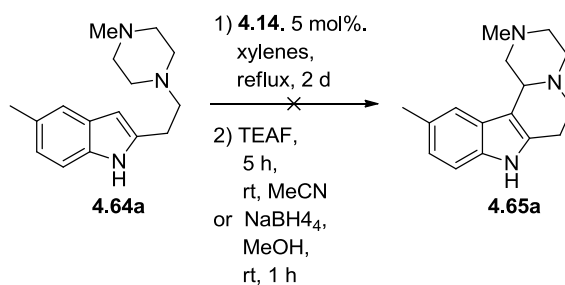
Scheme 4.17 Attempted incorporation of 5-methylsubsituted indole 4.64a into the cyclisation protocol.

4.3   Summary and future work

Various different conditions and methodologies have been assessed to optimise the synthesis of polycyclic indoles *via* metal catalysed amine dehydrogenation. TEAF has been evaluated during the reduction of over-oxidation product **4.21** formed during the cyclisation reaction and it has been shown to give a yield enhancement over the previous conditions (using NaBH$_4$).The requirement for the use of a reductive work-up was itself not desirable and other catalytic systems were assessed in an attempt to optimise the conditions. Whilst some success was seen with the copper acetate systems, poorer yields than those with the standard conditions were observed. Future work to improve upon the initial work with copper catalysts or to assess other catalysts similar to Xiao catalyst **4.48** could potentially provide a less energy intensive and economic method to form polycyclic indoles, and to carry out telescoped reactions.

A telescoped method for the formation of polycyclic indoles, directly from alcohols rather than tertiary indole amines was investigated. The reason for lack of success observed was hypothesised to have been due to the multi-component reaction proceeding *via* multiple reaction pathways, leading to the production of a large range of products, observed *via* TLC analysis. Polymerisation was a viable by-product however the low solubility did not allow for structural analysis and determination to confirm this hypothesis.

A test reaction with a new indole amine that was functionalised on the aryl ring of the indole was also carried out. 5-Methylindole analogue **4.64a** was not successfully incorporated into the reaction with only starting material observed. A preliminary hypothesis was that steric hindrance was precluding the reaction of the 5-methyl substituted indole. The incorporation of further amines that are functionalised on the indole nitrogen will be a continued goal for

this work, with the ultimate aim of accessing an industrially relevant protocol for the production of dimebolin type motifs (**4.42**) and examination of their biological effects.

Chapter 5 The Evaluation of Further Nucleophiles

5.1   Introduction

The research discussed in Chapters 2 and 4 about primary and secondary amine dehydrogenation, has shown that amines readily undergo dehydrogenation with an iridium catalyst. Primary amines were most facile, however as has been shown in the literature, *N*-alkylation occurs rapidly with primary amines.[96] Whilst the *N*-alkylation itself is an efficacious process, proven to be desirable to industry,[152] it limits the scope of products synthesisable by this process. Indeed *N*-alkylation is the most common reaction with iridium catalysed hydrogen-borrowing of amines.[39] The literature review (Chapter 1) described a number of nucleophilic addition reactions of imines[81-83, 85-89] and Chapter 3 discussed the intramolecular cyclisation reactions of indoles, *via* an iminium ion intermediate. The success of the cyclisation reaction is achieved as formation of *N*-alkylation products is not possible with tertiary amines. The formation of aldimines or ketimines is a useful transformation and it would be useful to extend the scope of the reactants to other nucleophiles beyond amines. As such, further reagents (cyanide, ammonia and dimethylsulfoxonium methylide) were evaluated in an attempt to establish new functionalisation protocols for amines *via* iridium catalysed hydrogen transfer reactions (Scheme 5.1).
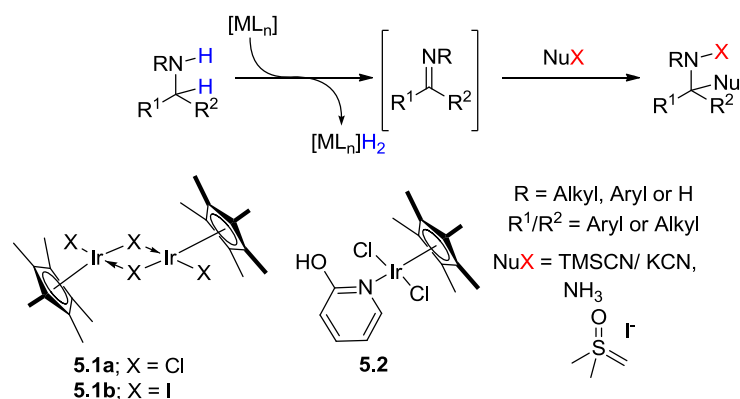
Scheme 5.1 Proposed incorporation of various nucleophiles into iridium catalysed hydrogen borrowing.

5.2 Addition of Cyanide to Imines

5.2.1 Background and Synthetic Rationale

The Strecker reaction, is a highly useful reaction (Scheme 5.2). The formation of α-amino nitrile **5.3** is itself an interesting transformation, however further attractiveness is added as the product after homologation is functionalisable.[153] Strecker product **5.3**, can be hydrolysed to form β-amino acid **5.4** with the potential to form unnatural amino acids (Scheme 5.2a). Further reactivity can be achieved when **5.3** is reduced, thus forming diamine **5.5** which can be useful in several other reactions (Scheme 5.2b).[154-156] Use of a base and then electrophile allows for further functionalization to form compound **5.6**[157] (Scheme 5.2c) with subsequent reduction or hydrolysis still possible.
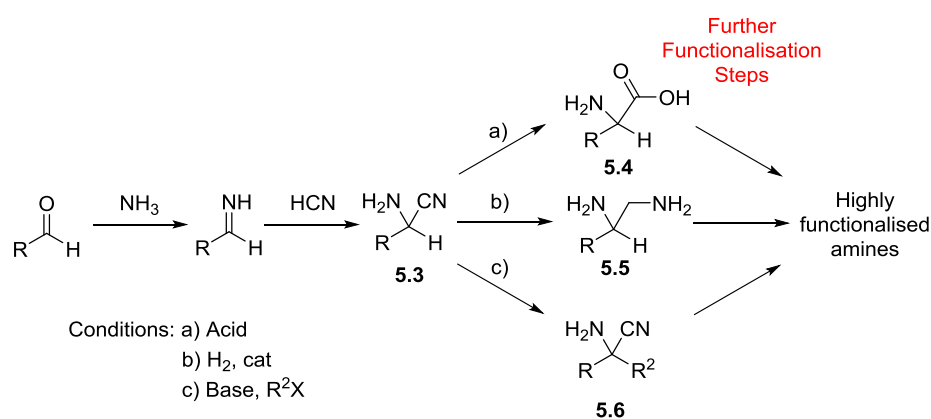
Scheme 5.2 A generalised Strecker reaction with post reaction functionalization to: a) β-amino acid 5.4, b) diamine 5.5 or c) further alkylated product 5.6.

Work carried out previously has described the formation of α-amino nitriles using biochemical transformations. Turner and co-workers' have disclosed a MAO-N D5 catalysed method for the formation of fused α-cyano-pyrrolidines (Scheme 1.28a). This methodology is currently applicable to only these fused pyrrolidines, however a similarly successful method that can form acid **1.113** over two steps from fused pyrrolidine **1.111** *via* α-cyano-pyrrolidine intermediate, **1.112** would be desirable.

Whilst Murahashi[139] and others[158-162] have shown that similar homogeneous or heterogeneous transition metal catalysed reactions are possible (Scheme 5.3). Many of these methods are only tolerant of tertiary amines, whereas this new methodology might be applicable to primary and secondary amines. This methodology may also avoid the use of an

external oxidant, such as the atomic oxygen employed in Murahashi's work. The formation of Ir-imine complex should facilitate the addition of the cyanide nucleophile, especially if amine concentration is kept low relative to the cyanide nucleophile then selective addition should be possible. The iridium catalysed formation of α-amino nitriles from amines was evaluated.
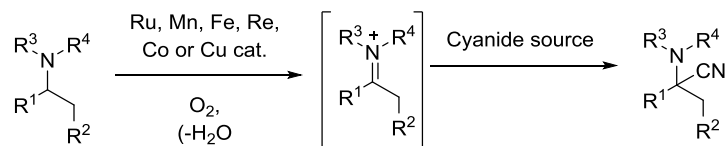
Scheme 5.3 Ruthenium[139], copper[158], rhenium[159], manganese[160], iron[161], or cobalt[162] catalysed synthesis of tertiary-α-aminonitriles *via* iminium ion formation.

5.2.2 Result and Discussions

The initial research focused on the use of sodium cyanide (NaCN), a hard and strongly nucleophilic cyanide source,. In this form the cyanide anion has the potential to react rapidly with the imine, envisaged to overcome the problems observed previously in primary amine dehydrogenation (Chapter 2), due to *N*-alkylation with unreacted starting material (Scheme 5.4).
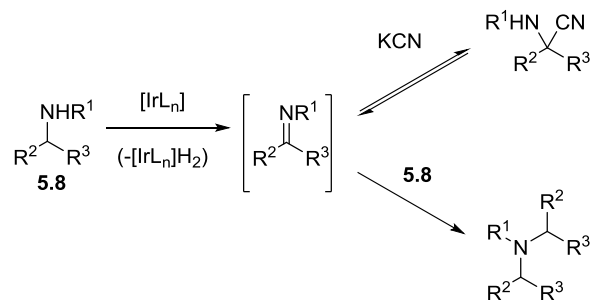
Scheme 5.4 Proposed use of potassium cyanide as the cyanide source during Strecker type reaction, with molar excess of cyanide source overcoming *N*-alkylation.

An initial reaction was carried out where iridium Cp* iodide catalyst, **5.1a** (1 mol%) was stirred with potassium cyanide (0.79 equiv.) and amine **5.8**, a cheap and commercially available amine (1 equiv.), in deionised water at 100 °C (Scheme 5.5 and Table 5.1, Entry 1). Monitoring of the reaction by either TLC or GC-MS proved difficult due to poor solubility of the amine in the bulk aqueous solution. Aqueous extraction, followed by

solvent removal *in vacuo* and NMR analysis of the crude reaction mixture showed that instead of α-aminonitrile **5.10**, homo-dimerisation to secondary amine **5.11** had occurred. Evaluation of a range of different reaction conditions was carried out investigating changes to concentrations of reagents, the solvents, different catalyst effects and the evaluation of different cyanide sources, to try and establish a successful method for the synthesis of the desired α-amino nitrile (Table 5.1).
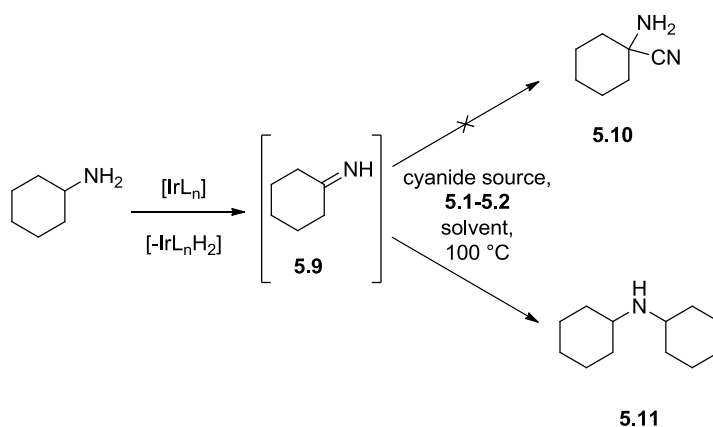
Scheme 5.5 General procedure for the evaluation of cyanide sources in iridium catalysed amine dehydrogenation reactions.

Table 5.1 Conditions screened during SCRAM catalysed cyanide addition to imines[a]

Entry	Cyanide Source and quantity / mol equiv.	Catalyst	Catalyst Loading / mol%	Overall Concentration of reactants in solution / N	Product Observed *via* GC-MS
1	KCN, 0.79	**5.1b**	1	0.57	**5.11**[b]
2	KCN, 4	**5.1b**	1	2.09	**5.12 or 5.13**
3	KCN, 4	**5.1a**	1	2.09	**5.12 or 5.13**
4	KCN, 4	**5.2**	2	2.09	**5.12 or 5.13**
5	KCN, 4	**5.2**	2	2.09	**5.12 or 5.13**
6	TMSCN, 1.5	**5.1b**	1	1.25	No[c]

[a] Amine **5.9** (2 equiv.), iridium catalyst (1 mol%), cyanide source (5 equiv.) and water (5 mL) were heated to reflux for 24-60 hours.

[b] Product observed *via* analysis of crude NMR and comparison to commercially available **5.11**

[c] Reaction carried out in toluene

5.2.2.1 Reactant concentration

A higher reactant concentration of 2.09 M failed to give any product (Table 5.1, Entry 2). However, during GC-MS analysis of the 2.09 M reaction, two by-product peaks with *m/z* 134 and 139 were observed in minor quantities. The compound with *m/z* 139 was tentatively assigned the structure of enamide **5.12**, formed *via* reaction with acetonitrile (the GC-MS solvent) and subsequent water hydrolysis (Scheme 5.6). Structure **5.13** was tentatively assigned to the compound with mass *m/z* = 134 and might be formed by double addition of cyanide to the imine. The formation of this product could provide a potentially useful entry into the drug gabapentin, **5.14** (Figure 5.1). Compounds **5.12** and **5.13** did not appear in ^{1}H-NMR analysis and were not isolable from the reaction mixture, appearing instead to be artefacts of the analysis process.[163]
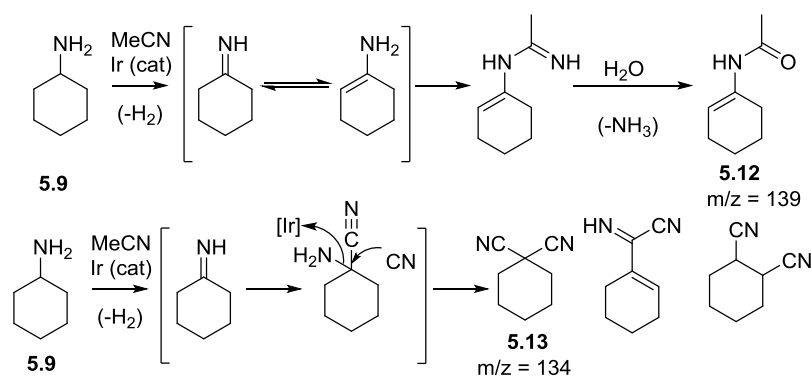
Scheme 5.6 Formation of enamide 5.12 and dinitrile 5.13 from the reaction of cyclohexylamine with MeCN and cyanide respectively.
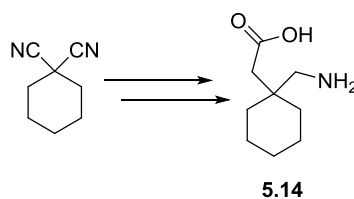
Figure 5.1 Gabapentin.[163]

5.2.2.2 Catalyst screening

In Chapter 2, different catalysts were shown to have different activities in amine dehydrogenation. Accordingly a series of catalysts were evaluated (Table 5.1, Entries 2-5). Amine **5.9** and potassium cyanide (4 equiv.) were heated to reflux in the presence of

catalysts **5.1b**, **5.2** or **5.1a** in deionised water and the reaction monitored *via* GC-MS. The catalyst loadings were normalised to ensure that the same number of moles of iridium were available in each reaction. After 24 h GC analysis indicated that two species were present in the reaction mixture at 5.2 min with *m/z* = 139 and at 5.6 min. with *m/z* = 134 that were tentatively assigned structures **5.12** and **5.13**, which had been observed previously (*vide supra*).

5.2.2.3 Evaluation of a different cyanide source

Barton and co-workers' developed a Strecker reaction in organic media using trimethyl silylcyanide (TMSCN) as the cyanide source (Chapter 1, Scheme 1.9).[14] To evaluate whether the solubility of the amine was affecting the reaction, the reaction was carried out with TMSCN, in organic media (Table 5.1, Entry 5). Amine **5.9** was stirred with complex **5.1b** (1 mol%) and TMSCN (1.5 equiv.) in anhydrous toluene at 100 °C for 60 hours. No reaction was observed by GC-MS, an indication that the TMSCN was not nucleophilic enough to react with the imine.

5.2.3 Conclusion

A range of conditions have been evaluated for the synthesis of α-amino nitriles by a Strecker type synthesis from primary amines, using hydrogen transfer methodology to form an imine *in situ,* all conditions have proven unsuccessful. The species observed, during analysis of the reaction mixtures, indicated that homo-dimerisation, by-product formation (that could be potentially useful) or no-reaction was observed. As primary and not secondary or tertiary amines were evaluated, these may prove more fruitful endeavours in α-aminonitrile synthesis as has been shown in the literature, *in situ* generation of the desired imine from carbonyl and amine attack and these avenues will constitute the bulk of future efforts.

5.3   Novel aziridine formation

5.3.1 Background and synthetic rationale

The formation of aziridines is very important in organic synthesis, as noted in Sweeney's review of the moiety.[87] Aziridines can be considered umpolung synthons during retrosynthetic analysis and, as such, they are highly useful reagents in natural product synthesis (Figure 5.2).
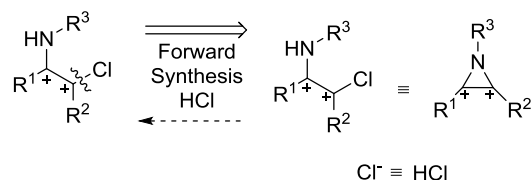
Figure 5.2 Example of an umpolung situation in retrosynthetic analysis, leading to an aziridine being a potential synthon.

The aziridine moiety has been used recently as an intermediate in the synthesis of a number of antibiotics including **5.15-5.18**, synthesised from the key fused cyclohexane-aziridine structure, **5.14** (Figure 5.3).[164]
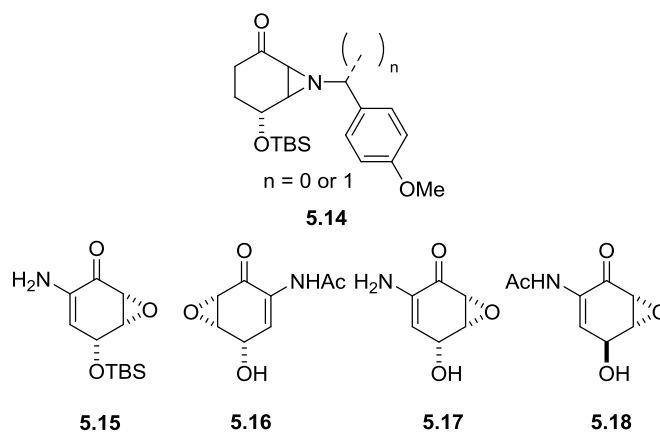
Figure 5.3 Intermediate 5.14 used in the synthesis of antibiotics 5.15-5.18.

It was envisioned that the imine formed *in situ* during iridium catalysed amine dehydrogenation would react with a nucleophile containing a potential leaving group, for example a sulfonium (**5.19**) or sulfoxonium ylide (**5.20**) as in the Johnson-Corey-Chaykovsky reaction (Scheme 5.7).[165, 166]
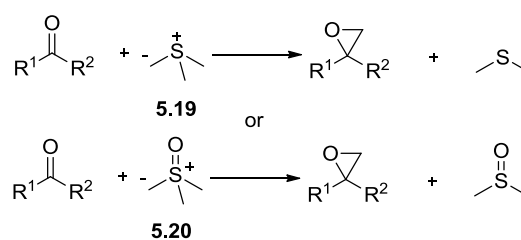
Scheme 5.7 Epoxide formation using the Johnson-Corey-Chaykovsky reaction, with dimethylsulfonium (5.19) or dimethylsulfoxonium (5.20) ylides.

This new method would not require the use of potentially hazardous diazo compounds, which have been used previously to form aziridines *via* Lewis acid[167] and rhodium catalysis.[168] Therefore, due to the importance of the aziridine moiety and the significant potential of its synthesis directly from amines *via* iridium catalysed hydrogen-transfer reactions, the evaluation of its formation was tested using the standard dehydrogenation conditions and dimethylsulfoxonium methylide.

5.3.2 Results and discussions

The dimethylsulfoxonium methylide (**5.20**) nucleophile used to evaluate the potential formation of aziridines through the iridium catalysed dehydrogenation of amines was formed *via* deprotonation of trimethylsulfoxonium iodide (**5.21**) using the conditions of Smith and co-workers (Scheme 5.8).[169] Dimethylsulfoxonium methylide was used as the DMSO formed during the reaction was preferred compared to the more volatile dimethsulfide formed with the sulfonium analogue.
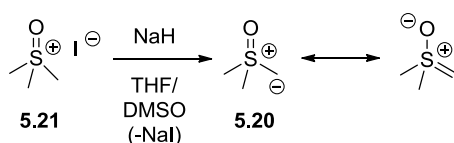
Scheme 5.8 Synthesis of dimethylsulfoxonium methylide, 5.20.

Ylide **5.20** reacts readily with water, therefore its use is potentially problematic during scale up due to the requirement for anhydrous conditions during ylide synthesis (Scheme 5.8). The negative-charge localised onto the amine nitrogen of zwitterionic species **5.22** would be available to attack the α-carbon to form the aziridine species (**5.23**) *via* concomitant loss of DMSO (Scheme 5.9).
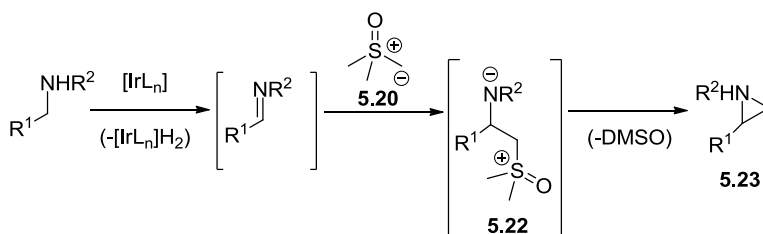
Scheme 5.9 The proposed use of dimethylsulfoxonium methylide (5.20) as the nucleophile during aziridine synthesis.

A standard of phenyl aziridine (**5.25**) was prepared from phenylglycinol (**5.24**) in 33% yield using Li's method (Scheme 5.10).[170] This standard was used for comparison in GC analysis during the study. When stored at room temperature, the phenyl aziridine standard was observed to decompose over several days at room temperature by NMR analysis.
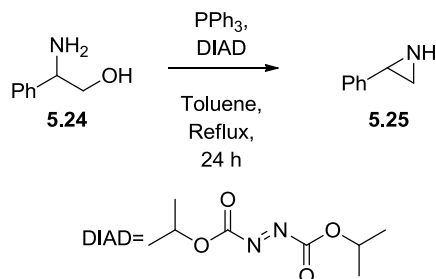
Scheme 5.10 Li's synthesis of phenyl aziridine, 5.25.[170]

Ylide **5.20** was initially tested as a nucleophile with benzylamine (**5.26**) activated *via* iridium catalysed dehydrogenation at reflux in xylenes (with dropwise addition of amine-ylide solution into the reaction, Scheme 5.11, Table 5.2, Entry 1). The formation of tentatively assigned aziridine **5.25** was observed *via* GC and GC-MS at 14% conversion *via* comparison to the separately prepared standard. Isolable quantities of aziridine **5.25** were not possible. The decomposition observed of the standard aziridine **5.25** indicated there may be associated problems due to thermal opening during the reaction, which have been observed in the formation of azomethine ylides and there subsequent reactions.[171-177]
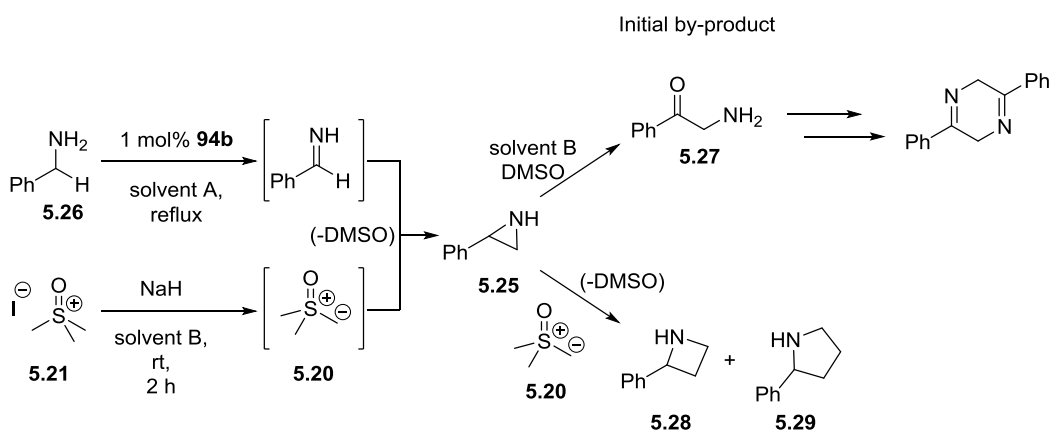
Scheme 5.11 *In situ* aziridination and subsequent azetidination or oxidation.

Table 5.2 Reaction conditions screened during aziridine formation study.[a]

Entry	Solvent A	Solvent B	Solvent C	Proposed Main Product / N^o	Product[b, c] / %
1	Xylenes	THF	n/a	**5.28**	14
2	PhMe	DMSO	n/a	**5.25**	32
3	PhMe	THF	n/a	**5.29**	20
4	Xylenes	THF	DMF	**5.25/ 5.27**	21/23
5	Xylenes	Anisole	n/a	No reaction	0

[a] Amine **5.26** (1.00 equiv.), iridium complex **5.1b** (1 mol%) in anhydrous solvent A (2 mL) were heated to reflux and a suspension of ylide **5.20** (1.5 equiv.) and solvent B (1 mL) were added slowly.

[b] Calculated *via* comparison to a biphenyl internal standard.

[c] Yield to the nearest percent, ±0.5%.

Several different reaction conditions were screened (Table 5.2), however isolation of aziridine **5.25** proved impossible. Various over-reaction products including: azetidine **5.28,** pyrrolidine **5.29** (Entries 1 and 3), as well as oxidation products that form in the presence of DMSO (**5.27**), were observed instead (Entry 4).
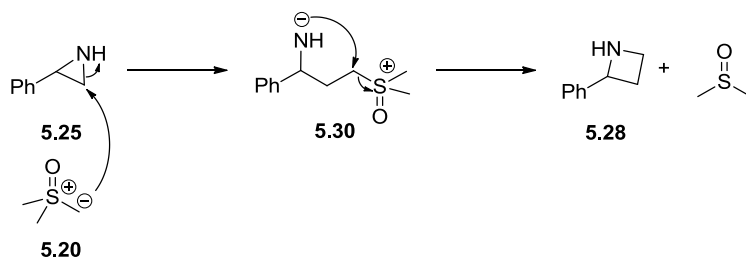
Scheme 5.12 Proposed mechanism for formation of azetidine 5.28.

The azetidine and pyrrolidine observed during GCMS analysis (Figure 5.4) are proposed to form due to an excess of ylide **5.20** in the reaction vessel (Scheme 5.12), as similar reactions have been described previously by Carrié and co-workers.[178, 179] Ylide **5.20** preferentially attacks the less substituted position to ring open aziridine **5.20**. The product of the ring opening, **5.30**, then itself ring closes to afford azetidine **5.28** and another equivalent of DMSO. Alternatively, the reaction may also occur without an initial ring closure to aziridine **5.25** (Scheme 5.13).
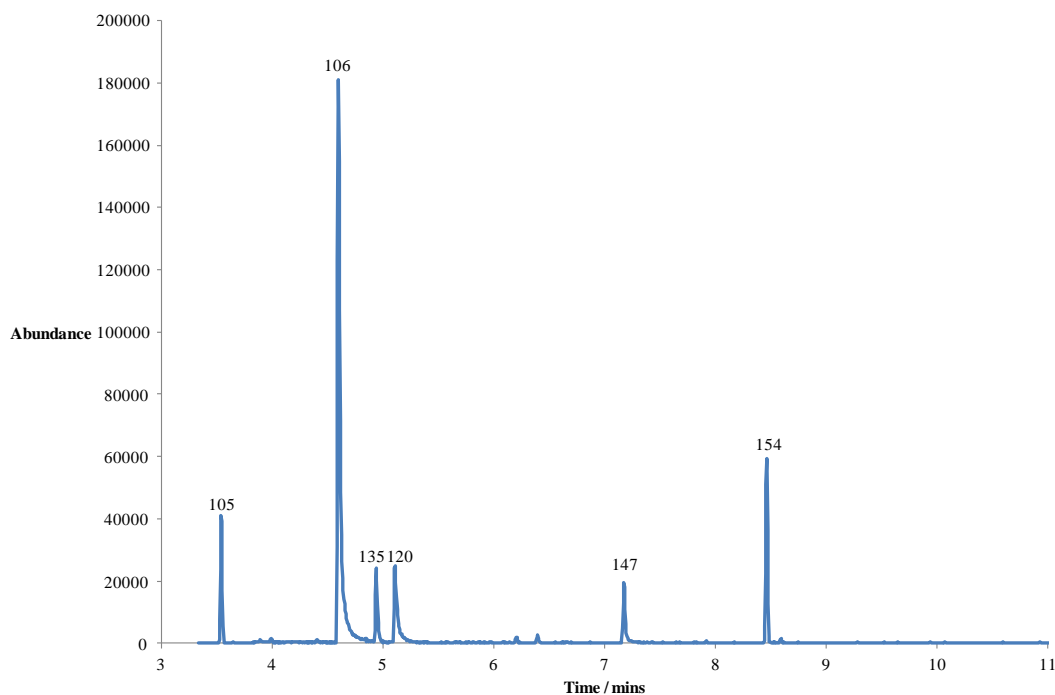
Figure 5.4 Total Ion Chromatogram for the iridium catalysed dehydrogenative nucleophilic reaction of amine 5.26 with ylide 5.20, showing the major ions and omitting the solvent peaks. 106 (benzylamine), 120 (rationalised as phenyl aziridine), 135 (rationalised as oxidation product 5.27), 147 (rationalised as phenyl pyrrolidine, 5.28), 154 (biphenyl standard).
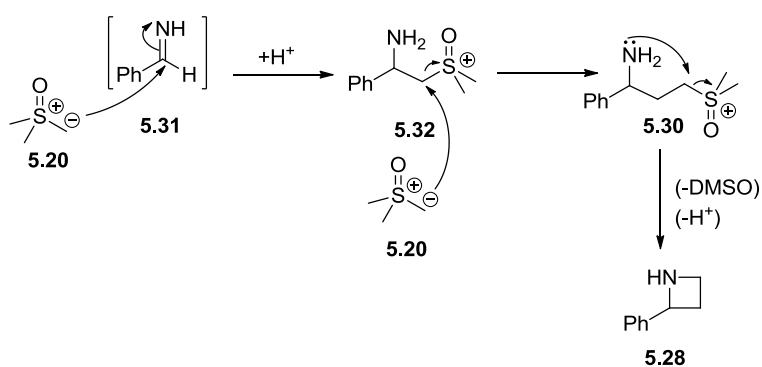
Scheme 5.13 Alternative proposed mechanism for azetidination 5.28 formation.

Phenyl pyrrolidine **5.29** formation was anticipated to occur *via* a second ring opening with subsequent ring closure analogous to that seen with azetidination (Scheme 5.14). The formation of the piperidine analogue of pyrrolidine **5.29,** was however not observed in the initial GC analysis or during isolation.
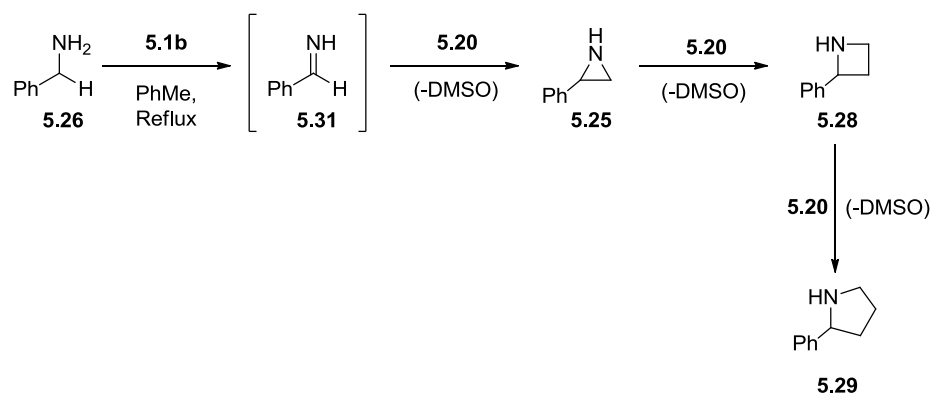
Scheme 5.14 Formation of pyrrolidine 5.29.

A range of polar aprotic solvents were assessed in the reaction. When DMSO was used as a solvent (Table 5.2, Entry 2), oxidation of aziridine **5.25** to 1-phenyl-2-aminoethanone (**5.27**), was observed as a peak at 4.9 min with *m/z* of 135 in GC-MS analysis. Analogous oxidations of aziridines to similar products by DMSO have been observed separately by Heine and Fujita (Scheme 5.11).[180-182] The use of DMSO as a solvent in the ylide forming reaction led to 32% to aziridine **5.25** and oxidation product **5.27** (3%) as measured by GC against an internal standard.

DMF was evaluated as a different high boiling aprotic solvent. The ylide **5.20** appeared soluble in DMF, allowing for the solvent to be changed from THF to DMF after the formation of ylide **5.20** (Table 5.2, Entry 4). During the reaction a mixture of compounds rationalised as aziridine **5.25** (21%), azetidine **5.28** (4%), pyrrolidine **5.29** (<1%) and oxidation product **5.27** (23%) were observed *via* GC analysis, as well as the starting amine **5.26** (47%). However, when the reaction was carried out in toluene at reflux, the pyrrolidine **5.29** was observed after 18 hours. Isolation of the aziridine **5.25** *via* column chromatography was carried out with different solvents, pH and media (silica and alumina) but separation proved elusive.

Anisole was evaluated as a further high boiling point (154 °C), polar aprotic solvent (Table 5.2, Entry 5), able to dissolve ylide **5.20** and allow for faster dehydrogenation, however no reaction was observed during the reaction.

5.3.3 Conclusions

Different conditions were screened to obtain phenyl aziridine **5.25**, however successful isolation proved impossible. Nevertheless, GC yields of upto 32% were observed by

comparing with both an authentic sample of phenyl aziridine and internal standard. The molecular ions of numerous by-products were observed *via* GC-MS analysis that included those due to ring expansion (**5.28** and **5.29**), through reaction with unreacted ylide **5.20**, or oxidation by DMSO (**5.27**). The evaluation of secondary amines may prove fruitful, due to the reduced nucleophilicity, however the thermal ring-opening that is known to occur with aziridines at the operating temperature will require the use of catalysts that are highly active even at lower temperatures or use of flow chemistry to allow for reduced time at high temperatures.

5.4   A novel method for the deprotection of amines

5.4.1 Introduction

The protection and deprotection of reactive functional groups is vitally important to organic synthesis, as it enables synthetic chemists to build a diverse array of molecules with varying sizes and complexities. Funtionalised amines are important to the pharmaceutical and fine chemical industries, as such their protection during the synthesis of APIs is exceptionally important. The textbooks by Kocieński[183] and Greene[184] provide a great insight and overview of the possible protecting group strategies available to the organic chemist for amines.

The C-N bond of an alkylated amine is not generally considered easy to break and is normally an irreversible process. The benzyl protecting group can be deprotected by hydrogenolysis to cleave the desired C-N bond to form the unprotected amine (Scheme 5.15).
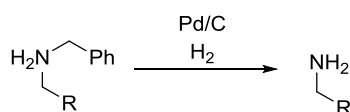
Scheme 5.15 General hydrogenolysis of *N*-benzyl protected amine.

In Chapter 2 ammonium salts were shown to partially inhibit *N*-alkylation of primary amines during iridium catalysed dehydrogenation, through reversing the *N*-alkylation equilibrium to enhance product primary amine and imine formation in Scheme 5.16.
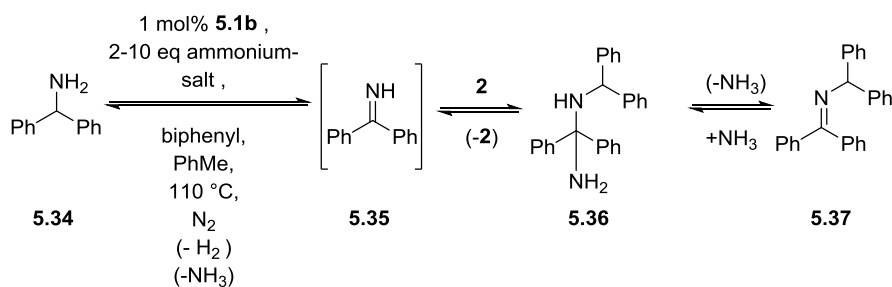
Scheme 5.16 Use of ammonium additives to reduce *N*-alkylation of amine 5.34.

The *N*-alkylation process is believed to be dependent upon the loss of ammonia (Scheme 5.16), so within a closed system an equilibrium will form. By carrying out dehydrogenation reactions with secondary and tertiary amines in the presence of an ammonia source, a de-alkylation to form two separate amines could be performed as the excess of ammonia would drive the equilibrium to increased primary amine formation. The successful implementation of this methodology would lead to a new protocol for the deprotection of amines that would make use of alternative reaction conditions to hydrogenolysis, establishing for example novel protecting groups such as the -methyl, -phenyl or -*tert*-butyl groups (Figure 5.5), which are not generally possible and would add further impact to the protocol. This work could thus allow for an expansion in the landscape of amine-based synthetic chemistry. In order to realise this objective, the synthesis of a range of secondary amines was carried out and these were analysed for successful deprotection by ammonia.
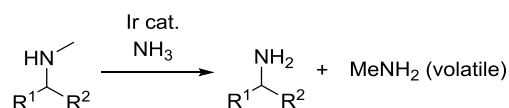
Figure 5.5 An *N*–methyl protected amine, a potential novel protecting group that could be realised *via* iridium catalysis.

Beller and co-workers have previously shown that a ruthenium system based on Shvo's catalyst **5.38** and ammonia gas can form primary amines from secondary and tertiary amines (Scheme 5.17). [185] Whilst Beller's protocol was applicable to a range of alkylated acyclic and cyclic amines, benzylic (aryl) amines were poorly represented (50% yield, 56% conversion). The results reported were based on GC yields so the development of a method that isolated and fully characterised the amine products would be desirable.
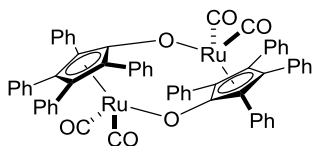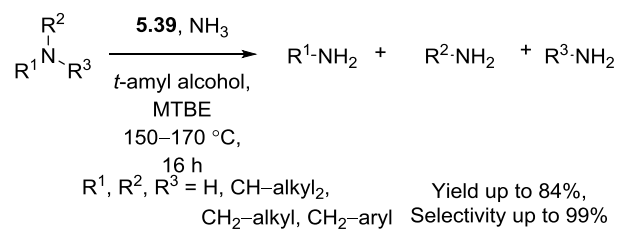
Scheme 5.17 Beller's synthesis of primary amines.

5.4.2 Results and Discussion

5.4.2.1 Starting material synthesis

A range of secondary amines were synthesised *via* reductive amination reactions using the modified literature procedures of Abdel-Magid[186] or Lai[187] and isolated as the hydrochloride salts (Scheme 5.18). With this range of secondary amines in hand, the screening of a various conditions was carried out to dealkylate secondary amines.
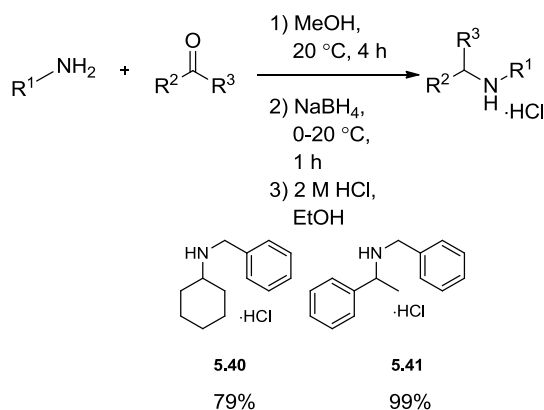
Scheme 5.18 Synthesis of secondary amine hydrochloride salts.

5.4.2.2 Conditions screened in attempted secondary amine deprotection

During the screening of reaction conditions for secondary amine deprotection, *N*-benzyl cyclohexylamine and *N*-benzyl-α-methyl benzylamine were chosen as model amine substrates.
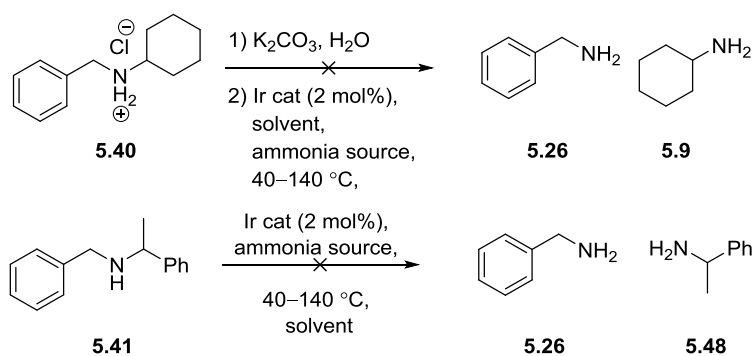
Scheme 5.19 Conditions trialled during unsuccessful amine deprotection.

Studying successful reactions with *N*-benzyl cyclohexylamine could give a further indication of mechanism, if labelling studies were carried out. Amines **5.40** and **5.41** were tested in a range of conditions: different ammonia sources; temperatures; solvents; closed or open systems were examined (Table 5.3).

Table 5.3 Conditions evaluated during deprotection study.[a]

Entry	Amine	Nucleophile Source	Temp / °C	Solvent	Sealed Tube	Yield of deprotected amine / %
1 [b]	**5.40**	NH_4OAc	110	PhMe	No	0
2	**5.40**	NH_4OH	55	MeCN	Yes	0
3	**5.40**	NH_4OAc	82	MeCN	No	0
4	**5.40**	NH_4OAc	90	*i*PrOH	Yes	0
5	**5.41**	NH_4OH	90	*i*PrOH	Yes	0
6	**5.41**	NH_3	40	*i*PrOH	Yes	0
7	**5.40**	$NH_2OH•HCl$, Na_2CO_3	reflux	MeOH	No	0
8	**5.41**	$NH_2OH(aq)$	reflux	CH_2Cl_2	No	0
9	**5.40**	$NH_2OH•HCl$, Na_2CO_3 (in CH_2Cl_2)[c]	reflux	xylenes	No	0
10	**5.40**	$NH_2OH•HCl$	reflux	PhMe	No	0
11	**5.40**	$NH_2OH•HCl$	reflux	MeCN	No	0
12	**5.40**	$NH_2OH•HCl$	reflux	THF	No	0
13	**5.40**	$NH_2OH•HCl$	reflux	^nBuOAc	No	0
14	**5.40**	$NH_2OH•HCl$	reflux	H_2O	No	0
15	**5.40**	$NH_2OH•HCl$, Na_2CO_3 (in CH_2Cl_2)	reflux	xylenes	No	0
16	**5.40**	NH_4OH, Na_2CO_3 (in MeCN)	reflux	xylenes	No	0

[a] Amine (1 equiv.), ammonia source, complex **5.1b** (1 mol%) in solvent (2 mL) were heated and monitored by GC-MS, LC-MS and ^{1}H-NMR analysis.

[b] Formed *in situ* from iridium complex **5.1a** and KI.

[c] Dropwise addition of amine to reaction.

Analysis of all reactions by LC-MS and ^{1}H NMR indicated that only starting material was present in the crude mixture. Two conclusions can be drawn from the screening experiments as to the reason for their failure (Table 5.3): either no reaction was occurring, which was possible due to the literature precedent for inactive, insoluble iridium-amine species being formed[77] or that the equilibrium lies far to the side of *N*-alkylation and the equilibrium constant, K_c, is less than one for the required reaction shown in Scheme 5.16 (as supported by evidence in Chapter 2).

When an open reaction vessel was used ammonia could evaporate resulting in a loss of reagent (Table 5.3, Entries 1, 3, 6, 8-18). The higher boiling ammonium acetate was then used to overcome this issue. However, the formation of the desired amine was not observed. This result would lead to the second conclusion being true, however a further hypothesis could be that the rate of *N*-alkylation is far greater than that for dealkylation. The operating temperature that Beller used during dealkylation were higher than those achievable (150 170 °C) for sealed tube reactions using the apparatus available.[185] The vessel used for the deprotection with ammonia dissolved in isopropanol reached an internal temperature of 55 °C due to the requirement for a specially designed metal jacket, which was harder to heat uniformly, indeed Beller had to use specialised equipment to carry out his deprotections.

5.4.3 Conclusions

Successful deprotection of secondary amines has proven elusive. In spite of a wide range of conditions being screened, there has been no evidence for the formation of primary amines. The reason for this may lie in the fact that the primary amines formed rapidly undergo the reverse reaction, as it has been observed previously (Chapter 2), or that iridium-amine complexes are being formed that precipitate out of solution and also inhibit the dehydrogenation process. A similar system to that which has been used in the literature was evaluated, however the pressures of ammonia that would have formed in the reaction vessel are not desirable on a laboratory scale, furthermore, the use of jacketed vessels inhibited the heating of the reaction and so high temperatures were not achievable.

5.5   Overall Conclusions

A range of nucleophiles have been evaluated to try to broaden the scope of iridium catalysed hydrogen transfer reactions. For the formation of α-cyano amine **5.10** from primary amines, homo-dimerisation has predominated, which has been rationalised by the reversibility of the cyanide addition and the facile nature of *N*-alkylation at the operating conditions. Due to the

forcing conditions of the reaction, even when formation of aziridine **5.25** had been observed *via* GC, secondary reactions were observed, leading to low yields of aziridine products and mixtures of products. Trying to exploit the equilibrium formed during *N*-alkylation to reverse the process and form primary amines from secondary amines has not been successful. This result was rationalised as the facile nature of imine alkylation and encouraged further by iridium coordination of the imine intermediates.

Chapter 6 Overall Conclusions and Future Work

Functionalised amines are important molecules to the chemical industries, in both functional and economic terms. The methods to make functionalised amines are varied, but tend to require multi-step reactions that produce stoichiometric waste streams and can require the use of hazardous reagents that must be controlled, especially in API synthesis. These facets of amine functionalisation can add further cost to the formation of amines on an industrial scale; however attempts have been made to functionalise amines *via in situ* activation.

Previous published work has focused on the functionalisation of amines using stoichiometric oxidants,[15, 16, 139] a drawback of these reactions is that the oxidants are hazardous and can be expensive to use on anything above a laboratory scale. There has also been a focus on new metal catalysed methodologies for the functionalisation of molecules that has been a direct evolution of hydrogenation and transfer hydrogenation chemistry. Hydrogen-transfer reactions have risen to prominence in recent years,[39] with the attraction of being a cost-effective, greener methodology to activate low cost materials to reactions that produce higher value products. Hydrogen-transfer methodology activates often-considered non-electrophilic substrates to nucleophilic attack, forming imines, carbonyls and alkenes from amines, alcohols and alkanes, respectively.

Hydrogen-transfer reactions have been thoroughly explored with alcohols, however there remains an opportunity to extend this methodology further to incorporate amines. Hydrogen-transfers have been used with amines to form single stereoisomers through kinetic resolution and then racemisation of non-reactive stereo-centres,[74, 76, 77, 96] to reduce waste during reactions. The methodology is used to carry out *N*-alkylation reactions of amines. Whilst these reactions have showcased the technology with respect to amines, further functionalisation reactions can be exploited to help form numerous different products including: α-aminonitriles, β-nitroamines, aziridines and (hetero)-cyclic compounds, *via* nucleophilic reactions of imines formed *in situ*. The potential for industrially important contributions using this method has been exemplified through Pfizer's multi-kilo API intermediate synthesis using hydrogen-transfer activation of an alcohol to carry out an *N*-alkylation.[152] There are several potential problems that may arise with this method that include homo-dimerisation of the amine used once it has dehydrogenated and by-product formation, due to the reactive nature of imines (primary imines especially).[96]

The research carried out during PhD studies has shown that the selective formation and isolation of imines is not facile *via* iridium catalysed dehydrogenation methodology. Chapter 2 described how in the case of primary imines especially, after formation they will rapidly and readily undergo *N*-alkylation reactions, as has been disclosed previously within the literature. This process can be tuned to form *N*-alkylated amines faster. Conversely to previous literature reports, a rate enhancement can be seen using molecular oxygen as an oxidant (with an air sparge), which is not observed using only a nitrogen sparge. This result supported the mechanistic hypothesis that the cleavage of the iridium-hydride bond to reform the active catalyst was rate limiting. The equilibrium formed during the dehydrogenation and *N*-alkylation reactions, by the addition of a source of ammonia, to facilitate the formation of small quantities of imine, was also exploited; however *N*-alkylation product was still formed. Deuterium labelling experiments could potentially give further insight into the reactions probed. For example, these reactions could definitively prove whether or not dicyclohexylamine is dehydrogenating and the rate at which it is undergoing the process (Scheme 6.1), giving further mechanistic information. Furthermore, this reaction could also be used to probe any Secondary Kinetic Isotope Effects (SKIE) experienced by the C-H bond alpha to the amine group.

R = D or H
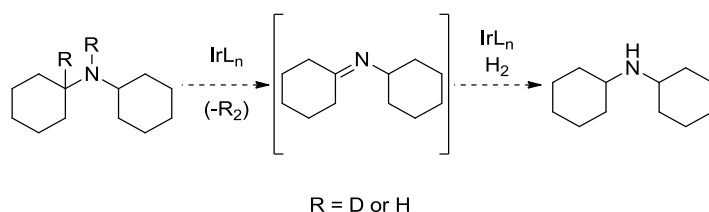
Scheme 6.1 Potential deuterium labelling experiments.

Chapter 3 outlined the mechanistic information that has been gained by various analytical methods, including NMR, MS and X-ray diffraction. Several different species have been observed that are potential intermediates during *N*-alkylation reactions. NMR analysis has shown that reaction can occur with several different species of iridium complex being formed and that many amines will bind to the iridium centre, with less sterically hindered amines showing a greater interaction. A potential *bis*-amine-iridium complex has also been observed, whose formation suggested that *N*-alkylation may occur *via* an inner sphere mechanism. The crystal structure of a mono-dentate iridium-benzylamine complex has been elucidated, suggesting a potential catalyst inhibition pathway for the reaction. A Hammett analysis of a range of 4-substituted benzylamines has not shown conclusively that the rate limiting step of the reaction involves the build-up of charge at the reactive centre. This

result would support the mechanistic hypothesis that iridium-hydride cleavage maybe the rate limiting step. Further mechanistic work is required, with the isolation and analysis of other amine bound iridium complexes being very important, as this may give further information on how this complex affects the reaction. Furthermore, *in silico* and molecular modelling studies focused on understanding how Fujita's and similar monomeric iridium systems, would give further understanding of the reaction.

Chapter 4 described findings from the functionalisation of tertiary amines with iridium catalysed iminium ion formation and cyclisation to form polycyclic indoles. The reaction benefits from the inability of the iminium ion to undergo *N*-alkylation, however the greater energetic demands of the process require higher reaction temperatures and there are lower substrate conversions and yields. Future work analogous to this could be highly profitable, as if a similar reaction to that disclosed previously was developed, this could allow access to several functionalised polycyclic isoquinolines which are medicinally important. (Scheme 6.2).[128]
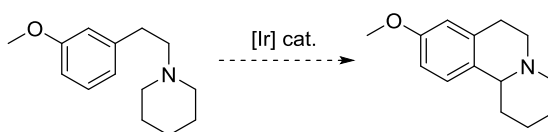
Scheme 6.2 Potential synthesis of isoquinolines using iridium catalysis.

Finally a range of other nucleophiles, including cyanide and sulphur ylides, have also been evaluated in their reactions with a range of primary amines. Homo-dimerisation tended to predominate or product degradation was observed during reaction monitoring. The use of iridium catalysts to synthesise α-amino nitriles, rather than ruthenium catalysts, in a similar fashion to Murahashi[139] is a further potential avenue that could be exploited (Scheme 6.3).
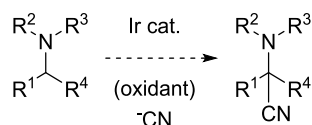
Scheme 6.3 Potential synthesis of α-amino nitriles, using iridium catalysed hydrogen transfer.

The cleavage of secondary amines to form two separate primary amines (using ammonia) or to form an amine and alcohol (using water or hydroxide) has also been evaluated with no

success observed. This result suggested that the rate of *N*-alkylation is faster than the backward reaction and a large excess of ammonia or hydroxyl are required, with respect to the ammonia reaction the pressures involved when heating ammonia have meant that this reaction has been hard to evaluate on a laboratory scale. In the future, the *in situ* formation of secondary imines *via* the reaction of amines with carbonyls (formed through transfer dehydrogenation of the parent alcohol) could potentially be successful with these more stable imines being more ready to react with nucleophiles (Scheme 6.4).
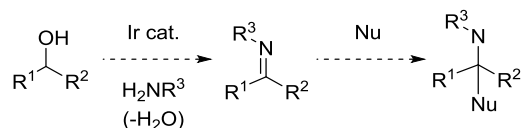
Scheme 6.4 Potential use of *in situ* N-alkylation to synthesise functionalised amines from alcohols.

Xiao's catalyst,[73, 137] described in Chapter 1, has recently received interest due to its increased activity compared to Fujita's catalyst, whilst it was not successful in its use in iridium catalysed polycyclic indole formation, the catalyst can successfully activate amines at lower temperatures than $[IrCp*I_2]_2$ and could potentially solve the thermal ring opening observed with aziridine formation (Scheme 6.5). Stabilised aziridine formation using amides could potentially overcome the instability problems observed. Furthermore, the potential formation of pyrrolidines and azetidines due to ring expansion of aziridines merits further investigation.
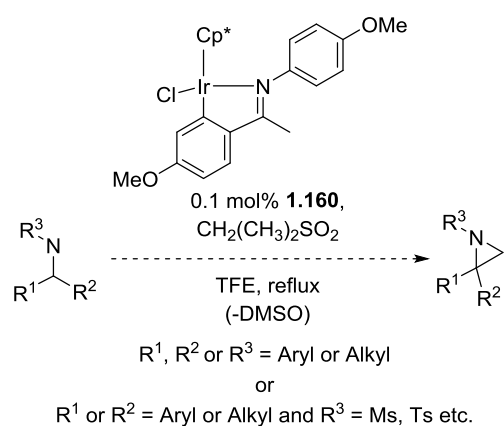
Scheme 6.5 Potential use of Xiao's catalyst to form aziridines at lower temperature or use of stabilised aziridines.

There is also work being carried out on immobilising SCRAM type catalysts,[138] putting reactions in flow systems, which may solve some of the problems associated with dimerization, by reducing the time the amine is available for the catalyst to dehydrogenate, and also the thermal ring opening associated with aziridines.

Chapter 7 Experimental Section

7.1 General methods

Unless otherwise stated, all the chemicals and reagents were obtained commercially from Sigma-Aldrich, Fisher Scientific, Alfa Aesar or Merck and used without further purification. Xiao's catalyst, **4.48**[73, 137] and immobilised catalyst **4.50**[138] were obtained from Yorkshire Process Technology and were used without further purification. Palladium complex **4.49**, was prepared by Dr. J. P. Cooksey using the method of Waymouth[188] and used without further purification. All solvents used were HPLC grade. Analytical Thin Layer Chromatography was performed on precoated silica gel plates (Kieselgel 60F254, Merck). Column chromatographic purifications were performed with flash silica gel. NMR spectra were recorded in $CDCl_3$, toluene-d_8, DMSO-d_6 or CD_3OD, unless otherwise stated, on DPX300, AV 500 MHz Bruker or Varian Inova 500 MHz NMR spectrometers. All chemical shifts are reported in δ ppm downfield of TMS and peak multiplicities as singlet (s), doublet (d), quartet (q), quintet (quin), septet (sep), doublet of doublets (dd), broad singlet (bs), and multiplet (m). Signal assignment, where possible/necessary, was made with the help of 2D-NMR techniques (COSY, HMQC, HMBC, and DOSY). High resolution mass spectra (HRMS) were obtained using either a Waters GCT Premier mass spectrometer, using electron impact (EI), a Bruker microTOF using electrospray ionisation (ESI), or a Bruker MaXis Impact, using electrospray ionisation (ESI). Electrospray ionisation mass-spectrometry (ESI-MS) were run on an Agilent 1200 LC system equipped with a Phenomenex Luna C18(2) 50 × 2 mm column, 5 μm particle size, on an acetonitrile/water gradient (5-95% acetonitrile, 0.1% formic acid, over 3 minutes) and a Bruker Daltonics HTCUltra™ system equipped with an ion trap MS detector. Infra-red (IR) analyses were performed using a Perkin Elmer FT-IR spectrometer or a Bruker Platinum-ATR system equipped with an Alpha FT-IR spectrometer and the samples were analysed as solids. Melting points were determined using a Griffin and George melting point apparatus and are uncorrected. Single crystal X-ray data were collected and structures resolved by Dr H. Sheppard or Dr C. Pask (University of Leeds) on a Bruker SMART APEX CCD area diffractometer with graphite monochromatized (Mo Kα = 0.71073Å) radiation at room temperature or Agilent Super Nova area diffractometer with mirror monochromatized ((Mo Kα = 0.71073Å). Gas chromatography was carried out using a HP 6890 series GC system, Agilent Technologies 7683 series injector and HP 7683 series autosampler. GC method (for conversion) Column = HP-5 5% polymethyl siloxane capillary column (30 m x

320 μm x 0.25 μm). Oven temperature = 60 °C isothermal for 2 min.; 15 °C min^{-1} ramp to 235 °C; 235 °C isothermal for 7 mins. Inlet pressure = 4.31 psi. Gas chromatography mass spectrometry was carried out using an HP 7683 series injector, HP 5973 mass selective detector, HP 6890 GC system, HP 7683 series auto sampler. GC-MS method (for crude mass measurements) Column = HP-5MS-Agilent 190915-413 capillary column (30 m x 320 μm x 0.25 μm). Oven temperature = 60 °C isothermal for 2 min; 15 °C min^{-1} ramp to 235 °C; 235 °C isothermal for 7 min. He flow = 4.30 psi, flow rate = 1.8 ml min^{-1}, with a 2.5 min solvent delay. GC yields are reported compared to an internal biphenyl standard, where isolation has been achieved these values are corrected using the internal response factor, *F*, for the analyte.

7.2   Experiments discussed in Chapter 2

7.2.1 Calibration of GC data and determination of *F*

Table 7.1 Values used for the calculation of internal response factor, *F*, for analytes in GC analysis.

Analyte	Analyte Mass / mg[b]	Peak Area Analyte[c]	Biphenyl Mass / mg[b]	Peak Area Biphenyl[c]	*F*[a]
Benzophenone imine, **2.7**	182	10952	63	4377	1.03
Benzylamine, **3.6**	132	5317	67	3950	0.48
Benzhydrylamine, **2.6**	183	11201	27	1738	1.11
N-benzhydryl diphenyl methanimine, **2.8**	20	454	17	1893	0.24
Cyclohexylamine, **2.31**	142	4230	10	575	0.71
Dicyclohexylamin, **2.34**	193	8845	10	700	0.76

[a] Biphenyl and analyte dissolved in 5 mL aliquot of acetonitrile, *F* determined using Equation 7..

[b] Mass +/- 0.5 mg.

[c] Peak area +/- 0.5 units

A 5 mL aliquot of biphenyl and the analyte was prepared in acetonitrile (5 mL) (Table 7.1). The solution was added to a sample vial and analysed *via* GC. The concentration of the biphenyl and analyte in the aliquot was calculated. The peak area of the analyte was then measured and compared to the peak area of the biphenyl. A ratio of the peak areas to concentrations for the analyte and biphenyl were calculated. The internal response factor, *F*, was calculated as the ratio of the analyte response to biphenyl response (Equation 7.).

$$F = \frac{\frac{A_x}{[X]}}{\frac{A_s}{[S]}}$$

Equation 7.1 Used for the calculation of internal response factor, during GC analysis.

F= Internal response factor.

A_x= Peak area of analyte.

[*X*]= Concentration of analyte

A_s= Peak area of standard

[*S*]= Concentration of standard.

7.2.2 Direct *N*-alkylation of benzyhydrylamine by benzophenone with different catalysts

Synthetic procedure 7.2.a

A general synthetic procedure was used with minor modifications to assess the effect of different catalysts on the *N*-alkylation of benzhydrylamine by benzophenone. The procedure is described briefly below:
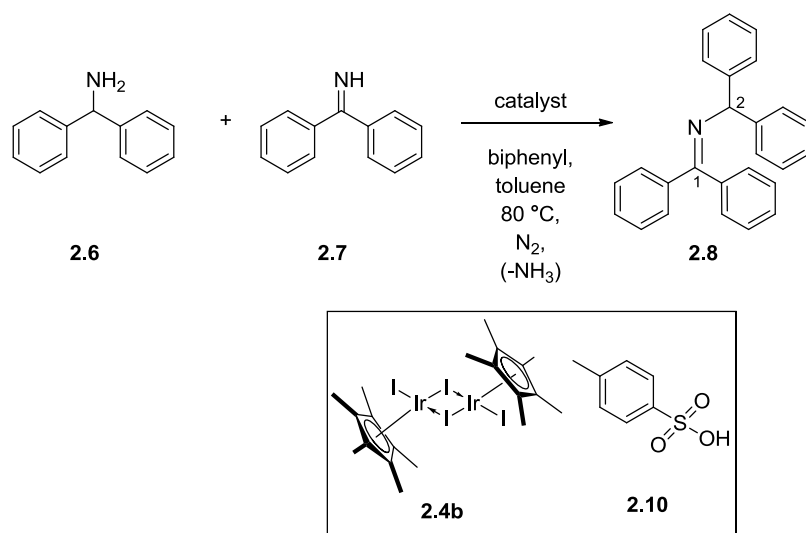
The imine, **2.7**, (168 μL, 0.97 mmol, 1 equiv.) was added to a solution of the catalyst, amine **2.6** (172 μL, 0.97 mmol, 1 equiv.) and internal standard biphenyl (155 mg, 1.00 mmol, 1.00 equiv.) in toluene (4 mL) and heated to 80 °C for 5 hours. The reaction was monitored by **GC** and **GC-MS** at regular intervals by sampling 10 μL and diluting in 5 mL of acetonitrile. 2 mL aliquots of the resulting solution were analysed by **GC** and **GC-MS**. 2 mL aliquots of the resulting mixture were then analysed and the concentration of the *N*-alkylation product **2.8** in the reaction calculated using Equation 7.1 (**GC** elution time: 16.0 min). The initial reaction rates were calculated by calculating the change in concentration of starting material over the first 0.25 hours of reaction.

Entry	Catalyst	Catalyst Loading / mol%	Compound 2.8[a] / %
1	[IrCp*I$_2$], **2.4b**	2	84
2	tosic acid, **2.10**	50	11
3	no catalyst	0	0

[a] Yield based on GC area percent and comparison to internal biphenyl standard, calculated to the nearest percent, ±0.5%.

Entry 1: General procedure **7.2.a** was followed. Pentamethyl-cyclopentadienyl iridium (III) iodide dimer (23 mg, 20 μmol, 2 mol%) was used. The formation of the *N*-alkylation product was confirmed *via* **GC** analysis (84%).

Entry 2: General procedure **7.2.a** was followed. Toluene sulfonic acid (**2.10**) was used (95.1 mg, 500 μmol, 0.5 equiv.). Removal of the solvent *in vacuo* gave the crude product, which was purified by column chromatography (SiO$_2$, 2:1 petroleum ether–dichloromethane) to afford
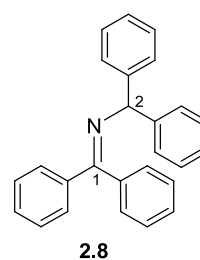
imine **2.8** [189,190] (38.5 mg, 111 µmols, 11%) as colourless needles; **m.p.** (dichloromethane-petroleum ether) 153-155 °C; R_f 0.31 (1:1 dichloromethane–petroleum ether); **^{1}H NMR** (500 MHz, CDCl$_3$) δ: 7.75–7.70 (m, 2H, C*Ar*H), 7.59 – 7.15 (m, 16H, C*Ar*H), 7.12-7.02 (m, 2H, C*Ar*H), 5.53 (s, 1H, C2H); **^{13}C NMR** (75 MHz, CDCl$_3$) 167.0 (C*I*N), 145.0 (C*Ar*), 139.9 (C*Ar*), 136.8 (C*Ar*), 130.2 (C*Ar*), 128.9 (C*Ar*), 128.6 (C*Ar*), 128.5 (C*Ar*), 128.5 (C*Ar*), 128.1 (C*Ar*), 127.9 (C*Ar*), 127.7 (C*Ar*), 126.8 (C*Ar*), 70.0 (C2N); **ESI-MS** (ES+): m/z = 348.2 [MH$^+$, 100%], 167.1 (10%); **HRMS** (ES+): *m/z* = 348.1751 [MH$^+$, 100 %]; calculated for C$_{26}$H$_{22}$N$_1$ [MH$^+$] found *m/z* = 347.1747. GC elution time: 16.0 min. (This compound was used as a standard for comparison during GC analysis).

Entry 3 No catalyst was used. No reaction was observed via GC after 90 min.

7.2.3 Dehydrogenation of primary amines at different temperatures

Synthetic Procedure 7.2.b

A general synthetic procedure was used with minor modifications to assess the dehydrogenation of primary amines at different temperatures. The procedure is described below:
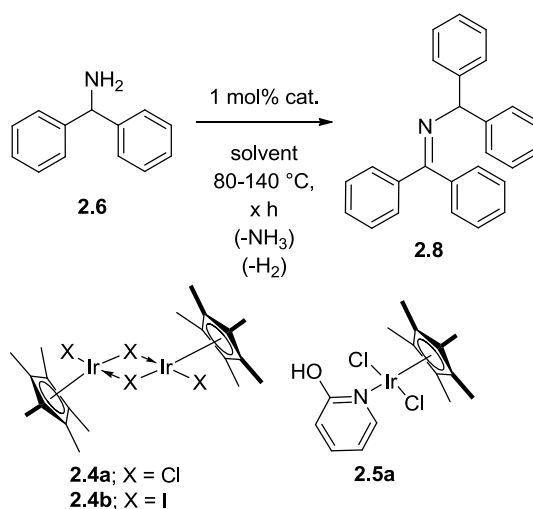
Benzhydrylamine, **2.6** (344 µL, 1.94 mmol, 1.94 equiv.) was added to a suspension of the pentamethylcyclopentadienyl-iridium catalyst (20 µmol, 2 mol%) and internal standard biphenyl (155.0 mg, 1.00 mmol, 1.00 equiv.) in the solvent chosen for the screening (0.5 M) and was heated to the required temperature for 5 hours. The reaction was monitored by GC and GC-MS at regular intervals by sampling 10-30 µL of the reaction mixture and diluting

into 25 mL of acetonitrile. 2 mL aliquots of the resulting mixture were then analysed and the concentration of the *N*-alkylation product **2.8** in the reaction calculated using Equation 7.1 (GC elution time: 16.0 min). The initial reaction rates were calculated by calculating the change in concentration of starting material over the first 0.25 hours of reaction.

Entry	Solvent	Catalyst	Temp / °C	Yield of 2.8 / %[a]
1	PhMe	**2.4b**	80	<1
2	PhMe	**2.4b**	110	34
3	Xylenes	**2.4b**	137-140	37
4	PhMe	**2.4a**	110	28
5	PhMe	**2.5a**	110	30

[a] Yield based on GC area percent and comparison to internal biphenyl standard. Yield calculated to the nearest percent, ±0.5%.

Entry 1 The general procedure **7.2.b** was followed (heated to 80 °C). Toluene (4 mL) and complex **2.4b** (23.3 mg, 20 µmol, 2 mol%) were used. The formation of the *N*-alkylation product was confirmed *via* **GC** analysis (<1%).

Entry 2 The general procedure **7.2.b** was followed (heated to 110 °C). Toluene (4 mL) and complex **2.4b** (23.3 mg, 20 µmol, 2 mol%) were used. The formation of the *N*-alkylation product was confirmed *via* **GC** analysis (34%).

Entry 3 The general procedure **7.2.b** was followed (heated to 137-140 °C). Xylenes (4 mL) and complex **2.4b** (23.3 mg, 20 µmol, 2 mol%) were used. The formation of the *N*-alkylation product was confirmed *via* **GC** analysis (37%).

Entry 4 The general procedure **7.2.b** was followed (heated to 110 °C).Toluene (4 mL) and complex **2.4a** (15.5 mg, 20 µmol, 2 mol%) were used. The formation of the *N*-alkylation product was confirmed *via* **GC** analysis (28%).

Entry 5 The general procedure **7.2.b** was followed (heated to 110 °C).Toluene (4 mL) and complex **2.5a** (9.87 mg, 20 µmol, 2 mol%) were used. The formation of the *N*-alkylation product was confirmed *via* **GC** analysis (30%).

7.2.4 Portion-wise addition of amine to the iridium catalysed dehydrogenation of primary amines
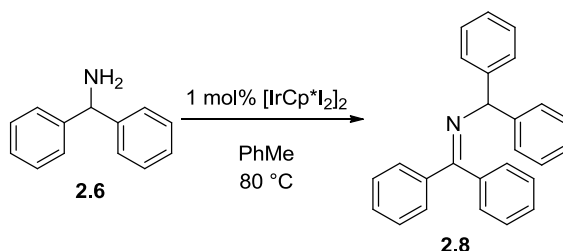
Diiodopentamethylcyclopentadienyliridium(III) dimer (23.3 mg, 20 μmol, 1 mol%) was added to a solution of internal standard biphenyl (155.0 mg, 1.00 mmol, 0.52 equiv.) in toluene (4 mL) and heated to 80 °C for 5 hours. After 2 min., benzhydrylamine (340 μL, 1.91 mmol, 1.91 equiv.) was added *via* portion-wise addition (20 μL every 10 min.) to the resulting solution. The reaction was monitored by GC and GC-MS at regular intervals by sampling 10 μL of the reaction mixture and diluting into 25 mL of acetonitrile. 2 mL aliquots of the resulting mixture were then analysed and the concentration of the *N*-alkylation product **2.8** in the reaction calculated using Equation 7.1 (**GC** elution time: 16.0 min). The formation of the *N*-alkylation product was confirmed *via* **GC** analysis (50%).

7.2.5 The evaluation of different sparging conditions on the iridium catalysed *N*-alkylation of benzhydrylamine

Synthetic Procedure 7.2.c

A general synthetic procedure was used with minor modifications to assess the dehydrogenation of primary amines. The procedure is described briefly below:

163
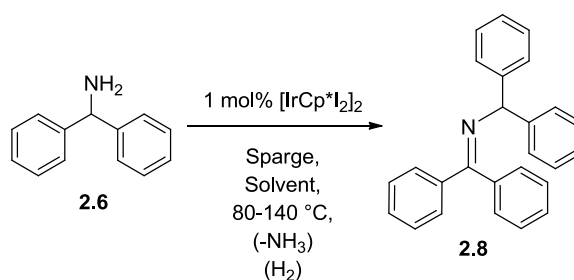
Diiodopentamethylcyclopentadienyliridium(III) dimer (23.3 mg, 20 μmol, 2 mol%), was added to a suspension of internal standard biphenyl (155.0 mg, 1.00 mmol, 1.00 equiv.) in 4 mL of the solvent chosen for the screening (0.5 M) and was saturated with oxygen for 15 min. and the condenser left open to air. The benzylamine, **2.6** (344 µL, 1.94 mmol, 1.94 equiv.) was added to the suspension, which was stirred at reflux whilst the sparge was maintained. The reaction was monitored by GC and GC-MS at regular intervals by sampling 10 µL of the reaction mixture and diluting into 25 mL of acetonitrile. 2 mL aliquots of the resulting mixture were then analysed by GC by comparison to an internal standard and the concentration of the *N*-alkylation product **2.6** in the reaction calculated using Equation 7.1 (**GC** elution time: 16.0 min.). The rate of conversion of **2.6** was determined by calucating the change in concentration of **2.6** after the first 0.25 hours.

Entry	Solvent	Temp / °C	Rate of conversion of 2.6 / mmols min^{-1}	Yield of 2.8[a] / %
1	Toluene	80	0.00628	2
2	Toluene	80	0.00830	2
3	Toluene	80	0.00321	2
4	Xylenes	137-140	0.03224	86
5	Toluene	80	0.00061	2
6	Xylenes	137-140	0.00165	67
7	Xylenes	137-140	0.01262	67

[a] Yield based on GC area percent and comparison to internal biphenyl standard. Yield calculated to the nearest percent, ±0.5%.

Entries 1-3 The general procedure **7.2.c** was followed (heated to 80 °C). Toluene (4 mL) and a sparge of compressed air were used. The formation of *N*-alkylation product **2.8** was confirmed *via* **GC** analysis (2%).

Entry 4 The general procedure **7.2.c** was followed (heated to 137-140 °C). Xylenes (4 mL) and a sparge of compressed air were used. The formation of the *N*-alkylation product **2.8** was confirmed *via* **GC** analysis (86%).

Entry 5 The general procedure **7.2.c** was followed (heated to 80 °C). Toluene (4 mL) and a sparge of nitrogen were used. The formation of the *N*-alkylation product **2.8** was confirmed *via* **GC** analysis (2%).

Entries 6 and 7 The general procedure **7.2.c** was followed (heated to 137-140 °C). Xylenes (4 mL) and a sparge of nitrogen were used. The formation of the *N*-alkylation product **2.8** was confirmed *via* **GC** analysis (67%).

7.2.6 Inhibition of benzhydrylamine *N*-alkylation by ammonium salt additives

Synthetic Procedure 7.2.d

A general synthetic procedure was used with minor modifications to assess the inhibition of *N*-alkylation product formation during primary amine dehydrogenation. The procedure is described briefly below:
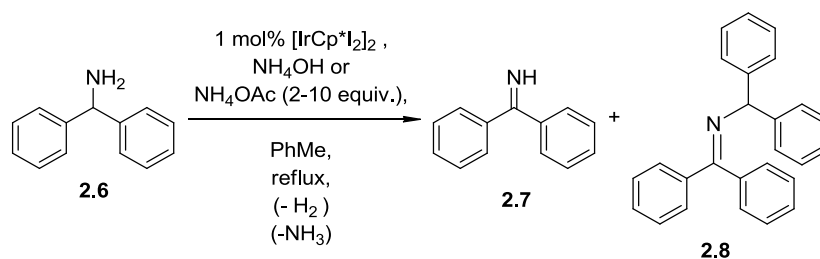
The amine **2.6** (344 µL, 1.94 mmol, 1.94 equiv.) was added to a suspension of diiodopentamethylcyclopentadienyliridium (III) catalyst (23.3 mg, 20 µmol, 1 mol%.), internal standard biphenyl (155 mg, 1.00 mmol, 1.00 equiv.) and ammonium additive in toluene (4 mL) and was heated to reflux. The resulting brick red suspension became homogeneous, fading to orange with gas evolution. The reaction was monitored by GC and GC-MS at regular intervals by sampling 10 µL of the reaction mixture and diluting into 25 mL of acetonitrile. 2 mL aliquots of the resulting mixture were then analysed and the concentration of the *N*-alkylation product **2.8** and the imine **2.7** in the reaction calculated using Equation 7.1 (**GC** elution times: 16.0 min. and 12.4 min., respectively).

Entry	Ammonium Additive	Quantity / mmols	Yield of imine / %	Yield of 2.8[a] / %
1	35% Aqueous Ammonia	2	17	38
2	35% Aqueous Ammonia	10	26	14
3	Ammonium Acetate	5	11	6

[a] Yield based on GC area percent and comparison to internal biphenyl standard. Yield calculated to the nearest percent, ±0.5%.

Entry 1 The general procedure **7.2.d** was followed. 35 % Aqueous ammonia (225 µL, 2.00 mmol, 2.00 equiv.) was used. The formation of the imine **2.7** was confirmed *via* **GC** analysis (17%). The formation of the *N*-alkylation product **2.8** was confirmed *via* **GC** analysis (38%).

Entry 2 The general procedure **7.2.d** was followed. 35% Aqueous ammonia (1135 µL, 10.00 mmol, 10.0 equiv.) was used. The formation of the imine was confirmed *via* **GC** analysis (26%). The formation of the *N*-alkylation product was confirmed *via* **GC** analysis (14%).

Entry 3 The general procedure **7.2.d** was followed. Ammonium acetate (405 mg, 5.26 mmol, 5.26 equiv.) was used. The formation of imine **2.7** was confirmed *via* **GC** analysis (11%). The formation of *N*-alkylation product **2.8** was confirmed *via* **GC** analysis (6%).

7.2.7 Iridium catalysed dehydrogenation of benzhydrylamine with dropwise addition of aqueous ammonia
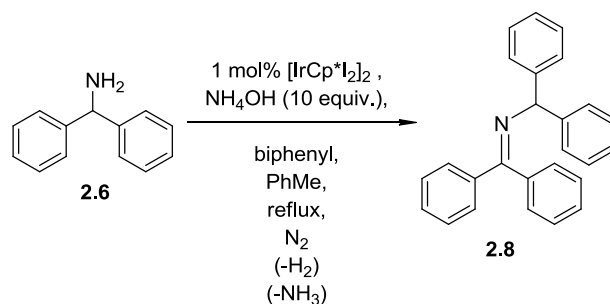
The amine **2.6** (688 μL, 3.88 mmol, 1.0 equiv.) was added to a suspension of diiodopentamethylcyclopentadienyliridium(III) dimer complex (46.6 mg, 40 μmol, 1 mol%), internal standard biphenyl (310 mg, 2.00 mmol, 0.5 equiv.) and 0.35% w/w aqueous ammonia (900 μL, 8.09 mmol, 2.00 equiv.) toluene (8 mL) and heated to reflux for 24 hours. Aqueous ammonia (1350 μL, 12.1 mmol, 1.5 equiv.) was added by syringe pump (0.763 cc hr^{-1}) to the resulting solution after 2 min. The resulting brick red heterogeneous solution became homogeneous and faded to orange with gas evolution. The reaction was monitored by GC and GC-MS at regular intervals by sampling 20 μL of the reaction mixture and diluting into 5 mL of acetonitrile. 2 mL aliquots of the resulting mixture were then analysed and the concentration of the *N*-alkylation product **2.8** in the reaction calculated using Equation 7.1 (GC elution times: 16.0 min). The *N*-alkylation product was confirmed *via* **GC** analysis (50%).

7.2.8 Iridium catalysed *N*-alkylation of (+)-α-methylbenzylamine

Synthetic Procedure 7.2.e

A general synthetic procedure was used with minor modifications to assess the dehydrogenation of primary amines. The procedure is described briefly below:
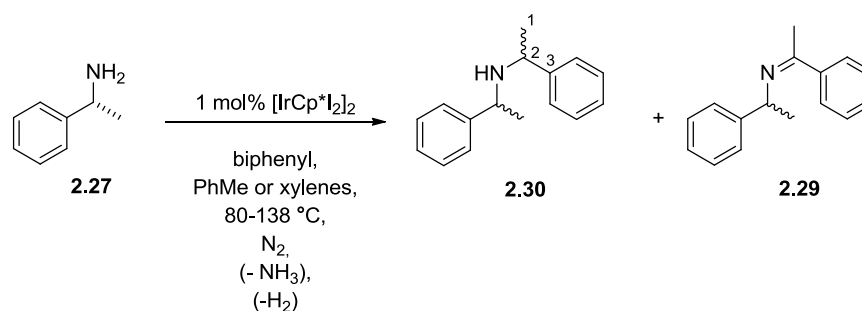
The amine (257 μL, 1.97 mmols, 1.97 equiv.) was added to a suspension of diiodopentamethylcyclopentadienyliridium(III) dimer complex (23.3 mg, 20 μmol, 1 mol%), internal standard biphenyl (155 mg, 1.00 mmol, 1.00 equiv.) in the solvent (0.5 M) and heated to the required temperature for 5 hours. The resulting brick red solution faded to light orange and grew darker with time. The reaction was monitored by GC and GC-MS at regular intervals by sampling 10 μL of the reaction mixture and diluting into 5 mL of acetonitrile. 2 mL aliquots of the resulting mixture were then analysed and the concentration of the saturated *N*-alkylation product **2.30** in the reaction and unsaturated *N*-alkylation product **2.29** calculated using Equation 7.1 (**GC** elution times: 12.3 min and

13.2 min). The unsaturated and saturated *N*-alkylation products (**2.29** and **2.30**, respectively) were confirmed *via* **GC-MS** analysis (m/z = 223 and 225).

Entry	Solvent	Temp / °C	Yield of 2.30[a] / %	Yield of 2.29 product[a] / %
1	Toluene	80	6	<1
2	Xylenes	137-140	82	9

[a] Yield based on GC area percent and comparison to internal biphenyl standard. Yield calculated to the nearest percent, ±0.5%

Entry 1 The general procedure **7.2.e** was followed (heated to 80 °C). Toluene (4 mL) was the solvent. The saturated *N*-alkylation product **2.29** was confirmed by **GC** analysis (6%). The unsaturated *N*-alkylation product **2.30** was confirmed by **GC** and **GC-MS** analysis (<1%).

Entry 2 The general procedure **7.2.e** was followed (heated to 137-140 °C). Xylenes (4 mL) was the solvent used. The saturated *N*-alkylation product **2.30** was confirmed by **GC** analysis (82%). The unsaturated *N*-alkylation product **2.29** was confirmed by **GC** and

2.30
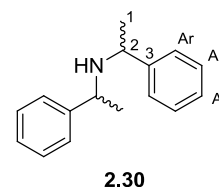
GC-MS analysis (9%). After 21.5 hours the reaction was cooled and the solvent removed *in vacuo*, the resulting orange oil was purified by column chromatography [SiO$_2$; ethyl acetate-petroleum ether; 1:4] to give the product **2.30** as an unknown mixture of diastereomers (702 mg, 3.12 mmols, 39%) as a yellow oil.[191, 192] R_f 0.33 (1:4 ethyl acetate–petroleum ether); **^{1}H NMR** (500 MHz, CDCl$_3$): δ = 7.35–7.18 (apparent m, 10H, C*Ar*H), 3.76 (q, J = 6.6 Hz, 1H, C2H), 3.50 (q, J = 6.7 Hz, 1H, C2H), 1.66 (broad s, NH), 1.35 (d, J = 6.6Hz, 3 H, C*1*H$_3$), 1.27 (d, J = 6.7 Hz, 3H, C*1*H$_3$). **^{13}C NMR** (75 MHz, CDCl$_3$): δ = 145.5 (C*3*), 128.5 (C*Ar*), 126.8 (C*Ar*), 126.6 (C*Ar*), 54.9 (C*2*), 22.9 (C*1*). **GC** elution time: 13.2 min. **ESI-MS** (ES+): m/z = 226 [MH$^+$, 100%]. **HRMS** (ES+): m/z = 226.1606 [MH$^+$, 100 %]; calculated for C$_{16}$H$_{20}$N [MH$^+$] m/z = 226.1596. **IR** (liquid film) ν = 3082, 3061, 3025, 2960, 2924, 2863, 1602, 1492 cm^{-1}.

7.2.9 Iridium catalysed *N*-alkylation of cyclohexylamine[151]
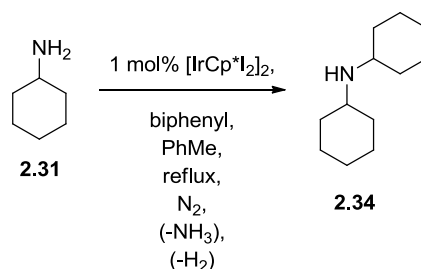
The amine **2.31** (1.38 mL, 7.76 mmol, 1.0 equiv.) was added to a suspension of diiodopentamethylcyclopentadienyliridium(III) dimer complex (92 mg, 0.08 mmol, 1 mol%) in toluene (16mL) and heated to reflux for 21.5 hours. The reaction was monitored by GC and GC-MS at regular intervals by sampling 10 µL of the reaction mixture and diluting into 5 mL of acetonitrile. 2 mL aliquots of the resulting mixture were then analysed and the concentration of the saturated *N*-alkylation product **2.34** in the reaction. Removal of the solvent *in vacuo* gave the crude product. Distillation by short path distillation by Kügelrohr gave the product **2.34** as a brown oil (43.4 mg, 240 µmol, 6%). R_f 0.31 (petroleum ether–ethyl acetate, 3:1), **^{1}H NMR** (500 MHz, CDCl$_3$) : δ = 2.48 (tt, *J* = 10.5, 3.6 Hz, 2H), 1.79 (d, *J* = 10.9 Hz, 4H), 1.64 (d, *J* = 13.2 Hz, 4H), 1.54 (dd, *J* = 9.1, 3.3 Hz, 2H), 1.33-0.43 (m, 11H). **^{13}C NMR** (75 MHz, CDCl$_3$): δ = 53.1, 34.4, 26.2, 25.3; **IR** (film); *ν* = 2925 cm^{-1}.

7.3 Experiments discussed in Chapter 3

7.3.1 General notes on NMR titration spectra

The ^{1}H NMR spectra taken during the titration experiments are reported for each individual spectrum at the specific amine equivalence or time interval, however each species within the spectrum is reported separately. The ratios are then given between each relevant species. Where more than one iridium species are present, the species are listed alphabetically for clarity in each individual spectrum.

7.3.2 Formation of catalyst-bound ammonia complex
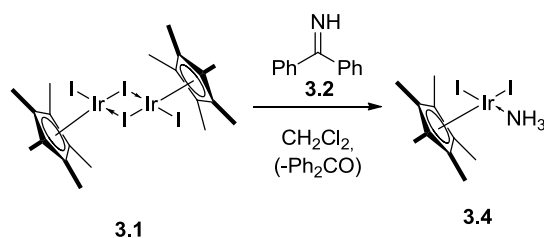
Diiodopentamethylcyclopentadienyliridium(III) dimer complex (19.9 mg, 17.1 µmols, 2.00 equiv.) was suspended in chloroform-d and benzophenone imine **3.2** (5.7 µl, 34.2 µmols, 1.0 equiv.) was added and the suspension shaken vigorously for 60 seconds. The solvent was removed and the resulting solid was recrystalised from dichloromethane *via* diffusion crystalisation. The resulting orange crystals were analysed by X-ray diffraction (performed by Dr H. Sheppard, University of Leeds).

Crystallographic data diiodopentamethylcyclopenatdienyliridium(III)-amine (3.4)

Single crystals of **3.4** were grown by slow evaporation of dichloromethane. An prismatic crystal of dimensions 0.41 x 0.41 x 0.12 mm was used for the data collection; T = 120(2) K; θ range = $5.44 \leq \theta \leq 60.36$ °, Formula = $C_{10}H_{18}I_2IrN$; Formula weight = 598.25; crystals belong to monoclinic, space group P 2_1/c; a = 8.9155 (9) Å, b = 8.0190 (7) Å, c = 21.087 (2) Å; α = 90 °, β = 100.533 °, γ = 90 °; Volume = 1482.1 (2) Å^3, Z = 4, Density (calculated): 2.681 mg mm^{-3}, μ = 13.145 mm^{-1}. Reflections collected 14319; Independent reflections 4358 [R(int) = 0.0341]; R value = 0.0291, $wR2$ = 0.0683.

7.3.3 Synthesis of bis(diphenylmethanamine)[193, 194] as an NMR standard
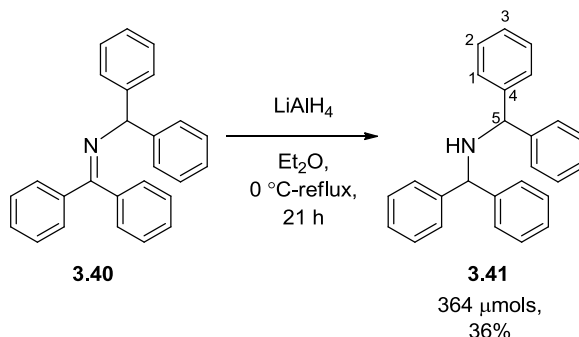
N-Benzhydryldiphenylmethanimine (347 mg, 1.00 mmols, 1.00 equiv.) was dissolved in diethyl ether (6 mL) at 0ºC. Lithium aluminium tetrahydride (184 mg, 5 mmols, 5 equiv.) was added portionwise to the resulting suspension, which gradually became a suspension. The suspension was slowly heated to reflux and stirred for 21 hours. Water (6 mL) was added portionwise to the solution at 0 ºC. The resulting suspension was filtered and the solvent removed from the solute *in vacuo*, washing the resulting solid with ice cold petroleum ether gave product **3.41** (127 mg, 364 µmols, 36%) as colourless crystalline needles. **m.p.** (diethyl ether) 139-142 ºC. **^{1}H NMR** (500 MHz, CDCl$_3$) δ: 7.34 (d, *J* = 6.7 Hz, 8H, C*1*H), 7.30 (t, *J* = 7.6 Hz, 8H, C2H), 7.22 (t, *J* = 7.2 Hz, 4H, C*3*H), 4.74 (s, 2H, C*5*H), 2.22 (s, 1H, NH). **^{13}C NMR** (126 MHz, CDCl$_3$) δ: 143.8 (C*4*), 128.5 (C*1*), 127.6 (C2), 127.0 (C*3*), 63.6 (C*5*). **ESI-MS** (ES+): *m/z* = 350.2 [MH$^+$, 100%]. **HRMS** (ES+): *m/z* = 350.1907 [MH$^+$, 100%); calculated for C$_{26}$H$_{24}$N [MH$^+$] found 350.1903. **IR** (liquid film) ν = 3349, 3061, 3025, 2846, 1597 cm^{-1}.
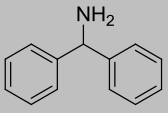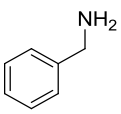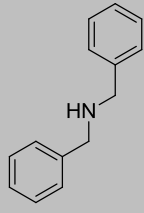
7.3.4 Amine/imine-catalyst binding analysis through NMR spectroscopy

General Procedure 7.4a

A general synthetic procedure was used with minor modifications to assess the binding of primary, secondary and tertiary amines to the catalyst complex. The procedure is described briefly below:

R^1 = Ph, Me or H
R^2 = Aryl
R^3 = H, Me or Bn
R_4 = H or Me
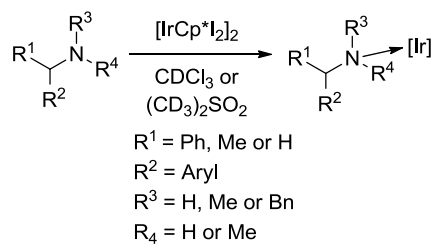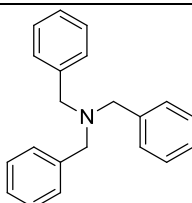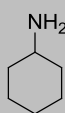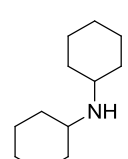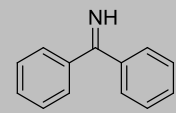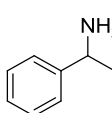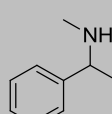
The diiodopentamethylcyclopentadienyliridium(III) dimer (0.5 equiv.; 1.0 equiv. of iridium) complex was suspended in deuterated solvent (0.7 mL) in an NMR tube. The resulting orange suspension was shaken vigorously for 60 seconds. The suspension was then analysed by ^{1}H-NMR spectroscopy. The amine or imine was added, vigorously for 60 seconds and the sample analysed by ^{1}H NMR spectroscopy. This process was repeated with the amine at 0.2, 0.5, 1, 2 and 10 equiv.

Entry	Amine	Amine added / equiv., μmols	Volume of 0.1 M amine in DMSO-d$_6$[a]/ μL
1	3.6	0.2	17.0
		0.5	25.0
		1.0	42.0
		2.0	84.0
		10.0	11.5[b]
2	3.11	0.2	22.5
		0.5	34.0
		1.0	78.0
		2.0	146.0
		10.0	10.0[b]
3	3.14	0.2	14.0
		0.5	21.0
		1.0	35.0
		2.0	71.0
		10.0	11.0[b]
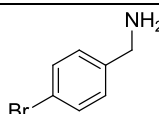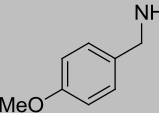
[a] Non-cumulative volume added

[b] Added as the pure amine

[c] Added as a solid

Entry	Amine	Amine added / equiv., μmols	Volume of 0.1 M amine in DMSO-d_6[a]/ μL
4	**3.15**	0.2	17.5
		0.5	26.5
		1.0	45.0
		2.0	130.0
		10.0	19.9 mg[c]
5	**3.10**	0.2	25.0
		0.5	37.0
		1.0	62.0
		2.0	124.0
		10.0	11.5[b]
6	**3.9**	0.2	40.0
		0.5	60.0
		1.0	99.0
		2.0	4.0[b]
		10.0	31.5[b]
7	**3.2**	0.2	14.0
		0.5	20.5
		1.0	34.5
		2.0	68.0
		10.0	6.0[b]
8[c]	**3.12**	0.2	21.5
		0.5	32.5
		1.0	54.0
		2.0	108.5
		10.0	12.5[b]
9[c]	**3.13**	0.2	23.5
		0.5	35.0
		1.0	58.5
		2.0	117.0
		10.0	13.5[b]

[a] Non-cumulative volume added

[b] Added as the pure amine

[c] Added as a solid

Entry	Amine	Amine added / equiv., μmols	Volume of 0.1 M amine in DMSO-d$_6$[a]/ μL
10	NH$_2$ ... Br **3.7**	0.5	41.0
		1.0	41.5
11	NH$_2$ ... MeO **3.8**	0.5	44.5
		1.0	45.0

[a] non-cumulative volume added.

[b] Added as the pure amine.

[c] Added as a solid.

[d] CDCl$_3$ was the deuterated solvent used for the reaction and the 0.1 N solution.

Entry 1 Synthetic procedure **7.4a** was followed. Benzhydrylamine and complex **3.1** (4.9 mg, 4.21 μmol) in DMSO-d$_6$ were used. Benzhydrylamine and iridium catalyst were observed in the ^{1}H NMR spectra (Figure 7.1):
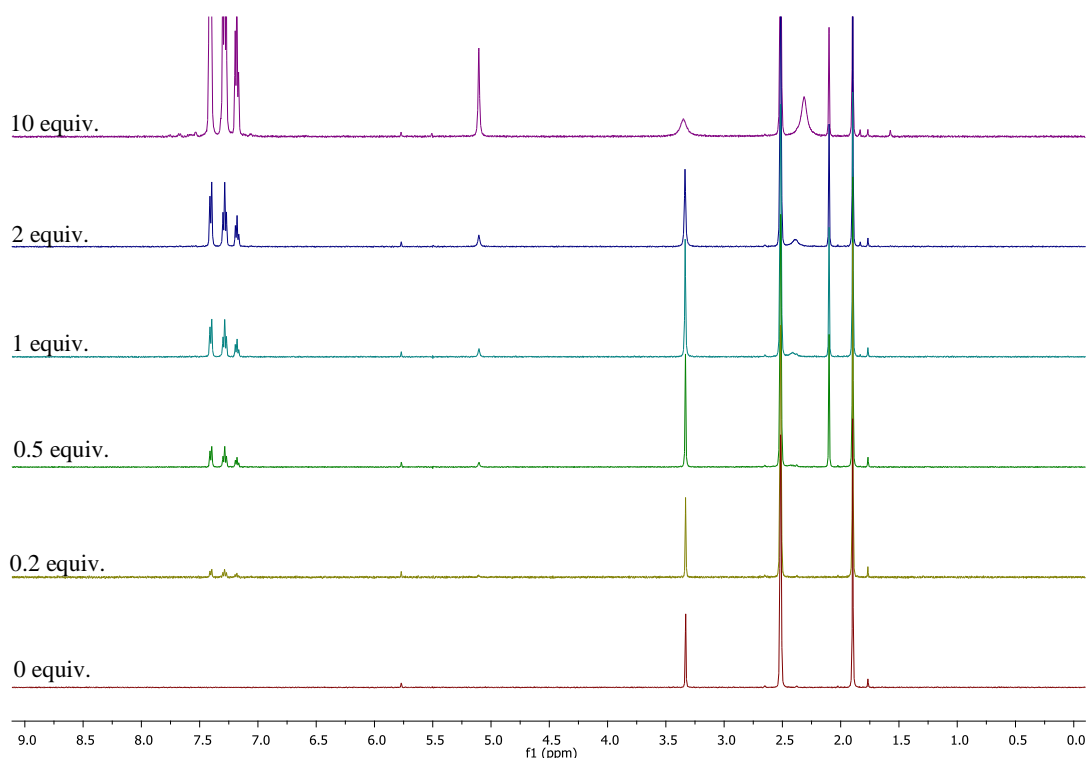
Figure 7.1 Stacked spectra for benzhydrylamine, 3.6 and iridium catalyst 7.3.4, Entry 1.171

0.00 equiv. of amine, iridium catalyst complex, **^{1}H NMR** (500MHz, DMSO-d$_6$) δ: 1.88 (s, 30H, C$_5$Me$_5$).

For 0.2 equiv. of amine **^{1}H NMR** (500MHz, DMSO-d$_6$) δ: 7.39 (d, *J* = 7.8 Hz, 4H, C*Ar*H), 7.27 (t, *J* = 7.7 Hz, 4H, C*Ar*H), 7.17 (t, *J* = 7.3 Hz, 2H, C*Ar*H), 5.76 (s, 2H, NH$_2$), 5.09 (s, 1H, C*Bn*H). Iridium catalyst complex, **^{1}H NMR** (500MHz, DMSO-d$_6$) δ: 1.88 (s, 30H, C$_5$Me$_5$).

For 0.5 equiv. of amine **^{1}H NMR** (500MHz, DMSO-d$_6$) δ: 7.39 (d, *J* = 7.5 Hz, 4H, C*Ar*H), 7.27 (t, *J* = 7.4 Hz, 4H, C*Ar*H), 7.16 (t, *J* = 7.3 Hz, 2H, C*Ar*H), 5.09 (s, 1H, C*Bn*H), 2.41 (br s, 2H, NH$_2$). Iridium catalyst complex **A**, **^{1}H NMR** (500MHz, DMSO-d$_6$) δ: 2.08 (s, 30H, C$_5$Me$_5$) and iridium catalyst complex **B**, **^{1}H NMR** (500MHz, DMSO-d$_6$) δ: 1.88 (s, 30H, C$_5$Me$_5$). Ratio 2.08 ppm complex: 1.88 ppm complex = 1:2.

For 1.00 equiv. of amine **^{1}H NMR** (500MHz, DMSO-d$_6$) δ: 7.39 (d, *J* = 7.5 Hz, 4H, C*Ar*H), 7.27 (t, *J* = 7.4 Hz, 4H, C*Ar*H), 7.16 (t, *J* = 7.3 Hz, 2H, C*Ar*H), 5.09 (s, 1H, C*Bn*H), 2.40 (br s, 2H, NH$_2$). Iridium catalyst complex **A**, **^{1}H NMR** (500MHz, DMSO-d$_6$) δ: 2.08 (s, 30H, C$_5$Me$_5$) and iridium catalyst complex **B**, **^{1}H NMR** (500MHz, DMSO-d$_6$) δ: 1.88 (s, 30H, C$_5$Me$_5$). Ratio 2.08 ppm complex: 1.88 ppm complex = 1:2.

For 2.00 equiv. of amine **^{1}H NMR** (500MHz, DMSO-d$_6$) δ: 7.39 (d, *J* = 7.5 Hz, 4H, C*Ar*H), 7.27 (t, *J* = 7.5 Hz, 4H, C*Ar*H), 7.17 (t, *J* = 7.3 Hz, 2H, C*Ar*H), 5.09 (s, 1H, C*Bn*H), 2.37 (br s, 2H, NH$_2$), 2.08 (s, 5H, C$_5$Me$_5$). Iridium catalyst complex **A**, **^{1}H NMR** (500MHz, DMSO-d$_6$) δ: 2.08 (s, 30H, C$_5$Me$_5$) and iridium catalyst complex **B**, **^{1}H NMR** (500MHz, DMSO-d$_6$) δ: 1.88 (s, 30H, C$_5$Me$_5$). Ratio 2.08 ppm complex: 1.88 ppm complex = 1:2.

For 10.0 equiv. of amine **^{1}H NMR** (500MHz, DMSO-d$_6$) δ: 7.39 (d, *J* = 7.4 Hz, 4H, C*Ar*H), 7.27 (t, *J* = 7.5 Hz, 4H, C*Ar*H), 7.17 (t, *J* = 7.2 Hz, 2H, C*Ar*H), 5.09 (s, 1H, C*Bn*H), 2.30 (br s, 2H, NH$_2$). Iridium catalyst complex **A**, **^{1}H NMR** (500MHz, DMSO-d$_6$) δ: 2.09 (s, 30H, C$_5$Me$_5$) and iridium catalyst complex **B**, **^{1}H NMR** (500MHz, DMSO-d$_6$) δ: 1.88 (s, 30H, C$_5$Me$_5$). Ratio 2.08 ppm complex: 1.88 ppm complex = 1:2

Entry 2 Synthetic procedure **7.4a** was followed. Benzylamine, **3.11** and complex **3.1** (6.5 mg, 5.59 μmols) in DMSO-d$_6$ were used. Benzylamine, iridium catalyst and the catalyst bound amine complex were observed by ^{1}H NMR (Figure 7.2):
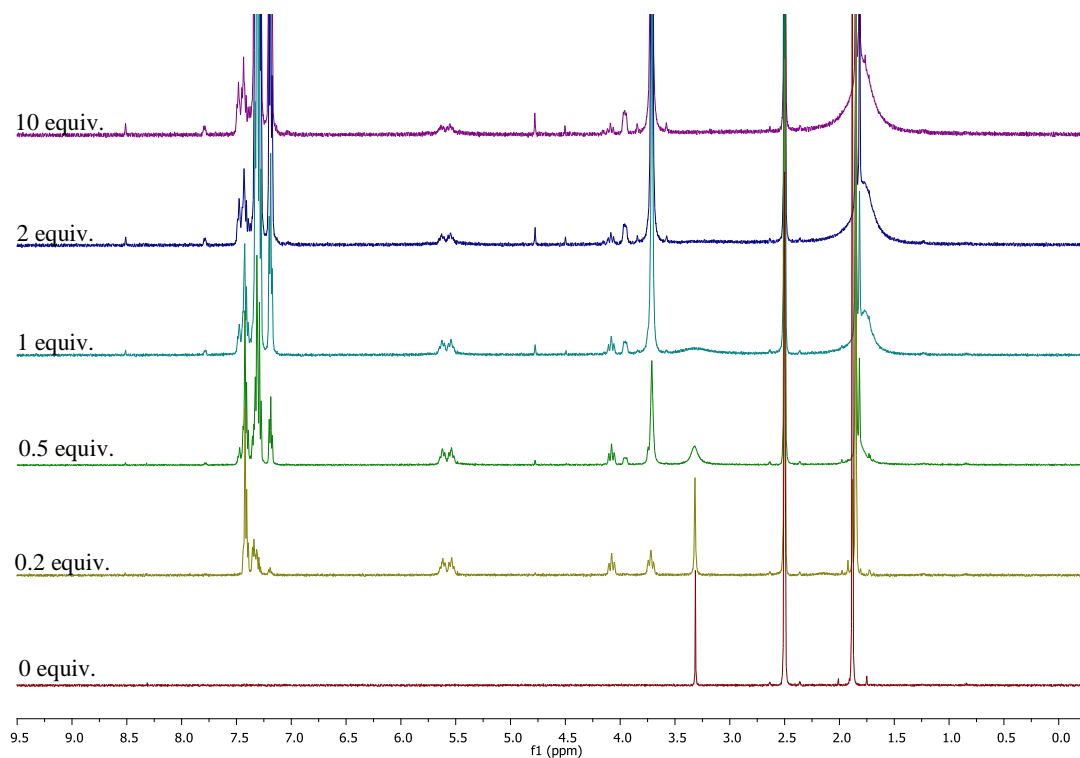
Figure 7.2 Stacked spectra for benzhydrylamine, 3.11 and iridium catalyst 7.3.4,

Entry 2.

0.00 equiv. of amine, iridium catalyst complex, **^{1}H NMR** (500MHz, DMSO-d$_6$) δ: 1.88 (s, 30H, C$_5$Me$_5$).

For 0.2 equiv. of amine, catalyst bound amine complex: **^{1}H NMR** (500MHz, DMSO-d$_6$) δ: 7.46-7.26 (m, 5H, C*Ar*H), 5.62 (t, J = 10.6 Hz, 1H, NH), 5.54 (t, J = 10.5 Hz, 1H, NH), 4.08 (t, J = 11.6 Hz, 1H, C*Bn*H), 3.72 (t, J = 11.5 Hz, 1H, C*Bn*H). Iridium catalyst complex **A**, **^{1}H NMR** (500MHz, DMSO-d$_6$) δ: 1.88 (s, 30H) and iridium catalyst complex **B**, **^{1}H NMR** (500MHz, DMSO-d$_6$) δ: 1.85 (s, 30H). Ratio of 1.88 ppm complex: 1.85 ppm complex = 2:13.

For 0.5 equiv. of amine, catalyst bound amine complex: **^{1}H NMR** (500MHz, DMSO-d$_6$) δ: 7.58-7.12 (m, 5H, C*Ar*H) 5.62 (d, J = 10.0 Hz, 1H, NH), 5.54 (d, J = 10.0 Hz, 1H, NH) 4.08 (t, J = 11.6 Hz, 1H, C*Bn*H) 3.72 (t, J = 11.6 Hz, 1H, C*Bn*H). Benzylamine: **^{1}H NMR** (500MHz, DMSO-d$_6$) δ: 7.46-7.26 (m, 5H, C*Ar*H), 3.71(apparent s, 1H, C*Bn*H), 1.83 (apparent br s, 2H, NH$_2$).Iridium catalyst complex **A**, **^{1}H NMR** (500MHz, DMSO) δ: 1.85 (s, 30H, C$_5$Me$_5$) and iridium catalyst complex **B**, **^{1}H NMR** (500MHz, DMSO-d$_6$) δ: 1.82 (s, 30H, C$_5$Me$_5$). Ratio of 1.85 ppm complex: 1.82 ppm complex = 23:7.

For 1.00 equiv. of amine, catalyst bound amine complex: **^{1}H NMR** (500MHz, DMSO-d$_6$) δ: 7.45-7.11 (apparent m, 5H, C*Ar*H), 5.63 (t, J = 10.4 Hz, 1H, NH), 5.54 (t, J = 10.2 Hz, 1H, NH), 4.08 (t, J = 12.1 Hz, 1H, C*Bn*H), 3.71 (apparent s, 1H, C*Bn*H). Benzylamine **^{1}H NMR** (500MHz, DMSO-d$_6$) δ: 7.45-7.11 (apparent m, 5H, CArH), 3.71 (s, 1H, CBnH$_2$), 1.77 (apparent br s, 2H, NH$_2$). Ratio benzyl amine: catalyst bound amine = 10:1. Iridium catalyst complex **A**: **^{1}H NMR** (500MHz, DMSO-d$_6$) δ: 1.85 (s, 30H, C$_5$Me$_5$) and iridium catalyst complex **B**: **^{1}H NMR** (500MHz, DMSO-d$_6$) δ: 1.82 (s, 30H, C$_5$Me$_5$). Ratio of 1.85 ppm complex: 1.82 ppm complex = 11:4.

For 2.00 equiv. of amine, catalyst bound amine complex: **^{1}H NMR** (500MHz, DMSO-d$_6$) δ: 7.52-7.07 (m, 5H, C*Ar*H) 5.63 (t, J = 10.8 Hz, 1H, NH), 5.55 (t, J = 10.7 Hz, 1H, NH) 4.08 (t, J = 12.0 Hz, 1H, C*Bn*H), 3.71 (apparent s, 1H, C*Bn*H). Benzylamine: **^{1}H NMR** (500MHz, DMSO-d$_6$) δ: 7.46-7.26 (m, 5H, C*Ar*H), 3.71(apparent s, 1H, C*Bn*H), 1.78 (apparent br s, 2H, NH$_2$).). Ratio benzyl amine: catalyst bound amine = 21:1. Iridium catalyst complex **A**, **^{1}H NMR** (500MHz, DMSO-d$_6$) δ: 1.85 (s, 30H, C$_5$Me$_5$) and iridium catalyst complex **B**: **^{1}H NMR** (500MHz, DMSO-d$_6$) δ: 1.82 (s, 30H, C$_5$Me$_5$). Ratio of 1.85 ppm complex: 1.82 ppm complex = 8:7.

For 10.0 equiv. of amine, catalyst bound amine complex: **^{1}H NMR** (500MHz, DMSO-d$_6$) δ: 7.52-7.07 (m, 5H, C*Ar*H) 5.63 (t, J = 10.8 Hz, 1H, NH), 5.55 (t, J = 10.7 Hz, 1H, NH) 4.08 (t, J = 12.0 Hz, 1H, C*Bn*H), 3.71 (apparent s, 1H, C*Bn*H). Benzylamine: **^{1}H NMR** (500MHz, DMSO-d$_6$) δ: 7.46-7.26 (m, 5H, C*Ar*H), 3.71(apparent s, 1H, C*Bn*H), 1.78 (apparent br s, 2H, NH$_2$). Ratio benzyl amine: catalyst bound amine = 35:1. Iridium catalyst complex **A**, **^{1}H NMR** (500MHz, DMSO-d$_6$) δ: 1.85 (s, 30H, C$_5$Me$_5$) and iridium catalyst complex **B**: **^{1}H NMR** (500MHz, DMSO-d$_6$) δ: 1.82 (s, 30H, C$_5$Me$_5$). Ratio of 1.85 ppm complex: 1.82 ppm complex = 8:7.

Entry 3 Synthetic procedure **7.4a** was followed. Dibenzylamine and complex **3.1** (4.1 mg, 3.53 μmols) in DMSO-d$_6$ were used. Dibenzylamine and iridium complexes were observed *via* ^{1}H NMR (Figure 7.3).
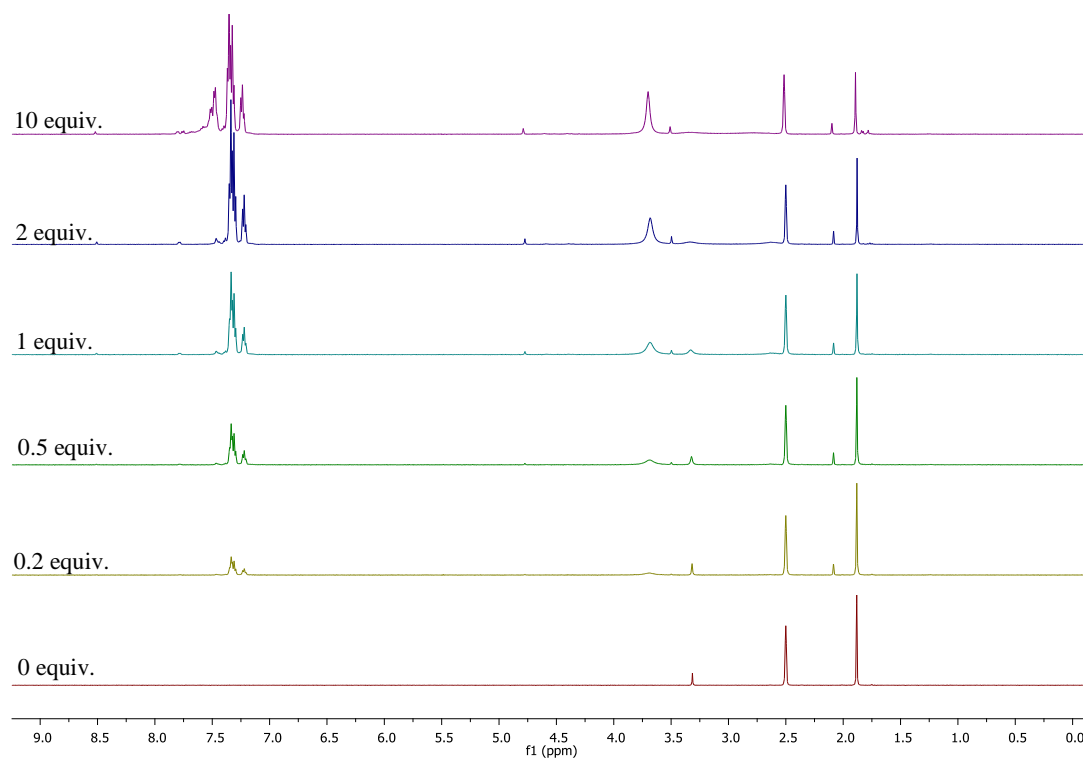
Figure 7.3 Stacked spectra dibenzyllamine, 3.14 and iridium catalyst 7.3.4, Entry 3.

For 0.0 equiv. of amine, iridium catalyst complex, **^{1}H NMR** (500MHz, DMSO-d$_6$) δ: 1.88 (s, 30H, C$_5$Me$_5$).

For 0.2 equiv. of amine, dibenzylamine: **^{1}H NMR** (500MHz, DMSO-d$_6$) δ: 7.36–7.28 (m, 8H, C*Ar*H), 7.22 (t, *J* = 6.9 Hz, 2H, C*Ar*H), 3.69 (s, 4H, C*Bn*H), 2.63 (s, 1H, NH). Iridium catalyst complex **A**: **^{1}H NMR** (500MHz, DMSO-d$_6$) δ: 2.09 (s, 30H, C$_5$Me$_5$) and iridium catalyst complex **B**: **^{1}H NMR** (500MHz, DMSO-d$_6$) δ: 1.88 (s, 30H, C$_5$Me$_5$). Ratio of 2.09 ppm complex: 1.88 ppm complex = 1:11.

For 0.5 equiv. of amine, dibenzylamine: **^{1}H NMR** (500MHz, DMSO-d$_6$) δ: 7.36–7.28 (m, 8H, C*Ar*H), 7.22 (t, *J* = 6.9 Hz, 2H, C*Ar*H), 3.69 (s, 4H, C*Bn*H), 2.63 (s, 1H, NH). Iridium catalyst complex **A**: **^{1}H NMR** (500MHz, DMSO-d$_6$) δ: 2.08 (s, 30H, C$_5$Me$_5$) and iridium catalyst complex **B**: **^{1}H NMR** (500MHz, DMSO-d$_6$) δ: 1.88 (s, 30H, C$_5$Me$_5$). Ratio of 2.08 ppm complex: 1.88 ppm complex = 1:8.

For 1.0 equiv. of amine, dibenzylamine: **^{1}H NMR** (500MHz, DMSO-d$_6$) δ: 7.36-7.28 (m, 8H, C*Ar*H), 7.22 (t, *J* = 6.9 Hz, 2H, C*Ar*H), 3.69 (s, 4H, C*Bn*H), 2.63 (s, 1H, NH). Iridium catalyst complex **A**: **^{1}H NMR** (500MHz, DMSO-d$_6$) δ: 2.08 (s, 30H, C$_5$Me$_5$) and iridium

catalyst complex **B**: **^{1}H NMR** (500MHz, DMSO-d$_6$) δ: 1.88 (s, 30H, C$_5$Me$_5$). Ratio of 2.08 ppm complex: 1.88 ppm complex = 1:7.

For 2.0 equiv. of amine, dibenzylamine: **^{1}H NMR** (500MHz, DMSO-d$_6$) δ: 7.36-7.28 (m, 8H, C*Ar*H), 7.22 (t, *J* = 6.9 Hz, 2H, C*Ar*H), 3.69 (s, 4H, C*Bn*H), 2.63 (s, 1H, NH). Iridium catalyst complex **A**: **^{1}H NMR** (500MHz, DMSO-d$_6$) δ: 2.08 (s, 30H, C$_5$Me$_5$) and iridium catalyst complex **B**: **^{1}H NMR** (500MHz, DMSO-d$_6$) δ: 1.88 (s, 30H, C$_5$Me$_5$). Ratio of 2.08 ppm complex: 1.88 ppm complex = 1:7.

For 10.0 equiv. of amine, dibenzylamine: **^{1}H NMR** (500MHz, DMSO-d$_6$) δ: 7.36-7.28 (m, 8H, C*Ar*H), 7.22 (t, *J* = 6.9 Hz, 2H, C*Ar*H), 3.69 (s, 4H, C*Bn*H), 2.63 (s, 1H, NH). Iridium catalyst complex **A**: **^{1}H NMR** (500MHz, DMSO-d$_6$) δ: 2.08 (s, 30H, C$_5$Me$_5$), iridium catalyst complex **B**: **^{1}H NMR** (500MHz, DMSO-d$_6$) δ: 1.88 (s, 30H, C$_5$Me$_5$) iridium catalyst complex **C**: **^{1}H NMR** (500MHz, DMSO-d$_6$) δ: 1.82 (s, 30H, C$_5$Me$_5$), iridium catalyst complex **D**: **^{1}H NMR** (500MHz, DMSO-d$_6$) δ: 1.81 (s, 30H, C$_5$Me$_5$) and iridium catalyst complex **E**: **^{1}H NMR** (500MHz, DMSO-d$_6$) δ: 1.77 (s, 30H, C$_5$Me$_5$). Ratio of 2.08 ppm complex: 1.88 ppm complex: 1.82 ppm complex: 1.81 ppm complex: 1.77 ppm complex = 8:46:3:2:4.

Entry 4 Synthetic procedure **7.4a** was followed. Tribenzylamine and complex **3.1** (5.1 mg, 4.39 μmols) in DMSO-d$_6$ were used. Tribenzylamine and iridium complexes were observed *via* ^{1}H NMR (Figure 7.4).
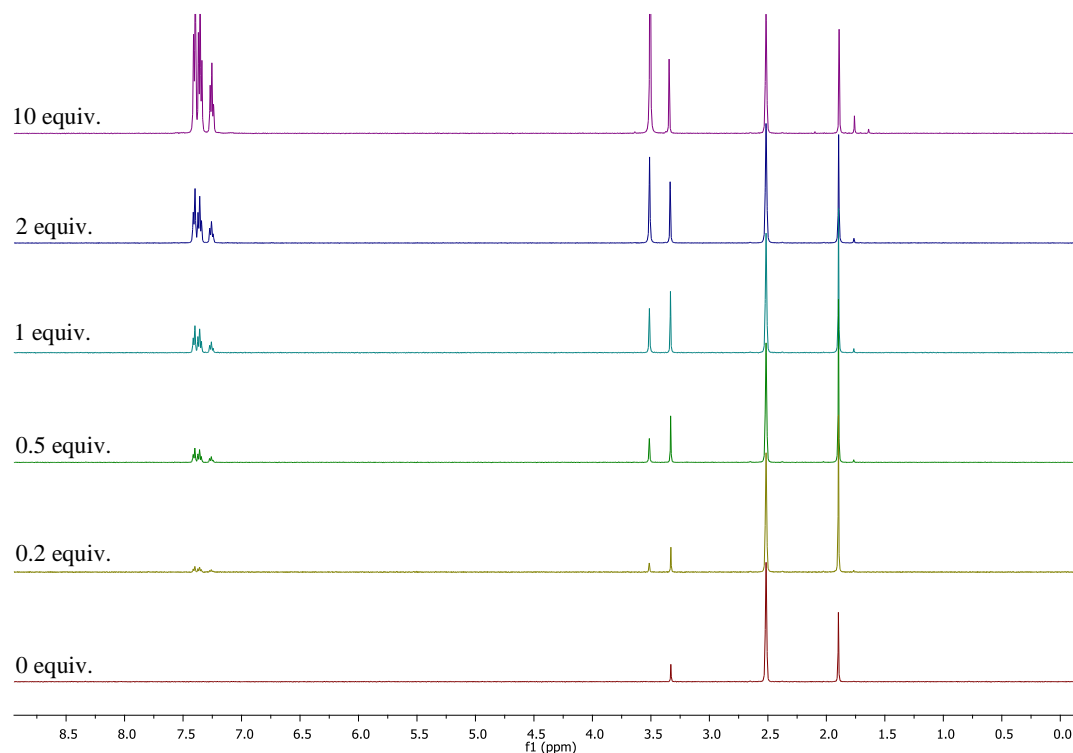
Figure 7.4 Stacked spectra for tribenzylamine, 3.17 and iridium catalyst 7.3.4, Entry 4.

For 0.0 equiv. of amine, iridium catalyst complex, **¹H NMR** (500MHz, DMSO-d$_6$) δ: 1.88 (s, 30H, C$_5$Me$_5$).

For 0.2 equiv. of amine, tribenzylamine: **¹H NMR** (500MHz, DMSO-d$_6$) δ: 7.39 (d, *J* = 7.1 Hz, 6H, C*Ar*H), 7.34 (t, *J* = 7.2 Hz, 6H, C*Ar*H), 7.24 (t, *J* = 7.3 Hz, 3H, C*Ar*H), 3.50 (s, 6H, C*Bn*H). Iridium catalyst complex: **¹H NMR** (500MHz, DMSO-d$_6$) δ: 1.88 (s, 30H, C$_5$Me$_5$).

For 0.5 equiv. of amine, tribenzylamine: **¹H NMR** (500MHz, DMSO-d$_6$) δ: 7.39 (d, *J* = 7.1 Hz, 6H, C*Ar*H), 7.34 (t, *J* = 7.2 Hz, 6H, C*Ar*H), 7.24 (t, *J* = 7.3 Hz, 3H, C*Ar*H), 3.50 (s, 6H, C*Bn*H). Iridium catalyst complex **A**: **¹H NMR** (500MHz, DMSO-d$_6$) δ: 1.88 (s, 30H, C$_5$Me$_5$) and iridium catalyst complex **B**: **¹H NMR** (500MHz, DMSO-d$_6$) δ: 1.75 (s, 30H, C$_5$Me$_5$). Ratio of 1.88 ppm complex: 1.75 complex = 59:1.

For 1.0 equiv. of amine, tribenzylamine: **¹H NMR** (500MHz, DMSO-d$_6$) δ: 7.39 (d, *J* = 7.1 Hz, 6H, C*Ar*H), 7.34 (t, *J* = 7.2 Hz, 6H, C*Ar*H), 7.24 (t, *J* = 7.3 Hz, 3H, C*Ar*H), 3.50 (s, 6H, C*Bn*H). Iridium catalyst complex **A**: **¹H NMR** (500MHz, DMSO-d$_6$) δ: 1.88 (s,

30H, C$_5$Me$_5$) and iridium catalyst complex **B**: **^{1}H NMR** (500MHz, DMSO-d$_6$) δ: 1.75 (s, 30H, C$_5$Me$_5$). Ratio of 1.88 ppm complex: 1.75 complex = 29:1.

For 2.0 equiv. of amine, tribenzylamine: **^{1}H NMR** (500MHz, DMSO-d$_6$) δ: 7.39 (d, *J* = 7.1 Hz, 6H, C*Ar*H), 7.34 (t, *J* = 7.2 Hz, 6H, C*Ar*H), 7.24 (t, *J* = 7.3 Hz, 3H, C*Ar*H), 3.50 (s, 6H, C*Bn*H). Iridium catalyst complex **A**: **^{1}H NMR** (500MHz, DMSO-d$_6$) δ: 1.88 (s, 30H, C$_5$Me$_5$) and iridium catalyst complex **B**: **^{1}H NMR** (500MHz, DMSO-d$_6$) δ: 1.75 (s, 30H, C$_5$Me$_5$). Ratio of 1.88 ppm complex: 1.75 complex = 29:1.

For 10.0 equiv. of amine, tribenzylamine: **^{1}H NMR** (500MHz, DMSO-d$_6$) δ: 7.39 (d, *J* = 7.1 Hz, 6H, C*Ar*H), 7.34 (t, *J* = 7.2 Hz, 6H, C*Ar*H), 7.24 (t, *J* = 7.3 Hz, 3H, C*Ar*H), 3.50 (s, 6H, C*Bn*H). Iridium catalyst complex **A**, **^{1}H NMR** (500MHz, DMSO-d$_6$) δ: 1.88 (s, 30H, C$_5$Me$_5$); iridium catalyst complex **B**, **^{1}H NMR** (500MHz, DMSO-d$_6$) δ: 1.75 (s, 30H, C$_5$Me$_5$) and iridium catalyst complex **C**, **^{1}H NMR** (500MHz, DMSO-d$_6$) δ: 1.62 (s, 30H, C$_5$Me$_5$). Ratio of 1.88 ppm complex: 1.75 ppm complex: 1.62 ppm complex = 25:4:1.

Entry 5 Synthetic procedure **7.4a** was followed. Cyclohexylamine and complex **3.1** (7.2 mg, 6.19 μmols) in DMSO-d$_6$ were used. Different iridium complexes were observed, elucidation of cyclohexylamine environments was not possible for all equivalences by ^{1}H NMR (Figure 7.5).
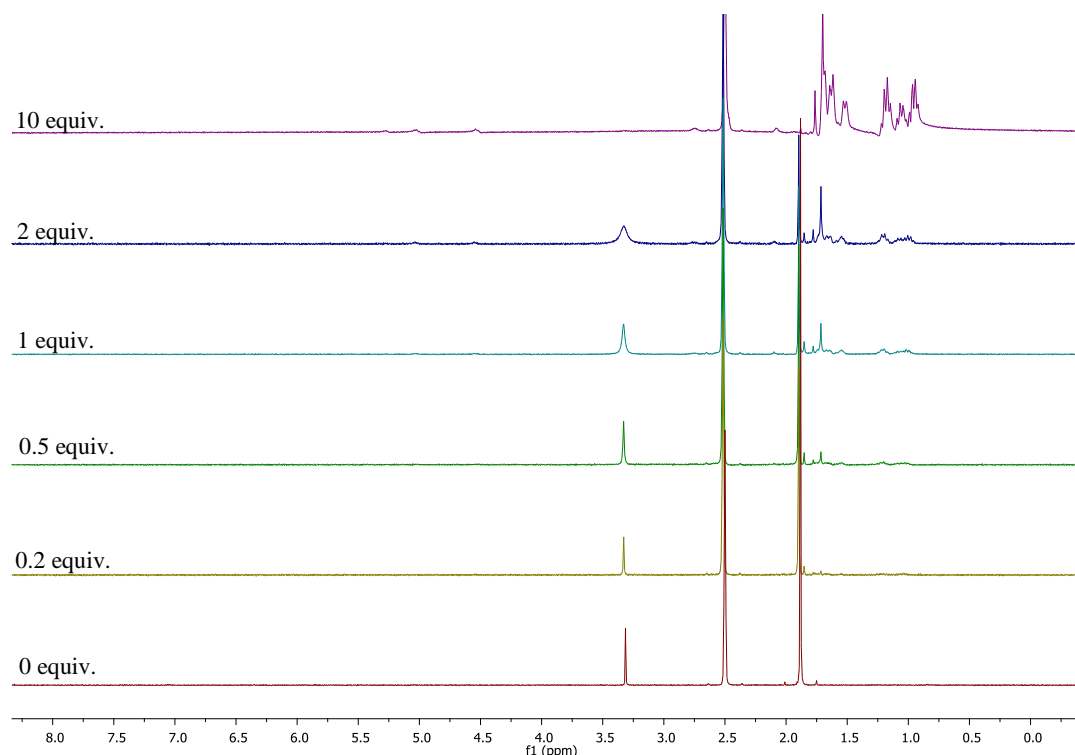
Figure 7.5 Stacked spectra for cyclohexylamine, 3.10 and iridium catalyst 7.3.4, Entry 5.

For 0.0 equiv. of amine, iridium catalyst complex, **^{1}H NMR** (500MHz, DMSO-d$_6$) δ: 1.88 (s, 30H, C$_5$Me$_5$).

For 0.2 equiv. of amine, iridium catalyst complex **A**, **^{1}H NMR** (500MHz, DMSO-d$_6$) δ: 1.88 (s, 30H, C$_5$Me$_5$), iridium catalyst complex **B**, **^{1}H NMR** (500MHz, DMSO-d$_6$) δ: 1.84 (s, 30H, C$_5$Me$_5$) and iridium catalyst complex **C**, **^{1}H NMR** (500MHz, DMSO-d$_6$) δ: 1.70 (s, 30H, C$_5$Me$_5$). Ratio of 1.88 ppm complex: 1.84 ppm complex: 1.70 ppm complex: = 90:5:2. Observation of the cyclohexylamine added was not possible at this concentration.

For 0.5 equiv. of amine, iridium catalyst complex **A**,**^{1}H NMR** (500MHz, DMSO-d$_6$) δ: 1.88 (s, 30H, C$_5$Me$_5$), iridium catalyst complex **B**, **^{1}H NMR** (500MHz, DMSO-d$_6$) δ: 1.84 (s, 30H, C$_5$Me$_5$), iridium catalyst complex **C**, **^{1}H NMR** (500MHz, DMSO-d$_6$) δ: 1.76 (s, 30H, C$_5$Me$_5$) and iridium catalyst complex **D**, **^{1}H NMR** (500MHz, DMSO-d$_6$) δ: 1.70 (s, 30H, C$_5$Me$_5$). Ratio of 1.88 ppm complex: 1.84 ppm complex: 1.76 ppm complex: 1.70 ppm complex: = 61:4:1:5. Observation of the cyclohexylamine added was not possible at this concentration.

For 1.0 equiv. of amine, iridium catalyst complex **A**, **^{1}H NMR** (500MHz, DMSO-d$_6$) δ: 1.88 (s, 30H, C$_5$Me$_5$), iridium catalyst complex **B**, **^{1}H NMR** (500MHz, DMSO-d$_6$) δ: 1.84 (s, 30H, C$_5$Me$_5$), iridium catalyst complex **C**, **^{1}H NMR** (500MHz, DMSO-d$_6$) δ: 1.76 (s, 30H, C$_5$Me$_5$) and iridium catalyst complex **D**, **^{1}H NMR** (500MHz, DMSO-d$_6$) δ: 1.70 (s, 30H, C$_5$Me$_5$). Ratio of 1.88 ppm complex: 1.84 ppm complex: 1.76 ppm complex: 1.70 ppm complex: = 18:2:1:4. Observation of the cyclohexylamine added was not possible at this concentration.

For 2.0 equiv. of amine, cyclohexylamine: **^{1}H NMR** (500 MHz, DMSO-d$_6$) δ 1.72-1.66 (m, 2H), 1.66-1.45 (m, 3H), 1.25-1.11 (m, 2H), 1.11-1.01 (m, 1H), 1.01-0.88 (m, 2H). Iridium catalyst complex **A**, **^{1}H NMR** (500MHz, DMSO-d$_6$) δ: 1.88 (s, 30H, C$_5$Me$_5$), iridium catalyst complex **B**, **^{1}H NMR** (500MHz, DMSO-d$_6$) δ: 1.84 (s, 30H, C$_5$Me$_5$), iridium catalyst complex **C**, **^{1}H NMR** (500MHz, DMSO-d$_6$) δ: 1.76 (s, 30H, C$_5$Me$_5$) and iridium catalyst complex **D**, **^{1}H NMR** (500MHz, DMSO-d$_6$) δ: 1.70 (s, 30H, C$_5$Me$_5$). Ratio of 1.88 ppm complex: 1.84 ppm complex: 1.76 ppm complex: 1.70 ppm complex: = 15:2:3:10.

For 10.0 equiv. of amine, cyclohexylamine: **^{1}H NMR** (500 MHz, DMSO-d$_6$) δ 1.72-1.66 (m, 2H), 1.66-1.45 (m, 3H), 1.25-1.11 (m, 2H), 1.11-1.01 (m, 1H), 1.01-0.88 (m, 2H). Iridium catalyst complex **A**, **^{1}H NMR** (500MHz, DMSO-d$_6$) δ: 1.88 (s, 30H, C$_5$Me$_5$), iridium catalyst complex **B**, **^{1}H NMR** (500MHz, DMSO-d$_6$) δ: 1.76 (s, 30H, C$_5$Me$_5$) and iridium catalyst complex **C**, **^{1}H NMR** (500MHz, DMSO-d$_6$) δ: 1.70 (s, 30H, C$_5$Me$_5$). Ratio of 1.88 ppm complex: 1.76 ppm complex: 1.70 ppm complex = 1:3:10.

Entry 6 Synthetic procedure **7.4a** was followed. Dicyclohexylamine and complex **3.1** (11.6 mg, 9.97 μmols) in DMSO-d$_6$ were used. Iridium catalyst complex and dicyclohexylamine were observed by ^{1}H NMR analysis (Figure 7.6). Not all dicyclohexyl protons were visible during analysis.
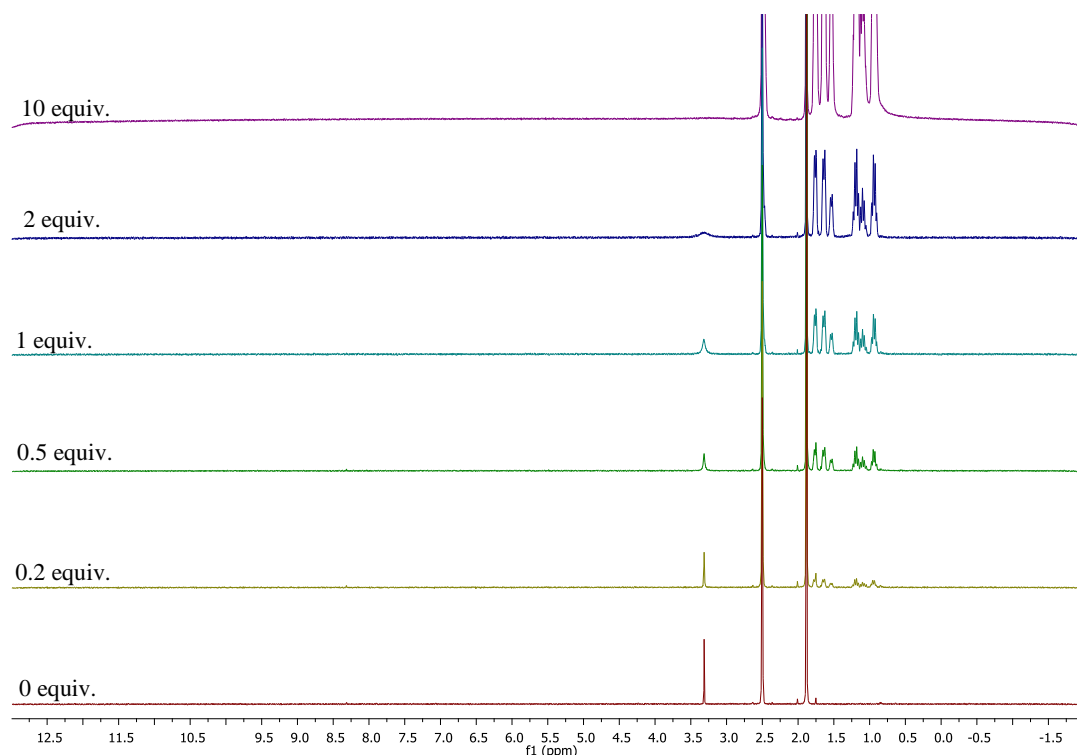
Figure 7.6 Stacked spectra for dicyclohexylamine, 3.9 and iridium catalyst 7.3.4, Entry 6.

For 0.0 equiv. of amine, iridium catalyst complex, **^{1}H NMR** (500MHz, DMSO-d$_6$) δ: 1.88 (s, 30H, C$_5$Me$_5$).

For 0.2 equiv. of amine, dicyclohexylamine, **^{1}H NMR** (500MHz, DMSO-d$_6$) δ: δ 1.80-1.73 (m, 4H), 1.69-1.60 (m, 4H), 1.54 (d, J = 12.0 Hz, 2H), 1.20 (q, J = 12.0 Hz, 4H), 1.09 (t, J = 12.0 Hz, 2H), 0.95 (q, J = 10.7 Hz, 4H). Iridium catalyst complex: **^{1}H NMR** (500MHz, DMSO-d$_6$) δ: 1.88 (s, 30H, C$_5$Me$_5$)

For 0.5 equiv. of amine, dicyclohexylamine: **^{1}H NMR** (500 MHz, DMSO-d$_6$) δ: 1.76 (d, J = 9.7 Hz, 4H), 1.64 (d, J = 9.6 Hz, 4H), 1.54 (d, J = 11.9 Hz, 2H), 1.19 (q, J = 12.3 Hz, 4H), 1.09 (q, J = 12.3 Hz, 2H), 0.93 (q, J = 9.8 Hz, 4H). Iridium catalyst complex: **^{1}H NMR** (500MHz, DMSO-d$_6$) δ: 1.88 (s, 30H, C$_5$Me$_5$).

For 1.0 equiv. of amine, dicyclohexylamine, **^{1}H NMR** (500 MHz, DMSO-d$_6$) δ: 1.76 (d, J = 9.7 Hz, 4H), 1.64 (d, J = 9.6 Hz, 4H), 1.54 (d, J = 11.9 Hz, 2H), 1.19 (q, J = 12.3 Hz, 4H), 1.09 (q, J = 12.3 Hz, 2H), 0.93 (q, J = 9.8 Hz, 4H). Iridium catalyst complex: **^{1}H NMR** (500MHz, DMSO-d$_6$) δ: 1.88 (s, 30H, C$_5$Me$_5$).

For 2.0 equiv. of amine, dicyclohexylamine, **¹H NMR** (500 MHz, DMSO-d₆) δ: 1.76 (d, *J* = 9.7 Hz, 4H), 1.64 (d, *J* = 9.6 Hz, 4H), 1.54 (d, *J* = 11.9 Hz, 2H), 1.19 (q, *J* = 12.3 Hz, 4H), 1.09 (q, *J* = 12.3 Hz, 2H), 0.93 (q, *J* = 9.8 Hz, 4H). Iridium catalyst complex: **¹H NMR** (500MHz, DMSO-d₆) δ: 1.88 (s, 30H, C₅Me₅).

For 10.0 equiv. of amine, dicyclohexylamine, **¹H NMR** (500 MHz, DMSO-d₆) δ: 1.76 (d, *J* = 9.7 Hz, 4H), 1.64 (d, *J* = 9.6 Hz, 4H), 1.54 (d, *J* = 11.9 Hz, 2H), 1.19 (q, *J* = 12.3 Hz, 4H), 1.09 (q, *J* = 12.3 Hz, 2H), 0.93 (q, *J* = 9.8 Hz, 4H). Iridium catalyst complex: **¹H NMR** (500MHz, DMSO-d₆) δ: 1.88 (s, 30H, C₅Me₅).

Entry 7 Synthetic procedure **7.4a** was followed. Benzophenone imine and complex **3.1** (4.0 mg, 3.44 μmols) in DMSO-d₆ were used. Benzophenone imine and iridium complex were observed by ¹H NMR (Figure 7.7).

Figure 7.7 Stacked spectra for benzophenone, 3.2 and iridium catalyst 7.3.4, Entry 7.

For 0.0 equiv. of amine, iridium catalyst complex, **¹H NMR** (500MHz, DMSO-d₆) δ: 1.88 (s, 30H, C₅Me₅).

For 0.2 equiv. of amine, benzophenone imine (500 MHz, DMSO-d$_6$) δ: 10.61 (s, 1H, NH), 7.55-7.41 (apparent m, 10H, CArH). Iridium catalyst complex: **^{1}H NMR** (500MHz, DMSO-d$_6$) δ: 1.88 (s, 30H, C$_5$Me$_5$).

For 0.5 equiv. of amine, benzophenone imine: **^{1}H NMR** (500MHz, DMSO-d$_6$) δ: 10.63 (s, 1H, NH), 7.60-7.38 (m, 10H, CArH). Iridium catalyst complex **A**, **^{1}H NMR** (500MHz, DMSO-d$_6$) δ: 1.88 (s, 30H, C$_5$Me$_5$) and iridium catalyst complex **B**, **^{1}H NMR** (500MHz, DMSO-d$_6$) δ: 1.83 (s, 30H, C$_5$Me$_5$). Ratio of 1.88 ppm complex: 1.83 ppm complex = 29:1.

For 1.0 equiv. of amine, benzophenone imine: **^{1}H NMR** (500MHz, DMSO-d$_6$) δ: 10.63 (s, 1H, NH), 7.52 (t, J = 6.8 Hz, 6H, CArH), 7.49-7.44 (apparent m, 4H, CArH). Iridium catalyst complex **A**, **^{1}H NMR** (500MHz, DMSO-d$_6$) δ: 1.88 (s, 30H, C$_5$Me$_5$); iridium complex **B**, **^{1}H NMR** (500MHz, DMSO-d$_6$) δ: 1.83 (s, 30H, C$_5$Me$_5$) and iridium catalyst complex **C**, **^{1}H NMR** (500MHz, DMSO-d$_6$) δ: 1.75 (s, 30H, C$_5$Me$_5$). Ratio of 1.88 ppm complex: 1.83 ppm complex: 1.75 ppm complex = 73:4.

For 2.0 equiv. of amine, benzophenone imine: **^{1}H NMR** (500MHz, DMSO-d$_6$) δ: 10.65 (s, 1H, NH), 7.52 (t, J = 6.8 Hz, 6H, CArH), 7.49-7.43 (apparent m, 4H, CArH). Iridium catalyst complex **A**, **^{1}H NMR** (500MHz, DMSO-d$_6$) δ: 2.08 (s, 30H, C$_5$Me$_5$) iridium catalyst complex **B**, **^{1}H NMR** (500MHz, DMSO-d$_6$) δ: 1.88 (s, 30H, C$_5$Me$_5$) and iridium catalyst complex **C**, **^{1}H NMR** (500MHz, DMSO-d$_6$) δ: 1.83 (s, 30H, C$_5$Me$_5$). Ratio of 2.08 ppm complex: 1.88 ppm complex: 1.83 ppm complex = 8:20:2.

For 10.0 equiv. of amine, benzophenone imine: **^{1}H NMR** (500MHz, DMSO-d$_6$) δ: 10.65 (s, 1H, NH), 7.52 (t, J = 6.8 Hz, 6H, CArH), 7.49-7.43 (apparent m, 4H, CArH). Iridium catalyst complex **A**, **^{1}H NMR** (500MHz, DMSO-d$_6$) δ: 2.08 (s, 30H, C$_5$Me$_5$) iridium catalyst complex **B**, **^{1}H NMR** (500MHz, DMSO-d$_6$) δ: 1.88 (s, 30H, C$_5$Me$_5$) and iridium catalyst complex **C**, **^{1}H NMR** (500MHz, DMSO-d$_6$) δ: 1.83 (s, 30H, C$_5$Me$_5$) iridium catalyst complex **D**, **^{1}H NMR** (500MHz, DMSO-d$_6$) δ: 1.82 (s, 30H, C$_5$Me$_5$). Ratio of 2.08 ppm complex: 1.88 ppm complex: 1.83 ppm complex: 1.82 ppm complex = 8:14:4:4.

Entry 8 Synthetic procedure **7.4a** was followed. α-Methyl benzylamine and complex **3.1** (6.8 mg, 5.85 μmols) in CDCl$_3$ were used. α-Methyl benzylamine and iridium complexes were observed by ^{1}H NMR (Figure 7.8).
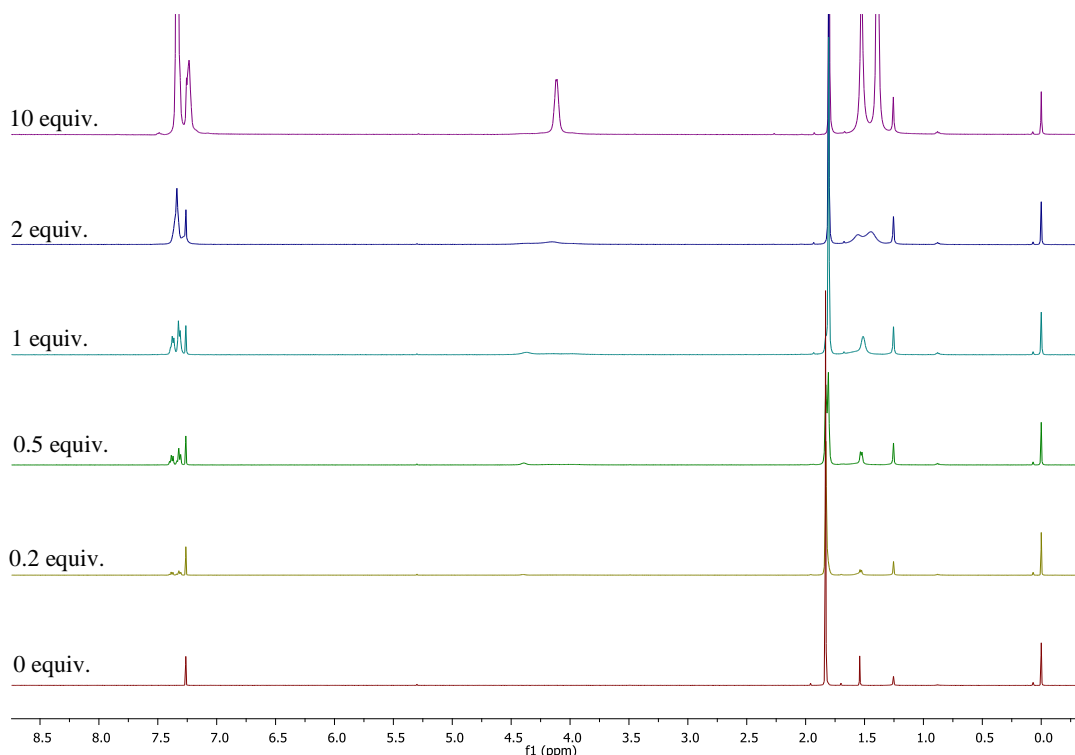
Figure 7.8 Stacked spectra for α-methyl benzylamine, 3.12 and iridium catalyst 7.3.4, Entry 8.

For 0.0 equiv. of amine, iridium catalyst complex: **^{1}H NMR** (500MHz, CDCl$_3$) δ: 1.83 (s, 30H, C$_5$Me$_5$).

For 0.2 equiv. of amine, α-methyl benzylamine: **^{1}H NMR** (500MHz, CDCl$_3$) δ: 7.39 (t, *J* = 7.3 Hz, 2H, C*Ar*H), 7.31 (d, *J* = 8.2 Hz, 2H, C*Ar*H),7.27-7.24 (apparent m, 1H, C*Ar*H), 4.39 (s, 1H, C*Bn*H), 1.53 (d, *J* = 6.7 Hz, 3H, (*CH*)CH$_3$). Iridium complex: **^{1}H NMR** (500MHz, CDCl$_3$) δ: 1.83 (s, 30H, C$_5$Me$_5$).

For 0.5 equiv. of amine, α-methyl benzylamine: **^{1}H NMR** (500MHz, CDCl$_3$) δ: 7.38 (t, *J* = 7.2 Hz, 2H, C*Ar*H), 7.32 (t, *J* = 7.8 Hz, 3H, C*Ar*H), 4.39 (s, 1H, C*Bn*H), 1.69 (d, *J* = 10.4, 3H, (*CH*)CH$_3$). Iridium catalyst complex **A**, **^{1}H NMR** (500MHz, CDCl$_3$) δ: 1.83 (s, 30H, C$_5$Me$_5$) and iridium catalyst complex **B**, **^{1}H NMR** (500MHz, CDCl$_3$) δ: 1.81 (s, 30H, C$_5$Me$_5$). Ratio of 1.83 ppm complex: 1.81 ppm complex = 1:1.

For 1.0 equiv. of amine, α-methyl benzylamine: **^{1}H NMR** (500MHz, CDCl$_3$) δ: : 7.38 (t, *J* = 7.1 Hz, 2H, C*Ar*H), 7.32 (apparent d, *J* = 7.3 Hz, 3H, C*Ar*H), 4.37 (s, 1H, C*Bn*H), 1.51 (apparent br s, 4H, (*CH*)CH$_3$ and NH). Iridium catalyst complex **A**, **^{1}H NMR** (500MHz,

CDCl$_3$) δ: 1.83 (s, 30H, C$_5$Me$_5$) and iridium catalyst complex **B**, **^{1}H NMR** (500MHz, CDCl$_3$) δ: 1.80 (s, 30H, C$_5$Me$_5$). Ratio of 1.83 ppm complex: 1.80 ppm complex = 1:4.

For 2.0 equiv. of amine, α-methyl benzylamine: **^{1}H NMR** (500MHz, CDCl$_3$) δ: 7.47-7.20 (apparent m, 5H, C*Ar*H), 4.15 (apparent s, 1H, C*Bn*H), 1.56 (apparent br s, 2H, NH), 1.45 (apparent br s, 3H, (*CH*)CH$_3$). Iridium catalyst complex: **^{1}H NMR** (500MHz, CDCl$_3$) δ: 1.80 (s, 30H, C$_5$Me$_5$).

For 10.0 equiv. of amine, α-methyl benzylamine: **^{1}H NMR** (500MHz, CDCl$_3$) δ: 7.57-6.95 (apparent m, 5H, C*Ar*H), 4.11 (apparent d, 1H, C*Bn*H), 1.53 (br s, 2H, NH), 1.39 (d, *J* = 5.5 Hz, 3H, (*CH*)CH$_3$). Iridium catalyst complex: **^{1}H NMR** (500MHz, CDCl$_3$) δ: 1.80 (s, 30H, C$_5$Me$_5$).

Entry 9 Synthetic procedure **7.4a** was followed. *N*-Methyl-α-methylbenzylamine and complex **3.1** (6.3 mg, 5.42 μmols, 0.5 equiv.) in CDCl$_3$ were used. *N*-methyl-α-methylbenzylamine, and iridium complexes were observed by ^{1}H NMR analysis (Figure 7.9).
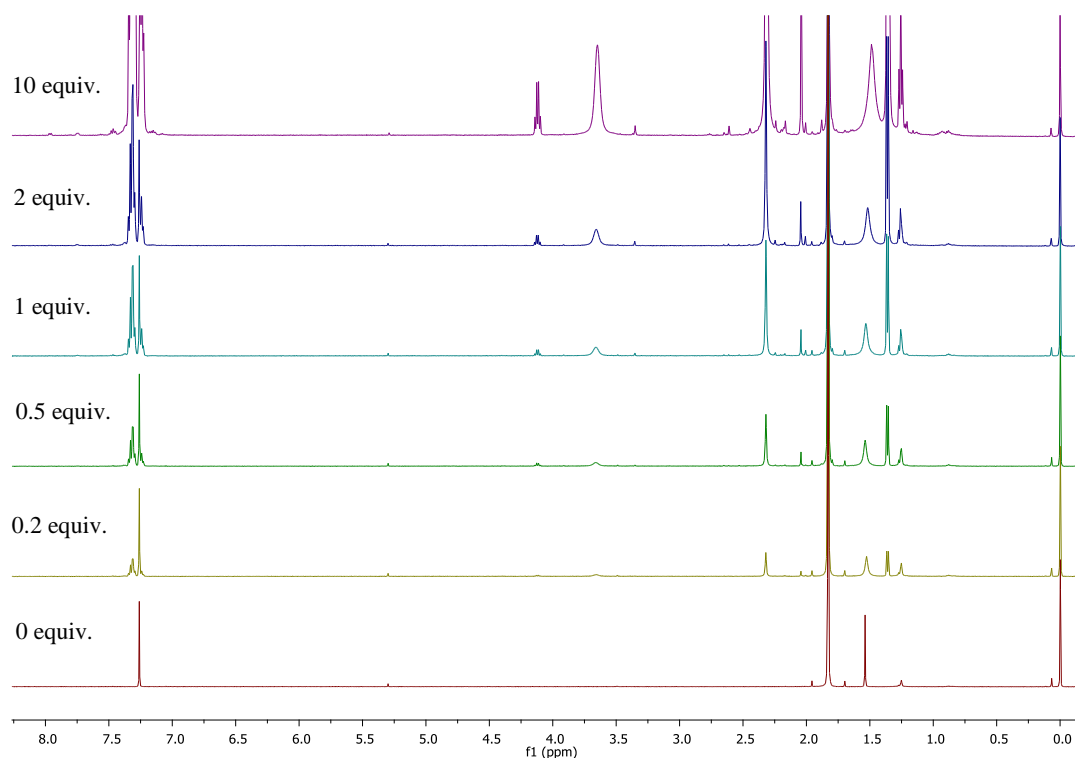
Figure 7.9 Stacked spectra for *N*-methyl-α-methyl benzylamine, 3.13 and iridium catalyst 7.3.4, Entry 9.

For 0.0 equiv. of amine, iridium catalyst complex: **^{1}H NMR** (500MHz, CDCl$_3$) δ: 1.83 (s, 30H, C$_5$Me$_5$).

For 0.2 equiv. of amine, *N*-methyl-α-methyl benzylamine: **^{1}H NMR** (500MHz, CDCl$_3$) δ: 7.36-7.27 (apparent m, 4H, C*Ar*H), 7.23 (apparent d, *J* = 7.0 Hz, 1H, C*Ar*H), 3.66 (s, 1H, C*Bn*H), 2.32 (s, 3H, *N*CH$_3$), 1.53 (s, 1H, NH), 1.36 (d, *J* = 6.6 Hz, 3H, CH$_3$). Iridium complex: **^{1}H NMR** (500MHz, CDCl$_3$) δ: 1.83 (s, 30H, C$_5$Me$_5$).

For 0.5 equiv. of amine, *N*-methyl-α-methyl benzylamine: **^{1}H NMR** (500MHz, CDCl$_3$) δ: 7.42-7.08 (apparent m, 5H, C*Ar*H), s, 1H,), 3.66 (s, 1H, C*Bn*H), 2.32 (s, 3H, *N*CH$_3$), 1.54 (s, 1H, NH), 1.36 (d, *J* = 6.6 Hz, 3H, CH$_3$). Iridium catalyst complex **A**: **^{1}H NMR** (500MHz, CDCl$_3$) δ: 2.04 (s, 30H, C$_5$Me$_5$) and iridium catalyst complex **B**: **^{1}H NMR** (500MHz, CDCl$_3$) δ: 1.83 (s, 30H, C$_5$Me$_5$). Ratio of 2.04 ppm complex: 1.83 ppm complex = 1:71.

For 1.0 equiv. of amine, *N*-methyl-α-methyl benzylamine: **^{1}H NMR** (500MHz, CDCl$_3$) δ: 7.39-7.19 (m, 5H, C*Ar*H), 3.66 (s, 1H, C*Bn*H), 2.32 (s, 3H, *N*CH$_3$), 1.53 (s, 1H, NH), 1.36 (d, *J* = 6.6 Hz, 3H, CH$_3$). Iridium catalyst complex **A**: **^{1}H NMR** (500MHz, CDCl$_3$) δ: 2.04 (s, 30H, C$_5$Me$_5$) and iridium catalyst complex **B**: **^{1}H NMR** (500MHz, CDCl$_3$) δ: 1.83 (s, 30H, C$_5$Me$_5$). Ratio of 2.04 ppm complex: 1.83 ppm complex = 1:40.

For 2.0 equiv. of amine, *N*-methyl-α-methyl benzylamine: **^{1}H NMR** (500MHz, CDCl$_3$) δ: 7.49-7.10 (apparent m, 5H, C*Ar*H), 3.66 (s, 1H, C*Bn*H), 2.32 (s, 3H, *N*CH$_3$), 1.52 (s, 1H, NH), 1.36 (d, *J* = 6.6 Hz, 3H, CH$_3$). Iridium catalyst complex **A**: **^{1}H NMR** (500MHz, CDCl$_3$) δ: 2.04 (s, 30H, C$_5$Me$_5$) and iridium catalyst complex **B**: **^{1}H NMR** (500MHz, CDCl$_3$) δ: 1.83 (s, 30H, C$_5$Me$_5$). Ratio of 2.04 ppm complex: 1.83 ppm complex = 2:41.

For 10.0 equiv. of amine, *N*-methyl-α-methyl benzylamine: **^{1}H NMR** (500MHz, CDCl$_3$) δ: 7.56-7.08 (m, 5H, C*Ar*H), 3.65 (s, 1H, C*Bn*H), 2.31 (s, 3H, *N*CH$_3$), 1.49 (s, 1H, NH), 1.36 (d, *J* = 6.6 Hz, 3H, CH$_3$). Iridium catalyst complex **A**: **^{1}H NMR** (500MHz, CDCl$_3$) δ: 2.04 (s, 30H, C$_5$Me$_5$) and iridium catalyst complex **B**: **^{1}H NMR** (500MHz, CDCl$_3$) δ: 1.83 (s, 30H, C$_5$Me$_5$). Ratio of 2.04 ppm complex: 1.83 ppm complex = 2:9.

Entry 10 Synthetic procedure **7.4a** was followed. 4-Bromo-benzylamine and complex **3.1** (6.7 mg, 5.76 μmols) in DMSO-d$_6$ were used. Iridium bound 4-bromo-benzylamine and iridium complexes were observed *via* ^{1}H NMR analysis (Figure 7.10).
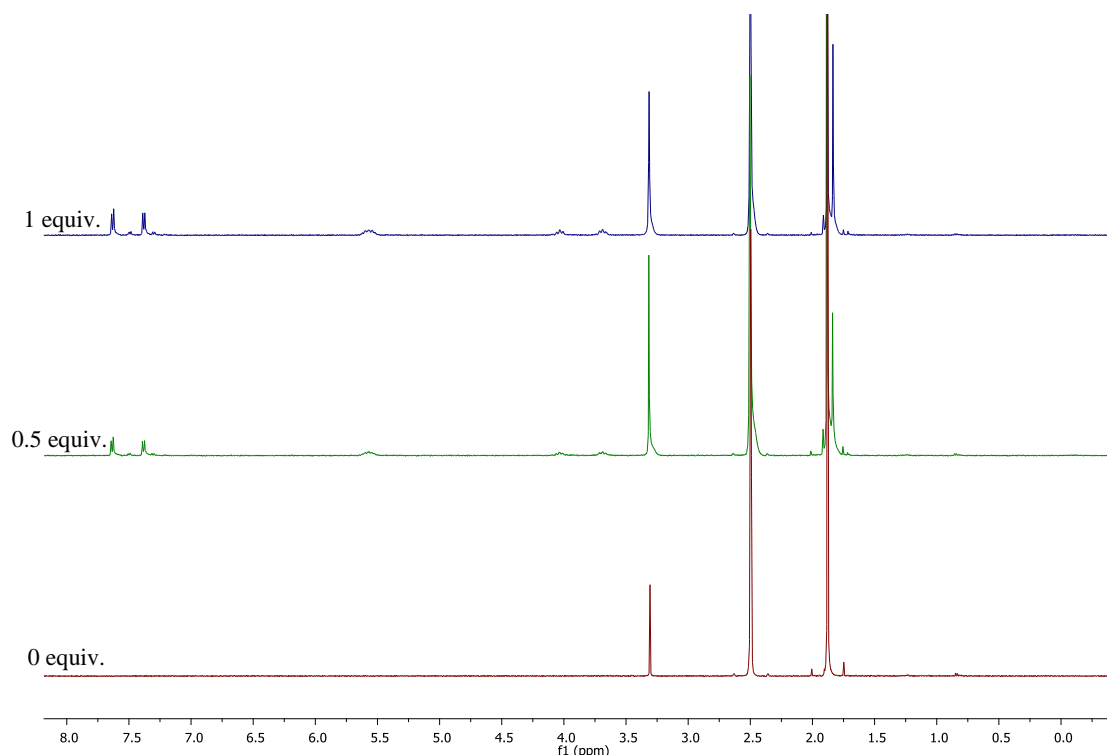
Figure 7.10 Stacked spectra for 4-bromobenzylamine, 3.7 and iridium catalyst 7.3.4, Entry 10.

For 0.0 equiv. of amine, iridium catalyst complex, **^{1}H NMR** (500MHz, DMSO-d$_6$) δ: 1.88 (s, 30H, C$_5$Me$_5$).

For 0.5 equiv. of amine, catalyst bound 4-bromobenzylamine: **^{1}H NMR** (500MHz, DMSO-d$_6$) δ: 7.63 (d, *J* = 8.4 Hz, 2H, C*Ar*H), 7.38 (d, *J* = 8.4 Hz, 2H, C*Ar*H), 5.56 (s, 2H, NH$_2$), 4.03 (t, *J* = 12.8 Hz, 1H, C*Bn*H), 3.68 (t, *J* = 12.6 Hz, 1H, C*Bn*H). Iridium catalyst complex **A**: **^{1}H NMR** (500MHz, DMSO-d$_6$) δ: 1.91 (s, 30H, C$_5$Me$_5$); iridium catalyst complex **B**: **^{1}H NMR** (500MHz, DMSO-d$_6$) δ: 1.88 (s, 30H, C$_5$Me$_5$) and iridium catalyst complex **C**: **^{1}H NMR** (500MHz, DMSO-d$_6$) δ: 1.83 (s, 30H, C$_5$Me$_5$). Ratio of 1.91 ppm complex: 1.88 ppm complex: 1.83 ppm complex = 1:22:7.

For 1.0 equiv. of amine, catalyst bound 4-bromobenzylamine: **^{1}H NMR** (500MHz, DMSO-d$_6$) δ: 7.63 (d, *J* = 8.2 Hz, 2H, C*Ar*H), 7.38 (d, *J* = 8.3 Hz, 2H, C*Ar*H), 5.55 (s, 2H, NH$_2$), 4.03 (t, *J* = 11.9 Hz, 1H, C*Bn*H), 3.68 (t, *J* = 12.1 Hz, 1H, C*Bn*H). Iridium catalyst complex **A**: **^{1}H NMR** (500MHz, DMSO-d$_6$) δ: 1.91 (s, 30H, C$_5$Me$_5$); iridium catalyst complex **B**: **^{1}H NMR** (500MHz, DMSO-d$_6$) δ: 1.88 (s, 30H, C$_5$Me$_5$) and iridium catalyst

complex **C**: **¹H NMR** (500MHz, DMSO-d$_6$) δ: 1.83 (s, 30H, C$_5$Me$_5$). Ratio of 1.91 ppm complex: 1.88 ppm complex: 1.83 ppm complex = 1:19:10.

Entry 11 Synthetic procedure **7.4a** was followed. 4-Methoxy-benzylamine, iridium complex **3.1** (5.2 mg, 4.47 µmols, 0.5 equiv.) and DMSO-d$_6$ were used. Iridium complexes and catalyst bound 4-methoxybenzylamine were observed by ¹H-NMR analysis (Figure 7.11).

Figure 7.11 Stacked spectra for 4-methoxybenzylamine, 3.8 and iridium catalyst 7.3.4, Entry 11.

For 0.0 equiv. of amine, For 0.0 equiv. of amine, iridium catalyst complex, **¹H NMR** (500MHz, DMSO-d$_6$) δ: 1.88 (s, 30H, C$_5$Me$_5$).
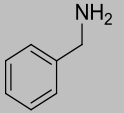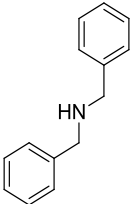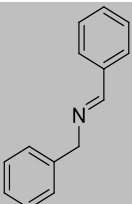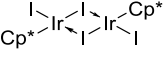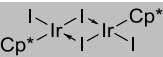
For 0.5 equiv. of amine, catalyst bound 4-methoxybenzylamine: **¹H NMR** (500MHz, DMSO-d$_6$) δ: 7.34 (d, *J* = 8.2 Hz, 2H, C*Ar*H), 6.96 (d, *J* = 8.2 Hz, 2H, C*Ar*H), 5.58-5.39 (apparent m, 2H, NH$_2$), 3.98 (t, *J* = 12.5 Hz, 1H, C*Bn*H), 3.74 (t, *J* = 12.5 Hz, 1H, C*Bn*H). Iridium catalyst complex **A**: **¹H NMR** (500MHz, DMSO-d$_6$) δ: 1.92 (s, 30H, C$_5$Me$_5$); iridium catalyst complex **B**: **¹H NMR** (500MHz, DMSO-d$_6$) δ: 1.88 (s, 30H, C$_5$Me$_5$) and

iridium catalyst complex **C**: **^{1}H NMR** (500MHz, DMSO-d$_6$) δ: 1.84 (s, 30H, C$_5$Me$_5$). Ratio of 1.92 ppm complex: 1.88 ppm complex: 1.84 ppm complex = 2:21:7.

For 1.0 equiv. of amine, catalyst bound 4-bromobenzylamine: **^{1}H NMR** (500MHz, DMSO-d$_6$) δ: 7.34 (d, *J* = 8.6 Hz, 2H, C*Ar*H), 6.96 (d, *J* = 8.6 Hz, 2H, C*Ar*H), 5.55-5.40 (apparent m, 2H, NH$_2$), 3.99 (t, *J* = 11.7 Hz, 1H, C*Bn*H), 3.67-3.59 (apparent m, 1H, C*Bn*H). Iridium catalyst complex **A**: **^{1}H NMR** (500MHz, DMSO-d$_6$) δ: 1.92 (s, 30H, C$_5$Me$_5$); iridium catalyst complex **B**: **^{1}H NMR** (500MHz, DMSO-d$_6$) δ: 1.88 (s, 30H, C$_5$Me$_5$) and iridium catalyst complex **C**: **^{1}H NMR** (500MHz, DMSO-d$_6$) δ: 1.84 (s, 30H, C$_5$Me$_5$). Ratio of 1.92 ppm complex: 1.88 ppm complex: 1.84 ppm complex = 3:13:13.

7.3.5 2D NMR analysis of benzylamine bound iridium complex *via* ^{1}H-^{1}H-diffusion ordered spectroscopic (DOSY spectroscopy)
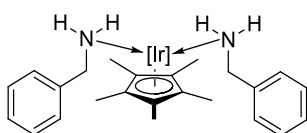
Analyte in standard	Moles of analyte / μmols	Mass of analyte added or volume of 0.1 M analyte added	Volume of DMSO-d$_6$/ mL	Concentration / mM
	6.25	62.50 μL	0.5375	12.50
	6.25	62.50 μL	0.5375	12.50
	6.25	62.50 μL	0.5375	12.50
	3.13	3.60 mg	0.6000	6.25
	6.25	7.28 mg	0.6000	12.50

Standards of diiodopentamethylcyclopentadienyliridium(III) dimer complex (6.25 mM and 12.5 mM), benzylamine (12.5 mM), *N*-benzylidene benzyl amine (12.5 mM) and dibenzylamine (12.5 mM) were prepared in DMSO-d_6. All the standards were analysed by DOSY NMR spectroscopy (spectra recorded and processed by Dr. J. Fisher, University of Leeds) and their diffusion coefficients determined. Separately, benzylamine (62.5 μL of 0.1 M solution in DMSO-d_6, 6.25 μmol, 2.00 equiv.) was added to a suspension of diiodopentamethylcyclopentadienyliridium (III) dimer complex (3.6 mg, 3.13 μmol, 1.00 equiv.) in DMSO-d_6 (0.5375 mL) and shaken vigorously for 60 seconds. The DOSY spectrums were recorded on a Varia Inova Unity 500 MHz instrument, using the oneshot pulse sequence. A sweep width of 6000 Hz, recycle delay of 10 seconds, and 16 transients were used. Fifteen gradient levels were employed, with a diffusion delay of 0.002 seconds was included, as was an unbalancing factor of 0.2. Data was processed with a $1H_2$ line broadening prior to Fourier transformation, then phased and base line corrected to produce the DOSY plot. The diffusion coefficient of the standards were obtained from their DOSY spectra and the spectra were compared to that of the sample and a mass range was determined. Catalyst bound amine complex: **^{1}H NMR** (500MHz, DMSO-d_6) δ: 7.45-7.11 (apparent m, 5H, C*Ar*H), 5.63 (t, *J* = 10.4 Hz, 1H, NH), 5.54 (t, *J* = 10.2 Hz, 1H, NH), 4.08 (t, *J* = 12.1 Hz, 1H, C*Bn*H), 3.71 (apparent s, 1H, C*Bn*H). Iridium catalyst complex: **^{1}H NMR** (500MHz, DMSO-d_6) δ: 1.85 (s, 30H, C_5Me_5). Ratio of 1.85 ppm Cp* protons: amine protons at 4.08 ppm = 15:2. Diffusion coefficient, (D): 1.59 x 10^{-10} m^2s^{-1} ≡ mass > 6000 Da.

7.3.6 NMR analysis of iridium catalysed amine dehydrogenation at elevated temperature

General Procedure 7.4b

A general synthetic procedure was used with minor modifications to assess the dehydrogenation of primary, secondary and tertiary amines at elevated temperature. The procedure is described briefly below:

$$R^1 \overset{R^3}{\underset{R^2}{\overset{|}{\longrightarrow}}} N\text{-}R^4 \quad \xrightarrow[\substack{C_7D_8 \text{ or} \\ (CD_3)_2SO_2 \\ 115\text{-}120\ °C}]{[IrCp^*I_2]_2} \quad R^1 \overset{R^3}{\underset{R^2}{\overset{|}{\longrightarrow}}} N\overset{[Ir]}{\underset{R^4}{\longrightarrow}}$$

$R^1 = $ Ph, Me or H
$R^2 = $ Aryl
$R^3 = $ H, Me or Bn
$R_4 = $ H or Me
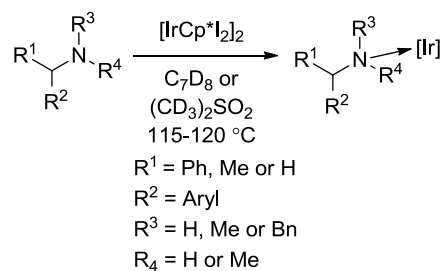
Diiodopentamethylcyclopentadienyliridium(III) dimer complex was suspended in deuterated solvent (0.7 mL) in an NMR tube, shaken for 60 seconds and analysed by ^{1}H NMR spectroscopy. The amine was added to the resultant suspension and shaken for 60 seconds and heated. The reaction was monitored by cooling the NMR tube to room temperature and analysing by ^{1}H NMR spectroscopy.

Entry 1 Synthetic procedure **7.4b** was followed. Benzhydrylamine (169 μLs of 0.1M amine in DMSO-d_6 and 11.5 μLs of pure amine, 84.3 μmols, 20 equiv.), iridium complex **3.1** (4.9 mg, 4.21 μmols, 1.00 equiv.) and DMSO-d_6 were used and the reaction was heated by an oil bath (115 °C). The reaction was monitored at 0, 0.25, 0.5, 1, 2, 3, 4 and 27 hours. Iridium complexes, benzhydrylamine (**3.6**), *N*-benzhydryl-diphenylmethanimine (**3.40**) and *N,N*-dibenzhydrylamine (**3.41**) were observed (Figure 7.12).
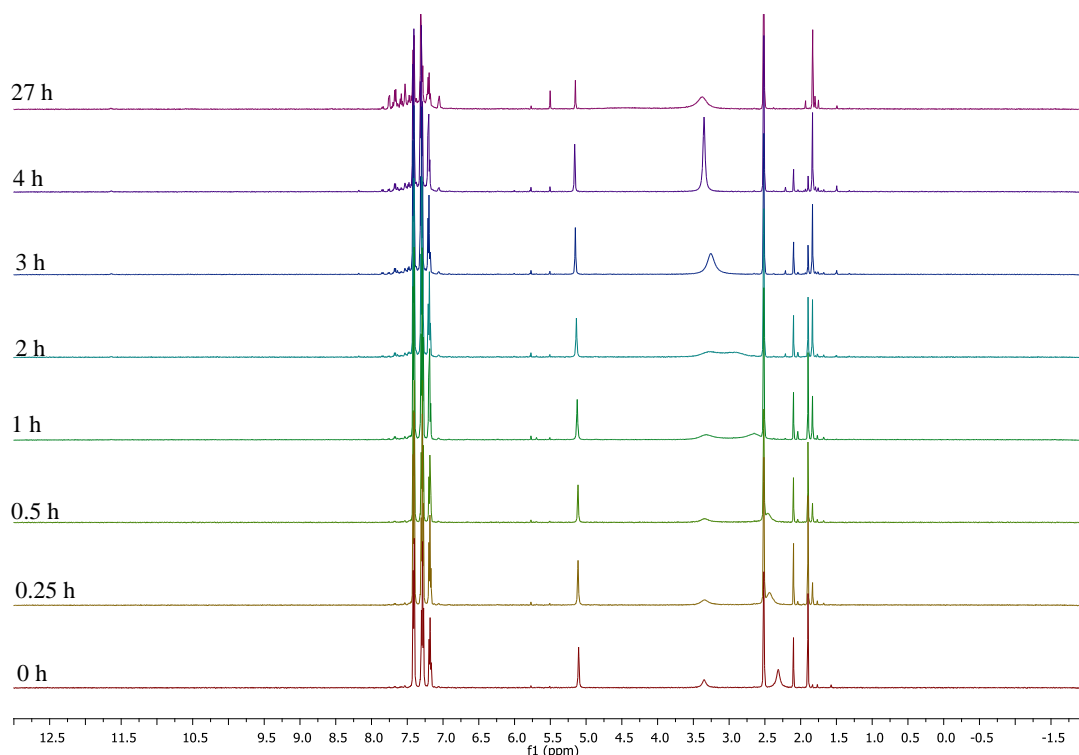
Figure 7.12 Stacked spectra for benzhydrylamine, 3.6 and iridium catalyst 7.3.6, Entry 1.

For 0.0 equiv. of amine, iridium catalyst complex, **¹H NMR** (500MHz, DMSO-d₆) δ: 1.88 (s, 30H, C₅Me₅).

For 10.0 equiv. of amine, benzhydrylamine, **¹H NMR** (500MHz, DMSO-d₆) δ: 7.39 (d, *J* = 7.4 Hz, 4H, C*Ar*H), 7.27 (t, *J* = 7.5 Hz, 4H, C*Ar*H), 7.17 (t, *J* = 7.2 Hz, 2H, C*Ar*H), 5.09 (s, 1H, C*Bn*H), 2.30 (br s, 2H, NH₂). Iridium catalyst complex **A**: **¹H NMR** (500MHz, DMSO-d₆) δ: 2.09 (s, 30H, C₅Me₅) and iridium catalyst complex **B**: **¹H NMR** (500MHz, DMSO-d₆) δ: 1.88 (s, 30H, C₅Me₅). Ratio of 2.09 ppm complex: 1.88 ppm complex = 1:2.

For 0.25 hours at 110 °C, benzhydrylamine, **¹H NMR** (500MHz, DMSO-d₆) δ: 7.39 (d, *J* = 7.4 Hz, 4H, C*Ar*H), 7.27 (t, *J* = 7.5 Hz, 4H, C*Ar*H), 7.17 (t, *J* = 7.2 Hz, 2H, C*Ar*H), 5.09 (s, 1H, C*Bn*H), 2.42 (br s, 2H, NH₂). Iridium catalyst complex **A**: **¹H NMR** (500 MHz, DMSO-d₆) δ: 2.08 (s, 30H, C₅Me₃), iridium catalyst complex **B**: **¹H NMR** (500 MHz, DMSO-d₆) δ: 1.88 (s, 30H, C₅Me₅) and iridium catalyst complex **C**: **¹H NMR** (500 MHz, DMSO-d₆) δ: 1.82 (s, 30H, C₅Me₅). Ratio of 2.09 ppm complex: 1.88 ppm complex: 1.82 ppm complex = 2:4:1.

For 0.5 hours at 110 °C, benzhydrylamine, **¹H NMR** (500MHz, DMSO-d₆) δ: 7.39 (d, *J* = 7.4 Hz, 4H, C*Ar*H), 7.27 (t, *J* = 7.5 Hz, 4H, C*Ar*H), 7.17 (t, *J* = 7.2 Hz, 2H, C*Ar*H), 5.09 (s, 1H, C*Bn*H), 2.45 (br s, 2H, NH₂). Iridium catalyst complex **A**: **¹H NMR** (500 MHz, DMSO-d₆) δ: 2.08 (s, 30H, C₅Me₃), iridium catalyst complex **B**: **¹H NMR** (500 MHz, DMSO-d₆) δ: 1.88 (s, 30H, C₅Me₅) and iridium catalyst complex **C**: **¹H NMR** (500 MHz, DMSO-d₆) δ: 1.82 (s, 30H, C₅Me₅). Ratio of 2.09 ppm complex: 1.88 ppm complex: 1.82 ppmcomplex = 2:4:1.

For 1 hour at 110 °C, benzhydrylamine, **¹H NMR** (500MHz, DMSO-d₆) δ: 7.39 (d, *J* = 7.4 Hz, 4H, C*Ar*H), 7.27 (t, *J* = 7.5 Hz, 4H, C*Ar*H), 7.17 (t, *J* = 7.2 Hz, 2H, C*Ar*H), 5.09 (s, 1H, C*Bn*H), 2.64 (br s, 2H, NH₂). Iridium catalyst complex **A**: **¹H NMR** (500 MHz, DMSO-d₆) δ: 2.08 (s, 30H, C₅Me₃), iridium catalyst complex **B**: **¹H NMR** (500 MHz, DMSO-d₆) δ: 2.03 (s, 30H, C₅Me₅), iridium catalyst complex **C**: **¹H NMR** (500 MHz, DMSO-d₆) δ: 1.88 (s, 30H, C₅Me₅) and iridium catalyst complex **D**: **¹H NMR** (500 MHz, DMSO-d₆) δ: 1.82 (s, 30H, C₅Me₅). Ratio of 2.09 ppm complex: 2.03 ppm complex: 1.88 ppm complex: 1.82 ppm, complex = 6:2:13:9.

For 2 hours at 110 °C, benzhydrylamine, **¹H NMR** (500MHz, DMSO-d₆) δ: 7.39 (d, *J* = 7.4 Hz, 4H, C*Ar*H), 7.27 (t, *J* = 7.5 Hz, 4H, C*Ar*H), 7.17 (t, *J* = 7.2 Hz, 2H, C*Ar*H), 5.09 (s, 1H, C*Bn*H), 2.91 (br s, 2H, NH₂). Iridium catalyst complex **A**: **¹H NMR** (500 MHz, DMSO-d₆) δ: 2.08 (s, 30H, C₅Me₃), iridium catalyst complex **B**: **¹H NMR** (500 MHz, DMSO-d₆) δ: 2.03 (s, 30H, C₅Me₅), iridium catalyst complex **C**: **¹H NMR** (500 MHz, DMSO-d₆) δ: 1.88 (s, 30H, C₅Me₅) and iridium catalyst complex **D**: **¹H NMR** (500 MHz, DMSO-d₆) δ: 1.82 (s, 30H, C₅Me₅). Ratio of 2.09 ppm complex: 2.03 ppm complex: 1.88 ppm complex: 1.82 ppmcomplex = 6:1:10:12.

For 3 hours at 110 °C, benzhydrylamine, **¹H NMR** (500MHz, DMSO-d₆) δ: 7.39 (d, *J* = 7.4 Hz, 4H, C*Ar*H), 7.27 (t, *J* = 7.5 Hz, 4H, C*Ar*H), 7.17 (t, *J* = 7.2 Hz, 2H, C*Ar*H), 5.09 (s, 1H, C*Bn*H), 3.24 (br s, 2H, NH₂). Iridium catalyst complex **A**: **¹H NMR** (500 MHz, DMSO-d₆) δ: 2.08 (s, 30H, C₅Me₃), iridium catalyst complex **B**: **¹H NMR** (500 MHz, DMSO-d₆) δ: 2.03 (s, 30H, C₅Me₅), iridium catalyst complex **C**: **¹H NMR** (500 MHz, DMSO-d₆) δ: 1.88 (s, 30H, C₅Me₅), iridium catalyst complex **D**: **¹H NMR** (500 MHz, DMSO-d₆) δ: 1.82 (s, 30H, C₅Me₅) and iridium catalyst complex **E**: **¹H NMR** (500 MHz, DMSO-d₆) δ: 1.81 (s, 30H, C₅Me₅). Ratio of 2.09 ppm complex: 2.03 ppm complex: 1.88 ppm complex: 1.82 ppm complex: 1.81 ppm complex = 5:6:14:3.

For 4 hours at 110 °C, benzhydrylamine, ^{1}**H NMR** (500MHz, DMSO-d_6) δ: 7.39 (d, J = 7.4 Hz, 4H, CArH), 7.27 (t, J = 7.5 Hz, 4H, CArH), 7.17 (t, J = 7.2 Hz, 2H, CArH), 5.09 (s, 1H, CBnH), 3.34 (br s, 2H, NH$_2$). Iridium catalyst complex **A**: ^{1}**H NMR** (500 MHz, DMSO-d_6) δ: 2.08 (s, 30H, C$_5$Me$_3$), iridium catalyst complex **B**: ^{1}**H NMR** (500 MHz, DMSO-d_6) δ: 2.03 (s, 30H, C$_5$Me$_5$), iridium catalyst complex **C**: ^{1}**H NMR** (500 MHz, DMSO-d_6) δ: 1.88 (s, 30H, C$_5$Me$_5$), iridium catalyst complex **D**: ^{1}**H NMR** (500 MHz, DMSO-d_6) δ: 1.82 (s, 30H, C$_5$Me$_5$) and iridium catalyst complex **E**: ^{1}**H NMR** (500 MHz, DMSO-d_6) δ: 1.81 (s, 30H, C$_5$Me$_5$). Ratio of 2.09 ppm complex: 2.03 ppm complex: 1.88 ppm complex: 1.82 ppm complex: 1.81 ppm complex = 4:3:16:3.

For 27 hours at 110 °C, benzhydrylamine, ^{1}**H NMR** (500MHz, DMSO-d_6) δ: 7.5-7.2 (apparent m, 10H, CArH), 5.09 (s, 1H, CBnH), 3.34 (br s, 2H, NH$_2$) *N*-benzhydryldiphenylmethanimine, ^{1}**H NMR** (500MHz, DMSO-d_6) δ: 7.75-7.4 (apparent m, 10H, CArH), 5.49 (s, 1H, CBnH). Iridium catalyst complex **A**: ^{1}**H NMR** (500 MHz, DMSO-d_6) δ: 1.92 (s, 30H, C$_5$Me$_5$), iridium catalyst complex **B**: ^{1}**H NMR** (500 MHz, DMSO-d_6) δ: 1.82 (s, 30H, C$_5$Me$_5$), iridium catalyst complex **C**: ^{1}**H NMR** (500 MHz, DMSO-d_6) δ: 1.78 (s, 30H, C$_5$Me$_5$) and iridium catalyst complex **D**: ^{1}**H NMR** (500 MHz, DMSO-d_6) δ: 1.74 (s, 30H, C$_5$Me$_5$). Ratio of 1.92 ppm complex: 1.82 ppm complex: 1.78 ppm complex: 1.74 ppm complex = 2:20:3:2.

Entry 2 Synthetic procedure **7.4b** was followed. Benzylamine (3.5 μLs, 33.3 μmols, 8 equiv.), iridium complex **3.1** (4.9 mg, 4.21 μmols, 1 equiv.) and DMSO-d_6 were used and the reaction was heated by an oil bath (115 °C). The reaction was monitored at 0, 0.25, 0.5, 1.08, 2, 3, 4 and 28 hours. Benzylamine (**3.11**) and *N*-benzylidene benzylamine (**3.17**) and iridium complexes were observed by ^{1}H NMR analysis (Figure 7.13).
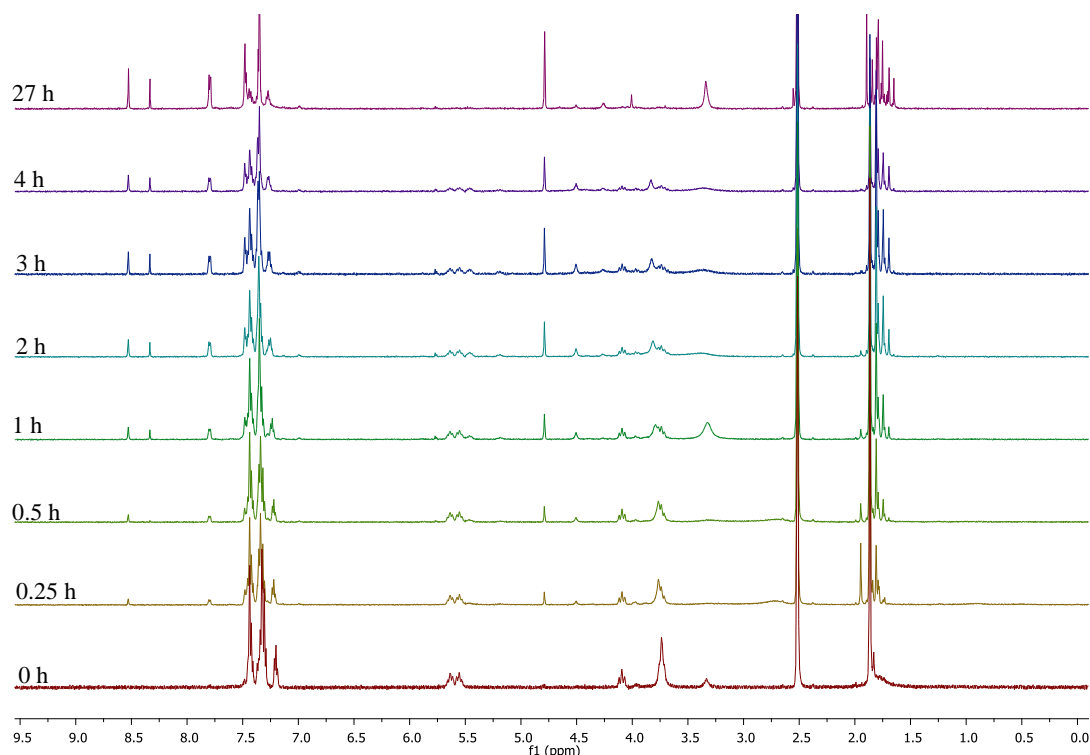
Figure 7.13 Stacked spectra for benzylamine, 3.11 and iridium catalyst 7.3.6, Entry 2.

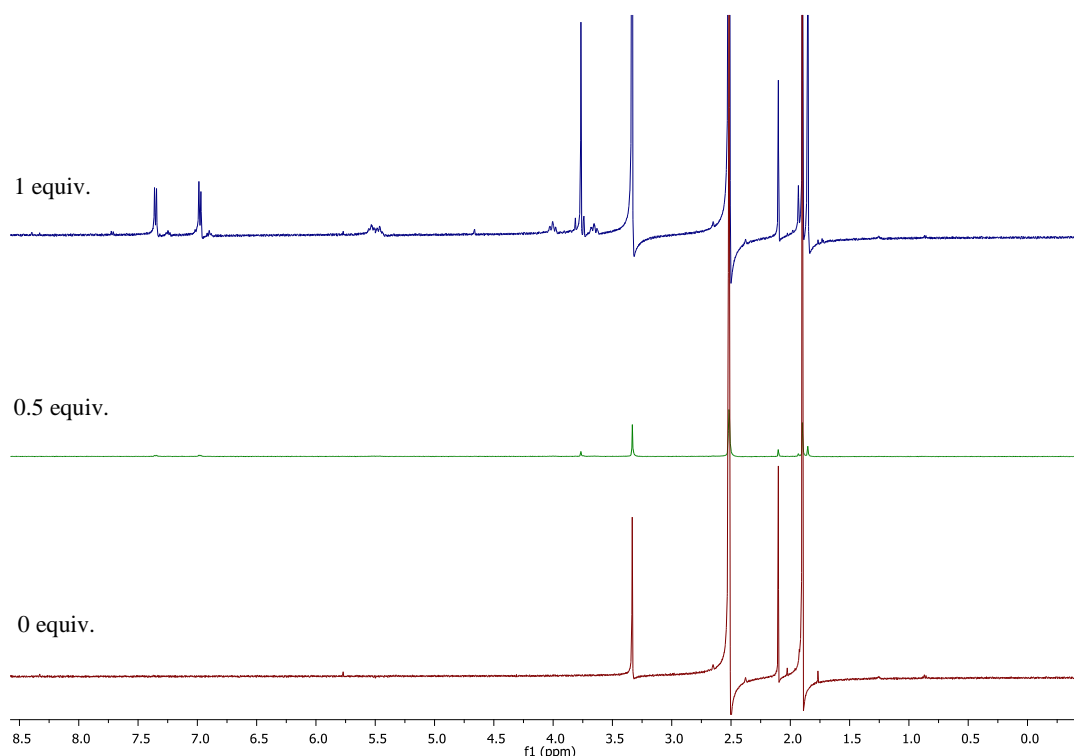For 0.0 equiv. of amine, iridium catalyst complex, **^{1}H NMR** (500MHz, DMSO-d$_6$) δ: 1.88 (s, 30H, C$_5$Me$_5$).

For 10.0 equiv. of amine, catalyst bound benzylamine, **^{1}H NMR** (500MHz, DMSO-d$_6$) δ: 7.53-7.38 (m, 2H, C*Ar*H), 7.36-7.24 (m, 2H, C*Ar*H), 7.24-7.13 (m, 1H, C*Ar*H), 5.62 (t, *J* = 10.5 Hz, 1H, NH), 5.54 (t, *J* = 10.5 Hz, 1H, NH), 4.08 (t, *J* = 11.6 Hz, 1H, C*Bn*H), 3.72 (t, *J*= 11.6, 1H, C*Bn*H) and free benzylamine, **^{1}H NMR** (500MHz, DMSO-d$_6$) δ: 7.53-7.38 (m, 2H, C*Ar*H), 7.36-7.24 (m, 2H, C*Ar*H), 7.24–7.13 (m, 1H, C*Ar*H), 3.72 (t, J= 11.6, 2H, C*Bn*H) 1.78 (br s, 2H, NH$_2$). Ratio of free amine protons at 3.72 ppm: to catalyst bound amine protons at 4.08 ppm = 1:3. Iridium catalyst complex **A**: **^{1}H NMR** (500MHz, DMSO-d$_6$) δ: 1.85 (s, 30H, C$_5$Me$_5$) and iridium catalyst complex **B**: **^{1}H NMR** (500MHz, DMSO-d$_6$) δ: 1.82 (s, 30H, C$_5$Me$_5$). Ratio of 1.85 ppm complex: 1.82 ppm complex = 13:2.

For 0.25 hours at 110 °C, catalyst bound benzylamine, **^{1}H NMR** (500MHz, DMSO-d$_6$) δ: 7.42-7.17 (m, 5H, C*Ar*H), 5.62 (t, J = 10.5 Hz, 1H, NH), 5.54 (t, J = 10.5 Hz, 1H, NH), 4.08 (t, J = 11.6 Hz, 1H, C*Bn*H), 3.72 (t, J= 11.6, 1H, C*Bn*H), *N*-benzylidene benzylamine, **^{1}H NMR** (500MHz, DMSO-d$_6$) δ: 8.51 (s, 1H, C*imine*H), 7.78 (d, *J* = 5.6 Hz, 2H, C*Ar*H), 7.42-7.17 (m, 8H, C*Ar*H), 4.78 (s, 2H, C*Bn*H) and free benzylamine, **^{1}H NMR** (500MHz,

DMSO-d_6) δ: 7.42-7.17 (m, 5H, CArH), 3.72 (s, 2H, CBnH) 2.70 (br s, 2H, NH$_2$). Ratio of free benzylamine: catalyst bound benzylamine: N-benzylidene benzylamine = 20:8:1. Iridium catalyst complex **A**: **^{1}H NMR** (500 MHz, DMSO-d_6) δ: 1.93 (s, 30H, C$_5$Me$_3$), iridium catalyst complex **B**: **^{1}H NMR** (500 MHz, DMSO-d_6) δ: 1.85 (s, 30H, C$_5$Me$_5$) and iridium catalyst complex **C**: **^{1}H NMR** (500 MHz, DMSO-d_6) δ: 1.78 (s, 30H, C$_5$Me$_5$). Ratio of 1.93 ppm complex: 1.85 ppm complex: 1.78 ppm complex = 3:21:5.

For 0.5 hours at 110 °C, catalyst bound benzylamine, **^{1}H NMR** (500MHz, DMSO-d_6) δ: 7.53-7.13 (m, 5H, CArH), 5.62 (t, J = 10.5 Hz, 1H, NH), 5.54 (t, J = 10.5 Hz, 1H, NH), 4.08 (t, J = 11.6 Hz, 1H, CBnH), 3.72 (t, J= 11.6, 1H, CBnH), N-benzylidene benzylamine, **^{1}H NMR** (500MHz, DMSO-d_6) δ: 8.51 (s, 1H, C$imine$H), 7.78 (d, J = 5.6 Hz, 2H, CArH), 7.42-7.17 (m, 8H, CArH), 4.78 (s, 2H, CBnH) and and free benzylamine, **^{1}H NMR** (500MHz, DMSO-d_6) δ: 7.53-7.13 (m, 5H, CArH), 3.72 (s, 2H, CBnH) 2.70 (br s, 2H, NH$_2$). Ratio of free benzylamine: catalyst bound benzylamine: N-benzylidene benzylamine = 15:6:1. Iridium catalyst complex **A**: **^{1}H NMR** (500 MHz, DMSO-d_6) δ: 1.93 (s, 30H, C$_5$Me$_3$), iridium catalyst complex **B**: **^{1}H NMR** (500 MHz, DMSO-d_6) δ: 1.85 (s, 30H, C$_5$Me$_5$), iridium catalyst complex **C**: **^{1}H NMR** (500 MHz, DMSO-d_6) δ: 1.79 (s, 30H, C$_5$Me$_5$) and iridium catalyst complex **D**: **^{1}H NMR** (500 MHz, DMSO-d_6) δ: 1.73 (s, 30H, C$_5$Me$_5$). Ratio of 1.93 ppm complex: 1.85 ppm complex: 1.79 ppm complex: 1.73 ppm complex = 1:20:6:2.

For 1.08 hours at 110 °C, catalyst bound benzylamine, **^{1}H NMR** (500MHz, DMSO-d_6) δ: 7.53-7.13 (m, 5H, CArH), 5.62 (t, J = 10.5 Hz, 1H, NH), 5.54 (t, J = 10.5 Hz, 1H, NH), 4.08 (t, J = 11.6 Hz, 1H, CBnH), 3.72 (t, J= 11.6, 1H, CBnH), N-benzylidene benzylamine (major isomer), **^{1}H NMR** (500MHz, DMSO-d_6) δ: 8.51 (s, 1H, C$imine$H), 7.78 (d, J = 5.6 Hz, 2H, CArH), 7. 42-7.17 (m, 8H, CArH), 4.78 (s, 2H, CBnH), N-benzylidene benzylamine (minor isomer) **^{1}H NMR** (500MHz, DMSO-d_6) δ: 8.32 (s, 1H, C$imine$H), 7.78 (d, J = 5.6 Hz, 2H, CArH), 7. 42-7.17 (m, 8H, CArH), 4.78 (s, 2H, CBnH) and free benzylamine, **^{1}H NMR** (500MHz, DMSO-d_6) δ: 7.53-7.13 (m, 5H, CArH), 3.72 (s, 2H, CBnH) 3.30 (br s, 2H, NH$_2$). Ratio of free benzylamine: catalyst bound benzylamine: N-benzylidene benzylamine (major): N-benzylidene benzylamine (minor) = 18:6:2:1. Iridium catalyst complex **A**: **^{1}H NMR** (500 MHz, DMSO-d_6) δ: 1.93 (s, 30H, C$_5$Me$_3$), iridium catalyst complex **B**: **^{1}H NMR** (500 MHz, DMSO-d_6) δ: 1.85 (s, 30H, C$_5$Me$_5$), iridium catalyst complex **C**: **^{1}H NMR** (500 MHz, DMSO-d_6) δ: 1.79 (s, 30H, C$_5$Me$_5$) and iridium catalyst complex **D**: **^{1}H NMR** (500 MHz, DMSO-d_6) δ: 1.73 (s, 30H, C$_5$Me$_5$). Ratio of 1.93 ppm complex: 1.85 ppm complex: 1.79 ppm complex: 1.73 ppm complex = 1:28:14:5.

For 2 hours at 110 °C, catalyst bound benzylamine, **¹H NMR** (500MHz, DMSO-d$_6$) δ: 7.53-7.13 (m, 5H, C*Ar*H), 5.62 (t, J = 10.5 Hz, 1H, NH), 5.54 (t, J = 10.5 Hz, 1H, NH), 4.08 (t, J = 11.6 Hz, 1H, C*Bn*H), 3.72 (t, J= 11.6, 1H, C*Bn*H), *N*-benzylidene benzylamine (major isomer), **¹H NMR** (500MHz, DMSO-d$_6$) δ: 8.51 (s, 1H, C*imine*H), 7.78 (d, *J* = 5.6 Hz, 2H, C*Ar*H), 7. 42-7.17 (m, 8H, C*Ar*H), 4.78 (s, 2H, C*Bn*H), *N*-benzylidene benzylamine (minor isomer) **¹H NMR** (500MHz, DMSO-d$_6$) δ: 8.32 (s, 1H, C*imine*H), 7.78 (d, *J* = 5.6 Hz, 2H, C*Ar*H), 7. 42-7.17 (m, 8H, C*Ar*H), 4.78 (s, 2H, C*Bn*H) and free benzylamine, **¹H NMR** (500MHz, DMSO-d$_6$) δ: 7.53-7.13 (m, 5H, C*Ar*H), 3.72 (s, 2H, C*Bn*H) 3.30 (br s, 2H, NH$_2$). Ratio of free benzylamine: catalyst bound benzylamine: *N*-benzylidene benzylamine (major): *N*-benzylidene benzylamine (minor) = 16:4:2:1. Iridium catalyst complex **A**: **¹H NMR** (500 MHz, DMSO-d$_6$) δ: 1.85 (s, 30H, C$_5$Me$_3$), iridium catalyst complex **B**: **¹H NMR** (500 MHz, DMSO-d$_6$) δ: 1.79 (s, 30H, C$_5$Me$_5$), iridium catalyst complex **C**: **¹H NMR** (500 MHz, DMSO-d$_6$) δ: 1.73 (s, 30H, C$_5$Me$_5$) and iridium catalyst complex **D**: **¹H NMR** (500 MHz, DMSO-d$_6$) δ: 1.68 (s, 30H, C$_5$Me$_5$). Ratio of 1.85 ppm complex: 1.79 ppm complex: 1.73 ppm complex: 1.68 ppm complex = 26:21:8:3.

For 3 hours at 110 °C, catalyst bound benzylamine, **¹H NMR** (500MHz, DMSO-d$_6$) δ: 7.53-7.13 (m, 5H, C*Ar*H), 5.62 (t, J = 10.5 Hz, 1H, NH), 5.54 (t, J = 10.5 Hz, 1H, NH), 4.08 (t, *J* = 11.6 Hz, 1H, C*Bn*H), 3.72 (t, *J*= 11.6 Hz, 1H, C*Bn*H), *N*-benzylidene benzylamine (major isomer), **¹H NMR** (500MHz, DMSO-d$_6$) δ: 8.51 (s, 1H, C*imine*H), 7.78 (d, *J* = 5.6 Hz, 2H, C*Ar*H), 7. 42-7.17 (m, 8H, C*Ar*H), 4.78 (s, 2H, C*Bn*H), *N*-benzylidene benzylamine (minor isomer) **¹H NMR** (500MHz, DMSO-d$_6$) δ: 8.32 (s, 1H, C*imine*H), 7.78 (d, *J* = 5.6 Hz, 2H, C*Ar*H), 7. 42-7.17 (m, 8H, C*Ar*H), 4.78 (s, 2H, C*Bn*H) and free benzylamine, **¹H NMR** (500MHz, DMSO-d$_6$) δ: 7.53-7.13 (m, 5H, C*Ar*H), 3.72 (s, 2H, C*Bn*H) 3.30 (br s, 2H, NH$_2$). Ratio of free benzylamine: catalyst bound benzylamine: *N*-benzylidene benzylamine (major): *N*-benzylidene benzylamine (minor) = 10:2:2:1. Iridium catalyst complex **A**, **¹H NMR** (500 MHz, DMSO-d$_6$) δ: 1.85 (s, 30H, C$_5$Me$_3$), iridium catalyst complex **B**, **¹H NMR** (500 MHz, DMSO-d$_6$) δ: 1.79 (s, 30H, C$_5$Me$_5$), iridium catalyst complex **C**, **¹H NMR** (500 MHz, DMSO-d$_6$) δ: 1.73 (s, 30H, C$_5$Me$_5$) and iridium catalyst complex **D**, **¹H NMR** (500 MHz, DMSO-d$_6$) δ: 1.68 (s, 30H, C$_5$Me$_5$). Ratio of 1.85 ppm complex: 1.79 ppm complex: 1.73 ppm complex: 1.68 ppm complex = 6:6:2:1.

For 4 hours at 110 °C, catalyst bound benzylamine, **¹H NMR** (500MHz, DMSO-d$_6$) δ: 7.53-7.13 (m, 5H, C*Ar*H), 5.62 (t, J = 10.5 Hz, 1H, NH), 5.54 (t, J = 10.5 Hz, 1H, NH), 4.08 (t, J = 11.6 Hz, 1H, C*Bn*H), 3.72 (t, J= 11.6, 1H, C*Bn*H), *N*-benzylidene benzylamine (major isomer), **¹H NMR** (500MHz, DMSO-d$_6$) δ: 8.51 (s, 1H, C*imine*H), 7.78 (d, *J* = 5.6 Hz, 2H, C*Ar*H), 7. 42-7.17 (m, 8H, C*Ar*H), 4.78 (s, 2H, C*Bn*H), *N*-benzylidene benzylamine (minor

isomer) **^{1}H NMR** (500MHz, DMSO-d$_6$) δ: 8.32 (s, 1H, C*imine*H), 7.78 (d, *J* = 5.6 Hz, 2H, C*Ar*H), 7. 42-7.17 (m, 8H, C*Ar*H), 4.78 (s, 2H, C*Bn*H) and free benzylamine, **^{1}H NMR** (500MHz, DMSO-d$_6$) δ: 7.53-7.13 (m, 5H, C*Ar*H), 3.72 (s, 2H, C*Bn*H) 3.30 (br s, 2H, NH$_2$). Ratio of free benzylamine: catalyst bound benzylamine: *N*-benzylidene benzylamine (major): *N*-benzylidene benzylamine (minor) = 7:2:2:1. Iridium catalyst complex **A**, **^{1}H NMR** (500 MHz, DMSO-d$_6$) δ: 1.85 (s, 30H, C$_5$Me$_3$), iridium catalyst complex **B**, **^{1}H NMR** (500 MHz, DMSO-d$_6$) δ: 1.79 (s, 30H, C$_5$Me$_5$), iridium catalyst complex **C**, **^{1}H NMR** (500 MHz, DMSO-d$_6$) δ: 1.73 (s, 30H, C$_5$Me$_5$) and iridium catalyst complex **D**, **^{1}H NMR** (500 MHz, DMSO-d$_6$) δ: 1.68 (s, 30H, C$_5$Me$_5$). Ratio of 1.85 ppm complex: 1.79 ppm complex: 1.73 ppm complex: 1.68 ppm complex = 12:14:5:2.

For 27 hours at 110 °C, *N*-benzylidene benzylamine (major isomer), **^{1}H NMR** (500MHz, DMSO-d$_6$) δ: 8.51 (s, 1H, C*imine*H), 7.78 (d, *J* = 5.6 Hz, 2H, C*Ar*H), 7. 42-7.17 (m, 8H, C*Ar*H), 4.78 (s, 2H, C*Bn*H) and *N*-benzylidene benzylamine (minor isomer) **^{1}H NMR** (500MHz, DMSO-d$_6$) δ: 8.32 (s, 1H, C*imine*H), 7.78 (d, *J* = 5.6 Hz, 2H, C*Ar*H), 7. 42-7.17 (m, 8H, C*Ar*H), 4.78 (s, 2H, C*Bn*H). Ratio of *N*-benzylidene benzylamine (major): *N*-benzylidene benzylamine (minor) = 3:1. Iridium catalyst complex **A**, **^{1}H NMR** (500 MHz, DMSO-d$_6$) δ: 1.87 (s, 30H, C$_5$Me$_3$), iridium catalyst complex **B**, **^{1}H NMR** (500 MHz, DMSO-d$_6$) δ: 1.82 (s, 30H, C$_5$Me$_5$), iridium catalyst complex **C**, **^{1}H NMR** (500 MHz, DMSO-d$_6$) δ: 1.79 (s, 30H, C$_5$Me$_5$), iridium catalyst complex **D**, **^{1}H NMR** (500 MHz, DMSO-d$_6$) δ: 1.73 (s, 30H, C$_5$Me$_5$), iridium catalyst complex **E**, **^{1}H NMR** (500 MHz, DMSO-d$_6$) δ: 1.68 (s, 30H, C$_5$Me$_5$) and iridium catalyst complex **F**, **^{1}H NMR** (500 MHz, DMSO-d$_6$) δ: 1.63 (s, 30H, C$_5$Me$_5$). Ratio of 1.87 ppm complex: 1.82 ppm complex: 1.79 ppm complex: 1.73 ppm complex: 1.68 ppm complex: 1.63 ppm complex = 6:3:2:5:3:2.

Entry 3 Synthetic procedure **7.4b** was followed. Benzylamine (11.8 μLs, 108 μmols, 20.0 equiv.), iridium complex **3.1** (6.3 mg, 5.42 μmols, 1.00 equiv.) and toluene-d$_8$ (0.8 mL) were used and the temperature of the oil bath was 120 °C. An orange precipitate formed upon heating. The reaction was monitored at 0, 0.25, 0.5, 1, 1.5, 2 and 3 hours. Benzylamine (**3.11**) and iridium complexes were observed by **^{1}H NMR** (Figure 7.14).
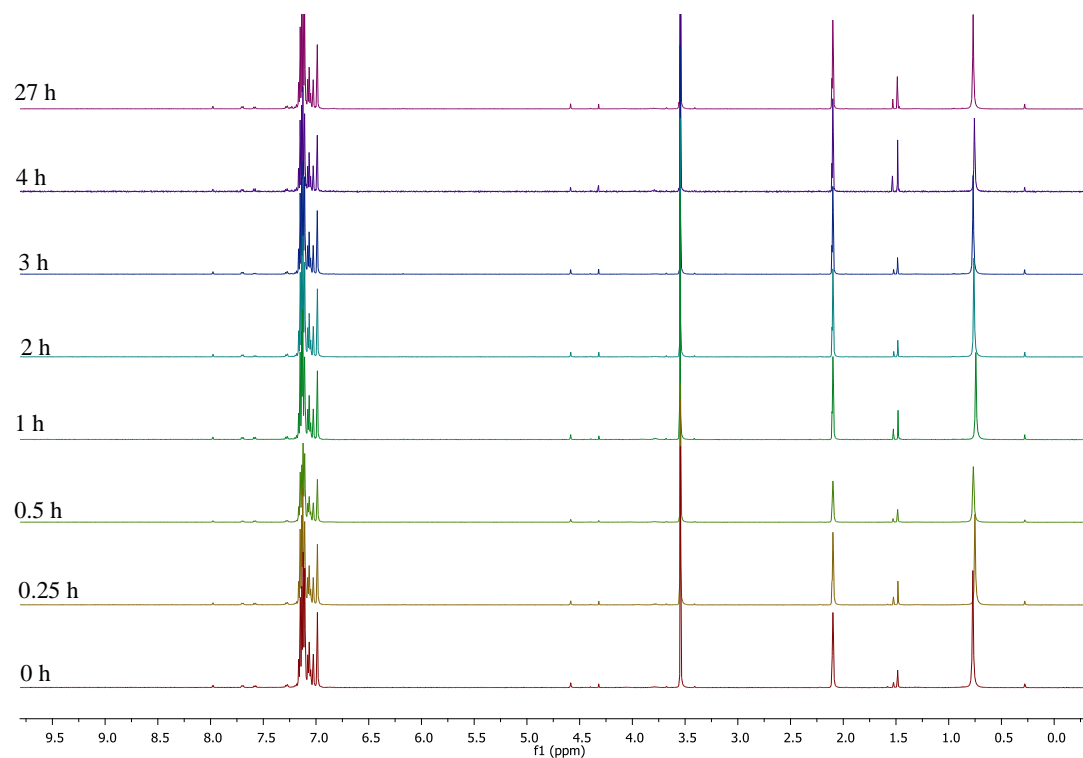
Figure 7.14 Stacked spectra for benzylamine, 3.11 and iridium catalyst 7.3.6, Entry 3.

For 0 hours, benzylamine, **¹H NMR** (500 MHz, toluene-d$_8$) δ 7.18-7.03 (m, 5H. CArH), 3.54 (s, 2H, CBnH), 0.76 (s, 2H, NH$_2$). Iridium catalyst complex **A**, **¹H NMR** (500MHz, toluene-d$_8$) δ: 1.57 (s, 30H, C$_5$Me$_5$), iridium catalyst complex **B**, **¹H NMR** (500MHz, toluene-d$_8$) δ: 1.52 (s, 30H, C$_5$Me$_5$) and iridium catalyst complex **C**, **¹H NMR** (500MHz, toluene-d$_8$) δ: 1.48 (s, 30H, C$_5$Me$_5$). Ratio of 1.57 ppm complex: 1.52 ppm complex: 1.47 ppm complex =2:7:46.

For 0.25 hours, benzylamine, **¹H NMR** (500 MHz, toluene-d$_8$) δ 7.18-7.03 (m, 5H. CArH), 3.54 (s, 2H, CBnH), 0.76 (s, 2H, NH$_2$). Iridium catalyst complex **A**, **¹H NMR** (500MHz, toluene-d$_8$) δ: 1.52 (s, 30H, C$_5$Me$_5$) and iridium catalyst complex **B**, **¹H NMR** (500MHz, toluene-d$_8$) δ: 1.47 (s, 30H, C$_5$Me$_5$). Ratio of 1.52 ppm complex: 1.47 ppm complex =1:3.

For 0.5 hours, benzylamine, **¹H NMR** (500 MHz, toluene-d$_8$) δ 7.18-7.03 (m, 5H. CArH), 3.54 (s, 2H, CBnH), 0.76 (s, 2H, NH$_2$). Iridium catalyst complex **A**, **¹H NMR** (500MHz, toluene-d$_8$) δ: 1.52 (s, 30H, C$_5$Me$_5$) and iridium catalyst complex **B**, **¹H NMR** (500MHz, toluene-d$_8$) δ: 1.47 (s, 30H, C$_5$Me$_5$). Ratio of 1.52 ppm complex: 1.47 ppm complex =2:7.

For 1 hour, benzylamine, **¹H NMR** (500 MHz, toluene-d$_8$) δ 7.18-7.03 (m, 5H. C*Ar*H), 3.54 (s, 2H, C*Bn*H), 0.76 (s, 2H, NH$_2$). Iridium catalyst complex **A**, **¹H NMR** (500MHz, toluene-d$_8$) δ: 1.52 (s, 30H, C$_5$Me$_5$) and iridium catalyst complex **B**, **¹H NMR** (500MHz, toluene-d$_8$) δ: 1.47 (s, 30H, C$_5$Me$_5$). Ratio of 1.52 ppm complex: 1.47 ppm complex =1:3.

For 1.5 hours, benzylamine, **¹H NMR** (500 MHz, toluene-d$_8$) δ 7.18-7.03 (m, 5H. C*Ar*H), 3.54 (s, 2H, C*Bn*H), 0.76 (s, 2H, NH$_2$). Iridium catalyst complex **A**, **¹H NMR** (500MHz, toluene-d$_8$) δ: 1.52 (s, 30H, C$_5$Me$_5$) and iridium catalyst complex **B**, **¹H NMR** (500MHz, toluene-d$_8$) δ: 1.47 (s, 30H, C$_5$Me$_5$). Ratio of 1.52 ppm complex: 1.47 ppm complex =1:3.

For 2 hours, benzylamine, **¹H NMR** (500 MHz, toluene-d$_8$) δ 7.18-7.03 (m, 5H. C*Ar*H), 3.54 (s, 2H, C*Bn*H), 0.76 (s, 2H, NH$_2$). Iridium catalyst complex **A**, **¹H NMR** (500MHz, toluene-d$_8$) δ: 1.52 (s, 30H, C$_5$Me$_5$) and iridium catalyst complex **B**, **¹H NMR** (500MHz, toluene-d$_8$) δ: 1.47(s, 30H, C$_5$Me$_5$). Ratio of 1.52 ppm complex: 1.47 ppm complex =2:7.

For 3 hours, benzylamine, **¹H NMR** (500 MHz, toluene-d$_8$) δ 7.18-7.03 (m, 5H. C*Ar*H), 3.54 (s, 2H, C*Bn*H), 0.76 (s, 2H, NH$_2$). Iridium catalyst complex **A**, **¹H NMR** (500MHz, toluene-d$_8$) δ: 1.52 (s, 30H, C$_5$Me$_5$) and iridium catalyst complex **B**, **¹H NMR** (500MHz, toluene-d$_8$) δ: 1.47 (s, 30H, C$_5$Me$_5$). Ratio of 1.52 ppm complex: 1.47 ppm complex =1:3.

For 4 hours, benzylamine, **¹H NMR** (500 MHz, toluene-d$_8$) δ 7.18-7.03 (m, 5H. C*Ar*H), 3.54 (s, 2H, C*Bn*H), 0.76 (s, 2H, NH$_2$). Iridium catalyst complex **A**, **¹H NMR** (500MHz, toluene-d$_8$) δ: 1.52 (s, 30H, C$_5$Me$_5$), iridium catalyst complex **B**, **¹H NMR** (500MHz, toluene-d$_8$) δ: 1.47 (s, 30H, C$_5$Me$_5$) and iridium catalyst complex **C**, **¹H NMR** (500MHz, toluene-d$_8$) δ: 1.45 (s, 30H, C$_5$Me$_5$). Ratio of 1.52 ppm complex: 1.47 ppm complex: 1.45 ppm complex =2:6:1.

Entry 4 Synthetic procedure **7.4b** was followed. Dibenzylamine (141 μLs of 0.1 M solution in DMSO-d$_6$ and 11 μLs of pure amine, 70.6 μLs, 20 equiv.), iridium complex **3.1a** (4.1 mg, 3.53 μmols, 1 equiv.) and DMSO-d$_6$ were used and the reaction was heated by an oil bath (115 °C). The reaction was monitored at 0, 0.25, 0.5, 1, 2, 3, 4.08 hours. Dibenzylamine (**3.14**) and iridium catalyst complexes were observed during ¹H NMR analysis (Figure 7.15).
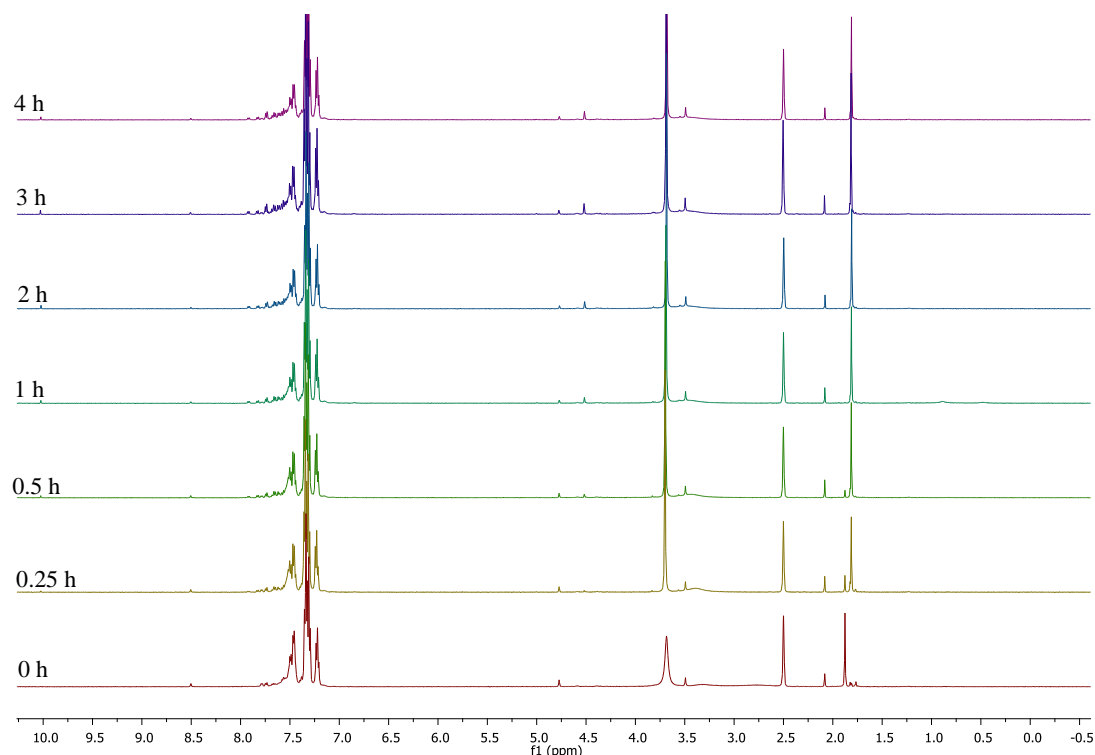
Figure 7.15 Stacked spectra for dibenzylamine, 3.14 and iridium catalyst 7.3.6,

Entry 4.

For 0.0 equiv. of amine, iridium catalyst complex, **^{1}H NMR** (500MHz, DMSO-d$_6$) δ: 1.88 (s, 30H, C$_5$Me$_5$).

For 10.0 equiv. of amine, dibenzylamine, **^{1}H NMR** (500MHz, DMSO-d$_6$) δ: 7.55-7.22 apparent m, 10H, C*Ar*H), 3.59 (s, 4H, C*Bn*H), 2.78 (s, 1H, NH). Iridium catalyst complex **A**, **^{1}H NMR** (500MHz, DMSO-d$_6$) δ: 2.08 (s, 30H, C$_5$Me$_5$) and iridium catalyst complex **B**, **^{1}H NMR** (500MHz, DMSO-d$_6$) δ: 1.88 (s, 30H, C$_5$Me$_5$). Ratio of 2.08 ppm complex: 1.88 ppm complex = 3:21.

For 0.25 hours, dibenzylamine, **^{1}H NMR** (500MHz, DMSO-d$_6$) δ: 7.55-7.22 apparent m, 10H, C*Ar*H), 3.59 (s, 4H, C*Bn*H), 3.39 (s, 1H, NH). Iridium catalyst complex **A**, **^{1}H NMR** (500MHz, DMSO-d$_6$) δ: 2.08 (s, 30H, C$_5$Me$_5$), iridium catalyst complex **B**, **^{1}H NMR** (500MHz, DMSO-d$_6$) δ: 1.88 (s, 30H, C$_5$Me$_5$) and iridium catalyst complex **C**, **^{1}H NMR** (500MHz, DMSO-d$_6$) δ: 1.81 (s, 30H, C$_5$Me$_5$). Ratio of 2.08 ppm complex: 1.88 ppm complex: 1.81 ppm complex = 1:1:6.

For 0.5 hours, dibenzylamine, **¹H NMR** (500MHz, DMSO-d$_6$) δ: 7.55-7.22 (apparent m, 10H, C*Ar*H), 3.59 (s, 4H, C*Bn*H), 3.45 (s, 1H, NH). Iridium catalyst complex **A**, **¹H NMR** (500MHz, DMSO-d$_6$) δ: 2.08 (s, 30H, C$_5$Me$_5$), iridium catalyst complex **B**, **¹H NMR** (500MHz, DMSO-d$_6$) δ: 1.88 (s, 30H, C$_5$Me$_5$) and iridium catalyst complex **C**, **¹H NMR** (500MHz, DMSO-d$_6$) δ: 1.81 (s, 30H, C$_5$Me$_5$). Ratio of 2.08 ppm complex: 1.88 ppm complex: 1.81 ppm complex = 2:1:7.

For 1 hour, dibenzylamine, **¹H NMR** (500MHz, DMSO-d$_6$) δ: 7.55-7.22 (apparent m, 10H, C*Ar*H), 3.59 (s, 4H, C*Bn*H), 3.45 (s, 1H, NH). Iridium catalyst complex **A**, **¹H NMR** (500MHz, DMSO-d$_6$) δ: 2.08 (s, 30H, C$_5$Me$_5$) and iridium catalyst complex **B**, **¹H NMR** (500MHz, DMSO-d$_6$) δ: 1.81 (s, 30H, C$_5$Me$_5$). Ratio of 2.08 ppm complex: 1.81 ppm complex = 1:8.

For 2 hours, dibenzylamine, **¹H NMR** (500MHz, DMSO-d$_6$) δ: 7.55-7.22 (apparent m, 10H, C*Ar*H), 3.59 (s, 4H, C*Bn*H), 3.49 (s, 1H, NH). Iridium catalyst complex **A**, **¹H NMR** (500MHz, DMSO-d$_6$) δ: 2.08 (s, 30H, C$_5$Me$_5$) and iridium catalyst complex **B**, **¹H NMR** (500MHz, DMSO-d$_6$) δ: 1.81 (s, 30H, C$_5$Me$_5$). Ratio of 2.08 ppm complex: 1.81 ppm complex = 1:9.

For 3 hours, dibenzylamine, **¹H NMR** (500MHz, DMSO-d$_6$) δ: 7.55-7.22 (apparent m, 10H, C*Ar*H), 3.59 (s, 4H, C*Bn*H), 3.49 (s, 1H, NH). Iridium catalyst complex **A**, **¹H NMR** (500MHz, DMSO-d$_6$) δ: 2.08 (s, 30H, C$_5$Me$_5$) and iridium catalyst complex **B**, **¹H NMR** (500MHz, DMSO-d$_6$) δ: 1.81 (s, 30H, C$_5$Me$_5$). Ratio of 2.08 ppm complex: 1.81 ppm complex = 1:10.

For 4 hours, dibenzylamine, **¹H NMR** (500MHz, DMSO-d$_6$) δ: 7.55-7.22 (apparent m, 10H, C*Ar*H), 3.59 (s, 4H, C*Bn*H), 3.49 (s, 1H, NH). Iridium catalyst complex **A**, **¹H NMR** (500MHz, DMSO-d$_6$) δ: 2.08 (s, 30H, C$_5$Me$_5$) and iridium catalyst complex **B**, **¹H NMR** (500MHz, DMSO-d$_6$) δ: 1.81 (s, 30H, C$_5$Me$_5$). Ratio of 2.08 ppm complex: 1.81 ppm complex = 1:12.

Entry 5 Synthetic procedure **7.4b** was followed. Tribenzylamine (176 μLs of 0.1 M solution in DMSO-d$_6$ and 19.9 mg of pure amine, 87.8 μmols, 1.0 equiv.), iridium complex **3.1** (5.1 mg, 4.39 μmols, 1 equiv.) were used and the reaction was heated by an oil bath (115 °C). The reaction was monitored at 0, 0.25, 0.5, 1, 2 hours. No reaction was observed *via* ¹H NMR analysis (Figure 7.16).
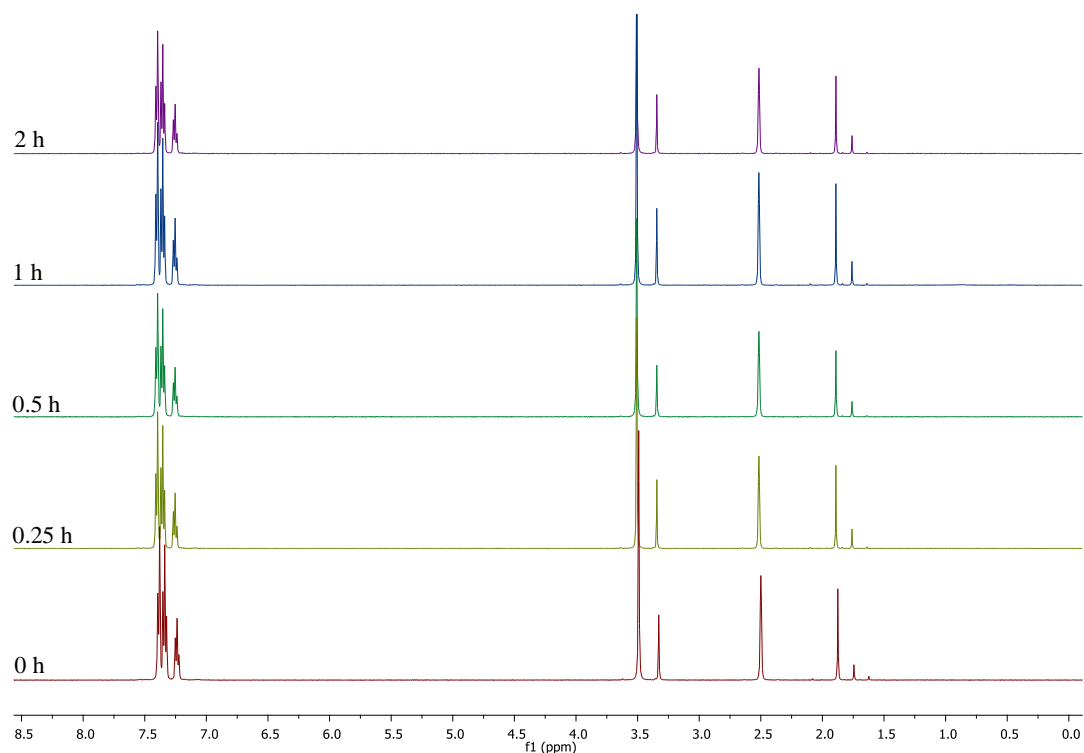
Figure 7.16 Stacked spectra for tribenzylamine, 3.15 and iridium catalyst 7.3.6,

Entry 5.

For 0.0 equiv. of amine, iridium catalyst complex, **¹H NMR** (500MHz, DMSO-d$_6$) δ: 1.88 (s, 30H, C$_5$Me$_5$).

For 10.0 equiv. of amine, tribenzylamine: **¹H NMR** (500MHz, DMSO-d$_6$) δ: 7.39 (d, J = 7.1 Hz, 6H, CArH), 7.34 (t, J = 7.2 Hz, 6H, CArH), 7.24 (t, J = 7.3 Hz, 3H, CArH), 3.50 (s, 6H, CBnH). Iridium catalyst complex **A**: **¹H NMR** (500MHz, DMSO-d$_6$) δ: 1.88 (s, 30H, C$_5$Me$_5$); iridium catalyst complex **B**: **¹H NMR** (500MHz, DMSO-d$_6$) δ: 1.75 (s, 30H, C$_5$Me$_5$) and iridium catalyst complex **C**: **¹H NMR** (500MHz, DMSO-d$_6$) δ: 1.62 (s, 30H, C$_5$Me$_5$). Ratio of 1.88 ppm complex: 1.75 ppm complex: 1.62 ppm complex = 25:4:1.

For 0.25 hours, tribenzylamine, **¹H NMR** (500MHz, DMSO-d$_6$) δ: 7.39 (d, J = 7.1 Hz, 6H, CArH), 7.34 (t, J = 7.2 Hz, 6H, CArH), 7.24 (t, J = 7.3 Hz, 3H, CArH), 3.50 (s, 6H, CBnH). Iridium catalyst complex **A**: **¹H NMR** (500MHz, DMSO-d$_6$) δ: 1.88 (s, 30H, C$_5$Me$_5$) and iridium catalyst complex **B**: **¹H NMR** (500MHz, DMSO-d$_6$) δ: 1.75 (s, 30H, C$_5$Me$_5$). Ratio of 1.88 ppm complex: 1.75 ppm complex = 4:1.

For 0.5 hours, tribenzylamine, ^{1}**H NMR** (500MHz, DMSO-d$_6$) δ: 7.39 (d, *J* = 7.1 Hz, 6H, C*Ar*H), 7.34 (t, *J* = 7.2 Hz, 6H, C*Ar*H), 7.24 (t, *J* = 7.3 Hz, 3H, C*Ar*H), 3.50 (s, 6H, C*Bn*H). Iridium catalyst complex **A**: ^{1}**H NMR** (500MHz, DMSO-d$_6$) δ: 1.88 (s, 30H, C$_5$Me$_5$) and iridium catalyst complex **B**: ^{1}**H NMR** (500MHz, DMSO-d$_6$) δ: 1.75 (s, 30H, C$_5$Me$_5$). Ratio of 1.88 ppm complex: 1.75 ppm complex = 4:1.

For 1 hour, tribenzylamine, ^{1}**H NMR** (500MHz, DMSO-d$_6$) δ: 7.39 (d, *J* = 7.1 Hz, 6H, C*Ar*H), 7.34 (t, *J* = 7.2 Hz, 6H, C*Ar*H), 7.24 (t, *J* = 7.3 Hz, 3H, C*Ar*H), 3.50 (s, 6H, C*Bn*H). Iridium catalyst complex **A**: ^{1}**H NMR** (500MHz, DMSO-d$_6$) δ: 1.88 (s, 30H, C$_5$Me$_5$) and iridium catalyst complex **B**: ^{1}**H NMR** (500MHz, DMSO-d$_6$) δ: 1.75 (s, 30H, C$_5$Me$_5$). Ratio of 1.88 ppm complex: 1.75 ppm complex = 4:1.

For 2 hours, tribenzylamine, ^{1}**H NMR** (500MHz, DMSO-d$_6$) δ: 7.39 (d, *J* = 7.1 Hz, 6H, C*Ar*H), 7.34 (t, *J* = 7.2 Hz, 6H, C*Ar*H), 7.24 (t, *J* = 7.3 Hz, 3H, C*Ar*H), 3.50 (s, 6H, C*Bn*H). Iridium catalyst complex **A**: ^{1}**H NMR** (500MHz, DMSO-d$_6$) δ: 1.88 (s, 30H, C$_5$Me$_5$) and iridium catalyst complex **B**: ^{1}**H NMR** (500MHz, DMSO-d$_6$) δ: 1.75 (s, 30H, C$_5$Me$_5$). Ratio of 1.88 ppm complex: 1.75 ppm complex = 4:1.

Entry 6 Synthetic procedure **7.4b** was followed. 4-Bromobenzylamine (21.4 mg, 115 μmols, 20 equiv.), iridium complex **3.1** (6.7 mg, 5.76 μmols, 1.00 equiv.) and toluene-d$_8$ (0.8 mL) were used and the reaction was heated by an oil bath (120 °C). The reaction was monitored at 0, 0.25, 0.5, 1, 1.5 2 and 3 hours. The formation of a yellow precipitate was observed (Figure 7.17).
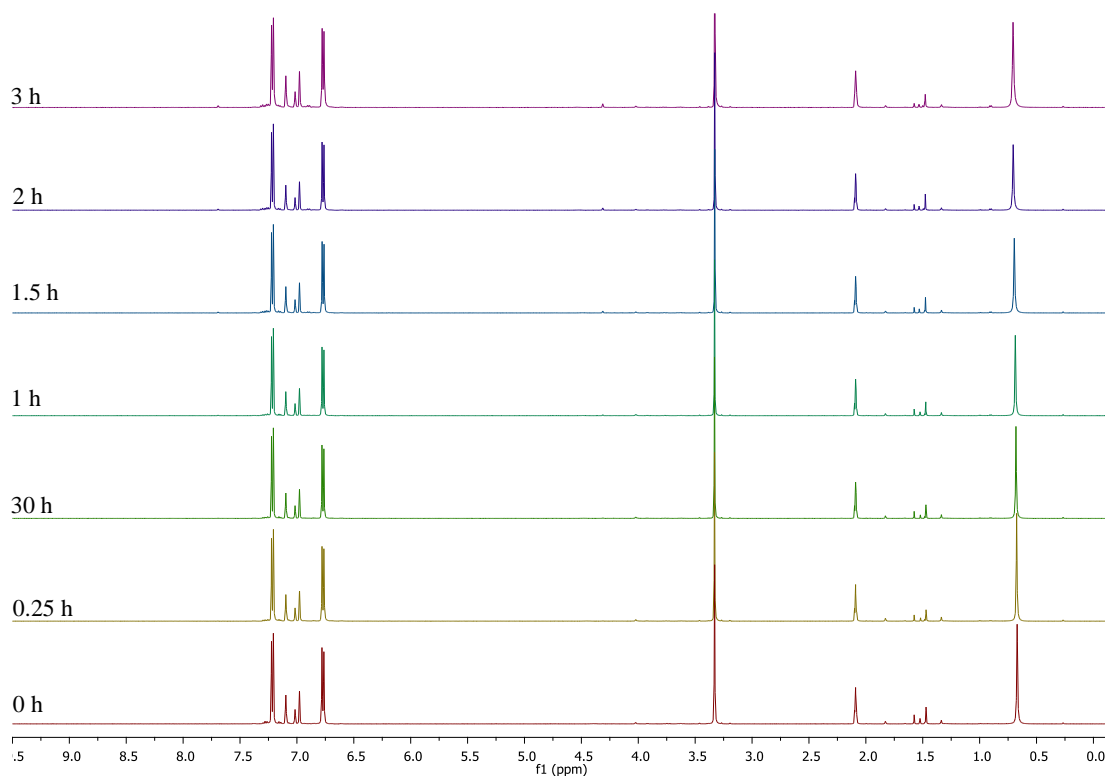
Figure 7.17 Stacked spectra for 4-bromobenzylamine, 3.7 and iridium catalyst 7.3.6, Entry 6.

For 0 hours, 4-bromobenzylamine, **¹H NMR** (500 MHz, toluene-d$_8$) δ 7.22 (d, *J* = 8.3 Hz, 2H. C*Ar*H), 6.77 (d, *J* = 8.3 Hz, 2H, C*Ar*H), 3.33 (s, 2H, C*Bn*H), 0.67 (s, 2H, NH$_2$). Iridium catalyst complex **A**: **¹H NMR** (500MHz, toluene-d$_8$) δ: 1.83 (s, 30H, C$_5$Me$_5$), Iridium catalyst complex **B**: **¹H NMR** (500MHz, toluene-d$_8$) δ: 1.58 (s, 30H, C$_5$Me$_5$), Iridium catalyst complex **C**: **¹H NMR** (500MHz, toluene-d$_8$) δ: 1.52 (s, 30H, C$_5$Me$_5$), Iridium catalyst complex **D**: **¹H NMR** (500MHz, toluene-d$_8$) δ: 1.47 (s, 30H, C$_5$Me$_5$) and iridium catalyst complex **E**: **¹H NMR** (500MHz, toluene-d$_8$) δ: 1.34 (s, 30H, C$_5$Me$_5$). Ratio of 1.83 ppm complex: 1.58 ppm complex: 1.52 ppm complex: 1.47 ppm complex: 1.34 ppm complex = 2:2:1:5:3.

For 0.25 hours, 4-bromobenzylamine, **¹H NMR** (500 MHz, toluene-d$_8$) δ 7.22 (d, *J* = 8.3 Hz, 2H. C*Ar*H), 6.77 (d, *J* = 8.3 Hz, 2H, C*Ar*H), 3.33 (s, 2H, C*Bn*H), 0.67 (s, 2H, NH$_2$). Iridium catalyst complex **A**: **¹H NMR** (500MHz, toluene-d$_8$) δ: 1.83 (s, 30H, C$_5$Me$_5$), Iridium catalyst complex **B**: **¹H NMR** (500MHz, toluene-d$_8$) δ: 1.58 (s, 30H, C$_5$Me$_5$), Iridium catalyst complex **C**: **¹H NMR** (500MHz, toluene-d$_8$) δ: 1.52 (s, 30H, C$_5$Me$_5$), Iridium catalyst complex **D**: **¹H NMR** (500MHz, toluene-d$_8$) δ: 1.47 (s, 30H, C$_5$Me$_5$) and iridium catalyst complex **E**: **¹H NMR** (500MHz, toluene-d$_8$) δ: 1.34 (s, 30H, C$_5$Me$_5$). Ratio

of 1.83 ppm complex: 1.58 ppm complex: 1.52 ppm complex: 1.47 ppm complex: 1.34 ppm complex = 2:2:1:5:3.

For 0.5 hours, 4-bromobenzylamine, **^{1}H NMR** (500 MHz, toluene-d$_8$) δ 7.22 (d, J = 8.3 Hz, 2H. C*Ar*H), 6.77 (d, J = 8.3 Hz, 2H, C*Ar*H), 3.33 (s, 2H, C*Bn*H), 0.67 (s, 2H, NH$_2$). Iridium catalyst complex **A**: **^{1}H NMR** (500MHz, toluene-d$_8$) δ: 1.83 (s, 30H, C$_5$Me$_5$), Iridium catalyst complex **B**: **^{1}H NMR** (500MHz, toluene-d$_8$) δ: 1.58 (s, 30H, C$_5$Me$_5$), Iridium catalyst complex **C**: **^{1}H NMR** (500MHz, toluene-d$_8$) δ: 1.52 (s, 30H, C$_5$Me$_5$), Iridium catalyst complex **D**: **^{1}H NMR** (500MHz, toluene-d$_8$) δ: 1.47 (s, 30H, C$_5$Me$_5$) and iridium catalyst complex **E**: **^{1}H NMR** (500MHz, toluene-d$_8$) δ: 1.34 (s, 30H, C$_5$Me$_5$). Ratio of 1.83 ppm complex: 1.58 ppm complex: 1.52 ppm complex: 1.47 ppm complex: 1.34 ppm complex = 2:1:1:5:3.

For 1 hour, 4-bromobenzylamine, **^{1}H NMR** (500 MHz, toluene-d$_8$) δ 7.22 (d, J = 8.3 Hz, 2H. C*Ar*H), 6.77 (d, J = 8.3 Hz, 2H, C*Ar*H), 3.33 (s, 2H, C*Bn*H), 0.67 (s, 2H, NH$_2$). Iridium catalyst complex **A**: **^{1}H NMR** (500MHz, toluene-d$_8$) δ: 1.83 (s, 30H, C$_5$Me$_5$), Iridium catalyst complex **B**: **^{1}H NMR** (500MHz, toluene-d$_8$) δ: 1.58 (s, 30H, C$_5$Me$_5$), Iridium catalyst complex **C**: **^{1}H NMR** (500MHz, toluene-d$_8$) δ: 1.52 (s, 30H, C$_5$Me$_5$), Iridium catalyst complex **D**: **^{1}H NMR** (500MHz, toluene-d$_8$) δ: 1.47 (s, 30H, C$_5$Me$_5$) and iridium catalyst complex **E**: **^{1}H NMR** (500MHz, toluene-d$_8$) δ: 1.34 (s, 30H, C$_5$Me$_5$). Ratio of 1.83 ppm complex: 1.58 ppm complex: 1.52 ppm complex: 1.47 ppm complex: 1.34 ppm complex = 1:1:1:5:2.

For 1.5 hours, 4-bromobenzylamine, **^{1}H NMR** (500 MHz, toluene-d$_8$) δ 7.22 (d, J = 8.3 Hz, 2H. C*Ar*H), 6.77 (d, J = 8.3 Hz, 2H, C*Ar*H), 3.33 (s, 2H, C*Bn*H), 0.67 (s, 2H, NH$_2$). Iridium catalyst complex **A**: **^{1}H NMR** (500MHz, toluene-d$_8$) δ: 1.83 (s, 30H, C$_5$Me$_5$), Iridium catalyst complex **B**: **^{1}H NMR** (500MHz, toluene-d$_8$) δ: 1.58 (s, 30H, C$_5$Me$_5$), Iridium catalyst complex **C**: **^{1}H NMR** (500MHz, toluene-d$_8$) δ: 1.53 (s, 30H, C$_5$Me$_5$), Iridium catalyst complex **D**: **^{1}H NMR** (500MHz, toluene-d$_8$) δ: 1.48 (s, 30H, C$_5$Me$_5$) and iridium catalyst complex **E**: **^{1}H NMR** (500MHz, toluene-d$_8$) δ: 1.34 (s, 30H, C$_5$Me$_5$). Ratio of 1.83 ppm complex: 1.58 ppm complex: 1.53 ppm complex: 1.48 ppm complex: 1.34 ppm complex = 1:1:1:4:2.

For 2 hours, 4-bromobenzylamine, **^{1}H NMR** (500 MHz, toluene-d$_8$) δ 7.22 (d, J = 8.3 Hz, 2H. C*Ar*H), 6.77 (d, J = 8.3 Hz, 2H, C*Ar*H), 3.33 (s, 2H, C*Bn*H), 0.67 (s, 2H, NH$_2$). Iridium catalyst complex **A**: **^{1}H NMR** (500MHz, toluene-d$_8$) δ: 1.83 (s, 30H, C$_5$Me$_5$), Iridium catalyst complex **B**: **^{1}H NMR** (500MHz, toluene-d$_8$) δ: 1.58 (s, 30H, C$_5$Me$_5$), Iridium

catalyst complex **C**: **^{1}H NMR** (500MHz, toluene-d$_8$) δ: 1.52 (s, 30H, C$_5$Me$_5$), Iridium catalyst complex **D**: **^{1}H NMR** (500MHz, toluene-d$_8$) δ: 1.47 (s, 30H, C$_5$Me$_5$) and iridium catalyst complex **E**: **^{1}H NMR** (500MHz, toluene-d$_8$) δ: 1.34 (s, 30H, C$_5$Me$_5$). Ratio of 1.83 ppm complex: 1.58 ppm complex: 1.52 ppm complex: 1.47 ppm complex: 1.34 ppm complex = 1:1:1:5:2.

For 3 hours, 4-bromobenzylamine, **^{1}H NMR** (500 MHz, toluene-d$_8$) δ 7.22 (d, *J* = 8.3 Hz, 2H. C*Ar*H), 6.77 (d, *J* = 8.3 Hz, 2H, C*Ar*H), 3.33 (s, 2H, C*Bn*H), 0.67 (s, 2H, NH$_2$). Iridium catalyst complex **A**: **^{1}H NMR** (500MHz, toluene-d$_8$) δ: 1.83 (s, 30H, C$_5$Me$_5$), Iridium catalyst complex **B**: **^{1}H NMR** (500MHz, toluene-d$_8$) δ: 1.58 (s, 30H, C$_5$Me$_5$), Iridium catalyst complex **C**: **^{1}H NMR** (500MHz, toluene-d$_8$) δ: 1.52 (s, 30H, C$_5$Me$_5$), Iridium catalyst complex **D**: **^{1}H NMR** (500MHz, toluene-d$_8$) δ: 1.50 (s, 30H, C$_5$Me$_5$), Iridium catalyst complex **E**: **^{1}H NMR** (500MHz, toluene-d$_8$) δ: 1.47 (s, 30H, C$_5$Me$_5$) and iridium catalyst complex **F**: **^{1}H NMR** (500MHz, toluene-d$_8$) δ: 1.34 (s, 30H, C$_5$Me$_5$). Ratio of 1.83 ppm complex: 1.58 ppm complex: 1.52 ppm complex: 1.50 ppm complex: 1.47 ppm complex: 1.34 ppm complex = 2:2:2:1:8:3.

Entry 7 Synthetic procedure **7.4b** was followed. 4-Methoxybenzylamine (15.0 μLs, 113 μmols, 20 equiv.), iridium complex **3.1** (6.6 mg, 5.67 μmols, 1.00 equiv.) and toluene-d$_8$ (0.8 mL) were used and the reaction was heated by an oil bath (120 °C). The reaction was monitored at 0, 0.25, 0.5, 1, 1.5, 2 and 3 hours. The formation of a yellow precipitate was observed, 4-methoxybenzylamine (**3.8**) and iridium complexes were observed by ^{1}H NMR analysis.
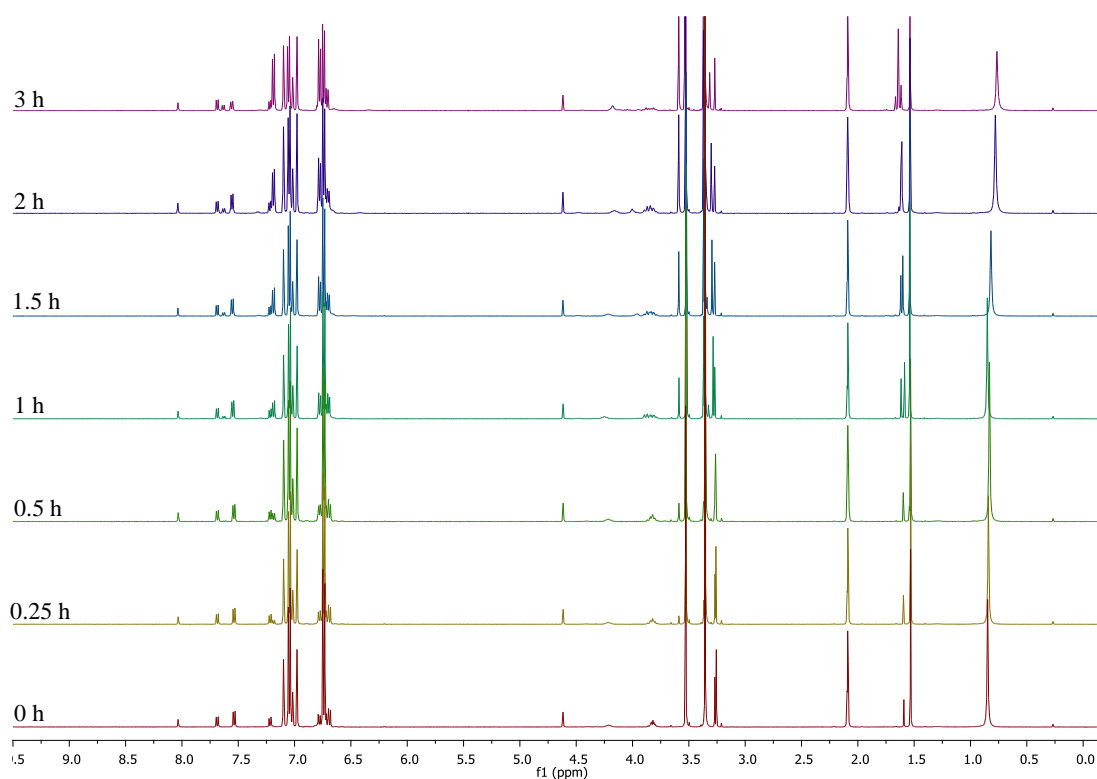
Figure 7.18 Stacked spectra for 4-methoxybenzylamine, 3.8 and iridium catalyst 7.3.6, Entry 7.

For 0 hours, 4-methoxybenzylamine, ^{1}**H NMR** (500 MHz, toluene-d$_8$) δ: 7.05 (d, J = 8.7 Hz, 2H, CArH), 6.74 (d, J = 8.6 Hz, 2H, CArH), 3.51 (s, 2H, CBnH), 3.36 (s, 3H, OCH$_3$), 0.85 (s, 2H, NH$_2$). Iridium catalyst complex **A**: ^{1}**H NMR** (500MHz, toluene-d$_8$) δ: 1.59 (s, 30H, C$_5$Me$_5$) and iridium catalyst complex **B**: ^{1}**H NMR** (500MHz, toluene-d$_6$) δ: 1.53 (s, 30H, C$_5$Me$_5$). Ratio of 1.59 ppm complex: 1.53 ppm complex = 1:7.

For 0.25 hours, 4-methoxybenzylamine, ^{1}**H NMR** (500 MHz, toluene-d$_8$) δ: 7.05 (d, J = 8.7 Hz, 2H, CArH), 6.74 (d, J = 8.6 Hz, 2H, CArH), 3.51 (s, 2H, CBnH), 3.36 (s, 3H, OCH$_3$), 0.85 (s, 2H, NH$_2$). Iridium catalyst complex **A**: ^{1}**H NMR** (500MHz, toluene-d$_8$) δ: 1.60 (s, 30H, C$_5$Me$_5$) and iridium catalyst complex **B**: ^{1}**H NMR** (500MHz, toluene-d$_8$) δ: 1.53 (s, 30H, C$_5$Me$_5$). Ratio of 1.59 ppm complex: 1.53 ppm complex = 1:7.

For 0.5 hours, 4-methoxybenzylamine, ^{1}**H NMR** (500 MHz, toluene-d$_8$) δ: 7.05 (d, J = 8.7 Hz, 2H, CArH), 6.74 (d, J = 8.6 Hz, 2H, CArH), 3.52 (s, 2H, CBnH), 3.36 (s, 3H, OCH$_3$), 0.85 (s, 2H, NH$_2$). 4-methoxybenzylamine species, ^{1}**H NMR** (500 MHz, toluene-d$_8$) δ: 7.19 (d, J = 8.7 Hz, 2H), 6.79 − 6.76 (m, 2H), 3.59 (s, 2H), 3.37 (s, 3H). Ratio of protons at 3.59 ppm: protons at 3.52 ppm = 1:17. Iridium catalyst complex **A**: ^{1}**H NMR** (500MHz,

toluene-d_8) δ: 1.60 (s, 30H, C_5Me_5) and iridium catalyst complex **B**: ^{1}**H NMR** (500MHz, toluene-d_8) δ: 1.53 (s, 30H, C_5Me_5). Ratio of 1.59 ppm complex: 1.53 ppm complex = 1:7.

For 1 hour, 4-methoxybenzylamine, ^{1}**H NMR** (500 MHz, toluene-d_8) δ: 7.05 (d, J = 8.7 Hz, 2H, C*Ar*H), 6.74 (d, J = 8.6 Hz, 2H, C*Ar*H), 3.52 (s, 2H, C*Bn*H), 3.36 (s, 3H, OCH_3), 0.85 (s, 2H, NH_2), 4-methoxybenzylamine species, ^{1}**H NMR** (500 MHz, toluene-d_8) δ: 7.19 (d, J = 8.7 Hz, 2H, C*Ar*H), 6.79-6.76 (m, 2H, C*Ar*H), 3.59 (s, 2H, C*Bn*H), 3.37 (s, 3H, OCH_3). Ratio of protons at 3.59 ppm: protons at 3.52 ppm = 1:6. Iridium catalyst complex **A**: ^{1}**H NMR** (500 MHz, toluene-d_8) δ: 1.62 (s, 30H, C_5Me_5), iridium catalyst complex **B**: ^{1}**H NMR** (500 MHz, toluene-d_8) δ: 1.59 (s, 30H, C_5Me_5) and iridium catalyst complex **C**: ^{1}**H NMR** (500 MHz, toluene-d_8) δ: 1.54 (s, 30H, C_5Me_5). Ratio of 1.62 ppm complex: 1.59 ppm complex: 1.53 ppm complex = 1:1:5.

For 1.5 hours, 4-methoxybenzylamine, ^{1}**H NMR** (500 MHz, toluene-d_8) δ: 7.05 (d, J = 8.7 Hz, 2H, C*Ar*H), 6.74 (d, J = 8.6 Hz, 2H, C*Ar*H), 3.52 (s, 2H, C*Bn*H), 3.36 (s, 3H, OCH_3), 0.85 (s, 2H, NH_2), 4-methoxybenzylamine species, ^{1}**H NMR** (500 MHz, toluene-d_8) δ: 7.19 (d, J = 8.7 Hz, 2H, C*Ar*H), 6.79-6.76 (m, 2H, C*Ar*H), 3.59 (s, 2H, C*Bn*H), 3.37 (s, 3H, OCH_3). Ratio of protons at 3.59 ppm: protons at 3.52 ppm = 1:4. Iridium catalyst complex **A**: ^{1}**H NMR** (500 MHz, toluene-d_8) δ: 1.62 (s, 30H, C_5Me_5), iridium catalyst complex **B**: ^{1}**H NMR** (500 MHz, toluene-d_8) δ: 1.60 (s, 30H, C_5Me_5) and iridium catalyst complex **C**: ^{1}**H NMR** (500 MHz, toluene-d_8) δ: 1.54 (s, 30H, C_5Me_5). Ratio of 1.62 ppm complex: 1.60 ppm complex: 1.53 ppm complex = 2:3:8.

For 2 hours, 4-methoxybenzylamine, ^{1}**H NMR** (500 MHz, toluene-d_8) δ: 7.05 (d, J = 8.7 Hz, 2H, C*Ar*H), 6.74 (d, J = 8.6 Hz, 2H, C*Ar*H), 3.53 (s, 2H, C*Bn*H), 3.36 (s, 3H, OCH_3), 0.85 (s, 2H, NH_2), 4-methoxybenzylamine species, ^{1}**H NMR** (500 MHz, toluene-d_8) δ: 7.19 (d, J = 8.7 Hz, 2H, C*Ar*H), 6.79-6.76 (m, 2H, C*Ar*H), 3.59 (s, 2H, C*Bn*H), 3.37 (s, 3H, OCH_3). Ratio of protons at 3.59 ppm: protons at 3.51 ppm = 2:5. Iridium catalyst complex **A**: ^{1}**H NMR** (500MHz, toluene-d_8) δ: 1.61 (s, 30H, C_5Me_5) and iridium catalyst complex **B**: ^{1}**H NMR** (500MHz, toluene-d_8) δ: 1.54 (s, 30H, C_5Me_5). Ratio of 1.61 ppm complex: 1.53 ppm complex = 1:1.

For 3 hours, 4-methoxybenzylamine, ^{1}**H NMR** (500 MHz, toluene-d_8) δ: 7.05 (d, J = 8.7 Hz, 2H, C*Ar*H), 6.74 (d, J = 8.6 Hz, 2H, C*Ar*H), 3.51 (s, 2H, C*Bn*H), 3.36 (s, 3H, OCH_3), 0.85 (s, 2H, NH_2), 4-methoxybenzylamine species, ^{1}**H NMR** (500 MHz, toluene-d_8) δ: 7.19 (d, J = 8.7 Hz, 2H, C*Ar*H), 6.79-6.76 (m, 2H, C*Ar*H), 3.59 (s, 2H, C*Bn*H), 3.37 (s, 3H, OCH_3). Ratio of protons at 3.59 ppm: protons at 3.51 ppm = 2:3. Iridium catalyst complex

A: ^{1}**H NMR** (500MHz, toluene-d$_8$) δ: 1.67 (s, 30H, C$_5$Me$_5$), iridium catalyst complex **B**: ^{1}**H NMR** (500MHz, toluene-d$_8$) δ: 1.64 (s, 30H, C$_5$Me$_5$), iridium catalyst complex **C**: ^{1}**H NMR** (500MHz, toluene-d$_8$) δ: 1.62 (s, 30H, C$_5$Me$_5$) and iridium catalyst complex **D**: ^{1}**H NMR** (500MHz, toluene-d$_8$) δ: 1.54 (s, 30H, C$_5$Me$_5$). Ratio of 1.67 ppm complex: 1.64 ppm complex: 1.612 ppm complex: 1.54 ppm complex = 1:5:1:5.

Entry 8 Synthetic procedure **7.4b** was followed. 4-Methylbenzylamine (14.0 µLs, 112 µmols, 20 equiv.), iridium complex **3.1** (6.5 mg, 5.59 µmols, 1.00 equiv.) and toluene-d$_8$ (0.8 mL) were used and the reaction was heated by an oil bath (120 °C). The reaction was monitored at 0, 0.25, 0.5, 1, 1.5, 2, 3 hours. The formation of an orange precipitate was observed, the reaction was filtered and the crystals washed with petrol (Figure 7.19). Recrystallisation from dichloromethane gave catalyst bound amine **3.19** (13 mg, 18.5 µmols, >99%) as orange crystals. **IR** (solid): ν = 3265, 3176, 3102, 2915, 1909, 1802, 1638 cm^{-1}.
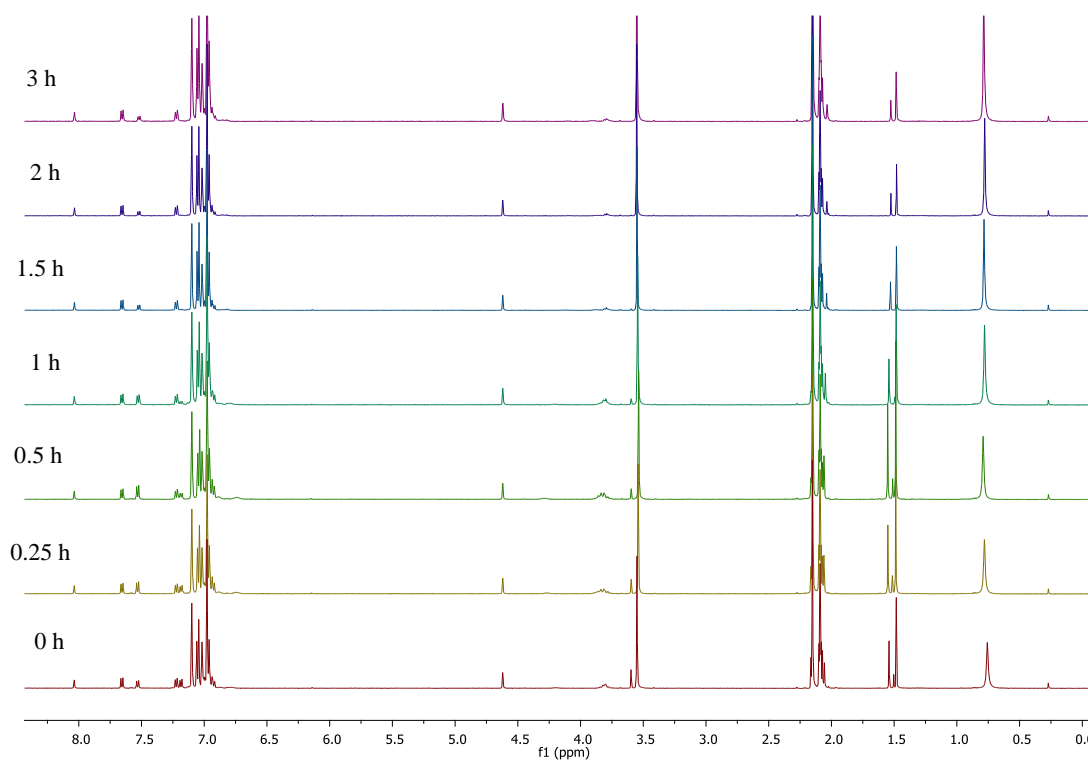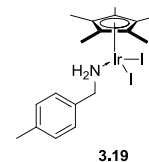
Figure 7.19 Stacked spectra for 4-methylbenzylamine, 3.27 and iridium catalyst 7.3.6, Entry 8.

For 0 hours, 4-methylbenzylamine, ^{1}**H NMR** (500 MHz, toluene-d$_8$) δ: 7.05 (d, *J* = 7.8 Hz, 2H, C*Ar*H), 6.97 (d, *J* = 8.1 Hz, 2H, C*Ar*H), 3.55 (s, 2H, C*Bn*H), 2.15 (s, 3H, CH$_3$), 0.79 (s,

2H, NH$_2$). Iridium catalyst complex **A**: ^{1}**H NMR** (500MHz, toluene-d$_8$) δ: 1.53 (s, 30H, C$_5$Me$_5$) and iridium catalyst complex **B**: ^{1}**H NMR** (500MHz, DMSO-d$_6$) δ: 1.48 (s, 30H, C$_5$Me$_5$). Ratio of 1.53 ppm complex: 1.48 ppm complex = 2:5.

For 0.25 hours, 4-methylbenzylamine, ^{1}**H NMR** (500 MHz, toluene-d$_8$) δ: 7.05 (d, *J* = 7.8 Hz, 2H, C*Ar*H), 6.97 (d, *J* = 8.1 Hz, 2H, C*Ar*H), 3.55 (s, 2H, C*Bn*H), 2.15 (s, 3H, CH$_3$), 0.79 (s, 2H, NH$_2$). Iridium catalyst complex **A**: ^{1}**H NMR** (500MHz, toluene-d$_8$) δ: 1.53 (s, 30H, C$_5$Me$_5$) and iridium catalyst complex **B**: ^{1}**H NMR** (500MHz, toluene-d$_8$) δ: 1.48 (s, 30H, C$_5$Me$_5$). Ratio of 1.53 ppm complex: 1.48 ppm complex = 2:5.

For 0.5 hours, 4-methylbenzylamine, ^{1}**H NMR** (500 MHz, toluene-d$_8$) δ: 7.05 (d, *J* = 7.8 Hz, 2H, C*Ar*H), 6.97 (d, *J* = 8.1 Hz, 2H, C*Ar*H), 3.55 (s, 2H, C*Bn*H), 2.15 (s, 3H, CH$_3$), 0.79 (s, 2H, NH$_2$). Iridium catalyst complex **A**: ^{1}**H NMR** (500MHz, toluene-d$_8$) δ: 1.53 (s, 30H, C$_5$Me$_5$) and iridium catalyst complex **B**: ^{1}**H NMR** (500MHz, toluene-d$_8$) δ: 1.48 (s, 30H, C$_5$Me$_5$). Ratio of 1.53 ppm complex: 1.48 ppm complex = 2:5.

For 1 hour, 4-methylbenzylamine, ^{1}**H NMR** (500 MHz, toluene-d$_8$) δ: 7.05 (d, *J* = 7.8 Hz, 2H, C*Ar*H), 6.97 (d, *J* = 8.1 Hz, 2H, C*Ar*H), 3.55 (s, 2H, C*Bn*H), 2.15 (s, 3H, CH$_3$), 0.79 (s, 2H, NH$_2$). Iridium catalyst complex **A**: ^{1}**H NMR** (500MHz, toluene-d$_8$) δ: 1.53 (s, 30H, C$_5$Me$_5$), iridium catalyst complex **B**: ^{1}**H NMR** (500MHz, toluene-d$_8$) δ: 1.50 (s, 30H, C$_5$Me$_5$) and iridium catalyst complex **C**: ^{1}**H NMR** (500MHz, toluene-d$_8$) δ: 1.48 (s, 30H, C$_5$Me$_5$). Ratio of 1.53 ppm complex: 1.50 ppm complex: 1.48 ppm complex = 5:1:10.

For 1.5 hours, 4-methylbenzylamine, ^{1}**H NMR** (500 MHz, toluene-d$_8$) δ: 7.05 (d, *J* = 7.8 Hz, 2H, C*Ar*H), 6.97 (d, *J* = 8.1 Hz, 2H, C*Ar*H), 3.55 (s, 2H, C*Bn*H), 2.15 (s, 3H, CH$_3$), 0.79 (s, 2H, NH$_2$). Iridium catalyst complex **A**: ^{1}**H NMR** (500MHz, toluene-d$_8$) δ: 1.55 (s, 30H, C$_5$Me$_5$), iridium catalyst complex **B**: ^{1}**H NMR** (500MHz, toluene-d$_8$) δ: 1.51 (s, 30H, C$_5$Me$_5$) and iridium catalyst complex **C**: ^{1}**H NMR** (500MHz, toluene-d$_8$) δ: 1.49 (s, 30H, C$_5$Me$_5$). Ratio of 1.53 ppm complex: 1.50 ppm complex: 1.48 ppm complex = 4:1:5.

For 2 hours, 4-methylbenzylamine, ^{1}**H NMR** (500 MHz, toluene-d$_8$) δ: 7.05 (d, *J* = 7.8 Hz, 2H, C*Ar*H), 6.97 (d, *J* = 8.1 Hz, 2H, C*Ar*H), 3.55 (s, 2H, C*Bn*H), 2.15 (s, 3H, CH$_3$), 0.79 (s, 2H, NH$_2$). Iridium catalyst complex **A**: ^{1}**H NMR** (500MHz, toluene-d$_8$) δ: 1.55 (s, 30H, C$_5$Me$_5$), iridium catalyst complex **B**: ^{1}**H NMR** (500MHz, toluene-d$_8$) δ: 1.51 (s, 30H, C$_5$Me$_5$) and iridium catalyst complex **C**: ^{1}**H NMR** (500MHz, toluene-d$_8$) δ: 1.49 (s, 30H, C$_5$Me$_5$). Ratio of 1.53 ppm complex: 1.50 ppm complex: 1.48 ppm complex = 3:1:5.

For 3 hours, 4-methylbenzylamine, ^{1}**H NMR** (500 MHz, toluene-d$_8$) δ: 7.05 (d, *J* = 7.8 Hz, 2H, C*Ar*H), 6.97 (d, *J* = 8.1 Hz, 2H, C*Ar*H), 3.55 (s, 2H, C*Bn*H), 2.15 (s, 3H, CH$_3$), 0.79 (s, 2H, NH$_2$). 4-methylbenzylamine species, ^{1}**H NMR** (500 MHz, toluene-d$_8$) δ: 7.19 (d, *J* = 7.9 Hz, 2H, C*Ar*H), 6.93 (d, *J* = 10.4 Hz, 2H, C*Ar*H), 3.60 (s, 2H, C*Bn*H), 2.16 (s, 3H, CH$_3$). Ratio of protons at 3.60: protons at 3.55 = 1:8. Iridium catalyst complex **A**: ^{1}**H NMR** (500MHz, toluene-d$_8$) δ: 1.55 (s, 30H, C$_5$Me$_5$), iridium catalyst complex **B**: ^{1}**H NMR** (500MHz, toluene-d$_8$) δ: 1.51 (s, 30H, C$_5$Me$_5$) and iridium catalyst complex **C**: ^{1}**H NMR** (500MHz, toluene-d$_8$) δ: 1.49 (s, 30H, C$_5$Me$_5$). Ratio of 1.53 ppm complex: 1.50 ppm complex: 1.48 ppm complex = 3:1:6.

Crystalallographic data of diiodopentamethylcyclopentadienyl-4-methyl-benzylamine-iridium(III) (3.19).

Orange block shaped crystals of **3.19** were grown by slow evaporation of a dichloromethane solution. An orange block crystal of approximate size 0.2 x 0.04 x 0.03 mm. θ range = 5.82 ≤ θ ≤ 52.74 °. Formula = C$_{18}$H$_{26}$I$_2$IrN; formula weight = 702.40; Crystals belong to monoclinic, *P*2$_1$/*n* space group, with one molecule in the asymmetric unit; *a* = 11.0247 (3) Å, *b* = 13.5771 (4) Å, *c* = 13.5644 (4) Å, *α* = 90.00 °, *β* = 95.194 (3) °, *γ* = 90.00 °, Volume = 2022.03 (11) Å^3, *Z* = 4, Density (calculated): 2.307 mg mm^{-3}, *μ* = 9.654 mm^{-1}, Reflections collected 19644; Independent reflections 4127 [*R*(int) = 0.0578]; *R* value = 0.0260, *wR2* = 0.0523.

Entry 9 Synthetic procedure **7.4b** was followed. 4-Chlorobenzylamine (14.0 μLs, 113 μmols, 20 equiv.), iridium complex **3.1** (6.6 mg, 5.67 μmols, 1.00 equiv.) and toluene-d$_8$ (0.8 mL) were used and the reaction was heated by an oil bath (120 °C). The reaction was monitored at 0, 0.25, 0.5, 1, 1.5, 2 and 3 hours. The formation of an orange precipitate was observed. 4-Chlorobenzylamine (**3.26**) and iridium complex were observed by ^{1}H NMR analysis (Figure 7.20).
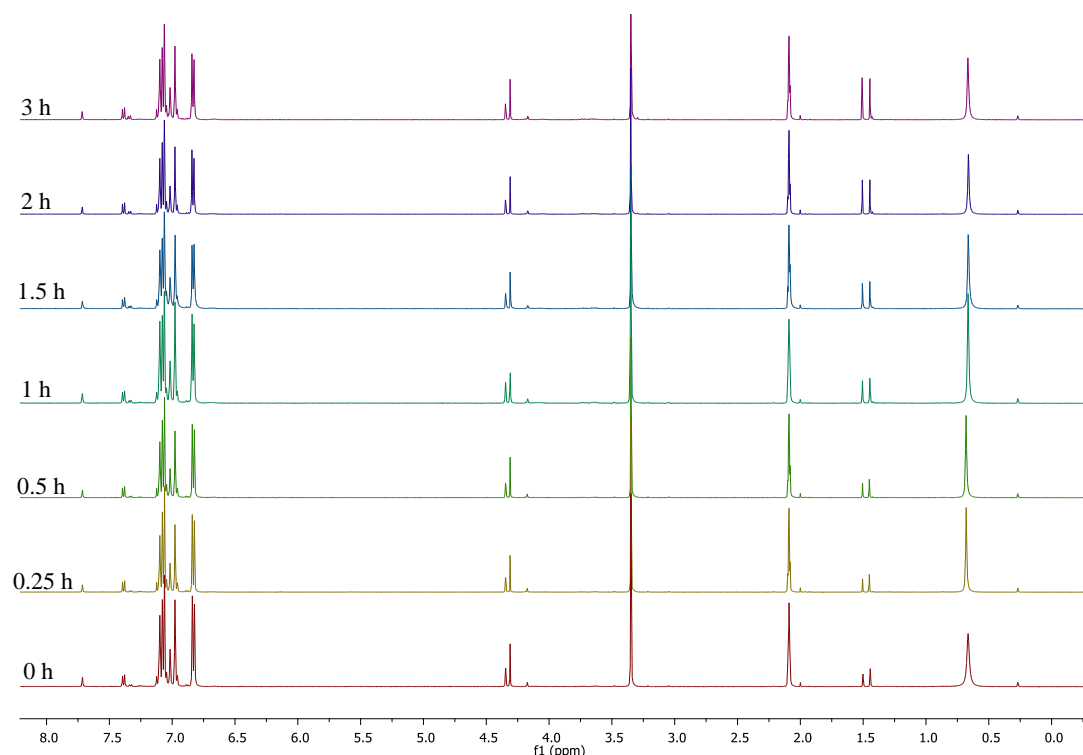
Figure 7.20 Stacked spectra for 4-chlorobenzylamine, 3.26 and iridium catalyst 7.3.6, Entry 9.

For 0 hours, 4-chlorobenzylamine, **^{1}H NMR** (500 MHz, toluene-d$_8$) δ: 7.07 (d, *J* = 8.3 Hz, 2H, C*Ar*H), 6.83 (d, *J* = 8.4 Hz, 2H, C*Ar*H), 3.35 (s, 2H, C*Bn*H), 0.66 (s, 2H, NH$_2$). Iridium catalyst complex **A**: **^{1}H NMR** (500MHz, toluene-d$_8$) δ: 1.50 (s, 30H, C$_5$Me$_5$) and iridium catalyst complex **B**: **^{1}H NMR** (500MHz, DMSO-d$_6$) δ: 1.44 (s, 30H, C$_5$Me$_5$). Ratio of 1.50 ppm complex: 1.44 ppm complex = 2:3.

For 0.25 hours, 4-chlorobenzylamine, **^{1}H NMR** (500 MHz, toluene-d$_8$) δ: 7.07 (d, *J* = 8.3 Hz, 2H, C*Ar*H), 6.83 (d, *J* = 8.4 Hz, 2H, C*Ar*H), 3.35 (s, 2H, C*Bn*H), 0.66 (s, 2H, NH$_2$). Iridium catalyst complex **A**: **^{1}H NMR** (500MHz, toluene-d$_8$) δ: 1.50 (s, 30H, C$_5$Me$_5$) and iridium catalyst complex **B**: **^{1}H NMR** (500MHz, DMSO-d$_6$) δ: 1.44 (s, 30H, C$_5$Me$_5$). Ratio of 1.50 ppm complex: 1.44 ppm complex = 2:3.

For 0.5 hours, 4-chlorobenzylamine, **^{1}H NMR** (500 MHz, toluene-d$_8$) δ: 7.07 (d, *J* = 8.3 Hz, 2H, C*Ar*H), 6.83 (d, *J* = 8.4 Hz, 2H, C*Ar*H), 3.35 (s, 2H, C*Bn*H), 0.66 (s, 2H, NH$_2$). Iridium catalyst complex **A**: **^{1}H NMR** (500MHz, toluene-d$_8$) δ: 1.50 (s, 30H, C$_5$Me$_5$) and iridium catalyst complex **B**: **^{1}H NMR** (500MHz, DMSO-d$_6$) δ: 1.44 (s, 30H, C$_5$Me$_5$). Ratio of 1.50 ppm complex: 1.44 ppm complex = 2:3.

For 1 hour, 4-chlorobenzylamine, **^{1}H NMR** (500 MHz, toluene-d$_8$) δ: 7.07 (d, *J* = 8.3 Hz, 2H, C*Ar*H), 6.83 (d, *J* = 8.4 Hz, 2H, C*Ar*H), 3.35 (s, 2H, C*Bn*H), 0.66 (s, 2H, NH$_2$). Iridium catalyst complex **A**: **^{1}H NMR** (500MHz, toluene-d$_8$) δ: 1.50 (s, 30H, C$_5$Me$_5$) and iridium catalyst complex **B**: **^{1}H NMR** (500MHz, DMSO-d$_6$) δ: 1.44 (s, 30H, C$_5$Me$_5$). Ratio of 1.50 ppm complex: 1.44 ppm complex = 1:1.

For 1.5 hours, 4-chlorobenzylamine, **^{1}H NMR** (500 MHz, toluene-d$_8$) δ: 7.07 (d, *J* = 8.3 Hz, 2H, C*Ar*H), 6.83 (d, *J* = 8.4 Hz, 2H, C*Ar*H), 3.35 (s, 2H, C*Bn*H), 0.66 (s, 2H, NH$_2$). Iridium catalyst complex **A**: **^{1}H NMR** (500MHz, toluene-d$_8$) δ: 1.50 (s, 30H, C$_5$Me$_5$) and iridium catalyst complex **B**: **^{1}H NMR** (500MHz, DMSO-d$_6$) δ: 1.44 (s, 30H, C$_5$Me$_5$). Ratio of 1.50 ppm complex: 1.44 ppm complex = 1:1.

For 2 hours, 4-chlorobenzylamine, **^{1}H NMR** (500 MHz, toluene-d$_8$) δ: 7.07 (d, *J* = 8.3 Hz, 2H, C*Ar*H), 6.83 (d, *J* = 8.4 Hz, 2H, C*Ar*H), 3.35 (s, 2H, C*Bn*H), 0.66 (s, 2H, NH$_2$). Iridium catalyst complex **A**: **^{1}H NMR** (500MHz, toluene-d$_8$) δ: 1.50 (s, 30H, C$_5$Me$_5$) and iridium catalyst complex **B**: **^{1}H NMR** (500MHz, DMSO-d$_6$) δ: 1.44 (s, 30H, C$_5$Me$_5$). Ratio of 1.50 ppm complex: 1.44 ppm complex = 1:1.

For 3 hours, 4-chlorobenzylamine, **^{1}H NMR** (500 MHz, toluene-d$_8$) δ: 7.07 (d, *J* = 8.3 Hz, 2H, C*Ar*H), 6.83 (d, *J* = 8.4 Hz, 2H, C*Ar*H), 3.35 (s, 2H, C*Bn*H), 0.66 (s, 2H, NH$_2$). Iridium catalyst complex **A**: **^{1}H NMR** (500MHz, toluene-d$_8$) δ: 1.50 (s, 30H, C$_5$Me$_5$) and iridium catalyst complex **B**: **^{1}H NMR** (500MHz, DMSO-d$_6$) δ: 1.44 (s, 30H, C$_5$Me$_5$). Ratio of 1.50 ppm complex: 1.44 ppm complex = 1:1.

7.4 Experiments discussed in Chapter 4

7.4.1 Synthesis of 3-methyl-2-iodo-aniline[195]
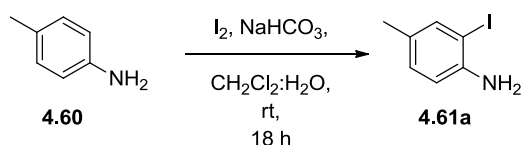
2-Iodo-4-methylaniline was synthesised following the procedure of Patel and co-workers,[195] with slight modifications. 4-Methylaniline (1.01 g, 9.44 mmols, 1.0 equiv.) was dissolved in dichloromethane (12 mL). Iodine (2.63 g, 20.9 mmols, 2.21 equiv.) and water (2 mL) were added to the solution. The resulting biphasic mixture was cooled to 0 °C and sodium

bicarbonate (8.72 g, 103 mmols, 10.9 equiv) was added. The biphasic mixture was stirred for 18 hours and then poured into dichloromethane (100 mL) and water (100 mL), the layers separated and the organics extracted with dichloromethane (2 x 100 mL). The combined organics were dried (sodium sulfate), filtered and the solvent removed *in vacuo* to give a brown oil as crude. Purification *via* column chromatography eluting with petroleum ether—ethyl acetate (SiO$_2$, gradient elution, 1:0 to 0:1) gave the title compound (1.52 g, 6.52 mmols, 69%) as a black oil. The product was used without further purification. **^{1}H NMR** (500 MHz, 298 K, CDCl$_3$): 7.52-7.42 (apparent m, 1H), 6.97 (dd, *J* = 7.8, 1.6 Hz), 6.74 (d, *J* = 8.1 Hz), 4.60 (s, 2H), 2.22 (s, 3H). LC-MS, 1.90 min (*m/z* = 234, 100%).

7.4.2 Synthesis of 3- or 4-substituted *N*-(methylsulfonyl)-2-iodo-anilines

General Procedure 7.3a

The method of Sakamoto[140] was followed with minor modifications for the synthesis of 3- or 4-substituted *N*-(methansulfonyl)-2-iodo-anilines, as described briefly below:
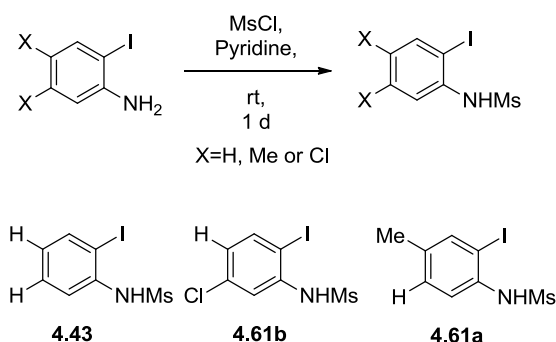
Methane sulfonyl chloride (1.5 equiv.) was added to a solution of the substituted 2-iodo-aniline (1.00 equiv.) in pyridine and stirred at room temperature for one day. The solvent was removed *in vacuo* to give a black or brown residue as crude. The crude product was dissolved in dichloromethane and washed sequentially with hydrochloric acid solution (aqueous, 1M), brine and sodium hydrogen carbonate (saturated, aqueous, 0.96M). The combined organics were dried over magnesium sulfate, filtered and the solvent removed *in vacuo* to give a brown solid as crude. Recrystalisation from the relevant solvent gave the product.

7.4.2.1 *N*-(Methylsulfonyl)-2-iodo-aniline[196]

N-(Methylsulfonyl)-2-iodo-aniline was synthesised using general procedure **7.2a** with slight modifications. Methanesulfonyl chloride (3.50 mL, 45.0 mmols), 2-iodoaniline (6.54 g, 29.7 mmols) in pyridine (40 mL) were used. The black residue was dissolved in dichloromethane (40 mL) and the organics were washed with hydrochloric acid solution (3M, aqueous, 3 x 30 mL), brine (30 mL) and saturated aqueous sodium hydrogen carbonate (30 mL). The combined organics were dried (magnesium sulfate), filtered and the solvent removed *in vacuo* to give a brown solid as crude. The solid was recrystallised from dichloromethane–*iso*-hexane to give *N*-(methylsulfonyl)-2-iodo-aniline[141, 196] (6.88 g, 23.2 mmols, 78%) as light brown rods. The product was used without further purification. **m.p.** (dichloromethane–iso-hexane) 92-95 °C (lit. 94-96 °C). **^{1}H NMR** (500 MHz, 298 K, CDCl$_3$): δ = 7.83 (dd, *J* = 8.0, 1.3 Hz, 1H, C*4*H); 7.65 (dd, *J* = 8.2, 1.5 Hz, 1H, C*1*H); 7.42-7.35 (m, 1H, C2H); 6.94 (td, *J* = 7.9, 1.5 Hz, 1H, NH); 3.19 (s, 3H, SO$_2$CH$_3$). **^{13}C NMR** (75 MHz, 298 K, CDCl$_3$): δ = 139.5 (C*4*), 137.6 (C*N*), 130.0 (C2), 127.3 (C*3*), 122.5 (C*1*), 92.1 (C*I*), 40.2 (SO$_2$CH$_3$). **ESI-MS** (ES+ mode): *m/z* = 319 [MNa$^+$, 100%]. **HRMS** (ES+ mode): *m/z* = 319.9212 [MNa$^+$, 100%]; calculated for C$_7$H$_8$INNaO$_2$S [MNa$^+$]: *m/z* = 319.9213. **IR** (solid) ν = 3275, 1583 cm^{-1}.
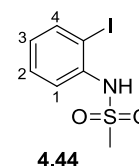
7.4.2.2 *N*-(Methylsulfonyl)-2-iodo-5-chloro-aniline

N-(Methylsulfonyl)-2-iodo-5-chloro-aniline was synthesised using the general procedure **7.2a** with slight modifications. Methansulfonyl chloride (700 μL, 9.04 mmols, 1.14 equiv.), 2-iodo-5-chloro-aniline (2.00 g, 7.91 mmols), pyridine (1 mL) and dichloromethane (15 mL) were used and stirred for one day. The crude reaction mixture was poured into dichloromethane (100 mL), the organics were washed with hydrochloric acid solution (1M, aqueous 150 mL) and then re-extracted with dichloromethane (2 x 100 mL). The combined organics were dried (magnesium sulfate), filtered and the solvent removed *in vacuo* to give a brown solid as crude. The crude product was recrystallised from *iso*-propanol to give *N*-(methylsulfonyl)-2-iodo-5-chloro-aniline (2.11 g, 6.36 mmols, 81%) as discoloured crystalline rods. The product was used without further purification. **m.p.** (*iso*propanol) 150-152 ºC. **^{1}H NMR** (500 MHz, 298 K, CDCl$_3$) δ: 7.73 (d, *J* = 8.5 Hz, 1H, C*1*H), 7.66 (d, *J* = 2.4 Hz, 1H, C*3*H), 6.94 (dd, *J* = 8.5, 2.4 Hz, 1H, C2H), 6.65 (br s, 1H, NH), 3.05 (s, 3H, *SO*$_2$CH$_3$). **^{13}C NMR** (75 MHz, 298 K, CDCl$_3$): δ = 140.0 (C2), 138.8 (C*1*), 136.1 (C*3*), 127.2 (C*4*) 121.6 (C5), 94.9 (C6), 40.4 (*SO*$_2$C). **ESI-MS** (ES- mode): *m/z* = 330 [M-H$^-$, 100%]. **HRMS** (ES+
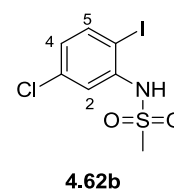
mode): $m/z = 353.8826$ [MNa$^+$, 100%]; calculated for C$_7$H$_7$ClINNaO$_2$S [MNa$^+$]: $m/z = 353.8828$. **IR** (solid) $\nu = 3286, 2806, 2593, 1574$ cm^{-1}.

7.4.2.3 *N*-(Methylsulfonyl)-2-iodo-4-methyl-aniline

N-(Methylsulfonyl)-2-iodo-4-methyl-aniline was synthesised using the general procedure **7.2a** with slight modifications. Methanesulfonyl chloride (7 mL, 90.4 mmols) added over 20 mins, crude 2-iodo-4-methyl-aniline (22.3 g, 95.8 mmols), pyridine (11.5 mL) and dichloromethane (200 mL) were used and were stirred for two hours. The resulting black viscous oil was dissolved in dichloromethane (1.00 L) and the organics were washed with hydrochloric acid solution (2M, aqueous 500 mL), sodium hydrogen carbonate (saturated aqueous, 500 mL). The combined organics were dried (magnesium sulfate), filtered and the solvent removed *in vacuo* to give a brown solid as crude. The solid was recrystallised from isopropanol to give *N*-(methylsulfonyl)-2-iodo-4-methyl-aniline (18.2 g, 58.5 mmols, 61%) as light brown crystalline rods. The product was used without further purification. **m.p.** (isopropanol) 105-108 ℃. **^{1}H NMR** (500 MHz, 298 K, CDCl$_3$) δ: 7.65 (s, 1H, C2H), 7.49 (d, *J* = 8.2 Hz, 1H, C5H), 7.17 (d, *J* = 8.2 Hz, 1H, C3H), 6.62 (s, 1H, NH*SO$_2$*), 2.98 (s, 3H, CH$_3$*SO$_2$*), 2.30 (s, 3H, CH$_3$*C4*). **^{13}C NMR** (75 MHz, 298 K, CDCl$_3$): δ = 140.4 (*C4*), 139.7, (*C1*), 139.5 (*C2*), 130.5 (*C3*), 122.8 (*C5*), 92.7 (*C6*), 39.7 (*SO$_2$CH$_3$*), 20.0 (CH$_3$*C4*). **ESI-MS** (ES+ mode): $m/z = 334$ [MNa$^+$, 100%]. **HRMS** (ES+ mode): $m/z = 333.9380$ [MNa$^+$, 100%]; calculated for C$_8$H$_{10}$INNaO$_2$S [MNa$^+$]: $m/z = 333.9375$. **IR** (solid): $\nu = 3252, 3026, 2934, 1484$ cm^{-1}.
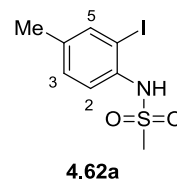
7.4.3 The synthesis of substituted (*N*-mesyl-(*1H*-indol-2-yl)) ethanols

General Procedure 7.3b

The Sakamoto[140] method was followed with minor modifications for the synthesis of 4-, 5- or non-substituted-(1H-indol-2-yl) ethanols, as described briefly below:
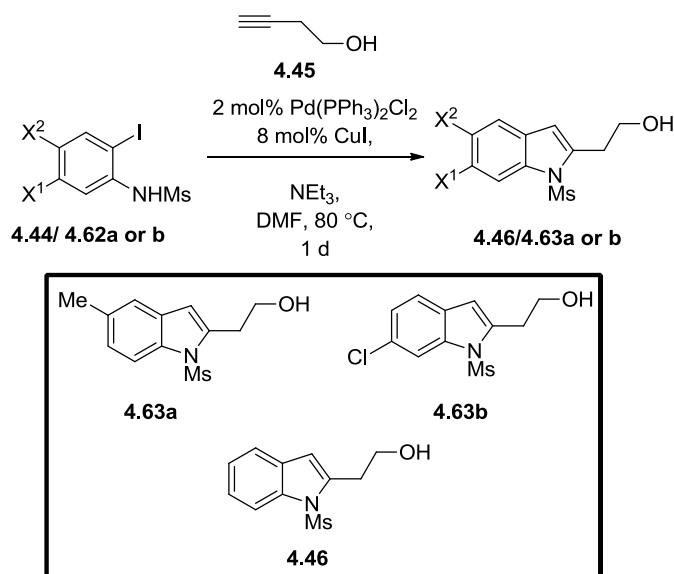
3-Butyn-1-ol (1.-1.83 equiv.) was added to a suspension of *N*-(methanesulfonyl)-2-iodo-aniline (1 equiv.), *bis*-(triphenylphosphine)palladium(II) chloride (2 mol%) and copper(I) iodide (2 mol%) in triethyl amine and *N,N*-dimethyl formamide which was heated to 80 °C for 1 day. The resulting dark brown solution was poured into water and the organics extracted with ethyl acetate or *tert*-butylmethyl ether. The combined organics were dried (magnesium sulphate), filtered and the solvent removed *in vacuo* to give a dark brown oil which was purified *via* column chromatography and recrystallised to give the product.

7.4.3.1 2-(1-(Methansulfonyl)-1*H*-(indol-2-yl)-ethanol[140]

2-(1-(Methansulfonyl)-1*H*-(indol-2-yl)-ethanol was synthesised using general procedure **7.3b** with slight modifications. 3-Butyn-1-ol (4.00 mL, 61.6 mmols, 1.83 equiv.) was added to a stirring suspension of *N*-mesyl-2-iodo-aniline (10.0 g, 33.7 mmols, 1.0 equiv.), bis (triphenylphosphine) palladium(II) chloride (500 mg, 701 µmols, 2 mol%) and copper(I) iodide (500 mg, 2.63 mmols, 7.8 mol%) in triethylamine (7 mL) and *N,N*-dimethyl formamide (13 mL), which was heated to 80 °C for one day. The resulting suspension became dark brown with time. The reaction was poured into water (250 mL) and the organics extracted with *tert*-butyl methyl ether (3 x 200 mL). The combined organics were dried (magnesium sulfate), filtered and the solvent removed *in vacuo*; purification *via* column chromatography [SiO$_2$, dichloromethane–methanol; gradient elution 1:0 to 0:1] gave 2-(1-(methylsulfonyl)-1*H*-indol-2-yl) ethanol **4.46** (8.49 g, 35.5 mmols, >99%) as a colourless crystals, which was used without further purification. **m.p.** (ethyl acetate-hexane): 80-81°C (lit. 80-81 °C). **^{1}H NMR** (500 MHz, 298 K, CDCl$_3$):
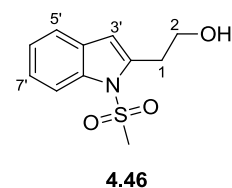
δ = 7.98 (d, *J* = 5.9, 1H, C*5′*H), 7.50 (d, *J* = 7.1, 1H, C*8′*H), 7.29 (t, *J* = 7.1, 1H, C*7′*H), 7.26 (t, *J* = 6.8, 1H, C*6′*H), 6.58 (s, 1H, C*3′*H), 4.00 (t, *J* = 6.1 Hz, 2H, C*1*H$_2$), 3.26 (t, *J* = 6.2, 2H, C2H$_2$), 3.04 (s, 3H, *SO$_2$*CH$_3$), 1.71 (s, 1H, OH). ^{13}**C NMR** (75 MHz, CDCl$_3$): δ = 138.5 (C*9′*), 137.0 (C*4′*), 129.8 (C*2′*), 124.5 (C*7′*), 124.0 (C*6′*), 120.7 (C*8′*), 114.3 (C*5′*), 110.5 (C*3′*), 61.9 (C*1*), 40.6 (*SO$_2$*CH$_3$), 32.2 (C2). **ESI-MS** (ES+ mode): *m/z* = 240 [MH$^+$, 100%]. **HRMS** (ES+ mode): *m/z* = 240.0681 [MH$^+$, 100%]; calculated for C$_{11}$H$_{14}$NO$_3$S [MH$^+$]: *m/z* = 240.0689.[197] **IR** (solid): ν = 3600-3000, 3010, 2933, 2884, 1592, 1567, 1474, 1451, 1354, 1305, 1246, 1217 cm^{-1}.

7.4.3.2 2-(5-Methane(1-(methanesulfonyl)-1*H*-(indol-2-yl)-ethanol
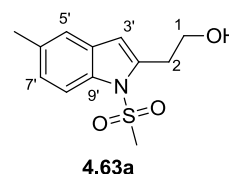
2-(5-Methane(1-(methanesulfonyl)-1*H*-(indol-2-yl)-ethanol   was synthesised using general procedure **7.3b** with slight modifications. 3-butyn-1-ol (5.44 mL, 71.9 mmols, 1.5 equiv.) was added in 250 μL portions over 70 min. *N*-Mesyl-2-iodo-4-methyl-laniline (15 g,

4.63a

48.0 mmols, 1.0 equiv.), bis (triphenylphosphine) palladium(II) chloride (240 mg, 342 μmols, 1 mol%), copper(I) iodide (264 mg, 1.39 mmols, 3 mol%), *N, N*-dimethylformamide (92 mL) and triethylamine (92 mL) were used and stirred at 80 °C. The resulting brown solution was cooled after four hours and stirred for 18 hours. The reaction was poured into water (200 mL) and the aqueous extracted with ethyl acetate (2 x 200 mL and 1 x 150 mL). The reaction was dried (magnesium sulphate), filtered and the solvent removed *in vacuo* to give the product as a brown viscuous oil, which was purified by column chromatography (0:1→1:0; Methanol–dichloromethane). Recrystalisation from ethyl acetate–petroleum ether gave the product as light brown crystalline rods (3.52 g, 13.9 mmol, 29%). **m.p.** (ethyl acetate-petroleum ether) 85-87 °C. ^{1}**H NMR** (500 MHz, 298 K, CDCl$_3$): δ 7.88 (d, *J* = 8.5 Hz, 1H, C*8′*H), 7.32 (s, 1H, C*5′* H), 7.14 (d, *J* = 8.4 Hz 1H, C*7′* H), 6.53 (s, 1H, C*3′*H), 4.00 (t, *J* = 6.1 Hz, 2H, C2H$_2$), 3.25 (t, *J* = 6.2 Hz, 2H, C*1*H$_2$), 3.02 (s, 3H, CH$_3$*SO$_2$*), 2.45(s, 3H, CH$_3$C*6′*), 1.95 (s, 1H, OH). ^{13}**C NMR** (75 MHz, 298 K, CDCl$_3$): 138.8 (C*2′*), 136.8 (C*9′*), 128.9 (C*6′*), 126.9 (C*4′*), 124.9 (C*7′*) δ 120.4 (C*5′*), 113.8 (C*8′*) 110.2 (C*3′*), 62.0 (C2), 40.0 (*SO$_2$*CH$_3$), 32.0, (C*1*), 21.0 (CH$_3$C*6′*). **ESI-MS** (ES+ mode): *m/z* = 276 [MNa$^+$, 100%] **HRMS** (ES+ mode): *m/z* = 254.0723 [MH$^+$, 100%]; calculated for C$_{12}$H$_{16}$NO$_3$S [MNa$^+$]: *m/z* = 254.0851. **IR** (solid): ν = 3373, 3009, 2929, 1588 cm^{-1}.

7.4.3.3 2-(4-Chloro-(1-(methanesulfonyl)-1*H*-(indol-2-yl)-ethanol

2-(4-Chloro-(1-(methanesulfonyl)-1*H*-(indol-2-yl)-ethanol was synthesised using general procedure **7.3b** with slight modifications. 3-Butyn-1-ol (600 μL, 61.6 mmols, 1.83 equiv.), 5-chloro-*N*-mesyl-2-iodo-aniline (1.75 g, 5.28 mmols, 1.0 equiv.), bis (triphenylphosphine) palladium (II) chloride (100 mg, 701 μmols, 2 mol%) and copper (I) iodide (106 mg, mmols, mol%) in triethylamine (2 mL) and *N*,*N*-dimethyl formamide (2 mL), which was heated to 80 °C for one day. The resulting suspension became dark brown with time. The reaction was poured into water (100 mL) and the organics extracted with ethyl acetate (2 x 100 mL) then diethyl ether (100 mL). The combined organics were dried (magnesium sulfate), filtered and the solvent removed *in vacuo*; purification *via* column chromatography [SiO$_2$, petroleum ether-ethyl acetate; gradient elution 1:0 to 0:1; then methanol] gave 2-(4-chloro-(1-(methanesulfonyl)-1*H*-(indol-2-yl)-ethanol **4.63b** (729.6 mg, 2.67 mmols, 51%) as colourless crystalline rods, which was used without further purification. **m.p.** (ethyl acetate-petroleum ether): 108-110 °C. **^{1}H NMR** (500 MHz, 298 K, CDCl$_3$): δ 8.01 (s, 1H, C*8'* H), 7.41 (d, *J* = 8.3 Hz, 1H, C*5'* H), 7.24 (dd, *J* = 8.3, 1.8 Hz, 1H, C*6'* H), 6.54 (s, 1H, C*3'* H), 3.97 (t, *J* = 6.1 Hz, 2H, C2H), 3.22 (t, *J* = 6.2 Hz, 2H, C*1*H), 3.06 (s, 3H, *SO$_2$*CH$_3$), 2.03 (s, 1H, OH). **^{13}C NMR** (75 MHz, CDCl$_3$) δ 139.1(C*2'*), 137.1 (C*9'*), 130.4 (C*Cl*), 128.8 (C*5'*), 124.5 (C*6'*), 121.2 (C*5'*), 114.5 (C*8'*), 109.8 (C*3'*), 61.8 (C2), 40.9 (C*SO$_2$*), 32.02 (C*1*). **ESI-MS** (ES+ mode): *m/z* = 274 [MH$^+$, 100%] **HRMS** (ES+ mode): *m/z* = 274.0310 [MH$^+$, 100%]; calculated for C$_{11}$H$_{13}$ClNO$_3$S [MH$^+$]: *m/z* = 274.0305. **IR** (solid) ν = 3364, 2967, 1586 cm^{-1}.
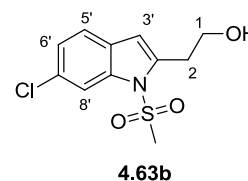
7.4.3.4 The synthesis of (1*H*-indol-2-yl) ethanol[198]
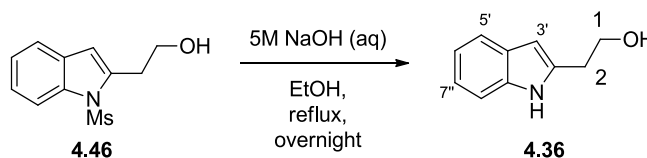
Crude 2-(1-(methylsulfonyl)-1H-indol-2-yl) ethanol **4.46** (8.49 g, 35.5 mmols, 1.0 equiv.) was dissolved in 5N aqueous sodium hydroxide (30 mL) and ethanol (65 mL) and heated to reflux for one day to give a light brown solution. The reaction was poured into dichloromethane (100 mL) and the organics extracted. The aqueous layer was acidified with 1M aqueous hydrochloric acid (200 mL) and neutralised to pH 7 with sodium hydrogen carbonate (saturated aqueous) and the organics were extracted with dichloromethane

(3 x 100 mL). The combined organics were dried (magnesium sulfate), filtered and concentrated in vacuo to give a thick viscous dark red oil, purification via column chromatography [dichloromethane–methanol] gave (*1H*-indol-2-yl) ethanol **4.36** (4.82 g, 29.9 mmols, 88% [from *N*-mesyl-2-iodoaniline, **4.46**]) as a dark red amorphous solid. **^{1}H NMR** (500 MHz, 298 K, CDCl$_3$): δ = 8.36 (1H, s, NH), 7.53 (1H, d, J = 7.9 Hz, C*5'* H), 7.25 (d, J = 7.9 Hz, 1H, C*8'* H), 7.12 (t, J = 7.5 Hz, 1H,C*7'* H), 7.07 (t, J = 7.5 Hz, 1H,C*6'*H) 6.24 (1H, s, C*3'* H), 3.81 (2H, t, J = 5.9 Hz, C*1*H), 2.86 (2H, t, J = 5.9 Hz, C2H), 2.19 (1H, br, s, OH). **^{13}C NMR** (75 MHz, 298 K, CDCl$_3$): δ = 137.1 (C*2'*), 136.2 (C*9'*), 128.6 (C*4'*), 121.3 (C*7'*), 119.9 (C*6'*), 119.7 (C*5'*), 110.7 (C*8'*), 100.2 (C*3'*), 62.2 (C*1*), 31.2 (C*2*). **ESI-MS** (ES− + mode): m/z = 160 [M−H, 100%]. **HRMS** (ES-): *m/z* = 160.0763 [M-H, 100%] calculated for C$_{10}$H$_{10}$NO [M-H]: *m/z* = 160.076788. **IR** (solid): ν = 3373 cm^{-1}.

7.4.4 The synthesis of substituted (*1H*-indol-2-yl) ethanamines

General Procedure 7.3c

The method of Marsden[95] was followed with minor modifications for the synthesis of 4-, 5- or non-substituted-(*N*-methanesulfonyl-(*1H*-indol-2-yl)) ethanamines, as described briefly below:

224
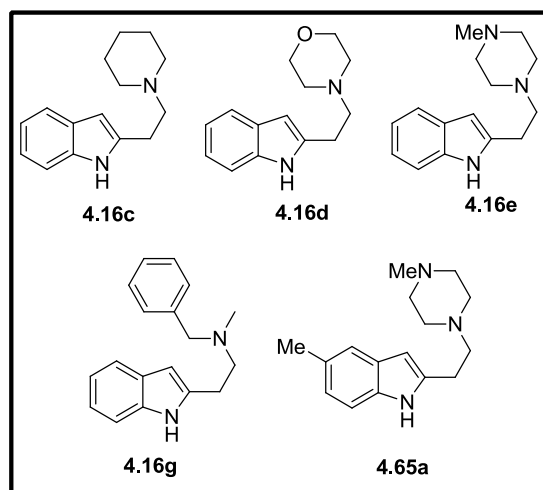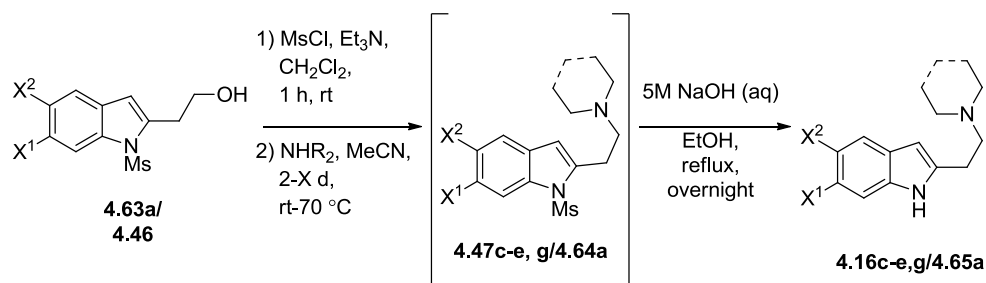
Methanesulfonyl chloride (1.2 equiv) was added dropwise to a solution of indole **4.63** or **4.46** (1.0 equiv) and triethylamine (1.5 equiv) in dichloromethane (15 mL) at room temperature and the resulting pale yellow solution stirred at room temperature for 1 hour. The reaction mixture was washed with hydrochloric acid (1M, aqueous, 20 mL) followed by sodium hydrogen carbonate (saturated aqueous; 20 mL), the layers separated and the organic layer dried (sodium sulfate), filtered and concentrated *in vacuo* to give the crude dimesylate as a pale yellow oil which was used with no further purification. The secondary amine (4.0 equiv) was added dropwise to the crude mesylate in acetonitrile (10 mL) at room temperature and the resulting pale yellow solution stirred at room temperature for 48 hours. The reaction mixture was quenched with sodium hydrogen carbonate (saturated aqueous; 20 mL), dichloromethane (20 mL) added, the layers separated and the aqueous layer extracted with dichloromethane (3 × 20 mL). The combined organic layers were dried (sodium sulfate), filtered and concentrated *in vacuo* to give the crude *N*-mesylate indole that was purified by column chromatography/recrystalisation using the solvents specified.

A solution of the *N*-mesylate indole (2.00 mmol, 1.0 equiv) in sodium hydroxide (5M, aqueous, 2 mL) and ethanol (5 mL) was heated under reflux for 18 hours. The reaction mixture was allowed to cool to room temperature and extracted with dichloromethane (3 × 20 mL). The combined organic layers were dried, filtered and the solvents removed *in vacuo* to give the crude indole that was purified by column chromatography and, or recrystallisation using the solvents specified.

7.4.4.1 2-(2-(Piperidin-1-yl)ethyl)-1*H*-indole

General Procedure **7.3c** was followed. Indole **4.46** (2.00 g, 8.36 mmols), methanesulfonyl chloride (780 μL, 10.0 mmol), triethylamine (1.74 mL, 12.5 mmol, 1.5 equiv), dichloromethane (50 mL) were used. The crude dimesylate was obtained after work up as a yellow oil which was used without further purification.
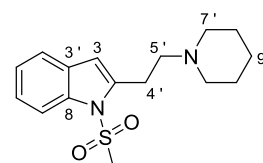
4.16c

Piperidine (3.3 mL, 33.4 mmol) and acetonitrile (30 mL) were stirred with the crude dimesylate for two days during the *N*-alkylation. The reaction was poured into sodium hydrogen carbonate solution (saturated aqueous, 50 mL) and dichloromethane (50 mL) was added, the organics were then extracted with dichloromethane (3 x 50 mL). The combined organics were dried (sodium sulphate), filtered and the solvent removed *in vacuo* to give the crude as a light brown oil. Purification by column chromatography (SiO$_2$, petroleum ether-ethyl acetate; 10:1 then→0:1) gave product **4.47c** (2.36 g, 7.71 mmol, 92%) which was used

without recrystallisation. **m.p.** (ethyl acetate-hexane) 105-107 °C. **¹H NMR** (500 MHz, CDCl₃): δ = 7.99 (1H, d, *J* = 7.8 Hz, C*4*H), 7.49 (1H, dd, *J* = 6.5, 2.1, C*7*H), 7.28 (1H, dt, *J* = 7.3, 1.7, C*6*H), 7.25 (1H, dt, *J* = 7.3, 1.7, C*5*H), 6.50 (1H, s, C*3*H), 3.18 (2H, t, *J* = 7.7, C*5′* H₂), 3.02 (3H, s, *SO₂*CH₃), 2.75 (2H, t, *J* = 7.7, C*7′* H₂), 2.55–2.43 (4H, m, C*8′* H₂), 1.61 (4H, apparent quint, *J* = 5.6 C*4′* H₂), 1.49–1.41 (2H, m, C*9′* H₂). **¹³C NMR** (75 MHz, CDCl₃): δ = 140.5 (C*8*), 136.7 (C*3′*), 129.8 (C2), 124.1 (C*6*), 123.8 (C*5*), 120.4 (C*7*), 114.2 (C*4*), 109.1 (C*3*), 58.7 (C*4′*), 54.6 (2C, C*7′*), 40.5 (*SO₂*CH₃), 26.5 (C*5′*), 26.1 (2C, C*8′*), 24.5 (C*9′*). **ESI-MS** (ES+ mode): *m/z* = 307 [MH⁺, 100%]. **HRMS** (ES+ mode): *m/z* = 307.1476 [MH⁺, 100%]; calculated for $C_{16}H_{23}N_2O_2S$ [MH⁺]: *m/z* = 307.1475. **IR** (solid): ν = 2925, 1591, 1566, 1453, 1400, 1359, 1271, 1223, 1158 cm⁻¹.

N-mesyl indole **4.47c**, sodium hydroxide (5M, aqueous, 2 mL) and ethanol (10 mL) were used and stirred under reflux for 18 hours. The reaction was poured into water (50 mL) and the organics extracted with dichloromethane (3 x 50 mL). The combined

4.16c

organics were dried (magnesium sulfate), filtered and the solvent removed *in vacuo* to afford the crude product. Purification by column chromatography (petroleum ether-ethyl acetate; 10:1 then→0:1) afforded the desired compound as a colourless solid (1.50g, 6.55 mmol 89%). **m.p**. (ethyl acetate-petroleum ether) 74-76 °C. **¹H NMR** (500 MHz, CDCl₃): δ = 9.49 (1H, s, NH), 7.52 (1H, d, *J* = 7.7, C*4*H), 7.32 (1H, d, *J* = 8.0, C*7*H), 7.11 (1H, td, *J* = 8.0, 0.7, C*6*H), 7.05 (1H, td, *J* = 8.0, 0.7, C*5*H), 6.22 (1H, s, C*3*H), 3.81 (4H, t, *J* = 4.5, C*8′* H₂), 2.94 (2H, t, *J* = 6.3, C*5′* H₂), 2.72 (2H, t, *J* = 6.3, C*4′* H₂), 2.58 (4H, broad s, C*7′* H₂). **¹³C NMR** (75 MHz, CDCl₃): δ = 139.1 (C*8*), 135.9 (C*3′*), 128.5 (C2), 121.0 (C*6*), 119.9 (C*4*), 119.6 (C*5*), 110.7 (C*7*), 99.5 (C*3*), 67.3 (2C, C*8′*), 58.2 (C*4′*), 53.7 (2C, C*7′*), 24.2 (C*5′*). **ESI-MS** (ES+ mode): *m/z* = 231 [MH⁺, 100%]. **HRMS** (ES+ mode): *m/z* = 231.1493 [MH⁺, 100%]; calculated for $C_{14}H_{19}N_2O$ [MH⁺]: *m/z* = 231.1492. **IR** (solid): ν = 3600–2400, 2920, 2222, 1901, 1869, 1840, 1793, 1653, 1621, 1579, 1505 cm⁻¹.

7.4.4.2 4-(2-(1*H*-Indol-2-yl)ethyl)morpholine

General Procedure **7.3c** was followed. Indole **4.46** (1.56 g, 4.85 mmols), methanesulfonyl chloride (450 µL, 5.82 mmol), triethylamine (1.01 mL, 7.28 mmol, 1.5 equiv), dichloromethane (15 mL) were used.. The crude dimesylate was obtained after work up as a yellow oil which was used without further purification.

4.47d

Morpholine (2.92 mL, 33.5 mmol) and acetonitrile (20 mL) were stirred with the crude dimesylate for two days during the *N*-alkylation. The reaction was poured into sodium

hydrogen carbonate (saturated aqueous, 50 mL) and dichloromethane (50 mL) was added, the organics were then extracted with dichloromethane (3 x 50 mL). The combined organics were dried (sodium sulphate), filtered and the solvent removed *in vacuo* to a yellow/orange solid. Purification by column chromatography [SiO_2, dichloromethane-ethylacetate (10:1)→(0:1)] gave **4.47d** (2.25 g, 7.29 mmol, 87%) a discoloured solid. **m.p.** (ethyl acetate/hexane) 101-104 °C. **^{1}H NMR** (500 MHz, CDCl$_3$): δ = 7.99 (1H, d, *J* = 7.9, C*4*H), 7.51–7.48 (1H, m, C*7*H), 7.25–7.30 (2H, m, C*5*H/C*6*H), 6.53 (1H, s, C*3*H), 3.73 (4H, t, *J* = 9.2, C*8′* H$_2$), 3.17 (2H, q, *J* = 7.5, C*5′* H$_2$), 3.01 (3H, s, *SO*$_2$CH$_3$), 2.78 (2H, t, *J* = 7.5, C*5′* H$_2$), 2.56 (4H, t, *J* = 3.9, C*7′* H$_2$). **^{13}C NMR** (75 MHz, CDCl$_3$): δ = 140.3 (C*8*), 137.1 (C*3′*), 130.2 (C*2*), 124.6 (C*6*), 124.2 (C*5*), 120.9 (C*7*), 114.6 (C*4*), 109.8 (C*3*), 67.3 (2C, C*8′*), 58.7 (C*5′*), 53.9 (2C, C*7′*), 40.8 (*SO*$_2$CH$_3$), 26.6 (C*4′*). **ESI-MS** (ES+ mode): *m/z* = 309 [MH$^+$, 100%]. **HRMS** (ES+ mode): *m/z* = 309.1278 [MH$^+$, 100%]; calculated for C$_{15}$H$_{21}$N$_2$O$_3$S [MH$^+$]: *m/z* = 309.1267. **IR** (solid): ν = 3300–2600, 2811, 1926, 1895, 1855, 1810, 1775, 1587, 1546, 1495, 1454, 1430 cm^{-1}.

N-mesyl indole **4.47d**, sodium hydroxide (5M, aqueous, 2 mL) and ethanol (10 mL) were used and stirred under reflux for 18 hours. The reaction was poured into water (50 mL) and the organics extracted with dichloromethane (3 x 50 mL). The combined organics were
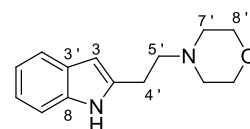
4.16d

dried (magnesium sulfate), filtered and the solvent removed *in vacuo* to give the crude product. Purification by column chromatography (petroleum ether/ethyl acetate; 10:1 then→0:1) afforded the desired compound as a colourless solid (1.11 g, 4.82 mmol, 70%). **m.p**. (ethyl acetae-hexane) 75-76 °C. **^{1}H NMR** (500 MHz, CDCl$_3$): δ = 9.36 (1H, s, NH), 7.39 (1H, d, *J* = 8.6, C*4*H), 6.83 (1 H, dd, *J* = 1.9, C*7*H), 6.73 (1H, dd, *J* = 8.6, 1.9, C*5*H), 6.14 (1H, s, C*3*H), 3.85 (3H, s, *O*CH$_3$), 3.82 (4H, t, *J* = 4.6, C*8′* H$_2$), 2.92 (2H, t, *J* = 6.2, C*5′*H$_2$), 2.72 (2H, t, *J* = 6.3, C*4′* H$_2$), 2.61–2.55 (4H, m, C*7′* H$_2$). **^{13}C NMR** (75 MHz, CDCl$_3$): δ = 155.6 (C*6*), 137.6 (C*8*), 136.4 (C*3′*), 122.7 (C*2*), 120.3 (C*4*), 109.2 (C*5*), 99.0 (C*3*), 94.6 (C*7*), 67.1 (2C, C*8′*), 58.2 (C*4′*), 55.7 (*O*CH$_3$), 53.6 (2C, C*7′*), 24.2 (C*5′*). **ESI-MS** (ES+ mode): *m/z* = 261 [MH$^+$, 100%]. **HRMS** (ES+ mode): *m/z* = 261.1598 [MH$^+$, 100%]; calculated for C$_{15}$H$_{21}$N$_2$O$_2$ [MH$^+$]: *m/z* = 261.1598. **IR** (solid): ν = 3800–2500, 2992, 1915, 1837, 1629, 1587, 1552, 1463, 1351 cm^{-1}.

7.4.4.3 2-(2-(4-Methylpiperazin-1-yl)ethyl)-1*H*-indole
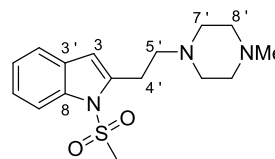
General Procedure **7.3c** was followed. Indole **4.46** (1.56 g, 4.85 mmols), methanesulfonyl chloride (450 µL, 5.82 mmol), triethylamine (1.01 mL, 7.28 mmol, 1.5 equiv), dichloromethane (15 mL) were used.. The crude dimesylate was obtained after work up as a yellow oil which was used without further purification. *N*-Methylpiperazine (3.71 mL, 33.4 mmol) and acetonitrile (20 mL) were stirred with the crude dimesylate for two days during the *N*-alkylation. The reaction was poured into sodium hydrogen carbonate (saturated aqueous, 50 mL) and dichloromethane (50 mL) was added, the organics were then extracted with dichloromethane (3 x 50 mL). The combined organics were dried (sodium sulphate), filtered and the solvent removed *in vacuo* to a yellow/orange solid. Purification by column chromatography [SiO$_2$, dichloromethane-ethyl acetate (10:1)→(0:1)] gave **4.47e** (2.41 g, 7.49 mmol, 90%) a discoloured solid. **m.p.** (ethyl acetate-hexane) 93-96 °C **^{1}H NMR** (500 MHz, CDCl$_3$): δ = 7.99 (1H, d, *J* = 7.8, C*4*H), 7.49 (1H, dd, *J* = 6.7, 1.9, C*7*H), 7.24–7.30 (2H, m, C*5*H/C*6*H), 6.51 (1H, s, C*3*H), 3.18 (2H, t, *J* = 7.7, C*5'* H$_2$), 3.01 (3H, s, *SO*$_2$CH$_3$), 2.80 (2H, t, C*4'* H$_2$), 2.70–2.36 (8H, m, C*7'* H$_2$/C*8'* H$_2$), 2.29 (3H, s, *N*CH$_3$). **^{13}C NMR** (75 MHz, CDCl$_3$): δ = 140.0 (C*8*), 136.6 (C*3'*), 129.7 (C*2*), 124.1 (C*6*), 123.6 (C*5*), 120.3 (C*7*), 114.1 (C*4*), 109.1 (C*3*), 57.7 (C*4'*), 55.0 (2C, C*7'*), 52.9 (2C, C*8'*), 46.0 (*N*CH$_3$), 40.4 (*SO*$_2$CH$_3$), 26.3 (C*5'*). **ESI-MS** (ES+ mode): *m/z* = 322 [MH$^+$, 100%]. **HRMS** (ES+ mode): *m/z* = 322.1582 [MH$^+$, 100%]; calculated for C$_{16}$H$_{24}$N$_3$O$_2$S [MH$^+$]: *m/z* = 322.1584. **IR** (solid): ν = 3074, 3015, 2937, 2788, 2697, 2317, 1934, 1899, 1676, 1593, 1568, 1455, 1410, 1396 cm^{-1}.

N-mesyl indole **4.47e** was used without recrystallization and sodium hydroxide (5M, aqueous, 2 mL) and ethanol (2 mL) were used and stirred under reflux for 18 hours. The reaction was poured into water (50 mL) and the organics extracted with dichloromethane (3 x 50 mL). The combined organics were dried (magnesium sulfate), filtered and the solvent removed *in vacuo* to give the crude product. Purification by column chromatography (SiO$_2$, petroleum ether-ethyl acetate; 10:1 then→0:1) gave indole **4.16e** as a colourless crystalline needles (1.34 g, 5.51 mmol, 79%). **m.p.** (ethyl acetate-hexane) 143–146 °C. **^{1}H NMR** (500 MHz, CDCl$_3$): δ = 9.70 (1H, s, NH), 7.52 (1H, d, *J* = 7.7, C*4*H), 7.32 (1H, d, *J* = 8.0, C*7*H), 7.10 (1H, t, *J* = 7.5, C*6*H), 7.05 (1H, t, *J* = 7.4, C*5*H), 6.21 (1H, s, C*3*H), 2.93 (3H, t, *J* = 6.2, C*5'* H$_2$), 2.72 (3H, t, *J* = 6.2, C*4'* H$_2$), 2.48–2.60 (8H, m, C*7'* H$_2$/C*8'* H$_2$), 2.33 (4H, s, *N*CH$_3$). **^{13}C NMR** (75 MHz, CDCl$_3$): δ = 139.3 (C*8*),
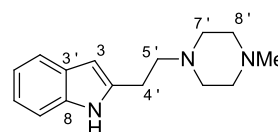
135.8 (*C3 '*), 128.5 (*C2*), 120.8 (*C6*), 119.8 (*C4*), 119.4 (*C5*), 110.7 (*C7*), 99.2 (*C3*), 57.6 (*C4'*), 55.6 (*C7'*), 53.1 (*C8'*), 46.2 (*N*CH$_3$), 24.4 (*C5*). **ESI-MS** (ES+ mode): *m/z* = 244.2 [MH$^+$, 100%]. **HRMS** (ES+ mode): *m/z* = 244.1801 [MH$^+$, 100%]; calculated for C$_{15}$H$_{22}$N$_3$ [MH$^+$]: *m/z* = 244.1808. **IR** (solid): ν = 3800–2400, 2925, 1905, 1871, 1739, 1618, 1621, 1548, 1456 cm^{-1}.

7.4.4.4 *N*-Benzyl-2-(1*H*-indol-2-yl)-*N*-methylethanamine

General Procedure **7.3c** was followed. Indole **4.46** (1.58 g, 4.93 mmols), methanesulfonyl chloride (450 μL, 5.82 mmol), triethylamine (1.01 mL, 7.28 mmol, 1.5 equiv), dichloromethane (15 mL) were used. The crude dimesylate was obtained after work up as a yellow oil which was used without further purificatio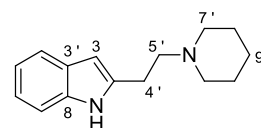n. *N*-Methylbenzylamine (2.44 mL, 18.9 mmol, 4.0 equiv.) and acetonitrile (22.5 mL) were stirred with the crude dimesylate for two days during the *N*-alkylation. The reaction was poured into sodium hydrogen carbonate (saturated aquesou, 50 mL) and dichloromethane (50 mL) was added, the organics were then extracted with dichloromethane (3 x 50 mL). The combined organics were dried (sodium sulphate), filtered and the solvent removed *in vacuo* to give the crude as a light brown oil. Purification by column chromatography (SiO$_2$, petroleum ether-ethyl acetate; 10:1 then→0:1) gave product **4.47g** (1.55 g, 4.54 mmol, 96%) as a yellow oil which. **^{1}H NMR** (500 MHz, CDCl$_3$): δ = 7.98 (1H, d, *J* = 7.9, *C4*H), 7.48 (1H, dd, *J* = 7.0, 1.4, *C7*H), 7.21–7.29 (7H, m, *C6*H/*C5*H/Ph), 6.46 (1H, s, *C3*H), 3.59 (2H, s, *C7'* H$_2$), 3.19 (2H, t, *J* = 7.3, *C5'* H$_2$), 2.95 (3H, s, *SO$_2$*CH$_3$), 2.82 (2H, t, *J* = 7.3, *C4'* H$_2$), 2.31 (3H, s, *C8'* H$_3$). **^{13}C NMR** (75 MHz, CDCl$_3$): δ = 140.3 (*C8*), 139.0 (Ph), 136.7 (*C3'*), 129.8 (*C2'*), 129.1 (2C, Ph), 128.2 (2C, Ph), 127.0 (Ph), 124.1 (*C6*), 123.7 (*C5*), 120.4 (*C7*), 114.2 (*C4*), 109.4 (*C3*), 62.3 (CH$_2$*Ph*), 56.6 (*C4'*), 42.3 (*C8'*), 40.4 (*SO$_2$*CH$_3$), 26.8 (*C5'*). **ESI-MS** (ES+ mode): *m/z* = 343 [MH$^+$, 100%]. **HRMS** (ES+ mode): *m/z* = 343.1473 [MH$^+$, 100%]; calculated for C$_{16}$H$_{23}$N$_2$O$_2$S [MH$^+$]: *m/z* = 343.1475. **IR** (solid): ν = 3061, 3026, 2931, 2841, 2792, 1591, 1567, 1494, 1453 1366 cm^{-1}.
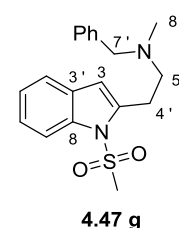
N-mesyl indole **4.47g** and sodium hydroxide (5M, aqueous, 2 mL) and ethanol (10 mL) were used and stirred under reflux for 18 hours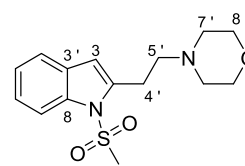. The reaction was poured into water (50 mL) and the organics extracted with dichloromethane (3 x 50 mL). The combined organics were dried (magnesium sulfate), filtered and the solvent removed *in vacuo* to afford the crude product. Purification by column chromatography (petroleum ether-ethyl acetate; 10:1 then→0:1) afforded the desired compound as a colourless solid (1.00 g, 3.78 mmols, 93%).
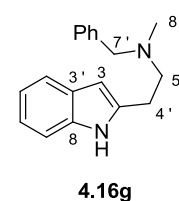
m.p. (ethyl acetate-hexane) 46-48 °C.**^{1}H NMR** (500 MHz, CDCl$_3$): δ = 9.72 (1H, s, NH), 7.52 (1H, d, *J* = 7.6, C*4*H), 7.27-7.36 (6H, m, C*7*H/Ph), 7.11 (1H, t, *J* = 7.4, C*6*H), 7.05 (1H, t, *J* = 7.1, C*5*H), 6.20 (1H, s, C*3*H), 3.58 (2H, s, C*7′* H$_2$), 2.96 (2H, t, *J* = 6.1, C*5′* H$_2$), 2.78 (2H, t, *J* = 6.1, C*4′* H$_2$), 2.31 (3H, s, (2H, t, *J* = 6.1, C*8′* H$_3$). **^{13}C NMR** (75 MHz, CDCl$_3$): δ = 139.5 (C*8*), 138.6 (Ph), 135.9 (C*3′*), 129.3 (2C, Ph), 128.6 (3C, C2/Ph), 127.4 (Ph), 120.8 (C*6*), 119.8 (C*4*), 119.5 (C*5*), 110.7 (C*7*), 99.1 (C*3*), 62.8 (CH$_2$Ph), 57.0 (C*4′*), 41.6 (C*8′*), 25.0 (C*5′*). **ESI-MS** (ES+ mode): *m/z* = 265 [MH$^+$, 100%]. **HRMS** (ES+ mode): *m/z* = 265.1706 [MH$^+$, 100%]; calculated for C$_{18}$H$_{21}$N$_2$ [MH$^+$]: *m/z* = 265.1699. **IR** (solid): ν = 3500-2300, 2849, 1976, 1958, 1910, 1874, 1839, 1819, 1795, 1759, 1651, 1620, 1589, 1549, 1494, 1455, 1390 cm^{-1}.

7.4.4.5 *N*-mesyl indole5-methyl-2-(2-(piperidin-1-yl)ethyl)-1*H*-indole

General Procedure **7.3c** was followed. Indole **4.65a** was synthesised directly from **4.63.** 5-Methyl-2-(1-(methanesulfonyl)-1*H*-(indol-2-yl)-ethanol (1.00 g,

4.64a
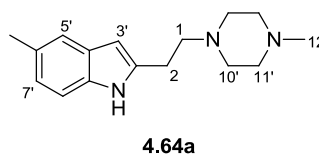
3.95 mmols), methanesulfonyl chloride (350 µL, 4.35 mmol), triethylamine (850 µL, 5.93 mmol), dichloromethane (20 mL) were used. The crude dimesylate was obtained after work up as a yellow oil which was used without further purification. *N*-Methylpiperazine (700 mL, 6.32 mmol), dichloromethane (2 mL) and acetonitrile (20 mL) were stirred with the crude dimesylate for two days during the *N*-alkylation. The reaction was poured into sodium hydrogen carbonate (saturated aqueous, 50 mL) and dichloromethane (50 mL) was added, the organics were then extracted with dichloromethane (3 x 50 mL). The combined organics were dried (sodium sulphate), filtered and the solvent removed *in vacuo* to give crude **4.64a** as a yellow/orange solid which was used without further purification. Crude **4.64a** (760 mg), sodium hydroxide (5M, aqueous, 1 mL) and ethanol (20 mL) were used. The reaction was poured into 2M hydrochloric acid (2M, aqueous, 2.5 mL) and diluted in water (50 mL), the organics were extracted with dichloromethane (3 x 50 mL). The combined organic layers were dried (sodium sulphate), filtered and the solvents removed *in vacuo* to give the crude indole, purification by column chromatography (SiO$_2$, gradient elution, dichloromethane -MeOH; 1:0→0:1) gave the title compound (106.8 mg, 416 µmols, 18% [from **4.63**]) as a discoloured solid. **m.p**. (*iso*propanol) 128-132 °C. **^{1}H NMR** (300 MHz, CDCl$_3$) δ: 9.49 (s, 1H, NH), 7.23 (s, 1H, C*5′*H), 7.16 (d, *J* = 8.1 Hz, 1H, C*7′*H), 6.89 (dd, *J* = 8.2, 1.4 Hz, 1H, C*6′*H), 6.11 (s, 1H, C*3′* H), 2.77 (t, *J* = 6.2 Hz, 2H, C2H$_2$), 2.57 (t, *J* = 6.3 Hz, 2H, C*1*H$_2$), 2.50 (apparent s, 4H, C*10′* H$_2$), 2.36 (s, 3H, CH$_3$C*6′*), 2.32 (s, 3H, C*12′* H$_3$), 1.61 (s, 4H, C*11′* H$_2$). **^{13}C NMR** (75 MHz, CDCl$_3$) δ: 138.9 (C*2′*), 136.4 (C*8′*),130.5 (C*6′*), 127.4 (C*4′*), 121.6 (C*5′*), 118.1 (C*7′*), 109.8 (C*8′*), 100.6 (C*3′*) 57.4

(C*11'*), 54.5 (C*10'*), 45.8 (C*12'*), 35.8 (C*1*), 21.5 (C2), 21.3(CH$_3$C*6'*). **ESI-MS** (ES+ mode): *m/z* = 258 [MH$^+$, 100%]. **HRMS** (ES+ mode): *m/z* = 258.2011 [MH$^+$, 100%]; calculated for C$_{16}$H$_{24}$N$_3$ [MH$^+$]: *m/z* = 258.1970. **IR** (solid) ν = 3363, 1558 cm^{-1}.

7.4.5 Pentamethyl-cyclopentadienyl-(5-trifluoromethyl-2-hydroxypyridyl) iridium dichloride, 4.14
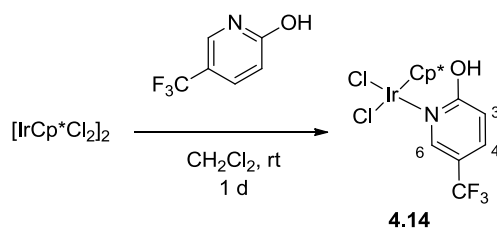
Pentamethylcyclopentadienyl-(5-trifluoromethyl-2-hydroxypyridyl) iridium dichloride was synthesised using the procedure of Fujita.[69] The 2-hydroxy-5-(trifluoromethyl)-pyridine (75.5 mg, 463 μmols, 1.85 equiv.) was added to a stirring solution of pentamethylcyclopentdienyl iridium (III) dichloride dimer (199 mg, 250 μmols, 1.0 equiv.) in dichloromethane (5 mL) and stirred for 1 hour. The resulting dark red suspension was concentrated in vacuo and recrystallized from dichloromethane–*iso*-hexane to give pentamethyl-cyclopentadienyl-(5-trifluoromethyl-2-hydroypyridyl) iridium(III) dichloride **4.14** as yellow crystalline needles (163 mg, 290 μmols, 58%). **m.p.** (dichloromethane-*iso*-hexane) decomposition at 250 °C. **^{1}H NMR** (500 MHz, 298 K, CDCl$_3$): δ = 11.33 (1H, broad s, OH), 8.87 (1H, broad s, C*4*H), 7.75 (1H, broad s, C*6*H), 6.86 (1H, broad s, C*3*H), 1.56 (15H, broad s, C$_5$Me$_5$). **ESI-MS** (ES+ mode): m/z = 490 [M−2Cl, 100%]. **HRMS** (ES+ mode): m/z = 548.0537 [MNa−HCl, 100%]; calculated for C$_{16}$H$_{18}$ClIrF$_3$NNaO [MNa-HCl]: m/z = 548.0550. **IR** (solid): ν = 3800-2600, 2978, 1629, 1574, 1505, 1378, 1349, 1321, 1228, 1209 cm^{-1}.

7.4.6 Screening reactions for the one-pot dehydrogenation-cyclisation strategy for the synthesis of polycyclic amines:

General Procedure 7.3f

A general procedure with slight modifications was used for the evaluation of various conditions for the synthesis of polycyclic indoles *via* a dehydrogenation-cyclisation strategy. The procedure is described briefly below:
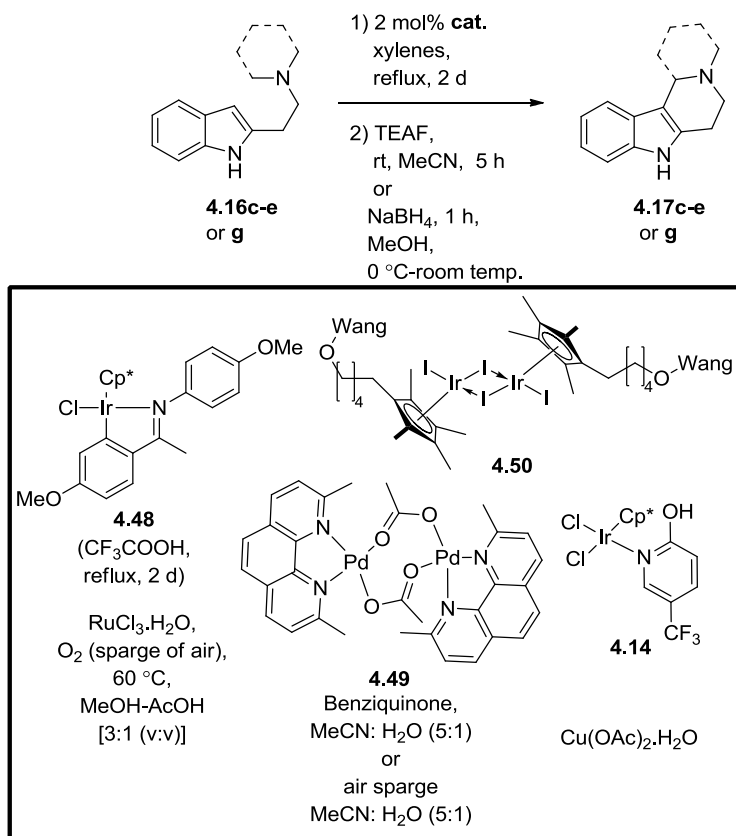
A suspension of 2-amino-indole **4.16c-e** or **g** (1.0 equiv) and catalyst **4.14**, **4.48-4.50**, copper acetate monohydrate or ruthenium chloride monohydrate was heated in solvent for 1-5 days. The reaction was cooled. The crude reaction mixture was diluted in methanol or acetonitrile, and triethylamine–formic acid azeotropic solution [2:5 (TEAF)] or sodium borohydride was added and the solution stirred for 1-5 hours. The reaction mixture was diluted in water, and the aqueous extracted with ethyl acetate and dichloromethane. The organics were washed with saturated aqueous sodium hydrogen carbonate and brine. The combined organics were dried (sodium sulfate or magnesium sulfate), filtered and the solvent removed *in vacuo* to give crude product as a brown oil. Purification by column chromatography [dichloromethane–methanol (5:1)] gave the product as colourless needles.

7.4.6.1 1,2,3,4,6,7,8,12c-octahydroindolo[3,2-a]quinolizine

1,2,3,4,6,7,8,12c-octahydroindolo[3,2-a]quinolizine was synthesised using general procedure **7.3f** with slight modifications. 2-(2-(piperidin-1-yl)ethyl)-*1H*-indole **4.16c** (100 mg, 438 μmol), pentamethylcyclopentadienyl-(5-trifluoromethyl-2-hydroypyridyl)iridium(III) dichloride **4.14** (6.2 mg, 11.3 μmol, 2 mol%) and xylenes (1.1 mL) were used and heated to reflux for 2 days. Acetonitrile (1 mL) and

4.17c
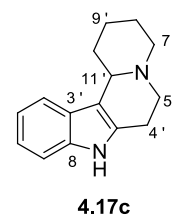
triethylamine–formic acid azeotropic solution (1.43 mL formic acid–3.57 mL triethylamine) were used for the reduction and stirred at room temperature for 5 hours. The reaction mixture was diluted in water (20 mL), and the aqueous extracted with ethyl acetate (2 × 20 mL) and dichloromethane (20 mL). The organics were washed with saturated aqueous sodium hydrogen carbonate (20 mL) and brine (20 mL). The combined organics were dried (sodium sulfate), filtered and the solvent removed *in vacuo* to give crude product as a brown oil. Purification by column chromatography [dichloromethane–methanol (5:1)] gave 1,2,3,4,6,7,8,12c-octahydroindolo[3,2-a] quinolizine[95] **4.17c** (77.6 mg, 343 μmol, 78%) as colourless needles. **m.p.** (ethanol-water) 212–213 °C. **^{1}H NMR** (500 MHz, CDCl$_3$): δ = 7.96 (1H, s, NH), 7.57 (1H, d, *J* = 7.8, C*4*H), 7.26–7.23 (1H, m, C*7*H), 7.08 (1H, t, *J* = 7.3, C*6*H), 7.04 (1H, t, *J* = 7.3, C*5*H), 3.37 (1H, d, *J* = 8.4, C*11'* H), 3.14–3.07 (1H, m, C*7'* $H_A H_B$), 3.02 (1H, dd, *J* = 10.7, 6.5, C*5'* $H_A H_B$), 3.05–2.98 (1H, m, C*4'* $H_A H_B$), 2.70–2.58 (3H, m, C*5'* $H_A H_B$/C*7'* $H_A H_B$/C*10'* $H_A H_B$), 2.50 (1H, td, *J* = 11.6, 3.0, C*4'* $H_A H_B$), 1.93–1.87 (1H, m, C*9'* $H_A H_B$), 1.83–1.71 (2H, m, C*8*H$_2$), 1.61–1.51 (2H, m, C*9'* $H_A H_B$/C*10'* $H_A H_B$). **^{13}C NMR** (75 MHz, CDCl$_3$): δ = 136.5 (C*8*), 132.5 (C*3'*), 126.0 (C*2*), 120.9 (C*6*), 119.4 (C*4*), 119.3 (C*5*), 112.5 (C*3*), 110.9 (C*7*), 61.4 (C*11'*), 56.2 (C*4'*), 52.6 (C*5'*), 31.4 (C*10'*), 26.2 (C*8'*), 24.9 (C*9'*), 24.4 (C*7'*). **ESI-MS** (ES+ mode): *m/z* = 227 [MH$^+$, 100%]. **HRMS** (ES+ mode): *m/z* = 227.1551 [MH$^+$, 100%]; calculated for C$_{15}$H$_{19}$N$_2$ [MH$^+$]: *m/z* = 227.1543. **IR** (solid): ν = 3600–2400, 2920, 2222, 1901, 1869, 1840, 1793, 1653, 1621, 1579, 1505, 1455 cm^{-1}.

7.4.6.2 1,2,3,4,6,7,8,12c-octahydroindolo[3,2-a]quinolizine

1,2,3,4,6,7,8,12c-octahydroindolo[3,2-a]quinolizine was synthesised using general procedure **7.3f** with slight modifications. 2-(2-(piperidin-1-yl)ethyl)-*1H*-indole **4.16c** (508 mg, 2.24 mmol), pentamethylcyclopentadienyl-5-trifluoromethyl-2-hydroypyridyl)iridium(III) dichloride **4.14** (26.1 mg, 47.6 μmol, 2 mol%)
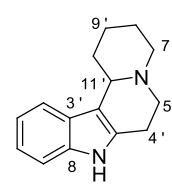
4.17c

and xylenes (5.5 mL) were used and heated to reflux for 2 days. Methanol (25 mL) and sodium borohydride (331 mg, 8.76 mmol, 4.0 equiv.) were used for the reduction and stirred at room temperature for 1 hour. The reaction mixture was quenched in sodium hydrogen carbonate (saturated aqueous, 50 mL) and the organics extracted with dichloromethane (3 x 50 mL). The organics were washed with saturated aqueous sodium hydrogen carbonate (20 mL) and brine (20 mL). The combined organics were dried (magnesium sulfate), filtered and the solvent removed *in vacuo* to give the crude product as a brown oil. Purification by column chromatography [SiO$_2$, dichloromethane-methanol (5:1)] gave

1,2,3,4,6,7,8,12c-octahydroindolo[3,2-a]quinolizine[95] **4.17c** (233 mg, 1.03 mmol, 46%) as colourless needles. Spectroscopic data was identical to that previously report (*vide supra*).

7.4.6.3 3,4,6,7,8,12c-Hexahydro-1H-[1,4]oxazino[4',3':1,2]pyrido[4,3-b]indole

3,4,6,7,8,12c-Hexahydro-1H-[1,4]oxazino[4',3':1,2]pyrido[4,3-b]indole was synthesised using general procedure **7.3f** with slight modifications. Indole amine **4.16d** (100 mg, 435 μmols) and pentamethyl-cyclopentadienyl-(5-trifluoromethyl-2-hydroypyridyl) iridium (III) dichloride (8.4 mg, 14.9 μmols, 3 mol%) in acetonitrile (1 mL) and triethylamine–formic acid solution (1 mL, triethylamine (0.3 mL): formic acid (0.7 mL)) was heated to reflux for two days. The solvent was removed *in vacuo* to give crude 3,4,6,7,8,12c-Hexahydro-1H-[1,4]oxazino[4',3':1,2]pyrido[4,3-b]indole[95] **4.17d** (9%, NMR yield) as a discoloured solid (NMR yield calculated via comparison of the integrals of C3H of indole **4.16d** and C10'H of the product indole **4.17d**); **¹H NMR** (500 MHz, 298 K, CDCl₃): δ = 8.19 (1H, s, N*H*), 4.68 (1H, dd, J = 11.0, 2.7, C*10'* H). lit.[95] **¹H NMR** (500 MHz, CDCl₃): δ = 8.19 (1H, s, N*H*), 7.44 (1H, d, *J* = 7.7, C*4*H), 7.20 (1H, d, *J* = 7.8, C*7*H), 7.09 (1H, td, *J* = 7.6, 1.1, C*6*H), 7.05 (1H, td, *J* = 7.6, 1.1, C*5*H), 4.68 (1H, dd, *J* = 11.0, 2.7, C*10'* H), 3.93 (1H, d, *J* = 10.6, C*8'* *H*ₐHᵦ), 3.84 (1H, td, *J* = 10.6, 4.0, C*8'* Hₐ*H*ᵦ), 3.67 (1H, dd, *J* = 10.1, 1.9, C*9'* *H*ₐHᵦ), 3.53 (1H, t, *J* = 10.6, C*9'* Hₐ*H*ᵦ), 3.00–3.08 (2H, m, C*5'H*ₐHᵦ /C*4'* *H*ₐHᵦ), 2.79–2.85 (2H, m, C*7'* Hₐ*H*ᵦ), 2.70–2.75 (1H, m, C*5'* Hₐ*H*ᵦ), 2.57 (1H, dd, *J* = 14.7, 4.9, C*4'* Hₐ*H*ᵦ).
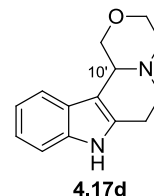
7.4.6.4 3,4,6,7,8,12c-Hexahydro-1*H*-[1,4]oxazino[4',3':1,2]pyrido[4,3-b]indole

3,4,6,7,8,12c-Hexahydro-1H-[1,4]oxazino[4',3':1,2]pyrido[4,3-b]indole was synthesised using general procedure **7.3f** with slight modifications. Indole amine **4.16d** (116 mg, 509 μmols) and copper acetate monohydrate (6.3 mg, 31.6 μmols, 6 mol%) in xylenes (2.5 mL) were used and heated to reflux for one day. The solvent was removed *in vacuo* and the crude was washed with hydrochloric acid (1N, aqueous, 100 mL) and then the organics extracted with dichloromethane (100 mL). The aqueous was neutralised with sodium hydrogen carbonate (saturated aqueous, 100 mL) and the organics extracted with dichloromethane (3 x 100 mL). The combined organics were dried (magnesium sulfate), filtered and the solvent removed *in vacuo* to give a brown oil as crude 3,4,6,7,8,12c-Hexahydro-1*H*-[1,4]oxazino[4',3':1,2]pyrido[4,3-b]indole[95] **4.17d** (4%, NMR yield) as a discoloured solid (NMR yield calculated via comparison of the integrals of C3H of indole **4.16d** and C*10'* H
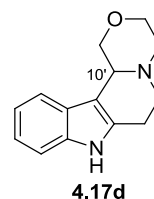
of the product indole **4.17d**); **¹H NMR** (500 MHz, 298 K, CDCl₃): δ = 8.19 (1H, s, NH), 4.68 (1H, dd, J = 11.0, 2.7, C*10′* H), which were in accordance with the literature reported previously (*vide supra*).

7.4.6.5 Attempted formation of 3,4,6,7,8,12c-Hexahydro-1H-[1,4]oxazino[4',3':1,2]pyrido[4,3-b]indole

Attempted synthesis of 3,4,6,7,8,12c-Hexahydro-1H-[1,4]oxazino[4',3':1,2]pyrido[4,3-b]indole was carried out using general procedure **7.3f** with slight modifications. 2-(2-(piperidin-1-yl)ethyl)-*1H*-indole **4.16d** (111 mg, 483 µmol), iridum complex **4.48**. (2.8 mg, 4.66 µmol, 1 mol%) and 2,2,2-tetrafluoroethanol (2.95 mL) were used and heated to reflux for 2 days. Acetonitrle (5 mL) and TEAF solution (5:2 azeotropic solution, 1 mL) were used for the reduction and stirred at room temperature for 18 hours. The reaction mixture was poured into water (50 mL) and the organics extracted with dichloromethane (3 x 50 mL). The combined organics were dried (magnesium sulfate), filtered and the solvent removed *in vacuo* to give the crude as a brown oil. No product formation was observed by **¹H NMR** or **LC-MS** analysis.
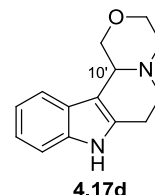
7.4.6.6 Attempted formation of 3,4,6,7,8,12c-Hexahydro-1H-[1,4]oxazino[4',3':1,2]pyrido[4,3-b]indole

Attempted synthesis of 3,4,6,7,8,12c-Hexahydro-1H-[1,4]oxazino[4',3':1,2]pyrido[4,3-b]indole was carried out using general procedure **7.3f** with slight modifications. 2-(2-(piperidin-1-yl)ethyl)-*1H*-indole **4.16d** (111 mg, 434 µmol), immobilised iridium complex **4.50** (81 mg, 4.34 µmol, 1 mol%) and xylenes (10 mL) were used and heated to reflux for 2 days. Methanol (5 mL) and sodium borohydride (43.5 mg, 1.15 mmol, 2.65 equiv.) were used for the reduction and stirred at room temaperature for 1 hour. The reaction mixture was poured into water (50 mL) and the organics extracted with dichloromethane (3 x 50 mL). The combined organics were dried (magnesium sulfate), filtered and the solvent removed *in vacuo* to give the crude as a brown oil. No product formation was observed by **¹H NMR** or **LC-MS** analysis.
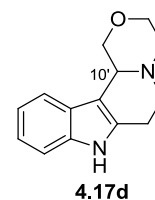
7.4.6.7 1,2,3,4,6,7,8,12c-octahydroindolo[3,2-a]quinolizine

1,2,3,4,6,7,8,12c-octahydroindolo[3,2-a]quinolizine was synthesised using general procedure **7.3f** with slight modifications. Triethylamine–formic acid solution (1 mL, triethylamine (0.3 mL): formic acid (0.7 mL)) was slowly added to a solution of indole amine **4.16c** (111 mg, 487 μmols) and pentamethyl-cyclopentadienyl-(5-trifluoromethyl-2-hydroypyridyl) iridium(III)dichloride 1.33 (11.6 mg, 20.6 μmols, 4 mol%) in acetonitrile (2 mL) and was heated in a sealed tube at 110 °C for one day then 140 °C for one day. The solvent was removed *in vacuo* to give crude 1,2,3,4,6,7,8,12c-octahydroindolo[3,2-a]quinolizine[95] (41%, NMR yield) as a brown oil (NMR yield calculated via comparison of the integrals of C*3*H of indole **4.16c** and C*11'* H of the product indole **4.17c**); **¹H NMR** (500 MHz, 298 K, CDCl₃): δ = 7.96 (1H, s, NH), 3.37 (1H, d, J = 8.4, C*11'* H), which were in agreement with those previously reported (*vide supra*).
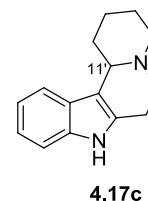
7.4.6.8 Attempted formation of 2-Methyl-1,2,3,4,6,7,8,12c-octahydropyrazino[1',2':1,2] pyrido[4,3-*b*]indole

2-Methyl-1,2,3,4,6,7,8,12c-octahydropyrazino[1',2':1,2]pyrido[4,3-*b*]indole was synthesised using general procedure **7.3f** with slight modifications. A suspension of palladium catalyst **4.49** (6 mg, 8.46 μmols, 2 mol%), indole **4.16e** (102 mg, 423 μmols) and 1,4-benzoquinone (100 mg, 925 μmols, 2.19 equiv.) in acetonitrile: water (5:1, 1 mL) was stirred for 3.5 hours at room temperature. The reaction grew black with time. The solvent was removed *in vacuo* and methanol (5 mL) was added and the reaction was cooled to 0 °C, sodium borohydride (63.1 mg, 1.66 mmols, 1.79 equiv.) was added and the solution stirred for one hour at room temperature. The reaction was poured into sodium hydrogen carbonate (saturated aqueous, 50 mL) and the organics extracted with dichloromethane (3 x 50 mL). The combined organics were dried (magnesium sulfate), filtered and solvent removed *in vacuo* to give a black viscous oil. No reaction was observed *via* ¹H NMR and LC-MS analysis.
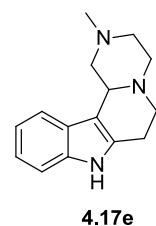
7.4.6.9 Attempted formation of 2-Methyl-1,2,3,4,6,7,8,12c-octahydropyrazino[1',2':1,2] pyrido[4,3-*b*]indole

2-Methyl-1,2,3,4,6,7,8,12c-octahydropyrazino[1',2':1,2]pyrido[4,3-*b*]indole was synthesised using general procedure **7.3f** with slight modifications. A suspension of palladium catalyst **4.49** (6 mg, 8.46 μmols, 2 mol%), indole **4.16e** (102 mg, 423 μmols) in acetonitrile: water (5:1, 1 mL) was sparged with air for 3.5 hours at room temperature. The reaction grew black with time. The solvent was removed *in vacuo* and methanol (5 mL) was added and the reaction was cooled to 0 °C, sodium borohydride (63.1 mg, 1.66 mmols, 1.79 equiv.) was added and the solution stirred for one hour at room temperature. The reaction was poured into sodium hydrogen carbonate (saturated aqueous, 50 mL) and the organics extracted with dichloromethane (3 x 50 mL). The combined organics were dried (magnesium sulfate), filtered and solvent removed in vacuo to give a black viscous oil. No reaction was observed *via* ^{1}H NMR and LC-MS analysis.
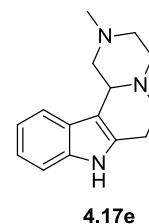
7.4.6.10   Attempted incorporation of ruthenium trichloride for cyclisation of *N*-benzyl-2-(1*H*-indol-2-yl)-*N*-methylethanamine

Evaluation of ruthenium trichloride in the cyclisation of *N*-benzyl-2-(1*H*-indol-2-yl)-*N*-methylethanamine was carried out using general procedure **7.3f** with slight modifications. Indole **4.16g** (165 mg, 625 μmol, 1 equiv.), ruthenium trichloride monohydrate (8.8 mg, 39.3 μmol, 6 mol%), methanol (1.2 mL) and acetic acid (0.6 mL) were used. The reaction was heated to 65 °C (hot plate) with an air sparge for 2 days. Solvent was removed *in vacuo* to give a brown oil. No reaction was observed *via* **^{1}H NMR** or **LC-MS** analysis.
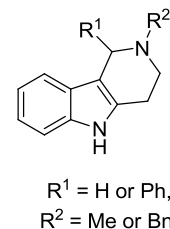
7.4.7 Synthesis of 1,2,3,4,6,7,8,12c-Octahydroindolo[3,2-a]quinolizine *via* a one-pot dehydrogenation-alkylation protocol
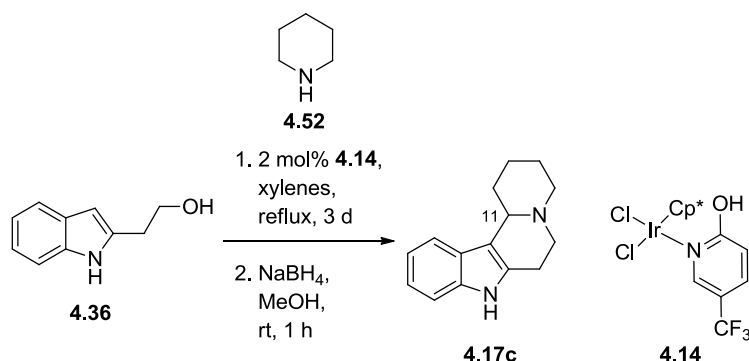
A suspension of the indolyl alcohol **4.36** (181 mg, 1.12 mmol, 1.0 equiv.), pentamethyl-cyclopentadienyl-(5-trifluoromethyl-2-hydroypyridyl) iridium (III) dichloride 1.33 (13.2 mg, 22.9 μmol, 2 mol%) and piperidine **4.52** (230 μL, 3.13 mmol, 2.79 equiv.) in xylenes (2.8 mL) was heated to reflux for 2.5 days. The reaction was cooled to 0 °C dissolved in methanol (5 mL), sodium borohydride (25 mg, 658 μmol, 0.588 equiv.) was added portionwise to the reaction which was allowed to warm to room temperature and stirred for an hour. The reaction was quenched with water (20 mL) and the organics extracted with dichloromethane (2 x 20 mL) and ethyl acetate (2 x 20 mL). The combined organics were dried, filtered and the solvent removed *in vacuo* to give crude 1,2,3,4,6,7,8,12c-octahydroindolo[3,2-a]quinolizine[95] **4.17c** as a brown oil. **^{1}H NMR** (500 MHz, 298 K, CDCl$_3$): δ = 7.96 (1H, s, NH), 3.37 (1H, d, *J* = 8.4, C*11'* H), which was in agreement with those reported previously (*vide supra*).
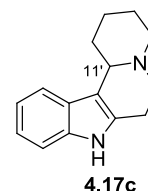
7.4.8 Reactions screened for the synthesis of 1,2,3,4,6,7,8,12c-octahydroindolo [3,2-a]quinolizine *via* a one-pot dehydrogenation-alkylation strategy

General Procedure 7.3e

A general procedure with slight modifications was used for the evaluation of various different conditions during the synthesis of 1,2,3,4,6,7,8,12c-octahydroindolo

[3,2-a]quinolizine *via* a one-pot sequential dehydrogenation-alkylation strategy. The procedure is described briefly below:
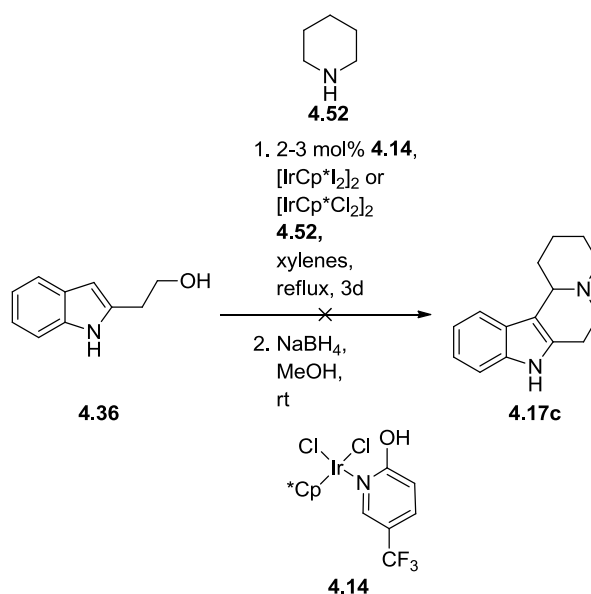
A suspension of the iridium catalyst (2-3 mol%), indolyl alcohol (97.2 mg, 604 μmol,1.0 equiv.) and piperidine (483-906 μmol, 0.8-1.5 equiv.) in solvent (1.5-2 mL) was heated for 3 days. Formation of 1,2,3,4,6,7,8,12c-octahydroindolo[3,2-a]quinolizine **4.17c** was not observed in all cases.

Entry	Solvent	Base	Catalyst	Piperidine / Equiv.	Yield of Product / %
1	Xylenes	No	**4.14**	0.8	0
2	Xylenes	No	**4.14**	1	0
3	Xylenes	No	**4.14**	1[a]	0
4	Xylenes	No	**4.14**	1.5	0
5	Piperidine	No	**4.14**	25.2	0
6	PhCl	No	**4.14**	1	0
7	PhCl	K_2CO_3	[IrCp*Cl$_2$]$_2$	1	0
8	PhCl	No	[IrCp*Cl$_2$]$_2$	1	0
9	PhCl	K_2CO_3	[IrCp*I$_2$]$_2$	1	0
10	PhCl	No	[IrCp*I$_2$]$_2$	1	0
11	PhCl	K_2CO_3	**4.14**	1	0
12	PhCl	No	**4.14**	1	0

[a] Dropwise addition over 1 hour.

Entry	Solvent	Base	Catalyst	Piperidine / Equiv.	Yield of Product / %
13	AcOH	No	**4.14**	1	0
14	PhCl	No	**4.14**	1	0
15	Xylenes	No	[IrCp*I$_2$]$_2$	1	0
16	Xylenes	TMG	**4.14**	1	0
17	Xylenes	No	**4.14**	1	0

Entry 1 Synthetic procedure **7.3e** was followed. Xylenes (1.5 mL), catalyst **4.14** (11 mg, 19.6 µmols, 3 mol%) and piperidine (47.5 µL, 483 mmols, 0.8 equiv,) were used. An insoluble black viscuous oil was formed, which was not characterisable, no evidence of cyclisation product was observed *via* **^{1}H NMR** or **HPLC** analysis.

Entry 2 Synthetic procedure **7.3e** was followed. Xylenes (1.5 mL), catalyst **4.14** (11 mg, 19.6 µmols, 3 mol%) and piperidine (59.5 µL, 604 µmols, 1 equiv.) were used. An insoluble black viscuous oil was formed, which was not characterisable, no evidence of cyclisation product was observed *via* **^{1}H NMR** or **HPLC** analysis.

Entry 3 Synthetic procedure **7.3e** was followed. Xylenes (1.5 ml), catalyst **4.14** (11 mg, 19.6 µmols, 3 mol%) and piperidine (59.5 µL, 604 µmols, 1.0 equiv.; added dropwise over one hour.). An insoluble black viscuous oil was formed, which was not characterisable, no evidence of cyclisation product was observed *via* **^{1}H NMR** or **HPLC** analysis.

Entry 4 Synthetic procedure **7.3e** was followed. Xylenes (1.5 mL), catalyst **4.14** (11 mg, 19.6 µmols, 3 mol%) and piperidine (89 µL, 906 µmols, 1.5 equiv.) were used. An insoluble black viscuous oil was formed, which was not characterisable, no evidence of cyclisation product was observed *via* **^{1}H NMR** or **HPLC** analysis.

Entry 5 Synthetic procedure **7.3e** was followed. Catalyst **4.14** (6.8 mg, 12.1 µmols, 2 mol%) and piperidine (1.5 mL, 15.2 mmols, 25.2 equiv.) were used. An insoluble black viscuous oil was formed, which was not characterisable, no evidence of cyclisation product was observed *via* **^{1}H NMR** or **HPLC** analysis.

Entry 6 Synthetic procedure **7.3e** was followed. Chlorobenzene (1.5 mL), catalyst **4.14** (11 mg, 19.6 µmols, 3 mol%) and piperidine (59.5 µL, 604 µmols, 1 equiv.) were used. An insoluble black viscuous oil was formed, which was not characterisable, no evidence of cyclisation product was observed *via* **^{1}H NMR** or **HPLC** analysis.

Entry 7 Synthetic procedure **7.3e** was followed. Chlorobenzene (1.5 mL), dichloro pentamethylcyclopentadienyliridium(III) dimer (15.6 mg, 19.6 μmols, 3 mol%), potassium carbonate (5.4 mg, 39.2 μmol, 6 mol%) and piperidine (59.5 μL, 604 μmols, 1 equiv.) were used. An insoluble black viscuous oil was formed, which was not characterisable, no evidence of cyclisation product was observed *via* **^{1}H NMR** or **HPLC** analysis.

Entry 8 Synthetic procedure **7.3e** was followed. Chlorobenzene (1.5 mL), dichloro pentamethylcyclopentadienyliridium(III) dimer (15.6 mg, 19.6 μmols, 3 mol%) and piperidine (59.5 μL, 604 μmols, 1 equiv.) were used. An insoluble black viscuous oil was formed, which was not characterisable, no evidence of cyclisation product was observed *via* **^{1}H NMR** or **HPLC** analysis.

Entry 9 Synthetic procedure **7.3e** was followed. Chlorobenzene (1.5 mL), diiodo pentamethylcyclopentadienyliridium(III) dimer (22.8 mg, 19.6 μmols, 3 mol%), potassium carbonate (5.4 mg, 39.2 μmols, 3 mol%) and piperidine (59.5 μL, 604 μmols, 1 equiv.) were used. An insoluble black viscuous oil was formed, which was not characterisable, no evidence of cyclisation product was observed *via* **^{1}H NMR** or **HPLC** analysis.

Entry 10 Synthetic procedure **7.3e** was followed. Chlorobenzene (1.5 mL), diiodo pentamethylcyclopentadienyliridium(III) dimer (22.8 mg, 19.6 μmols, 3 mol%) and piperidine (59.5 μL, 604 μmols, 1 equiv.) were used. An insoluble black viscuous oil was formed, which was not characterisable, no evidence of cyclisation product was observed *via* **^{1}H NMR** or **HPLC** analysis.

Entry 11 Synthetic procedure **7.3e** was followed. Chlorobenzene (1.5 mL), catalyst **4.14** (11 mg, 19.6 μmols, 3 mol%) and potassium carbonate and piperidine (59.5 μL, 604 μmols, 1 equiv.) were used. An insoluble black viscuous oil was formed, which was not characterisable, no evidence of cyclisation product was observed *via* **^{1}H NMR** or **HPLC** analysis*

Entry 12 Synthetic procedure **7.3e** was followed. Chlorobenzene (1.5 mL), catalyst **4.14** (11 mg, 19.6 μmols, 3 mol%) and piperidine (59.5 μL, 604 μmols, 1 equiv.) were used. An insoluble black viscuous oil was formed, which was not characterisable, no evidence of cyclisation product was observed *via* **^{1}H NMR** or **HPLC** analysis.

Entry 13 Synthetic procedure **7.3e** was followed. Acetic acid (1.5 mL), catalyst **4.14** (11 mg, 19.6 μmols, 3 mol%) and piperidine (59.5 μL, 604 μmols, 1 equiv.) were used. An

insoluble black viscuous oil was formed, which was not characterisable, no evidence of cyclisation product was observed *via* **¹H NMR** or **HPLC** analysis.

Entry 14 Synthetic procedure **7.3e** was followed. Xylenes (1.5 mL), dichloro pentamethylcyclopentadienyliridium(III) dimer (22.8 mg, 19.6 μmols, 3 mol%) and piperidine (59.5 μL, 604 μmols, 1 equiv.) were used. An insoluble black viscuous oil was formed, which was not characterisable, no evidence of cyclisation product was observed *via* **¹H NMR** or **HPLC** analysis.

Entry 15 Synthetic procedure **7.3e** was followed. Xylenes (1.5 mL), catalyst **4.14** (11 mg, 19.6 μmols, 3 mol%), were used. An insoluble black viscuous oil was formed, which was not characterisable, no evidence of cyclisation product was observed *via* **¹H NMR** or **HPLC** analysis.

Entry 16 Synthetic procedure **7.3e** was followed. Xylenes (1.5 mL), catalyst **4.14** (6.8 mg, 12.1 μmols, 2 mol%), 1,1,3,3-tetramethylguanidine (75.5 μL, 603 μmols, 1 equiv.) piperidine (59.5 μL, 604 μmols, 1 equiv.) were used. An insoluble black viscuous oil was formed, which was not characterisable, no evidence of cyclisation product was observed *via* **¹H NMR** or **HPLC** analysis.

Entry 17 Synthetic procedure **7.3e** was followed. Xylenes (1.5 mL), catalyst **4.14** (6.8 mg, 12.1 μmols, 2 mol%), (piperidine (59.5 μL, 604 μmols, 1 equiv.) were used. An insoluble black viscuous oil was formed, which was not characterisable, no evidence of cyclisation product was observed *via* **¹H NMR** or **HPLC** analysis.

7.4.9 Attempted formation of catalyst bound-(1H-indol-2-yl) ethanol
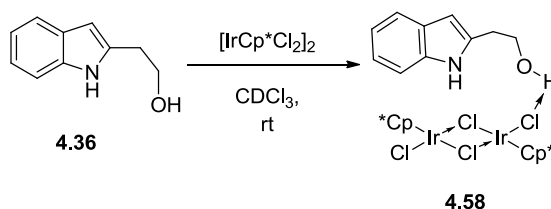
A solution of indolyl alcohol **4.36** (4.8 mg, 31.1 μmols, 1.0 equiv.), dichloropentamethylcyclcopentadienyliridium(III) dimer (17.8 mg, 31.1 μmols, 1.0 equiv.) in CDCl₃ (0.65 mL) was sonicated in an NMR tube for 30 minutes at room temperature. The

solvent was removed and the resulting orange solid was recrystallised from dichloromethane–petroleum ether to give the indolyl alcohol and pentamethylcyclcopentadienyl iridium (III) dichloride dimer complex **4.58**.

Crystallographic data complex 5.8

Single crystals of **4.58** were grown by slow evaporation of a dichloromethane-petroleum ether solution. An orange block crystal of dimensions 0.31 x 0.26 x 0.17 mm was used for the data collection; T = 120(2) K, θ range = 3.5 $\leq$ θ $\leq$ 60.5°, Crystals belong to Monoclinic; Space group $P2_1/c$; Formula = $C_{31}H_{43}Cl_6IrNO$; Formula weight = 1042.76; a = 9.1589(7) Å, b = 30.663(2) Å, c = 12.7932(10) Å, α = 90.00 °, β = 99.850(3) °, γ = 90.00 °; Volume = 3539.9(5) Å^3; Z = 4, D (calculated): 1.957 mg/mm^3, μ = 7.989 mm^{-1}, Reflections collected 41353; Independent reflections 10467 [R(int) = 0.0308]; R value = 0.0217, $wR2$ = 0.0445.

7.4.10 Synthesis of 3,4,6,7,8,12c-Hexahydro-1H-[1,4]oxazino[4',3':1,2] pyrido[4,3-b]indole *via* a one-pot dehydrogenation-alkylation strategy
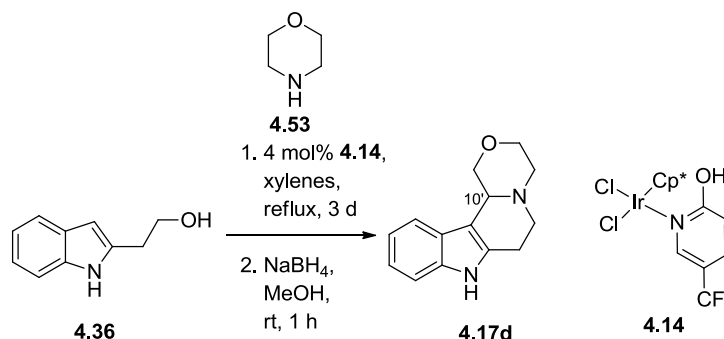
A suspension of indolyl alcohol **4.36** (97.3 mg, 603 µmol, 1.0 equiv.), pentamethyl-cyclopentadienyl-(5-trifluoromethyl-2-hydroypyridyl) iridium (III) dichloride **4.14** (12.8 mg, 22.2 µmol, 4 mol%) and morpholine, **4.53** (200 µL, 2.30 mmol, 3.81 equiv.) in xylenes (2 mL) was heated at reflux for three days. The reaction was cooled to 0 °C and dissolved in methanol (5 mL), sodium borohydride (78.5 mg, 2.07 mmol, 3.43 equiv.) was added portionwise to the reaction and the reaction was allowed to warm to room temperature and stirred for an hour. The reaction was quenched with water (20 mL) and the organics extracted with dichloromethane (2 x 20 mL) and ethyl acetate (2 x 20 mL). The combined organics were dried, filtered and the solvent removed *in vacuo* to give crude 3,4,6,7,8,12c-Hexahydro-1H-[1,4]oxazino[4',3':1,2]pyrido[4,3-b]indole[95] **4.17d** (15 mg,

65.8 µmols, 11%, crude material) as a brown oil. **¹H NMR** (500 MHz, 298 K, CDCl₃): δ = 8.19 (1H, s, NH), 4.68 (1H, dd, *J* = 11.0, 2.7, C10'H) which were in agreement with the literature[95] (*vide supra*).

7.4.11 Synthesis of (±)-Desbromoarborescidine A using a one-pot dehydrogenation-alkylation strategy
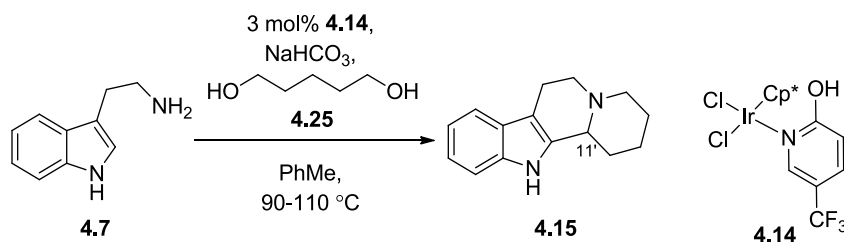
A suspension of tryptamine **4.7** (104 mg, 650 µmol, 1.0 equiv.), pentamethylcyclopentadienyl-(2-oxy-(5-trifluoromethyl)-pyridyl) iridium(III) dichloride **4.14** (11.4 mg, 20.3 µmol, 3 mol%) and 1,5-pentanediol **4.25** (60 µL, 499 µmol, 0.8 equiv.) in xylenes (2 mL) was heated to 100 °C for 4 hours, then reflux for 2 days. The reaction was acidified with 1M aqueous hydrochloric acid (20 mL) and the organics extracted with dichloromethane (2 x 20 mL). The aqueous was neutralised with aqueous saturated sodium hydrogen carbonate (20 mL) and the organics were extracted with dichloromethane (3 x 20 mL). The combined organics were dried (magnesium sulfate), filtered and the solvent removed *in vacuo*. Column chromatography [dichloromethane–methanol] gave impure (±)-Desbromoarborescidine A[95,28] **4.15** (10.7 mg, 47.3 µmols, 7%) as a dark brown solid. **¹H NMR** (500 MHz, 298 K, CDCl₃): δ = 3.24 (1H, broad d, J = 10.7, C*11'* H), lit.[95] **¹H NMR** (500 MHz, CDCl₃): δ = 7.71 (1H, broad s, NH), 7.47 (1H, d, *J* = 7.7, C*4*H), 7.29 (1H, d, *J* = 8.1, C7H), 7.12 (1H, t, *J* = 7.3, C6H) 7.08 (1H, t, *J* = 7.3, C5H), 3.24 (1H, broad d, *J* = 10.7, C*11'* H), 3.10–2.97 (3H, m, C*4'* *H*ₐHв/C5' *H*ₐHв/C7' *H*ₐHв), 2.74–2.67 (1H, m, C7' Hₐ*H*в), 2.63 (1H, td, *J* = 11.1, 4.4, C5' Hₐ*H*в), 2.39 (1H, td, *J* = 11.1, 3.4, C*4'* Hₐ*H*в), 2.06 (1H, dd, *J* = 12.4, 2.1, C*10'* *H*ₐHв), 1.90 (1H, broad d, *J* = 12.4, C9' *H*ₐHв), 1.82–1.69 (2H, m, C8' *H*ₐHв/C9' Hₐ*H*в), 1.60 (1H, qd, *J* = 12.4, 3.4, C*10'* Hₐ*H*в), 1.54–1.43 (1H, m, C8' Hₐ*H*в).

7.5 Experiments discussed in Chapter 5

7.5.1.1 Evaluation of potassium cyanide in the iridium catalysed dehydrogenation of amines

Synthetic Procedure 7.5a

A general synthetic procedure was used with minor modifications to assess the dehydrogenation of primary amines. The procedure is described briefly below:
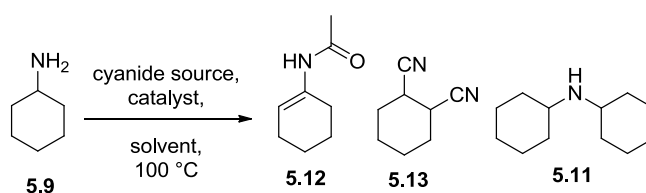
Cyclohexylamine was added to a suspension of the iridium catalyst, potassium cyanide in water and heated to reflux for 3 days. The resulting brown solution became colourless with time. The solution was cooled to room temperature. The mixture was poured into dichloromethane (20 mL), and the aqueous layer extracted with dichloromethane (3 x 20 mL), extracted, dried and the solvent removed *in vacuo*. Isolation of the reaction products was not possible. Samples were taken at regular intervals by sampling 50 μL and diluting in 5 mL of acetonitrile. 2 mL aliquots of the resulting solution were analysed by GC and GC-MS. Dicyclohexylamine and potential analysis artefacts were observed *via* **GC-MS** analysis, α-aminonitrile formation was not observed *via* **^{1}H NMR** or **GC-MS** analysis. The eneamide **5.12** was observed *via* **GC-MS**: elution time: 5.2 min., *m/z*: 139. The **5.13** was observed *via* **GC-MS**: elution time: 5.6 min., *m/z*: 134.

Entry	Cyanide Source and quantity / equiv.	Catalyst	Catalyst Loading / mol%	Overall Concentration of reactants in solution / N	Product Observed *via* GC-MS
1	KCN, 0.79	**5.1b**	1	0.57	**5.11**[b]
2	KCN, 4	**5.1b**	1	2.09	**5.12 or 5.13**
3	KCN, 4	**5.1a**	1	2.09	**5.12 or 5.13**
4	KCN, 4	**5.2**	2	2.09	**5.12 or 5.13**
5	KCN, 4	**5.2**	2	2.09	**5.12 or 5.13**

Entry 1 Synthetic procedure **7.5a** was followed. Amine **5.9** (288 μL, 2.52 mmols, 1.00 equiv.), diiodopentamethylcyclopentadienyliridium(III) dimer complex (23 mg, 20.0 μmol, 1 mol%), water (8 mL) and potassium cyanide (135 mg, 2 mmol, 0.79 equiv.) were used. Dicyclohexylamine was observed by **GC-MS** analysis.

Entry 2 Synthetic procedure **7.5a** was followed. Amine **5.9** (576 μL, 5.04 mmols, 1.00 equiv.), diiodopentamethylcyclopentadienyliridium(III) dimer complex (46 mg, 40.0 μmol, 1 mol%), water (12 mL) and potassium cyanide (1.35 g, 20 mmol, 4.00 equiv.) were used. Eneamide and dinitrile were observed by **GC-MS** analysis.

Entry 3 Synthetic procedure **7.5a** was followed. Amine **5.9** (288 μL, 2.52 mmols, 1.00 equiv.), diiodopentamethylcyclopentadienyliridium(III) dimer complex (16 mg, 20.0 μmol, 1 mol%), water (6 mL) and potassium cyanide (675 mg, 10 mmol, 4.00 equiv.) were used. The products of the reaction were not isolated. Eneamide and dinitrile were observed by **GC-MS** analysis.

Entry 4 Synthetic procedure **7.5a** was followed. Amine **5.9** (288 μL, 2.52 mmols, 1.00 equiv.), pentamethylcyclopentadienyl (2-hydroxy-5-(trifluoromethyl)-pyridine)iridium(III) dichloride (19.8 mg, 40.0 μmol, 2 mol%), water (6 mL) and potassium cyanide (675 mg, 10 mmol, 4.00 equiv.) were used. Eneamide and dinitrile were observed by **GC-MS** analysis.

Entry 5 Synthetic procedure **7.5a** was followed. Amine **5.9** (288 μL, 2.52 mmols, 1.00 equiv.), Fujita catalyst **5.2** (22.4 mg, 4.0 *μ*mol, 1 mol%), water (6 mL) and potassium cyanide (675 mg, 10 mmol, 4.00 equiv.) were used. Eneamide and dinitrile were observed by **GC-MS** analysis.

7.5.1.2 Evaluation of trimethylsilyl cyanide (TMSCN) in the iridium catalysed dehydrogenation of amines
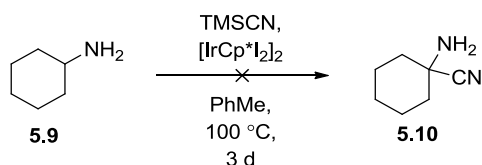
Amine **5.9** (458 *μ*L, 4.00 mmols), diiodopentamethylcyclopentadienyliridium(III) dimer complex (46 mg, 40.0 μmol, 1 mol%) and trimethylsilyl cyanide (750 μL, 6 mmol,

1.50 equiv.) in toluene (8 mL) were heated to 100 °C. The eneamide **5.12** was observed *via* **GC-MS**: elution time: 5.2 min., *m/z*: 139. The dinitrile **5.13** was observed *via* **GC-MS**: elution time: 5.6 min., *m/z*: 134.

7.5.1.3 The synthesis of a (*s*)-2-phenyl aziridine standard
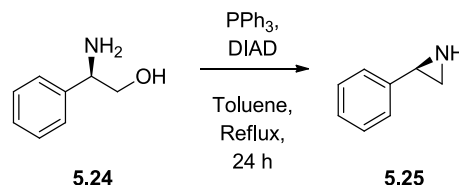
(*S*)-2-Phenyl aziridine was synthesised using the method of Xu with slight modifications.[170] (*S*)-2-Phenyl glycinol (550 mg, 4.01 mmol, 1.00 equiv.) was dissolved in toluene and cooled to 0 °C. Triphenyl phosphine (1.10 mg, 4.20 mmol, 1.05 equiv.) and toluene (9 mL) were added to the resulting solution. Diisopropyl azodicarboxylate (780 μL, mmol, equiv.) was slowly added to the resulting solution over 2 hours, which was slowly warmed to room temperature and then stirred at reflux for 24 hours. The resulting solution was yellow in colour which grew darker with time. The solution was poured into water (15 mL) and diethyl ether (15 mL). The solution was dried over magnesium sulfate and filtered. The solvent was removed *in vacuo*, diluted in diethyl ether (15 mL) and cooled to 0 °C for 3 hours. The resulting suspension was filtered. Removal of the solvent *in vacuo* gave the crude product as a dark orange oil. Purification via column chromatography (eluting with petroleum ether [1% triethylamine]–ethyl acetate; 5:1) gave (*S*)-phenyl aziridine[170, 199] (**5.25**) (161 mg, 1.35 mmol, 30%) as a yellow oil. *R*$_f$ 0.25 (Petroleum ether [1% triethylamine]–ethyl acetate 5:1); **¹H NMR** (500 MHz, CDCl₃) δ: 7.18–7.40 (m, 5 H), 3.02 (dd, *J* = 6.0, 3.4 Hz, 1 H), 2.21 (d, *J* = 6.0 Hz, 1 H), 1.51 (br s, 1 H), 1.81 (d, *J* = 3.4 Hz, 1 H); **¹³C NMR** (75 MHz, CDCl₃) δ:140.3, 128.4, 127.0, 125.6, 32.1, 29.2; **GC-MS**: elution time: 6.3 min, m/z; 118.

7.5.1.4 General procedure for the synthesis of dimethylsulfoxoniummethylide

Synthetic Procedure 7.5b

A general synthetic procedure based upon the methods of Jones[200] and Smith[169] was used with minor modifications to form dimethylsulfoxoniummethylide. The procedure is described briefly below:
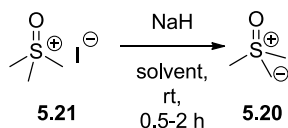
Under anhydrous conditions in a flame-dried round bottomed flask, sodium hydride (60% in mineral oil [145 mg, 5.00 mmol, 2.50 equiv.]) was washed 3 times with anhydrous THF (2 mL). Vacuum-dried sulfoxonium iodide salt **5.21** (444 mg, 2.00 mmol, 1.00 equiv.) was added to the dry mixture and anhydrous solvent (2 mL) was added slowly, the mixture was stirred at 20 °C to afford the ylide **5.20**. The solvent was partially evaporated. The resulting mixture was used without further purification.

Entry	Solvent	Time / hours
1	THF	2
2	DMSO	0.5
3	Anisole	2

Entry 1 Synthetic procedure **7.5b** was followed. Anhydrous THF was the solvent used and the suspension was stirred for 2 hours.

Entry 2 Synthetic procedure **7.5b** was followed. Anhydrous DMSO was the solvent used and the solution was stirred for 0.5 hours.

Entry 3 Synthetic procedure **7.5b** was followed. Anhydrous anisole was the solvent used and the suspension was stirred for 2 hours.

7.5.1.5 The evaluation of dimethyl sulfoxonium methylide in the iridium catalysed dehydrogenation of benzlyamine

Synthetic Procedure 7.5c

A general procedure with slight modifications was used for the evaluation of dimethylsulfoxonium methylide during benzyl amine dehydrogenation. The procedure is described briefly below:
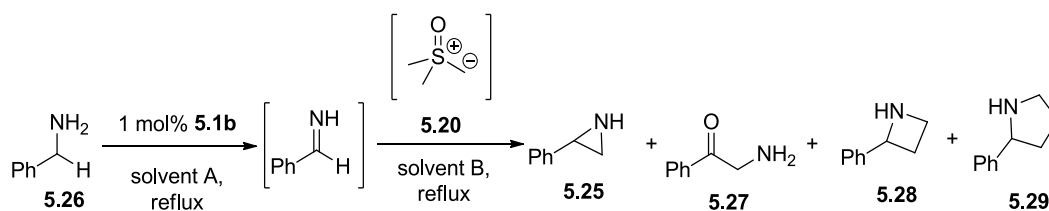
Under anhydrous conditions, benzylamine **5.26** (225 μL, 2.00 mmol, 2.00 equiv.) was added to a suspension of diiodopentamethylcyclopentadienyliridium (III) dimer complex (23 mg, 20.0 μmol, 1 mol%) and biphenyl (15.4 mg, 0.1 mmol, 0.10 equiv.) in solvent **A** (4 mL) and was stirred at reflux for 5 hours. The resulting brown solution rapidly became orange. Dimethylsulfoxonium methylide **5.20** dissolved in solvent B was added to the resulting solution *via* dropwise addition by syringe pump (2.03 mL min^{-1}). The resulting solution became orange over time. Isolation of the reaction products was not possible. Samples were taken at regular intervals by sampling 50 μL and diluting in 5 mL of acetonitrile. 2 mL aliquots of the resulting solution were analysed by GC and GC-MS. The formation of products **5.25** and **5.27**-**5.29** was observed *via* GC-MS analysis. Aziridine **5.25** was observed *via* **GC-MS** analysis: elution time: 5.1 min., *m/z*: 120 and comparison to a pre-prepared standard (*vide supra*); over-oxidation product **5.27** was observed *via* **GC-MS** analysis: elution time = 4.9 min., *m/z*: 135; azetidine **5.28** was observed *via* **GC-MS** analysis: elution time: 6.4 min., *m/z*: 134: pyrrolidine **5.29** was observed *via* **GC-MS** analysis: elution time: 7.2 min., *m/z*: 147. GC yields were calculated by comparison to the biphenyl internal standard using Equation 7.1, but without an internal response factor.

Entry	Solvent A	Solvent B	Solvent C	Proposed Main Product / N^o	Product[b] / %
1	Xylenes	THF	n/a	**5.28**	14
2	PhMe	DMSO	n/a	**5.25**	32
3	PhMe	THF	n/a	**5.29**	20
4	Xylenes	THF	DMF	**5.25/ 5.27**	21/23
5	Xylenes	Anisole	n/a	No reaction	0

[a] Amine **5.26** (1.00 equiv.), iridium complex (1 mol%) in anhydrous solvent A (2 mL) were heated to reflux and a suspension of ylide **5.20** (1.5 equiv.) and solvent B (1 mL) were added slowly.

[b] Calculated *via* comparison to a biphenyl internal standard. Yield calculated to the nearest percent, ±0.5%.

Entry 1 Synthetic procedure **7.5c** was followed. Xylenes (solvent A) and THF (solvent B) were used. The formation of azetidine **5.28** was observed *via* **GC** analysis **GC** conversion 14%.

Entry 2 Synthetic procedure **7.5c** was followed. Toluene (solvent A) and DMSO (solvent B) were used. Aziridine **5.25**, **GC** yield 32%. Oxidation product **5.30**, **GC** yield 3%.

Entry 3 Synthetic procedure **7.5c** was followed. Toluene (solvent A) and THF (solvent B) were used. Pyrrolidine **5.29**, **GC** conversion, 20%.

Entry 4 Synthetic procedure **7.5c** was followed. Xylenes (solvent A) and THF (solvent B) which was changed to DMF (2 ml, solvent C) were used. Aziridine **5.25**, **GC** conversion 21%. Oxidation product **5.27**, **GC** conversion 23%. Azetidine **5.28**, **GC** conversion 4%. Pyrrolidine **5.29**, **GC** conversion < 1%.

Entry 5 Synthetic procedure **7.5c** was followed. Xylenes (solvent A) and anisole (solvent B) were used. The solution of ylide **5.20** was added in one portion. No reaction was observed via **GC** analysis.

7.5.1.6 Synthesis of secondary amine hydrochloride salts

Synthetic Procedure 7.5d

The method of Abdel-Magid[186] was followed with minor modifications for the synthesis of secondary amines through reductive amination, as described below:
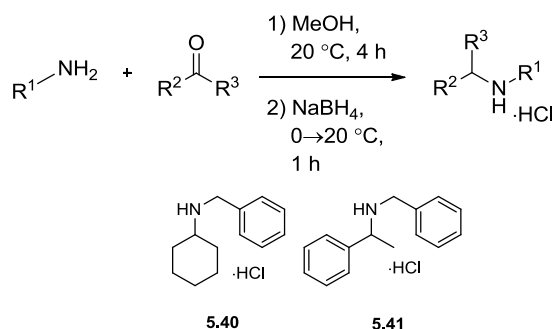
The amine (1.06 equiv.) was added to a solution of the ketone (1.0 equiv.) in anhydrous methanol (0.25M) and the reaction mixture was stirred under a nitrogen atmosphere at 20 °C for 4 hours. After complete consumption of the starting material by TLC analysis, the reaction was cooled to 0 °C. Sodium borohydride (1.6 equiv.) was added portionwise to the resulting mixture, which was subsequently allowed to warm to 20 °C and stirred for 1 hour. The reaction was quenched with 1M sodium hydroxide solution. The organic phase was

extracted with diethylether (3 x 150 mL) and washed with saturated sodium chloride solution (100 mL) and dried over anhydrous magnesium sulfate. The crude product obtained after the removal of solvent in vacuo was diluted in ether and isolated as hydrochloride salt, by acidification with 2M ethanolic hydrochloric acid solution and recrystalisation of the resulting solid.

3.2.3.1.2.   *N*-Benzyl cyclohexylamine hydrochloride salt[201-203]

Synthetic procedure **7.5d** was followed. Benzylamine (2.38 mL, 21.2 mmol, 1.06 equiv.); cyclohexanone (2.06 mL, 20 mmol, 1.0 equiv.); anhydrous methanol (80 mL); sodium borohydride (1.22 g, 32.0 mmol, 1.6 equiv.). The crude product obtained was a yellow oil (4.00 g). Acidification and recrystallisation from acetonitrile gave the title compound as colourless crystalline plates (3.31 g, 15.7 mmol, 79%).[201-203] **m.p.** (acetonitrile-ethanol): >230 °C (lit. 283-284 °C)[202]. **^{1}H NMR** (300 MHz, 298 K, CDCl$_3$): δ = 9.76 (2H, s, NH$_2$), 7.63 (2H, d, J = 7.2 Hz, C2H), 7.39 (t, J = 7.3 Hz, 2H, C3H), 7.34 (d, J = 7.3 Hz, 1H, C1H), 3.97 (s, 2H, C5H$_2$), 2.74 (1H, tt, J = 11.0, 3.3 Hz, C6H), 2.16 (1H, d, J = 10.7 Hz, C9H$_a$), 1.79 (1H, d, J = 12.8 Hz, C9H$_b$), 1.67-1.54 (4H, m, 2C7H$_2$), 1.32-1.02 (4H, m, 2C8H$_2$). **^{13}C NMR** (75 MHz, 298 K, CDCl$_3$): δ = 130.9 (*C2*), 130.5 (C6), 129.5 (C2), 129.3 (*C1*), 55.4 (C6), 47.4 (C5), 29.1 (C9), 25.0 (C8), 24.7 (C7). **ESI-MS** (ES+ mode): m/z = 190.1 [(M-Cl)$^+$, 100%]. **HRMS** (ES+ mode): m/z = 190.1590 [M-Cl$^-$, 100%]; calculated for C$_{13}$H$_{20}$N [(M-Cl)$^+$]: m/z = 190.1596. **IR** (solid): ν = 3200, 3050-2400, 2448, 1945, 1590, 1452, 1380, 997, 748, 692, 504 cm^{-1}.
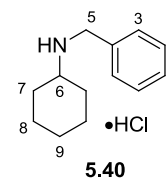
3.2.3.1.3.   *N*-Benzyl-α-methyl-benzylamine hydrochloride salt[201]

Synthetic procedure **7.5d** was followed. α-methyl benzylamine (1.35 mL, 10.5 mmol, 1.05 equiv.); benzaldehyde (1.02 mL, 10.0 mmols, 1.0 equiv.); anhydrous methanol (40 mL); sodium borohydride (646 mg, 17.1 mmol, 1.71 equiv.). Acidification and recrystallisation from acetonitrile–petroleum ether gave the title compound as yellow crystalline needles (2.45 g, 9.87 mmols, 99%). **m.p.** (acetonitrile-petroleum ether) 165-168 °C. **^{1}H NMR** (500 MHz, CD$_3$OD) δ 7.62 – 7.51 (m, 5H, C*Ar*H), 7.51-7.31 (m, 5H, C*Ar*H), 4.49 (q, J = 6.8 Hz, 1H, C5H), 4.17 (d, J = 13.1 Hz, 1H, C7H$_a$), 3.95 (d, J = 13.2 Hz, 1H, C7H$_b$), 1.76 (d, J = 6.9 Hz, 3H, C6H$_3$). **^{13}C NMR** (75 MHz, CD$_3$OD) δ: 135.8 (C8), 130.6 (*C4*), 129.4 (C*Ar*), 129.2 (C*Ar*), 128.2 (C*Ar*), 128.0 (C*Ar*), 127.5 (C*Ar*), 127.4 (C*Ar*), 70.5 (C6), 49.1 (C7), 16.3 (C5). **ESI-MS** (ES+ mode): m/z = 212 [(M-Cl)$^+$, 100%]. **HRMS**
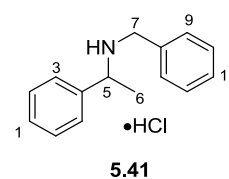
(ES+ mode): m/z = 212.1106 [M-Cl⁻, 100%]; calculated for $C_{15}H_{18}N$ [(M-Cl)⁺]: m/z = 212.1439. **IR** (solid): ν = 3405, 2940, 2720, 1598 cm⁻¹.

7.5.2 Attempted deprotection of secondary amines

Synthetic Procedure 7.5e

A general synthetic procedure was followed with slight modifications for the attempted deprotection of secondary amines. The procedure is described briefly below:
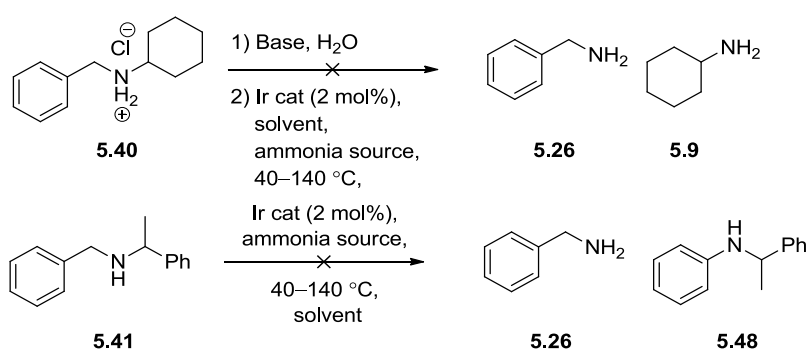
The amine hydrochloride salt was dissolved in solvent, the free base formed using a carbonate base and the resulting organics were extracted with ethyl acetate and or diethyl ether (50 mL). The combined organics were washed with water and then concentrated *in vacuo* to give the crude free amine, as a yellow oil. The crude free amine was added to a suspension of the solvent, ammonia source and iridium catalyst and heated either open to air or under pressure in a sealed tube for 1-7 days. The reaction was then poured into water (50 mL) and the organics extracted with dichloromethane (3 x 50 mL). The combined organics were then dried (magnesium sulfate), filtered and the solvent removed *in vacuo* to give the crude reaction mixture, which was then analysed by ¹H-NMR and/or LC-MS analysis to monitor the conversion to the desired primary amines. No primary amine was observed during **¹H-NMR** or **LC-MS** analysis.

Entry	Amine	Nucleophile Source	Temp / °C	Solvent	Sealed Tube	Yield of deprotected amine / %
1 [a]	**5.40**	NH_4OAc	110	PhMe	No	0
2	**5.40**	NH_4OH	55	MeCN	Yes	0
3	**5.40**	NH_4OAc	82	MeCN	No	0
4	**5.40**	NH_4OAc	90	*i*PrOH	Yes	0
5	**5.41**	NH_4OH	90	*i*PrOH	Yes	0
6	**5.41**	NH_3	40	*i*PrOH	Yes	0
7	**5.40**	$NH_2OH \cdot HCl$, Na_2CO_3	Reflux	MeOH	No	0
8	**5.41**	$NH_2OH(aq)$	Reflux	CH_2Cl_2	No	0
9	**5.40**	$NH_2OH \cdot HCl$, Na_2CO_3 (in CH_2Cl_2)[b]	Reflux	xylenes	No	0
10	**5.40**	$NH_2OH \cdot HCl$	Reflux	PhMe	No	0
11	**5.40**	$NH_2OH \cdot HCl$	Reflux	MeCN	No	0
12	**5.40**	$NH_2OH \cdot HCl$	Reflux	THF	No	0
13	**5.40**	$NH_2OH \cdot HCl$	Reflux	^nBuOAc	No	0
14	**5.40**	$NH_2OH \cdot HCl$	Reflux	H_2O	No	0
15	**5.40**	$NH_2OH \cdot HCl$, Na_2CO_3 (in CH_2Cl_2)	Reflux	xylenes	No	0
16	**5.40**	NH_4OH, Na_2CO_3 (in MeCN)	Reflux	xylenes	No	0

[a] Formed *in situ from* iridium complex **5.1a** and KI.

[b] Dropwise addition of amine to reaction.

Entry 1 Synthetic Procedure **7.5e** was followed. *N*-Cyclohexyl benzylamine hydrochloride salt (897 mg, 3.97 mmols, 1.00 equiv.), sodium hydroxide (aqueous, 2 N, 50 mL) and ethyl acetate (3 x 50 mL) were used to form the crude free amine as an oil. The crude free amine, dichloropentamethylcyclopentadienyliridium(III) dimer complex (37.1 mg, 46.5 μmols, 1 mol%), potassium iodide (16.2 mg, 97.6 μmols, 2 mol%), ammonium acetate (1.33 g,

17.3 mmols, 4.36 equiv.) and toluene (8 mL) were used and heated to reflux for one day. The reaction was poured into water (50 mL) and the organics extracted with ethyl acetate (2 x 50 mL) and dichloromethane (3 x 50 mL), the combined organics were dried magnesium sulfate, filtered and the solvent removed *in vacuo* to give the crude reaction mixture as a light brown oil. The crude was analysed by **¹H NMR** and **LC-MS** and no reaction was observed.

Entry 2 Synthetic Procedure **7.5e** was followed. *N*-Cyclohexyl benzylamine hydrochloride salt (387 mg, 1.71 mmols, 1.00 equiv.), sodium carbonate (saturated aqueous, 125 mL), ethyl acetate (50 mL) and diethyl ether (2 x 30 mL) were used to form the crude free amine as an oil. The crude free amine, diiodopentamethylcyclopentadienyliridium(III) dimer complex (26.8 mg, 23.0 μmols, 1 mol%), aqueous ammonia (35% w/w, 1.13 mL, 10 mmol, 5 equiv.) and acetonitrile (3 mL), were used and heated in a sealed tube by an oil bath (55 °C) for one day and a colourless precipitate formed for the attempted deprotection. The reaction was poured into water (50 mL) and the organics extracted with ethyl acetate (2 x 50 mL) and dichloromethane (3 x 50 mL), the combined organics were dried magnesium sulfate, filtered and the solvent removed *in vacuo* to give the crude reaction mixture as a light brown oil. The crude was analysed by **¹H NMR** and **LC-MS** and no reaction was observed.

Entry 3 Synthetic Procedure **7.5e** was followed. *N*-Cyclohexyl benzylamine hydrochloride salt (372 mg, 1.62 mmols, 1.00 equiv.), sodium hydrogen carbonate (saturated aqueous, 100 mL) and ethyl acetate (3 x 100 mL) were used to form the crude free amine as an oil. The crude free amine, diiodopentamethylcyclopentadienyliridium(III) dimer complex (27.4 mg, 23.6 μmols, 1 mol%), ammonium acetate (770 mg, 10 mmols, 6.17 equiv.) and acetonitrile (4 mL) were used and heated to reflux for five days for the attempted deprotection. The reaction was monitored by GC-MS and LC-MS. The reaction was poured into water (50 mL) and the organics extracted with ethyl acetate (3 x 150 mL), the combined organics were dried (magnesium sulfate), filtered and the solvent removed in vacuo to give a brown oil. The crude was analysed by **¹H NMR** and **LC-MS** and no reaction was observed.

Entry 4 Synthetic Procedure **7.5e** was followed. *N*-Cyclohexyl benzylamine hydrochloride salt (453 mg, 2.00 mmols, 1.00 equiv.), sodium hydrogen carbonate (saturated aqueous, 200 mL), ethyl acetate (150 mL), ethyl acetate–diethyl ether (1:1, 2 x 150 mL) and water (150 mL) were used to form the crude free amine as an oil. The crude free amine, diiodopentamethylcyclopentadienyliridium(III) dimer complex (26.9 mg, 23.1 μmols,

1 mol%), ammonium acetate (800 mg, 10.4 mmols, 5. 2 equiv.) and isopropanol (2 mL) were used and heated in a sealed tube by an oil bath (90 °C) for one day, then the temperature was raised (100 °C) for a total of 3.5 days for the attempted deprotection. The reaction was poured into water (50 mL) and the organics extracted with dichloromethane (100 mL), then ethyl acetate–diethyl ether (1:1, 3 x 100 mL). The combined organics were dried (sodium sulfate), filtered and the solvent removed *in vacuo* to give a brown solid as crude. The crude was analysed by **¹H NMR** and **LC-MS** and no reaction was observed.

Entry 5 Synthetic Procedure **7.5e** was followed. *N*-Cyclohexyl benzylamine hydrochloride salt (453 mg, 2.00 mmols, 1.00 equiv.), sodium hydrogen carbonate (saturated aqueous, 200 mL), ethyl acetate (150 mL), ethyl acetate–diethyl ether (1:1, 2 x 150 mL) and water (150 mL) were used to form the crude free amine as an oil. Ammonia was condensed and dissolved into isopropanol. The crude free amine, diiodopentamethylcyclopentadienyliridium(III) dimer complex (26.9 mg, 23.1 μmols, 1 mol%), aqueous ammonia (35% w/w, 1.13 mL, 10 mmol, 5 equiv.) in isopropanol (2 mL) were used and heated in a sealed tube by an oil bath (90 °C) for one day. The reaction was poured into water (50 mL) and the organics extracted with dichloromethane (100 mL), then ethyl acetate–diethyl ether (1:1, 3 x 100 mL). The combined organics were dried (sodium sulfate), filtered and the solvent removed *in vacuo* to give a brown solid as crude. The crude was analysed by **¹H NMR** and **LC-MS** and no reaction was observed.

Entry 6 Synthetic Procedure **7.5e** was followed. *N*-benzyl-a-methyl benzylamine hydrochloride salt (424 mg, 2.00 mmols, 1.00 equiv.), sodium hydrogen carbonate (saturated aqueous, 200 mL), ethyl acetate (150 mL), ethyl acetate–diethyl ether (1:1, 2 x 150 mL) and water (150 mL) were used to form the crude free amine as an oil. Ammonia was condensed and dissolved into isopropanol. The crude free amine, diiodopentamethylcyclopentadienyliridium(III) dimer complex (26.9 mg, 23.1 μmols, 1 mol%), ammonium dissolved in isopropanol (800 mg, 10.4 mmols, 5.2 equiv.) and isopropanol (2 mL) were used and heated in a sealed tube by an oil bath (90 °C) for one day. The reaction was poured into water (50 mL) and the organics extracted with dichloromethane (100 mL), then ethyl acetate–diethyl ether (1:1, 3 x 100 mL). The combined organics were dried (sodium sulfate), filtered and the solvent removed *in vacuo* to give a brown solid as crude. The crude was analysed by **¹H NMR** and **LC-MS** and no reaction was observed.

Entry 7 Synthetic Procedure **7.5e** was followed. *N*-Cyclohexyl benzylamine hydrochloride salt (453 mg, 2.00 mmols, 1.00 equiv.), sodium hydrogen carbonate (saturated aqueous, 200 mL), ethyl acetate (150 mL), ethyl acetate–diethyl ether (1:1, 2 x 150 mL) and water (150 mL) were used to form the crude free amine as an oil. The crude free amine, diiodopentamethylcyclopentadienyliridium(III) dimer complex (26.9 mg, 23.1 μmols, 1 mol%), hydroxylamine hydrochloride (695 mg, 10.0 mmols, 5.00 equiv.), sodium carbonate (1.06 g, 10.0 mmols, 5 equiv.) and methanol (4 mL) were used and heated to reflux for one day. The reaction was poured into water (50 mL) and the organics extracted with dichloromethane (100 mL), then ethyl acetate-diethyl ether (1:1, 3 x 100 mL). The combined organics were dried (sodium sulfate), filtered and the solvent removed *in vacuo* to give a brown oil. The crude was analysed by **^{1}H NMR** and **LC-MS** and no reaction was observed.

Entry 8 Synthetic Procedure **7.5e** was followed. *N*-Cyclohexyl benzylamine hydrochloride salt (453 mg, 2.00 mmols, 1.00 equiv.), sodium hydrogen carbonate (saturated aqueous, 200 mL), ethyl acetate (150 mL), ethyl acetate–diethyl ether (1:1, 2 x 150 mL) and water (150 mL) were used to form the crude free amine as an oil. The crude free amine, diiodopentamethylcyclopentadienyliridium(III) dimer complex (26.9 mg, 23.1 μmols, 1 mol%), aqueous hydroxylamine (50 wt %, 1 mL, 16.3 mmols, 8.15 equiv.) and dichloromethane (4 mL) were used and heated to reflux for one day. The reaction was poured into water (50 mL) and the organics extracted with dichloromethane (100 mL), then ethyl acetate–diethyl ether (1:1, 3 x 100 mL). The combined organics were dried over sodium sulfate, filtered and the solvent removed *in vacuo* to give a brown oil as crude. The crude was analysed by **^{1}H NMR** and **LC-MS** and no reaction was observed.

Entry 9 Synthetic Procedure **7.5e** was followed. *N*-Cyclohexyl benzylamine hydrochloride salt (453 mg, 2.00 mmols, 1.00 equiv.), sodium hydrogen carbonate (saturated aqueous, 200 mL), ethyl acetate (150 mL), ethyl acetate–diethyl ether (1:1, 2 x 150 mL) and water (150 mL) were used to form the crude free amine as an oil. The crude free amine, diiodopentamethylcyclopentadienyliridium(III) dimer complex (26.9 mg, 23.1 μmols, 1 mol%), hydroxylamine hydrochloride (695 mg, 10.0 mmols, 5.00 equiv.) in dichloromethane (0.5 mL, added dropwise over two hours once at temperature) and xylenes (2 mL) were used and heated to reflux for two days. The reaction was poured into water (50 mL) and the organics extracted with dichloromethane (100 mL), then ethyl acetate–diethyl ether (1:1, 3 x 100 mL). The combined organics were dried (sodium sulfate), filtered and the solvent removed *in vacuo* to give a brown solid as crude. The crude was analysed by **^{1}H NMR** and **LC-MS** and no reaction was observed.

Entry 10 Synthetic Procedure **7.5e** was followed. *N*-Cyclohexyl benzylamine hydrochloride salt (453 mg, 2.00 mmols, 1.00 equiv.), sodium hydrogen carbonate (saturated aqueous, 200 mL), ethyl acetate (150 mL), ethyl acetate–diethyl ether (1:1, 2 x 150 mL) and water (150 mL) were used to form the crude free amine as an oil. The crude free amine, diiodopentamethylcyclopentadienyliridium(III) dimer complex (26.9 mg, 23.1 μmols, 1 mol%), hydroxylamine hydrochloride (695 mg, 10.0 mmols, 5.00 equiv.) and toluene (2 mL) were used and to reflux for two days. The reaction was poured into water (50 mL) and the organics extracted with dichloromethane (100 mL), then ethyl acetate–diethyl ether (1:1, 3 x 100 mL). The combined organics were dried (sodium sulfate), filtered and the solvent removed *in vacuo* to give a brown solid as crude. The crude was analysed by ^{1}H NMR and **LC-MS** and no reaction was observed.

Entry 11 Synthetic Procedure **7.5e** was followed. *N*-Cyclohexyl benzylamine hydrochloride salt (453 mg, 2.00 mmols, 1.00 equiv.), sodium hydrogen carbonate (saturated aqueous, 200 mL), ethyl acetate (150 mL), ethyl acetate–diethyl ether (1:1, 2 x 150 mL) and water (150 mL) were used to form the crude free amine as an oil. The crude free amine, diiodopentamethylcyclopentadienyliridium(III) dimer complex (26.9 mg, 23.1 μmols, 1 mol%), hydroxylamine hydrochloride (695 mg, 10.0 mmols, 5.00 equiv.) and acetonitrile (2 mL) were used and heated to reflux for two days. The reaction was poured into water (50 mL) and the organics extracted with dichloromethane (100 mL), then ethyl acetate–diethyl ether (1:1, 3 x 100 mL). The combined organics were dried (sodium sulfate), filtered and the solvent removed *in vacuo* to give a brown solid as crude. The crude was analysed by ^{1}H NMR and **LC-MS** and no reaction was observed.

Entry 12 Synthetic Procedure **7.5e** was followed. *N*-Cyclohexyl benzylamine hydrochloride salt (453 mg, 2.00 mmols, 1.00 equiv.), sodium hydrogen carbonate (saturated aqueous, 200 mL), ethyl acetate (150 mL), ethyl acetate–diethyl ether (1:1, 2 x 150 mL) and water (150 mL) were used to form the crude free amine as an oil. The crude free amine, diiodopentamethylcyclopentadienyliridium(III) dimer complex (26.9 mg, 23.1 μmols, 1 mol%), hydroxylamine hydrochloride (695 mg, 10.0 mmols, 5.00 equiv.) and THF (2 mL) were used and heated to reflux for two days. The reaction was poured into water (50 mL) and the organics extracted with dichloromethane (100 mL), then ethyl acetate–diethyl ether (1:1, 3 x 100 mL). The combined organics were dried (sodium sulfate), filtered and the solvent removed *in vacuo* to give a brown solid as crude. The crude was analysed by ^{1}H NMR and **LC-MS** and no reaction was observed.

Entry 13 Synthetic Procedure **7.5e** was followed. *N*-Cyclohexyl benzylamine hydrochloride salt (453 mg, 2.00 mmols, 1.00 equiv.), sodium hydrogen carbonate (saturated aqueous, 200 mL), ethyl acetate (150 mL), ethyl acetate–diethyl ether (1:1, 2 x 150 mL) and water (150 mL) were used to form the crude free amine as an oil. The crude free amine, diiodopentamethylcyclopentadienyliridium(III) dimer complex (26.9 mg, 23.1 μmols, 1 mol%), hydroxylamine hydrochloride (695 mg, 10.0 mmols, 5.00 equiv.) and n-butyl acetate (2 mL) were used and heated to reflux for two days. The reaction was poured into water (50 mL) and the organics extracted with dichloromethane (100 mL), then ethyl acetate–diethyl ether (1:1, 3 x 100 mL). The combined organics were dried (sodium sulfate), filtered and the solvent removed *in vacuo* to give a brown solid as crude. The crude was analysed by **^{1}H NMR** and **LC-MS** and no reaction was observed.

Entry 14 Synthetic Procedure **7.5e** was followed. *N*-Cyclohexyl benzylamine hydrochloride salt (453 mg, 2.00 mmols, 1.00 equiv.), sodium hydrogen carbonate (saturated aqueous, 200 mL), ethyl acetate (150 mL), ethyl acetate–diethyl ether (1:1, 2 x 150 mL) and water (150 mL) were used to form the crude free amine as an oil. The crude free amine, diiodopentamethylcyclopentadienyliridium(III) dimer complex (26.9 mg, 23.1 μmols, 1 mol%), hydroxylamine hydrochloride (695 mg, 10.0 mmols, 5.00 equiv.) and water (2 mL) were used and heated to reflux for two days. The reaction was poured into water (50 mL) and the organics extracted with dichloromethane (100 mL), then ethyl acetate–diethyl ether (1:1, 3 x 100 mL). The combined organics were dried (sodium sulfate), filtered and the solvent removed *in vacuo* to give a brown solid as crude. The crude was analysed by **^{1}H NMR** and **LC-MS** and no reaction was observed.

Entry 15 Synthetic Procedure **7.5e** was followed. *N*-Cyclohexyl benzylamine hydrochloride salt (453 mg, 2.00 mmols, 1.00 equiv.), sodium hydrogen carbonate (saturated aqueous, 200 mL), ethyl acetate (150 mL), ethyl acetate–diethyl ether (1:1, 2 x 150 mL) and water (150 mL) were used to form the crude free amine as an oil. The crude free amine, diiodopentamethylcyclopentadienyliridium(III) dimer complex (26.9 mg, 23.1 μmols, 1 mol%), hydroxylamine hydrochloride (695 mg, 10.0 mmols, 5.00 equiv.) in dichloromethane (0.5 mL) and xylenes (2 mL) were used and heated to reflux for two days. The reaction was poured into water (50 mL) and the organics extracted with dichloromethane (100 mL), then ethyl acetate-diethyl ether (1:1, 3 x 100 mL). The combined organics were dried (sodium sulfate), filtered and the solvent removed *in vacuo* to give a brown solid as crude. The crude was analysed by **^{1}H NMR** and **LC-MS** and no reaction was observed.

Entry 16 Synthetic Procedure **7.5e** was followed. *N*-Cyclohexyl benzylamine hydrochloride salt (453 mg, 2.00 mmols, 1.00 equiv.), sodium hydrogen carbonate (saturated aqueous, 200 mL), ethyl acetate (150 mL), ethyl acetate–diethyl ether (1:1, 2 x 150 mL) and water (150 mL) were used to form the crude free amine as an oil. The crude free amine, diiodopentamethylcyclopentadienyliridium(III) dimer complex (26.9 mg, 23.1 μmols, 1 mol%), hydroxylamine hydrochloride (695 mg, 10.0 mmols, 5.00 equiv.) in acetonitrile (0.5 mL) and xylenes (2 mL) were used and heated to reflux for two days. The reaction was poured into water (50 mL) and the organics extracted with dichloromethane (100 mL), then ethyl acetate–diethyl ether (1:1, 3 x 100 mL). The combined organics were dried (sodium sulfate), filtered and the solvent removed *in vacuo* to give a brown solid as crude. The crude was analysed by **¹H NMR** and **LC-MS** and no reaction was observed.

References

1. E. Vitaku, E. A. Ilardi and J. T. Njarðarson, *Top 200 Pharmaceutical Products by US Retail Sales in 2011*, http://cbc.arizona.edu/njardarson/group/sites/default/files/Top%20200%20Pharmac eutical%20Products%20by%20US%20Retail%20Sales%20in%202011_small_0.pdf , Accessed 03/04, 2014.

2. W. H. Organization, *Asthma Fact Sheet*, http://web.archive.org/web/20110629035454/http://www.who.int/mediacentre/facts heets/fs307/en/, Accessed 04/04, 2014.

3. M. Breuer, K. Ditrich, T. Habicher, B. Hauer, M. Keßeler, R. Stürmer and T. Zelinski, *Angew. Chem., Int. Ed.*, 2004, **43**, 788-824.

4. J. P. Clayden, N. Greeves, S. Warren and P. D. Wothers, *Organic Chemistry*, Oxford University Press, Oxford, 2001.

5. S. Aalla, G. Gilla, D. S. Metil, R. R. Anumula, P. R. Vummenthala and P. R. Padi, *Org. Process. Res. Dev.*, 2012, **16**, 240-243.

6. D. P. Elder, A. M. Lipczynski and A. Teasdale, *J. Pharm. Biomed. Anal.*, 2008, **48**, 497-507.

7. D. P. Elder, A. Teasdale and A. M. Lipczynski, *J. Pharm. Biomed. Anal.*, 2008, **46**, 1-8.

8. J. J. Li, D. S. Johnson, D. R. Sliskovic and B. D. Roth, *Contemporary Drug Synthesis*, Wiley Interscience, 2004.

9. X. Li, R. K. Russell, J. Spink, S. Ballentine, C. Teleha, S. Branum, K. Wells, D. Beauchamp, R. Patch, H. Huang, M. Player and W. Murray, *Org. Process. Res. Dev.*, 2014, **18**, 321-330.

10. J. Magano and J. R. Dunetz, *Org. Process. Res. Dev.*, 2012, **16**, 1156-1184.

11. W.-C. Shieh, G.-P. Chen, S. Xue, J. McKenna, X. Jiang, K. Prasad, O. Repič, C. Straub and S. K. Sharma, *Org. Process. Res. Dev.*, 2007, **11**, 711-715.

12. G. Guercio, A. M. Manzo, M. Goodyear, S. Bacchi, S. Curti and S. Provera, *Org. Process. Res. Dev.*, 2009, **13**, 489-493.

13. Assessment and Control of DNA Reactive (Mutagenic) Impurities in Pharmaceuticals to Limit Potential Carcinogenic Risk M7 obtained from: http://www.ich.org/fileadmin/Public_Web_Site/ICH_Products/Guidelines/Multidisc iplinary/M7/M7_Step_2.pdf last accessed on 12/03/2014.

14.   D. H. R. Barton, A. Billion and J. Boivin, *Tetrahedron Lett.*, 1985, **26**, 1229-1232.

15.   J. Gutzwiller, G. Pizzolato and M. Uskokovic, *J. Am. Chem. Soc.*, 1971, **93**, 5907-5908.

16.   S. Murahashi, T. Naota and K. Yonemura, *J. Am. Chem. Soc.*, 1988, **110**, 8256-8258.

17.   Z. Li and C.-J. Li, *Eur. J. Org. Chem.*, 2005, **2005**, 3173-3176.

18.   A. J. Blacker, in *Handbook of Homogeneous Hydrogenation*, eds. J. G. de Vries and C. J. Elsevier, Wiley-VCH, Weinheim, Editon edn., 2007, vol. 3, pp. 1215-1244.

19.   F. Zaera, *Acc. Chem. Res.*, 2009, **42**, 1152-1160.

20.   M. Studer, H.-U. Blaser and C. Exner, *Adv. Synth. Catal.*, 2003, **345**, 45-65.

21.   M. Heitbaum, F. Glorius and I. Escher, *Angew. Chem., Int. Ed.*, 2006, **45**, 4732-4762.

22.   J. A. Osborn, F. H. Jardine, J. F. Young and G. Wilkinson, *J. Chem. Soc. A: Inorg. Phy. Theo. Chem.*, 1966, 1711-1732.

23.   A. Miyashita, A. Yasuda, H. Takaya, K. Toriumi, T. Ito, T. Souchi and R. Noyori, *J. Am. Chem. Soc.*, 1980, **102**, 7932-7934.

24.   G. Bringmann, A. J. Price Mortimer, P. A. Keller, M. J. Gresser, J. Garner and M. Breuning, *Angew. Chem., Int. Ed.*, 2005, **44**, 5384-5427.

25.   R. Noyori and H. Takaya, *Acc. Chem. Res.*, 1990, **23**, 345-350.

26.   W. Tang and X. Zhang, *Chem. Rev.*, 2003, **103**, 3029-3070.

27.   T. P. Dang and H. B. Kagan, *J. Chem. Soc. D: Chem. Commun.*, 1971, 481-481.

28.   F. Spindler; and H.-U. Blaser, *Enantioselective Hydrogenation of C=N Functions and Enamines*, Wiley-VCH, 2007.

29.   F. Spindler;, B. Pugin; and H.-U. Blaser, *Angew. Chem., Int. Ed.*, 1990, **29**, 558-559.

30.   H.-U. Blaser, H.-P. Buser, K. Coers, R. Hanreich, H.-P. Jalett, E. Jelsch, B. Pugin, H.-D. Schneider, F. Spindler and A. Wegmann, *CHIMIA International Journal for Chemistry*, 1999, **53**, 275-280.

31.   H.-U. Blaser, *Adv. Synth. Catal.*, 2002, **344**, 17-31.

32. R. Dorta, D. Broggini, R. Stoop, H. Rüegger, F. Spindler and A. Togni, *Chem. Eur. J.*, 2004, **10**, 267-278.

33. Z. Han, Z. Wang, X. Zhang and K. Ding, *Tetrahedron: Asymmetry*, 2010, **21**, 1529-1533.

34. A. Baeza and A. Pfaltz, *Chem. Eur. J.*, **16**, 4003-4009.

35. G. Brieger and T. J. Nestrick, *Chem. Rev.*, 1974, **74**, 567-580.

36. G. Zassinovich, G. Mestroni and S. Gladiali, *Chem. Rev.*, 1992, **92**, 1051-1069.

37. M. H. S. A. Hamid, P. A. Slatford and J. M. J. Williams, *Adv. Synth. Catal.*, 2007, **349**, 1555-1575.

38. A. J. A. Watson and J. M. J. Williams, *Science*, 2010, **329**, 635-636.

39. G. E. Dobereiner and R. H. Crabtree, *Chem. Rev.*, 2009, **110**, 681-703.

40. G. Guillena, D. J. Ramón and M. Yus, *Chem. Rev.*, 2009, **110**, 1611-1641.

41. S. Pan and T. Shibata, *ACS Catalysis*, 2013, **3**, 704-712.

42. C. Gunanathan and D. Milstein, *Science*, 2013, **341**.

43. K. R. Campos, *Chem. Soc. Rev.*, 2007, **36**, 1069-1084.

44. S.-I. Murahashi and D. Zhang, *Chem. Soc. Rev.*, 2008, **37**, 1490-1501.

45. S. Bähn, S. Imm, L. Neubert, M. Zhang, H. Neumann and M. Beller, *ChemCatChem*, 2011, **3**, 1853-1864.

46. S. E. Clapham, A. Hadzovic and R. H. Morris, *Coord. Chem. Rev.*, 2004, **248**, 2201-2237.

47. C. F. de Graauw, J. A. Peters, H. van Bekkum and J. Huskens, *Synthesis*, 1994, **1994**, 1007,1017.

48. H. Meerwein and R. Schmidt, *Leibigs Ann.*, 1925, **444**, 221-238.

49. W. Ponndorf, *Angew. Chem.*, 1926, **39**, 138-143.

50. A. Verley, *Bull. Soc. Chim. Fr.*, 1925, **37**.

51. N. Uematsu, A. Fujii, S. Hashiguchi, T. Ikariya and R. Noyori, *J. Am. Chem. Soc.*, 1996, **118**, 4916-4917.

52. R. L. Chowdhury and J.-E. Backvall, *J. Chem. Soc., Chem. Commun.*, 1991, 1063-1064.

53. J. S. M. Samec, A. H. Éll, J. B. Åberg, T. Privalov, L. Eriksson and J.-E. Bäckvall, *J. Am. Chem. Soc.*, 2006, **128**, 14293-14305.

54. A. J. Blacker and B. J. Mellor, *US Pat.*, *Transfer hydrogenation process and catalyst*, US6545188 B2, 1998.

55. J. Mao and D. C. Baker, *Org. Lett.*, 1999, **1**, 841-843.

56. N. J. Turner, *Chem. Rev.*, 2011, **111**, 4073-4087.

57. M. Largeron and M.-B. Fleury, *Science*, 2013, **339**, 43-44.

58. S. O. Sablin, V. Yankovskaya, S. Bernard, C. N. Cronin and T. P. Singer, *Eur. J. Biochem.*, 1998, **253**, 270-279.

59. M. Alexeeva, A. Enright, M. J. Dawson, M. Mahmoudian and N. J. Turner, *Angew. Chem., Int. Ed.*, 2002, **41**, 3177-3180.

60. C. J. Dunsmore, R. Carr, T. Fleming and N. J. Turner, *J. Am. Chem. Soc.*, 2006, **128**, 2224-2225.

61. R. Carr, M. Alexeeva, M. J. Dawson, V. Gotor-Fernández, C. E. Humphrey and N. J. Turner, *ChemBioChem*, 2005, **6**, 637-639.

62. D. Ghislieri, D. Houghton, A. P. Green, S. C. Willies and N. J. Turner, *ACS Catalysis*, 2013, 2869-2872.

63. V. Köhler, K. R. Bailey, A. Znabet, J. Raftery, M. Helliwell and N. J. Turner, *Angew. Chem., Int. Ed.*, 2010, **49**, 2182-2184.

64. V. Köhler, Y. M. Wilson, M. Dürrenberger, D. Ghislieri, E. Churakova, T. Quinto, L. Knörr, D. Häussinger, F. Hollmann, N. J. Turner and T. R. Ward, *Nat. Chem.*, 2013, **5**, 93-99.

65. R. Grigg, T. R. B. Mitchell, S. Sutthivaiyakit and N. Tongpenyai, *J. Chem. Soc., Chem. Commun.*, 1981, 611-612.

66. A. Loupy, D. Monteux, A. Petit, J. M. Aizpurua, E. Domínguez and C. Palomo, *Tetrahedron Lett.*, 1996, **37**, 8177-8180.

67. M. Kitamura, D. Lee, S. Hayashi, S. Tanaka and M. Yoshimura, *J. Org. Chem.*, 2002, **67**, 8685-8687.

68. X. Yang, L. Zhao, T. Fox, Z.-X. Wang and H. Berke, *Angew. Chem., Int. Ed.*, **49**, 2058-2062.

69.   K.-i. Fujita, N. Tanino and R. Yamaguchi, *Org. Lett.*, 2006, **9**, 109-111.

70.   J. S. M. Samec, A. H. Éll and J.-E. Bäckvall, *Chem. Eur. J.*, 2005, **11**, 2327-2334.

71.   I. Ibrahem, J. S. M. Samec, J. E. Bäckvall and A. Córdova, *Tetrahedron Lett.*, 2005, **46**, 3965-3968.

72.   R. Yamaguchi, C. Ikeda, Y. Takahashi and K.-i. Fujita, *J. Am. Chem. Soc.*, 2009, **131**, 8410-8412.

73.   J. Wu, D. Talwar, S. Johnston, M. Yan and J. Xiao, *Angew. Chem., Int. Ed.*, 2013, **52**, 6983-6987.

74.   M. Stirling, J. Blacker and M. I. Page, *Tetrahedron Lett.*, 2007, **48**, 1247-1250.

75.   A. J. Blacker, Unpublished Work

76.   A. J. Blacker, M. J. Stirling and M. I. Page, *Org. Process. Res. Dev.*, 2007, **11**, 642-648.

77.   A. J. Blacker, S. Brown, B. Clique, B. Gourlay, C. E. Headley, S. Ingham, D. Ritson, T. Screen, M. J. Stirling, D. Taylor and G. Thompson, *Org. Process. Res. Dev.*, 2009, **13**, 1370-1378.

78.   W. M. J. Ma, T. D. James and J. M. J. Williams, *Org. Lett.*, 2013, **15**, 4850-4853.

79.   O. Saidi, A. J. Blacker, M. M. Farah, S. P. Marsden and J. M. J. Williams, *Chem. Commun.*, 2010, **46**, 1541-1543.

80.   S. Michlik and R. Kempe, *Nat. Chem.*, 2013, **5**, 140-144.

81.   S. Kobayashi and H. Ishitani, *Chem. Rev.*, 1999, **99**, 1069-1094.

82.   M. S. Sigman and E. N. Jacobsen, *J. Am. Chem. Soc.*, 1998, **120**, 5315-5316.

83.   J. Blacker, L. A. Clutterbuck, M. R. Crampton, C. Grosjean and M. North, *Tetrahedron: Asymmetry*, 2006, **17**, 1449-1456.

84.   A. J. Blacker, Unpublished Work

85.   J. L. García Ruano, M. Topp, J. López-Cantarero, J. Alemán, M. J. Remuiñán and M. B. Cid, *Org. Lett.*, 2005, **7**, 4407-4410.

86.   T. Okino, S. Nakamura, T. Furukawa and Y. Takemoto, *Org. Lett.*, 2004, **6**, 625-627.

87.   J. B. Sweeney, *Chem. Soc. Rev.*, 2002, **31**, 247-258.

88. F. A. Davis, H. Liu, P. Zhou, T. Fang, G. V. Reddy and Y. Zhang, *J. Org. Chem.*, 1999, **64**, 7559-7567.

89. D. L. J. Clive and R. J. Bergstra, *J. Org. Chem.*, 1991, **56**, 4976-4977.

90. D. Morales-Morales, R. o. Redón, C. Yung and C. M. Jensen, *Inorganica Chimica Acta*, 2004, **357**, 2953-2956.

91. K.-i. Fujita and R. Yamaguchi, *Synlett*, 2005, **2005**, 560-571.

92. R. Kawahara, K.-i. Fujita and R. Yamaguchi, *J. Am. Chem. Soc.*, 2012, **134**, 3643-3646.

93. R. Kawahara, K.-i. Fujita and R. Yamaguchi, *J. Am. Chem. Soc.*, 2010, **132**, 15108-15111.

94. Y. Zhang, C.-S. Lim, D. S. B. Sim, H.-J. Pan and Y. Zhao, *Angew. Chem., Int. Ed.*, 2014, **53**, 1399-1403.

95. J. P. Cooksey, S. P. Marsden and A. J. Blacker, *Unpublished Results*, 2010.

96. O. Saidi, A. J. Blacker, M. M. Farah, S. P. Marsden and J. M. J. Williams, *Angew. Chem., Int. Ed.*, 2009, **48**, 7375-7378.

97. P. Fristrup, M. Tursky and R. Madsen, *Org. Biomol. Chem.*, 2012, **10**, 2569-2577.

98. H. Li, J. Jiang, G. Lu, F. Huang and Z.-X. Wang, *Organometallics*, 2011, **30**, 3131-3141.

99. L. Neubert, D. Michalik, S. Bähn, S. Imm, H. Neumann, J. Atzrodt, V. Derdau, W. Holla and M. Beller, *J. Am. Chem. Soc.*, 2012, **134**, 12239-12244.

100. K.-i. Fujita, Z. Li, N. Ozeki and R. Yamaguchi, *Tetrahedron Lett.*, 2003, **44**, 2687-2690.

101. K. F. Morris and C. S. Johnson, *J. Am. Chem. Soc.*, 1992, **114**, 3139-3141.

102. C. S. Johnson Jr, *Prog. Nucl. Magn. Reson. Spectrosc.*, 1999, **34**, 203-256.

103. T. D. W. Claridge, *High-Resolution NMR Techniques in Organic Chemistry*, Pergamon, Oxford, 1999.

104. E. Durand, M. Clemancey, A.-A. Quoineaud, J. Verstraete, D. Espinat and J.-M. Lancelin, *Energ. Fuel.*, 2008, **22**, 2604-2610.

105. H. Barjat, G. A. Morris, S. Smart, A. G. Swanson and S. C. R. Williams, *J. Magn. Reson., Ser. B*, 1995, **108**, 170-172.

106. D. P. Hinton and C. S. Johnson, *J. Phys. Chem.*, 1993, **97**, 9064-9072.

107. K. F. Morris and C. S. Johnson Jr, *J. Am. Chem. Soc.*, 1993, **115**, 4291-4299.

108. A. Chen, D. Wu and C. S. Johnson, *J. Am. Chem. Soc.*, 1995, **117**, 7965-7970.

109. A. Jerschow and N. Müller, *Macromolecules*, 1998, **31**, 6573-6578.

110. L. H. Lucas and C. K. Larive, *Concept. Magn. Reson. A*, 2004, **20A**, 24-41.

111. A. Ambrus, K. Friedrich and Á. Somogyi, *Anal. Biochem.*, 2006, **352**, 286-295.

112. S. Viel, L. Mannina and A. Segre, *Tetrahedron Lett.*, 2002, **43**, 2515-2519.

113. Adapted from ref. 102

114. J. H. Lee, S. Gupta, W. Jeong, Y. H. Rhee and J. Park, *Angew. Chem., Int. Ed.*, 2012, **51**, 10851-10855.

115. C.-L. Chang, M.-k. Leung and M.-H. Yang, *Tetrahedron*, 2004, **60**, 9205-9212.

116. P. Falus, Z. Boros, G. Hornyánszky, J. Nagy, F. Darvas, L. Ürge and L. Poppe, *Tetrahedron Lett.*, 2011, **52**, 1310-1312.

117. M. Szostak, B. Sautier, M. Spain and D. J. Procter, *Org. Lett.*, 2014, **16**, 1092-1095.

118. H. K. Hall, *J. Am. Chem. Soc.*, 1957, **79**, 5441-5444.

119. W. H. Carothers, C. F. Bickford and G. J. Hurwitz, *J. Am. Chem. Soc.*, 1927, **49**, 2908-2914.

120. L. P. Hammett, *J. Am. Chem. Soc.*, 1937, **59**, 96-103.

121. L. F. Blackwell, A. Fischer, I. J. Miller, R. D. Topsom and J. Vaughan, *J. Chem. Soc.*, 1964, 3588-3591.

122. S. Lucas, *The Synthesis of Group 9 Complexes for Use as Transfer Hydrogenation Catalysts and Anti-Cancer Agents*, University of Leeds, 2013.

123. A.-K. Jungton, C. Herwig, T. Braun and C. Limberg, *Chem. Eur. J.*, 2012, **18**, 10009-10013.

124. A. Pictet and T. Spengler, *Chem. Ber.*, 1911, **44**, 2030-2036.

125. G. R. Humphrey and J. T. Kuethe, *Chem. Rev.*, 2006, **106**, 2875-2911.

126. G. Hahn and H. Ludewig, *Chem. Ber.*, 1934, **67**, 2031-2035.

127. E. D. Cox and J. M. Cook, *Chem. Rev.*, 1995, **95**, 1797-1842.

128. J. Stöckigt, A. P. Antonchick, F. Wu and H. Waldmann, *Angew. Chem., Int. Ed.*, **50**, 8538-8564.

129. X. Zhang, L. Han and S.-L. You, *Chem. Sci.*, 2014.

130. D. Ghislieri, A. P. Green, M. Pontini, S. C. Willies, I. Rowles, A. Frank, G. Grogan and N. J. Turner, *J. Am. Chem. Soc.*, 2013, **135**, 10863-10869.

131. K.-i. Fujita, T. Fujii and R. Yamaguchi, *Org. Lett.*, 2004, **6**, 3525-3528.

132. G. Cami-Kobeci, P. A. Slatford, M. K. Whittlesey and J. M. J. Williams, *Bioorg. Med. Chem. Lett.*, 2005, **15**, 535-537.

133. M. E. J. Taylor, P., *Lilly Reports Fourth-Quarter and Full-Year 2011 Results* Financial Report, Eli Lilly, Indianapolis, 2011.

134. F. Group, *Novartis Group Annual Report 2012*, Novartis, Basel, 2012.

135. T. Kawasaki and K. Higuchi, *Nat. Prod. Rep.*, 2005, **22**, 761-793.

136. H. Dong, R. T. Latka and T. G. Driver, *Org. Lett.*, 2011, **13**, 2726-2729.

137. C. Wang, A. Pettman, J. Bacsa and J. Xiao, *Angew. Chem., Int. Ed.*, 2010, **49**, 7548-7552.

138. S. J. Lucas, B. D. Crossley, A. J. Pettman, A. D. Vassileiou, T. E. O. Screen, A. J. Blacker and P. C. McGowan, *Chem. Commun.*, 2013, **49**, 5562-5564.

139. S.-I. Murahashi, N. Komiya, H. Terai and T. Nakae, *J. Am. Chem. Soc.*, 2003, **125**, 15312-15313.

140. T. Sakamoto, Y. Kondo, S. Iwashita, T. Nagano and H. Yamanaka, *Chem. Pharm. Bull.*, 1988, **36**, 1305-1308.

141. R. Kuwano, K. Kaneda, T. Ito, K. Sato, T. Kurokawa and Y. I. . *Org. Lett.*, 2004, **6**, 2213-2215.

142. J. E. M. N. Klein, A. Perry, D. S. Pugh and R. J. K. Taylor, *Org. Lett.*, 2010, **12**, 3446-3449.

143. M. L. Deb, S. S. Dey, I. Bento, M. T. Barros and C. D. Maycock, *Angew. Chem., Int. Ed.*, 2013, **52**, 9791-9795.

144. Price of [IrCp*Cl2]2 obatined from http://www.sigmaaldrich.com/catalog/product/aldrich/357537?lang=en&region=GB and price of copper acetate monohydrate obtained from http://www.sigmaaldrich.com/catalog/product/aldrich/229601?lang=en&region=GB accessed on 09/06/2014 at 14:14

145. G. Zotti, S. Zecchin, G. Schiavon, R. Seraglia, A. Berlin and A. Canavesi, *Chem. Mater.*, 1994, **6**, 1742-1748.

146. A. Pezzella, A. Napolitano, M. d'Ischia and G. Prota, *Tetrahedron*, 1996, **52**, 7913-7920.

147. A. Laskin and A. Lifshitz, *J. Phys. Chem. A*, 1997, **101**, 7787-7801.

148. O. S. L. Bruinsma, P. J. J. Tromp, H. J. J. de Sauvage Nolting and J. A. Moulijn, *Fuel*, 1988, **67**, 334-340.

149. J. C. Mackie, M. B. Colket, P. F. Nelson and M. Esler, *Int. J. Chem. Kinet.*, 1991, **23**, 733-760.

150. A. Lifshitz, C. Tamburu and A. Suslensky, *J. Phys. Chem.*, 1989, **93**, 5802-5808.

151. R. Yamaguchi, S. Kawagoe, C. Asai and K.-i. Fujita, *Org. Lett.*, 2007, **10**, 181-184.

152. M. A. Berliner, S. P. A. Dubant, T. Makowski, K. Ng, B. Sitter, C. Wager and Y. Zhang, *Org. Process. Res. Dev.*, 2011, **15**, 1052-1062.

153. D. Enders and J. P. Shilvock, *Chem. Soc. Rev.*, 2000, **29**, 359-373.

154. Y. Fukuta, T. Mita, N. Fukuda, M. Kanai and M. Shibasaki, *J. Am. Chem. Soc.*, 2006, **128**, 6312-6313.

155. D. Lucet, T. Le Gall and C. Mioskowski, *Angew. Chem., Int. Ed.*, 1998, **37**, 2580-2627.

156. S. R. S. Saibabu Kotti, C. Timmons and G. Li, *Chem. Biol. Drug. Des.*, 2006, **67**, 101-114.

157. T. Opatz, *Synthesis*, 2009, **2009**, 1941-1959.

158. G. Zhang, Y. Ma, G. Cheng, D. Liu and R. Wang, *Org. Lett.*, 2014, **16**, 656-659.

159. A. Lin, H. Peng, A. Abdukader and C. Zhu, *Eur. J. Org. Chem.*, 2013, **2013**, 7286-7290.

160. K. Yamaguchi, Y. Wang and N. Mizuno, *ChemCatChem*, 2013, **5**, 2835-2838.

161. D. Verma, S. Verma, A. K. Sinha and S. L. Jain, *ChemPlusChem*, 2013, **78**, 860-865.

162. N. Sakai, A. Mutsuro, R. Ikeda and T. Konakahara, *Synlett*, 2013, **24**, 1283-1285.

163. P. G. Vasudev, N. Shamala, K. Ananda and P. Balaram, *Angew. Chem., Int. Ed.*, 2005, **44**, 4972-4975.

164. C. D. Maycock, P. Rodrigues and M. R. Ventura, *J. Org. Chem.*, 2014.

165. E. J. Corey and M. Chaykovsky, *J. Am. Chem. Soc.*, 1962, **84**, 867-868.

166. A. W. Johnson and R. B. LaCount, *J. Am. Chem. Soc.*, 1961, **83**, 417-423.

167. L. Casarrubios, J. A. Pérez, M. Brookhart and J. L. Templeton, *J. Org. Chem.*, 1996, **61**, 8358-8359.

168. V. K. Aggarwal, A. Thompson, R. V. H. Jones and M. C. H. Standen, *J. Org. Chem.*, 1996, **61**, 8368-8369.

169. R. H. Smith, B. D. Wladkowski, J. A. Herling, T. D. Pfaltzgraff, J. E. Taylor, E. J. Thompson, B. Pruski, J. R. Klose and C. J. Michejda, *J. Org. Chem.*, 1992, **57**, 6448-6454.

170. J. Xu, *Tetrahedron: Asymmetry*, 2002, **13**, 1129-1134.

171. I. Coldham, A. J. Collis, R. J. Mould and D. E. Robinson, *Synthesis*, 1995, **1995**, 1147-1150.

172. O. A. Attanasi, P. Davoli, G. Favi, P. Filippone, A. Forni, G. Moscatelli and F. Prati, *Org. Lett.*, 2007, **9**, 3461-3464.

173. E. A. Ilardi and J. T. Njardarson, *J. Org. Chem.*, 2013, **78**, 9533-9540.

174. T. M. V. D. Pinho e Melo, *Eur. J. Org. Chem.*, 2006, **2006**, 2873-2888.

175. K. Urbaniak, R. Szymański, J. Romański, G. Mlostoń, M. Domagała, A. Linden and H. Heimgartner, *Helv. Chim. Acta*, 2004, **87**, 496-510.

176. P. Dauban and G. Malik, *Angew. Chem., Int. Ed.*, 2009, **48**, 9026-9029.

177. I. Ungureanu, C. Bologa, S. Chayer and A. Mann, *Tetrahedron Lett.*, 1999, **40**, 5315-5318.

178. M. Vaultier, R. Danion-Bougot, D. Danion, J. Hamelin and R. Carrie, *J. Org. Chem.*, 1975, **40**, 2990-2992.

179. M. Vaultier, R. Danion-Bougot, D. Danion, J. Hamelin and R. Carrié, *Tetrahedron Lett.*, 1973, **14**, 1923-1926.

180. S. Fujita, T. Hiyama and H. Nozaki, *Tetrahedron Lett.*, 1969, **10**, 1677-1678.

181. S. Fujita, T. Hiyama and H. Nozaki, *Tetrahedron*, 1970, **26**, 4347-4352.

182. H. W. Heine and T. Newton, *Tetrahedron Lett.*, 1967, **8**, 1859-1860.

183. P. J. Kocieński, *Protecting Groups*, 3rd edn., Georg Thieme Verlag, Stuttgart, Germany, 2004.

184. P. G. M. Wuts and T. W. Greene, *Greene's Protective Groups in Organic Synthesis, 4th Edition*, 4th edn., Wiley, Frankfurt, 2006.

185. S. Bähn, S. Imm, L. Neubert, M. Zhang, H. Neumann and M. Beller, *Chem. Eur. J.*, 2011, **17**, 4705-4708.

186. A. F. Abdel-Magid, K. G. Carson, B. D. Harris, C. A. Maryanoff and R. D. Shah, *J. Org. Chem.*, 1996, **61**, 3849-3862.

187. J. T. Lai, *J. Org. Chem.*, 1980, **45**, 3671-3673.

188. N. R. Conley, L. A. Labios, D. M. Pearson, C. C. L. McCrory and R. M. Waymouth, *Organometallics*, 2007, **26**, 5447-5453.

189. D. Armesto, M. G. Gallego, W. M. Horspool and R. Perez-Ossorio, *J. Chem. Soc. Perkin Trans. 1.*, 1986, 799-803.

190. B. E. Love and J. Ren, *J. Org. Chem.*, 1993, **58**, 5556-5557.

191. X. Cui, X. Dai, Y. Deng and F. Shi, *Chem. Eur. J.*, 2013, **19**, 3665-3675.

192. J. A. Marshall and J. Lebreton, *J. Am. Chem. Soc.*, 1988, **110**, 2925-2931.

193. P. Eisenberger, A. M. Bailey and C. M. Crudden, *J. Am. Chem. Soc.*, 2012, **134**, 17384-17387.

194. K. N. Mehrotra and B. P. Giri, *Synthesis*, 1977, **1977**, 489-490.

195. M. Patel, S. S. Ko, R. J. McHugh Jr, J. A. Markwalder, A. S. Srivastava, B. C. Cordova, R. M. Klabe, S. Erickson-Viitanen, G. L. Trainor and S. P. Seitz, *Bioorg. Med. Chem. Lett.*, 1999, **9**, 2805-2810.

196. A. Varela-Fernández, J. A. Varela and C. Saá, *Synthesis*, 2012, **44**, 3285-3295.

197.   T. Sakamoto, Y. Kondo, S. Iwashita, T. Nagano and H. Yamanaka, *Chem. Pharm. Bull.*, 1988, **36**, 1305-1308.

198.   A. N. Kost, S. M. Gorbunova, L. P. Basova, V. K. Kiselev and V. I. Gorbunov, *Pharm. Chem. J.*, 1974, **8**, 74-78.

199.   X. Li, N. Chen and J. Xu, *Synthesis*, **2010**, 3423,3428.

200.   G. Jones, D. J. Tonkinson and P. C. Hayes, *J. Chem. Soc. Perkin Trans. 1.*, 1983, 2645-2648.

201.   A. R. Katritzky, G. Noble, B. Pilarski and P. Harris, *Chem. Ber.*, 1990, **123**, 1443-1445.

202.   B. Carboni, M. Vaultier and R. Carrié, *Tetrahedron*, 1987, **43**, 1799-1810.

203.   L. Xing, C. Cheng, R. Zhu, B. Zhang, X. Wang and Y. Hu, *Tetrahedron*, 2008, **64**, 11783-11788.